

INSTYTUT CHEMII ORGANICZNEJ POLSKIEJ AKADEMII NAUK



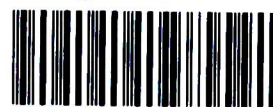
Synteza i właściwości fizykochemiczne koroli z podstawnikami amidowymi

mgr inż. Rafał Orłowski

Monotematyczny cykl publikacji z komentarzem przedstawiony Radzie Naukowej
Instytutu Chemii Organicznej Polskiej Akademii Nauk w celu uzyskania stopnia
naukowego doktora nauk chemicznych

Biblioteka Instytutu Chemii Organicznej PAN

Org.-B.426/21



80000000342847

Promotor: prof. dr hab. Daniel Tomasz Gryko

Warszawa 2021

A-21-6
K-c-130
K-c-125



B. Org. 426/21

Praca doktorska wykonana została w ramach projektów:



N A R O D O W E C E N T R U M N A U K I

„Synteza i samoorganizacja pochodnych koroli posiadających podstawniki amidowe”
realizowanego w ramach programu

PRELUDIUM 12 Narodowego Centrum Nauki

nr 2016/23/N/ST5/00052

oraz



N A R O D O W E C E N T R U M N A U K I

„Synteza, samoorganizacja i długodystansowe przeniesienie elektronu w
samoorganizujących się amidokorolach” realizowanego w ramach programu

Harmonia 10 Narodowego Centrum Nauki

nr 2016/22/M/ST5/00431

Pragnę serdecznie podziękować:

prof. Danielowi Gryko za opiekę naukową, poświęcony czas, zaangażowanie, a także za cenne uwagi podczas prowadzenia eksperymentów, analizy wyników i redagowania pracy.

Krzysztofowi Pulkiewiczowi za mentoring i otworenie nowych perspektyw.

Kolegom i koleżankom z zespołu X za miłą i sympatyczną atmosferę pracy.

Swoją pracę dedykuję
Ninie i Krzysztofowi Orłowski

SPIS TREŚCI

Spis treści

SPIS TREŚCI	9
1. SPIS PUBLIKACJI WCHODZĄCYCH W SKŁAD ROZPRAWY DOKTORSKIEJ	11
2. SPIS WYSTĄPIEŃ KONFERENCYJNYCH	12
3. SPIS PUBLIKACJI NIEWCHODZĄCYCH W SKŁAD ROZPRAWY DOKTORSKIEJ	13
4. WYKAZ SKRÓTÓW STOSOWANYCH W PRZEWODNIKU	14
5. STRESZCZENIE W JĘZYKU POLSKIM	15
6. ABSTRACT IN ENGLISH	16
7. PRZEWODNIK PO ROZPRAWIE DOKTORSKIEJ	17
7.1. Założenia i cel pracy	17
7.2. Obecny stan wiedzy dotyczący danej dziedziny chemii	19
7.3. Wyniki własne	26
7.3.1. Wpływ podstawników <i>mezo</i> korolu	26
7.3.2. Połączone kowalencyjnie bis(amido-korole)	29
7.3.3. Przepływ elektronów przez układy typu donor-mostek-akceptor	32
7.3.4. Podsumowanie	37
8. PUBLIKACJE ORYGINALNE	39

1. SPIS PUBLIKACJI WCHODZĄCYCH W SKŁAD ROZPRAWY DOKTORSKIEJ

1. „Synthesis of Corroles and Their Heteroanalogs”, **R. Orłowski**, D. Gryko, D. T. Gryko, *Chemical reviews*, **2017**, 117 (4), 3102-3137.
2. „Hydrogen Bonds Involving Cavity NH Protons Drives Supramolecular Oligomerization of Amido-Corroles”, **R. Orłowski**, M. Tasiar, O. Staszewska-Krajewska, Ł. Dobrzycki, W. Schilf, B. Ventura, M. K. Cyrański, D. T. Gryko, *Chemistry–A European Journal*, **2017**, 23 (42), 10195-10204.
3. „Covalently Linked Bis (Amido-Corroles): Inter-and Intramolecular Hydrogen-Bond-Driven Supramolecular Assembly”, **R. Orłowski**, G. Cichowicz, O. Staszewska-Krajewska, W. Schilf, M. K. Cyrański, D. T. Gryko, *Chemistry–A European Journal*, **2019**, 25 (41), 9658-9664.
4. „Role of intramolecular hydrogen bonds in promoting electron flow through amino acid and oligopeptide conjugates”, **R. Orłowski**, J. A. Clark, J. B. Derr, E. M. Espinoza, M. F. Mayther, O. Staszewska-Krajewska, J. R. Winkler, H. Jędrzejewska, A. Szumna, H. B. Gray, V. I. Vullev, D. T. Gryko, *P. Natl. Acad. Sci. USA*. **2021**, DOI: 10.1073/pnas.2026462118

2. SPIS WYSTĄPIEŃ KONFERENCYJNYCH

Część wyników zawartych w niniejszej rozprawie przedstawiona została na konferencjach w formie posterów i prezentacji ustnych:

1. International Conference on Porphyrins and Phthalocyanines-9, Nanjing, Chiny, 2016; poster: „Novel self-assembling corroles”
2. The Polish-German Conference, Warszawa, Polska, 2016; prezentacja: „Novel self-assembling corroles”
3. International Conference on Porphyrins and Phthalocyanines-10, Monachium, Niemcy, 2018; poster „Amide-Functionalized Self-Assembling Corroles”

3. SPIS PUBLIKACJI NIEWCHODZĄCYCH W SKŁAD ROZPRAWY DOKTORSKIEJ

1. „Self-assembling corroles”, **R. Orłowski**, O. Vakuliuk, M. P. Gullo, O. Danylyuk, B. Ventura, B. Koszarna, A. Tarnowska, N. Jaworska, A. Barbieri, D. T. Gryko, *Chemical Communications*, **2015**, 51 (39), 8284-8287.
2. „Strong solvent dependence of linear and non-linear optical properties of donor–acceptor type pyrrolo [3, 2-*b*] pyrroles”, **R. Orłowski**, M. Banasiewicz, G. Clermont, F. Castet, R. Nazir, M. Blanchard-Desce, D. T. Gryko, *Physical Chemistry Chemical Physics*, **2015**, 17 (37), 23724-23731.
3. „How does tautomerization affect the excited-state dynamics of an amino acid-derivatized corrole? ” J. A. Clark, **R. Orłowski**, D. T. Gryko, V. I. Vullev, *Photosynth. Res.* **2021**, DOI: 10.1007/s11120-021-00824-4



4. WYKAZ SKRÓTÓW STOSOWANYCH W PRZEWODNIKU

AcOH – kwas octowy

CT – transfer ładunku (*ang.* charge transfer)

DBA – donor-mostek-akceptor (*ang.* donor-bridge-acceptor)

DBU – 1,8-Diazabicyklo(5.4.0)undek-7-en

DCM – dichlorometan

DDQ – 2,3-dichloro-5,6-dicyjano-1,4-benzochinon

DIPEA – *N,N*-diizopropylaminyloaminy

DMAP – 4-dimetyloaminylopirydyna

DMF – dimetyloformamid

EDC – 1-etylo-3-(3-dimetyloaminylopropylo) karbodiimid

ET – transfer elektronów (*ang.* electron transfer)

FF – *L*-fenyloalaniny-*L*-fenyloalaniny

Fmoc – grupa 9-fluorenyloaminyloksykarbonylowa

HATU – heksafluorofosforan 1-[bis(dimetyloaminylo)metyleno-1*H*- 1,2,3-triazolo[4,5-*b*]pirydyniowego

HCl – kwas solny

HFIP – heksafluoroizopropanol

HT – transfer dziury (*ang.* hole transfer)

MeOH – metanol

PDI – perylenobisimid

TFA – kwas trifluorooctowy

THF – tetrahydrofuran

5. STRESZCZENIE W JĘZYKU POLSKIM

Głównym celem mojej rozprawy było zbadanie wpływu podstawników znajdujących się w pozycjach *mezo* na strukturę przestrzenną sieci wiązań wodorowych oraz na właściwości fizykochemiczne amido-koroli. W swojej pracy skupiłem się na syntezie oraz na badaniu konkurencji pomiędzy wewnątrz- i międzycząsteczkowymi wiązaniami wodorowymi. Moją pracę rozpocząłem od optymalizacji metody syntezy koroli posiadających w pozycjach *mezo*-5- i *mezo*-15 grupy $-CO_2Me$. Podstawniki te zapewniały wymaganą stabilność barwników i nie generowały znacznej zawady sterycznej, w przeciwieństwie do zwykle stosowanych grup arylowych. Pozwoliło mi to na ocenę wpływu wielkości tych podstawników na zdolność koroli do tworzenia zorganizowanych struktur. Moja uwaga skupiła się następnie na modyfikacji podstawników *mezo*-10 korolu. Gdy jego budowa pozwala na przyjmowanie swobodnej konformacji pełni on zarówno rolę inicjatora samoorganizacji oraz stabilizuje otrzymane agregaty zarówno w kryształach jak i w roztworze. W przypadku wprowadzenia krótkich łączników, tryb tworzenia wiązań wodorowych zmienia się – promowane są wiązania wewnątrzcząsteczkowe i zahamowana zostaje zdolność związku do samoorganizacji. Dalsze badania nad barwnikami składającymi się z dwóch połączonych kowalencyjnie jednostek koroli wykazały ciekawy wpływ rozpuszczalnika na motyw wytwarzanych wiązań wodorowych. Użycie polarnych, aprotycznych rozpuszczalników uniemożliwia samoorganizację otrzymanych bis(amido-koroli). Przeciwny efekt występuje gdy zastosuje się heksafloroizopropanol, który promuje agregację. W kryształach również obserwuje się wpływ rozpuszczalnika na strukturę wiązań wodorowych. Niepolarne rozpuszczalniki wspierają tworzenie wewnątrzcząsteczkowych wiązań wodorowych, podczas gdy dodatek polarnych rozpuszczalników zmienia tryb wiązań na międzycząsteczkowy. Zwieńczeniem mojej pracy było otrzymanie biomimetycznych koroli typu donor-mostek-akceptor (*ang.* donor-bridge-acceptor DBA). Inkorporacja w ramach jednej cząsteczki zarówno korolu jak i perylenobisimidu (PDI) połączonych mostkiem zbudowanym z różnych aminokwasów, pozwoliła na zbadanie czynników odpowiedzialnych za sposób przenoszenia elektronów. Odpowiedni dobór elementów układu DBA miał na celu umożliwienie samoorganizacji finalnych związków. Dzięki temu w momencie zastosowania aprotycznego środowiska pomiarów obserwujemy dowody na fałdowanie się związku i wewnątrzcząsteczkowe oddziaływanie, wspierane przez wiązania wodorowe pochodzące od aminokwasu z łącznika. Dzięki trzem kluczowym wewnątrzcząsteczkowym wiązaniom wodorowym odległość pomiędzy donorem elektronu i jego akceptorem jest relatywnie mała i transfer elektronu zachodzi niezwykle szybko. Otrzymane związki są świetnymi biomimetykami pozwalającymi na pogłębianie wiedzy nad transferem elektronów (*ang.* electron transfer ET) i transferem dziur (*ang.* hole transfer HT) w skomplikowanych układach naturalnych. Opracowane metodologie syntetyczne są wydajne, a

ciekawe właściwości zsyntezowanych związków sprawiają, że mają one duży przyszły potencjał aplikacyjny.

6. ABSTRACT IN ENGLISH

The main objective of my work was to investigate the influence of substituents in *meso* positions on the spatial structure of the hydrogen bond network and on the physicochemical properties of amide-corroles. In my venture, I focused on synthesis and on studying the competition between intra- and intermolecular hydrogen bonds. I started my work with the optimization of the method of synthesis of corroles with $-\text{CO}_2\text{Me}$ groups in the *meso*-5 and *meso*-15 positions. These substituents ensured the required stability of the obtained dyes and did not generate significant steric hindrance, in contrast to the commonly used aryl groups. This allowed the assessment of the influence of the size of these substituents on the ability of corroles to form organized structures. My further attention focused on the *meso*-10 corrole substituent. When the structure allows it to change its conformation, it acts both as an initiator of self-organization and stabilizes the obtained aggregates both in the crystal and in the solution. When short linkers are introduced, the mode of formed hydrogen bonds changes - intramolecular bonds are promoted and the ability of the compound to self-assembly is inhibited. Further research on molecules comprising of two covalently connected corroles showed an interesting dependence of the used solvent on the motif of the assembled hydrogen bonds. The use of polar, aprotic solvents prevents the self-assembly of the obtained bis(amido-corroles). The opposite effect is observed when hexafluoroisopropanol is used, which promotes aggregation. In the solid state, we observe the influence of the solvent by changing the mode of hydrogen bonds. Non-polar solvents support the formation of intramolecular hydrogen bonds, while the addition of polar solvents changes the bond mode to intermolecular. The culmination of my work was obtaining biomimetic donor-bridge-acceptor (DBA) corrole derivatives. The incorporation of corrole and perylene bisimide (PDI) in one molecule, linked by amino acid bridge, allowed to study the factors responsible for the rate of electro-transfer. The structure of the applied donor and elector acceptor promoted self-organization. As a result, when the aprotic measurement environment is applied, we observe compound folding and intramolecular interactions supported by hydrogen bonding from the amino acids in the linker. As a result of the existence of three key intramolecular hydrogen bonds, the through-space distance between electron-donor and electron-acceptor is small and the electron transfer is very fast. The obtained compounds are excellent biomimetics that allow to deepen the knowledge on both electron transfer (ET) and hole transfer (HT) in complex natural systems. The developed synthetic methodologies are efficient, and the interesting properties of the synthesized compounds give them great future application potential.

7. PRZEWODNIK PO ROZPRAWIE DOKTORSKIEJ

7.1. Założenia i cel pracy

Wyczerpywanie się rezerw paliw kopalnych w połączeniu z rosnącym zapotrzebowaniem na energię i negatywnym wpływem na środowisko konwencjonalnych źródeł energii skłoniły społeczność naukową do poszukiwania rozwiązań prowadzących do bardziej zrównoważonej gospodarki energetycznej.¹ Bezpośrednie wykorzystanie energii słonecznej wydaje się optymalnym sposobem na długoterminowe sprostanie temu zadaniu. Uczeni zajmujący się tym zagadnieniem muszą znaleźć rozwiązania wielu potencjalnych problemów. Jednym z nich jest konieczność zapewnienia długiej żywotności urządzenia w połączeniu ze zdolnością do efektywnego pochłaniania światła widzialnego. Rozwiązanie tego problemu może dostarczyć analiza niektórych szczepów oceanicznych bakterii. Dzięki zdolności znajdującego się w nich bakteriochlorofilu do tworzenia poprzez samoorganizację, koncentrycznych helikalnych rurek (chlorosomów), agregaty te cechują się zarówno większą efektywnością absorpcji światła (dzięki poszerzonemu pasmu absorpcji), jak i podwyższoną trwałością.² Tak wytworzone nanoagregaty są największymi i jednymi z najbardziej wydajnych systemów barwników absorbujących światło, spośród wszystkich znanych związków organicznych występujących w naturze.³ Pomimo ogromnego postępu w dziedzinie biomimetyki w ostatnich latach żaden sztuczny samoorganizujący się system nie zbliżył się do złożoności naturalnych chlorosomów.⁴

Drugim, nie mniej ważnym wyzwaniem jest poznanie zależności pomiędzy strukturą cząsteczek wielochromoforowych a przeniesieniem elektronu na duże odległości. Jak wykazał Gray i współpracownicy w białkach przeniesienie elektronu zachodzi albo poprzez przeskakiwanie (*ang.* hopping) albo tunelowanie (*ang.* tunnelling).⁵ Jednak prace te ze względu na brak kontroli nad strukturą naturalnie występujących białek mają swoje ograniczenia. Z kolei badania przeniesienia elektronu poprzez wiązania wodorowe do tej pory oparte były na raczej prostych układach modelowych. Zaprojektowanie i synteza skutecznych

¹ Nocera, D. G. *Acc.Chem.Res.* **2012**, *45*, 767.

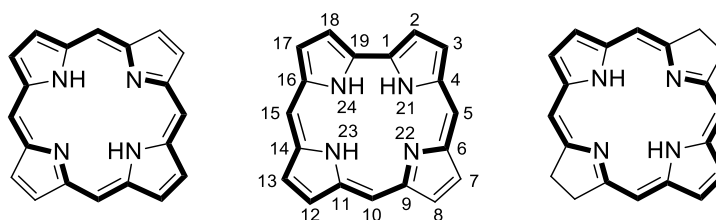
² Ganapathy, S.; Oostergetel, G. T.; Wawrzyniak, P. K.; Reus, M.; Gomez-Maqueo, C. A.; Buda, F.; Boekema, E. J.; Bryant, D. A.; Holzwarth A. R.; Groot, H. J. M. *Proc. Natl. Acad. Sci. USA* **2009**, *106*, 8525.

³ Pšenčík, J.; Ikonen, T. P.; Laurinmäki, P.; Merckel, M. C.; Butcher, S. J.; Serimaa, R. E.; Tuma R. *Biophys J.* **2004**, *87*, 1165.

⁴ a) Babu S. S.; Bonifazi, D. *ChemPlusChem* **2014**, *79*, 895. b) Huc, I. *Eur. J. Org. Chem.* **2004**, *17*. c) Qi, T.; Maurizot, V.; Noguchi, H.; Charoenraks, T.; Kauffmann, B.; Takafuji, M.; Ihara, H.; Huc, I. *Chem.Commun.* **2012**, *48*, 6337. d) Xia, B.; Bao, D.; Upadhyayula, S.; Jones G. II; Vullev, V. I. *J. Org. Chem.* **2013**, *78*, 1994.

⁵ a) Winkler, J. R.; Gray, H. B. *Chem. Rev.* **2014**, *114*, 3369. b) Gray, H. B.; Winkler, J. R. *Proc. Nat. Acad. Sci. U.S.A.* **2005**, *102*, 3534. Beratan, D. N.; Onuchic, J. N.; Winkler, J. R.; Gray, H. B. *Science* **1992**, *258*, 1740. c) Shih, C.; Museth, A. K.; Abrahamsson, M.; Blanco-Rodriguez, A. M.; Di Bilio, A. J.; Sudhamsu, J.; Crane, B. R.; Ronayne, K. L.; Towrie, M.; Vlcek, A., Jr.; Richards, J. H.; Winkler, J. R.; Gray, H. B. *Science* **2008**, *320*, 1760.

analogów funkcjonalnych naturalnie występujących kompleksów absorbujących światło, dopracowany przez miliardy lat ewolucji jest tematem przewodnim dla szeregu grup badawczych.⁶ W ostatnich latach zaproponowano wiele przykładów agregatów na bazie porfiryn, uformowanych dzięki wytwarzaniu wiązań wodorowych, π -stacking'u, oddziaływań typu metal-ligand lub oddziaływań hydrofobowych.⁷ Korole⁸ (**Rysunek 1**) są młodszymi i mniej symetrycznymi analogami porfiryn, co przekłada się na znacznie mniejszą ilość badań nad procesami ich samoorganizacji. Dotychczas opublikowane przykłady samoorganizujących się koroli obejmują oktabromo-korole,⁹ korole z ugrupowaniami $-\text{PO}(\text{OH})_2$,¹⁰ amfifilowe korole,¹¹ oraz korole zawierające jednostkę pirazolu.¹²



Rysunek 1. Od lewej: profiryryna, korol i bakteriochloryna.

Głównym celem mojej pracy było zbadanie wpływu podstawników znajdujących się w pozycjach *mezo* na strukturę przestrzenną sieci wiązań wodorowych oraz na właściwości fizykochemiczne amido-koroli. W tym kontekście skupiłem się na rozwinięciu unikalnego motywu samoorganizacji *trans-A₂B*-koroli indukowanego przez wprowadzenie do podstawnika fenyłowego znajdującego się w pozycji *mezo*-10 makrocyklu grupy *orto*- OCH_2CONHR .¹³ Przeprowadzone prace pozwoliły na określenie znaczenia zawady sterycznej generowanej przez pojedyncze cząsteczki w agregatach oraz ocenę wpływu długości i sztywności

⁶ a) Deisenhofer, J.; Epp, O.; Miki, K.; Huber, R.; Michel, H. *J. Mol. Biol.* **1984**, 180, 385. b) Bryant, D. A.; Holzwarth, A. R.; Groot, H. J. M. *Proc. Natl. Acad. Sci. USA* **2009**, 106, 8525. c) Balaban, T. S. *Acc. Chem. Res.* **2005**, 38, 612.

⁷ a) Charalambidis, G.; Georgilis, E.; Anson, C. E.; Powell, A. K.; Doyle, S.; Moss, D.; Jochum, T.; Horton, P. N.; Cole, S.; Linares, M.; Beljonne, D.; Naubron, J. V.; Conradt, J.; Kalt, H.; Mitraki, A.; Coutsolelos, A. G.; Balaban, T. S. *Nat. Commun.* **2016**, 7, 12657 b) Oliveras-Gonzalez, C.; Di Meo, F.; González-Campo, A.; Beljonne, D.; Norman, P.; Simón-Sorbed, M.; Linares, M.; Amabilino, D. B. *J. Am. Chem. Soc.* **2015**, 137, 15795.

⁸ a) Ghosh, A.; *Chem. Rev.* **2017**, 117, 3798. b) Gryko, D. T.; Fox, J. P.; Goldberg, D. P. *J. Porphyrins Phthalocyanines* **2004**, 8, 1091. c) Paolesse, R. *Synlett* **2008**, 2215. d) Orłowski, R.; Gryko, D.; Gryko, D. T. *Chem. Rev.* **2017**, 117, 3102.

⁹ Capar, J.; Conradie, J.; Beavers, C. M.; Ghosh, A. J. *Phys. Chem. A* **2015**, 119, 3452.

¹⁰ Stefanelli, M.; Monti, D.; Venanzi, M.; Paolesse, R.; *New J. Chem.* **2007**, 31, 1722.

¹¹ Randazzo, R.; Savoldelli, A.; Cristaldi, D. A.; Cunsolo, A.; Gaeta, M.; Fragalà, M. E.; Nardis, S.; D'Urso, A.; Paolesse, R.; Purrello, R. *J. Porphyrins Phthalocyanines* **2016**, 20, 1272.

¹² Gross, Z.; Sharma, V. K.; Saltsman, I.; Chen, Q.-C.; Fridman, N. *Eur. J. Org. Chem.* **2020**, 3142.

¹³ Orłowski, R.; Vakuliuk, O.; Gullo, M. P.; Danylyuk, O.; Ventura, B.; Koszarna, B.; Tarnowska, A.; Jaworska, N.; Barbieri, A.; Gryko, D. T. *Chem. Commun.* **2015**, 51, 8284.

zastosowanego łącznika między korolem a akceptorem wiązania wodorowego. W tym kontekście kluczowe było jednoznaczne potwierdzenie agregacji koroli w roztworze z zastosowaniem technik NMR. Jako kolejny cel wyznaczyłem sobie połączenie dwóch pierścieni korolu łącznikiem, który charakteryzował by się zróżnicowaną sztywnością. Ukoronowaniem pracy miało być otrzymanie układów bichromoforowych zawierających korol, akceptor elektronów oraz mostek typu peptydowego. W tym przypadku miałem nadzieję, że proces przeniesienia elektronu będzie zależny od typu mostka, a tym samym od układu wewnątrzcząsteczkowych wiązań wodorowych. Istotne więc było nie tylko otrzymanie złożonych barwników funkcjonalnych, ale również zbadanie właściwości fotofizycznych otrzymanych bichromoforowych barwników. W tym celu zamierzałem poprowadzić szereg pomiarów czasowo-zależnych pozwalających na zbadanie dynamiki otrzymanych układów.

7.2. Obecny stan wiedzy dotyczący danej dziedziny chemii

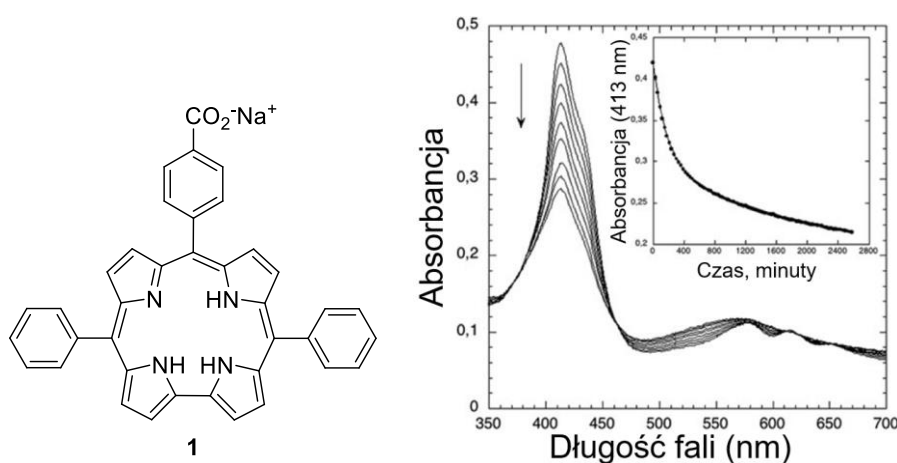
Chociaż w literaturze znajdujemy wiele prac poruszających temat samoorganizacji tetrapirolowych makrocycyli, takich jak porfiryny lub chloryny,¹⁴ niewiele z nich poświęconych jest zgłębieniu tego zjawiska dla pozostałych porifynoidów, a w szczególności koroli. Poza badaniami będącymi podstawą tej dysertacji, dostępnych jest łącznie 7 publikacji opisujących korole zdolne do tworzenia zorganizowanych struktur poprzez wiązania wodorowe. Znajdziemy w nich 25 przykładów takich związków nie będącymi kompleksami metali, przy czym tylko dla 9 została przeprowadzona rentgenowska analiza strukturalna ich monokryształów. Statystyki te wynikają bezpośrednio z dwóch powodów. Pierwszym był brak efektywnych metod syntezy koroli, który przez wiele lat hamował badania nad tymi tetrapirołami. Zmieniło się to dopiero w 2006 roku, kiedy opracowano pierwszą efektywną i uniwersalną metodę syntezy tych molekuł.¹⁵ Drugim powodem jest to, że korole w przeciwieństwie do swoich strukturalnych analogów – porfiryn charakteryzuje obniżona stabilność, co oznacza, że praca z tymi makrocycylami jest znacznie bardziej wymagająca.

Historycznie pierwszym przykładem syntezy samoorganizujących się koroli jest praca opublikowana w 2007 przez Monti i Paolesse.¹⁰ Zdolność do samoorganizacji związku została potwierdzona poprzez pomiary absorpcji związku **1** w różnych proporcjach układu rozpuszczalników woda:etanol (**Rysunek 2**). W zakresie składu od 50% do 100% etanolu (v / v) makrocycyl pozostaje w postaci monomerów, o czym świadczy kształt pasma Soreta przy

¹⁴ Drain, C. M.; Varotto, A.; Radivojevic, I. *Chem. Rev.* **2009**, *109*, 1630.

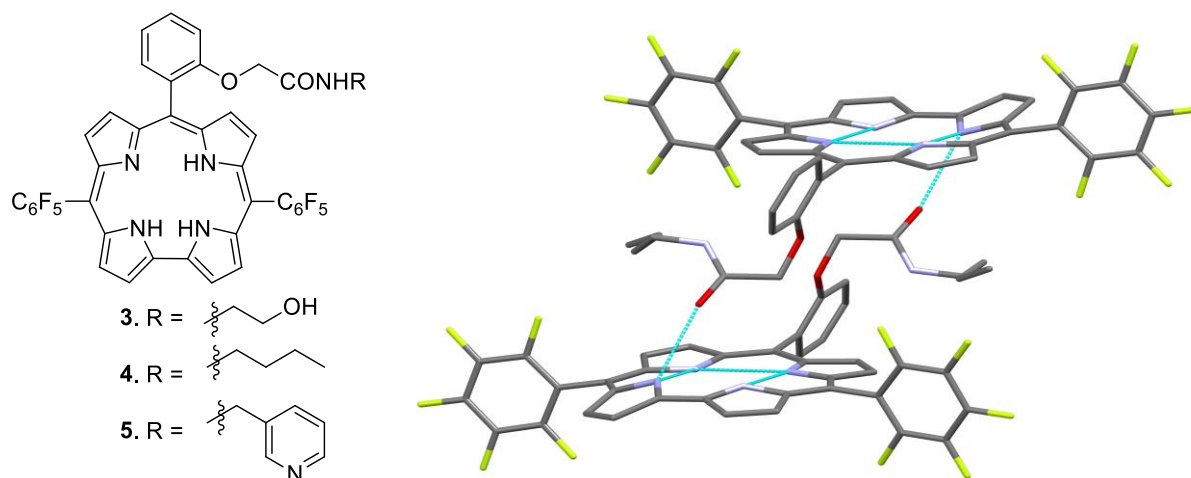
¹⁵ Koszarna, B.; Gryko, D. T. *J. Org. Chem.* **2006**, *71*, 3707.

413 nm. Dalszy wzrost udziału wody wyzwała proces agregacji, powodując poszerzenie i niewielkie przesunięcie hipsochromowe pasma Soreta (o ok. 2 nm).



Rysunek 2. Od lewej: korol 1, widmo a) 10-(4-karboxylanofenylo)-5,15-difenylokorołu sodu b) widmo UV-Vis związku 1 ($5 \cdot 10^{-6} \text{M}$).

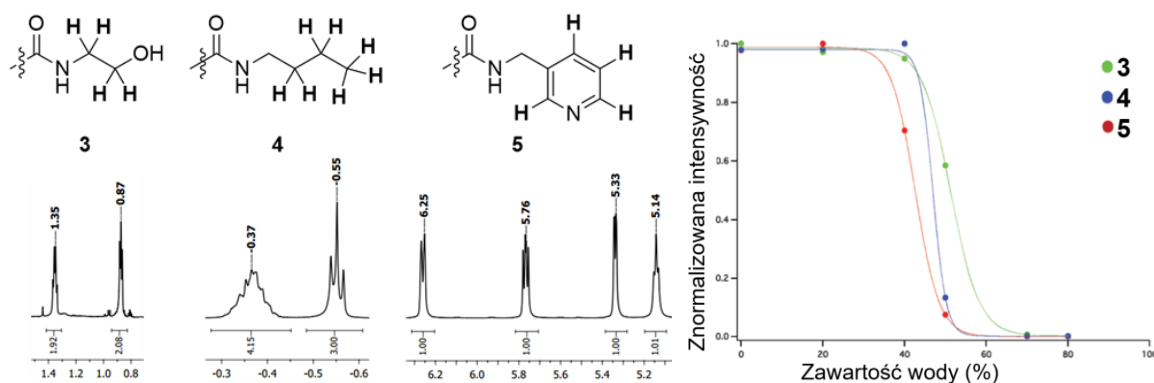
Autorzy zauważyli, że analogiczna porfiryryna w tych warunkach tworzy agregaty typu J. Odmiennie zachowanie się korolu zostało wytłumaczone różnicą w geometrii makrocyklu, spowodowaną obecnością bezpośredniego wiązania pirol-pirol. Ograniczenia wynikające z tej geometrii kierują agregację w kierunku formowania się supramolekularnych struktur typu głowa do głowy (ang. *face-to-face*), poprzez formowanie się wiązań wodorowych pomiędzy grupą karboksylową, a „wewnętrzny” atomami wodoru rdzenia korolu. Niestety nie udało się potwierdzić tej hipotezy poprzez badania NMR ani też otrzymać monokryształów związku 1, co uniemożliwiło zbadanie sposobu jego organizacji w kryształach.



Rysunek 3. Od lewej: korole 3-5 zdolne do samoorganizacji w ciele stałym, struktura krystalograficzna związku 4.

Opublikowana przeze mnie na łamach czasopisma *Chemical Communications* w 2015 roku praca stanowiła podwaliny moich dalszych badań.¹³ Otrzymałem bibliotekę trans-A₂B-podstawionych koroli zawierających grupę -OCH₂CONHR na podstawniku fenylovym znajdującym się w pozycji *mezo-10*, która indukowała ich zdolność do tworzenia silnych wiązań wodorowych (**Rysunek 3**).

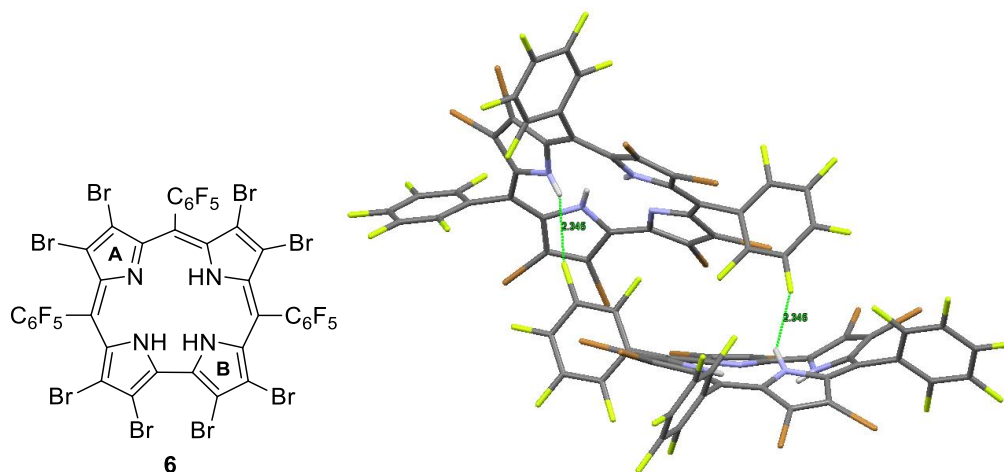
Sposób ułożenia otrzymanych cząsteczek w przestrzeni był zależny od rodzaju wprowadzonego podstawnika amidowego. Kluczowe dla tego procesu jest wytwarzanie silnych wiązań wodorowych pomiędzy wewnętrznymi protonami korolu, a tlenem karbonylowym bądź pirydynowym atomem azotu. Charakter wewnętrznego NH w rdzeniu korolu (służący jako donor wiązań wodorowych) jest bezpośrednio odpowiedzialny za silne właściwości samoorganizujące (w ciele stałym) tych związków. W połączeniu z akceptorem wiązania wodorowego - grupą -CONH- właściwości te prowadzą do tworzenia agregatów w stanie stałym. W roztworze analiza widm absorpcji UV-Vis i fluorescencji ujawniła formowanie się dużych agregatów w mieszaninach metanolu z wodą przy krytycznej zawartości wody wynoszącej około 40-50% (**Rysunek 4**). Tworzenie wiązań wodorowych było wyraźnie widoczne w strukturach krystalograficznych, a także w widmach ¹H NMR jako silne przesunięcia sygnałów ramienia amidowego w górę pola (**Rysunek 4**).



Rysunek 4. Fragmenty widm ¹H NMR i zmiana intensywności emisji przy λ_{\max} koroli **3**, **4** i **5** w mieszaninie wody i metanolu.

W 2015 Ghosh opublikował kolejny przykład samoorganizującego się korolu.⁹ W otrzymanym związku grupa NH w pierścieniu pierwszego korolu, angażuje się w wiązanie wodorowe z *meta*-F grupy pentafluorofenylovej sąsiedniej cząsteczki. Wytworzenie tego

wiązania wodorowe oraz zawada przestrzenna generowana przez wewnętrzne protony NH powodują znaczące zniekształcenie cząsteczki (**Rysunek 5**).

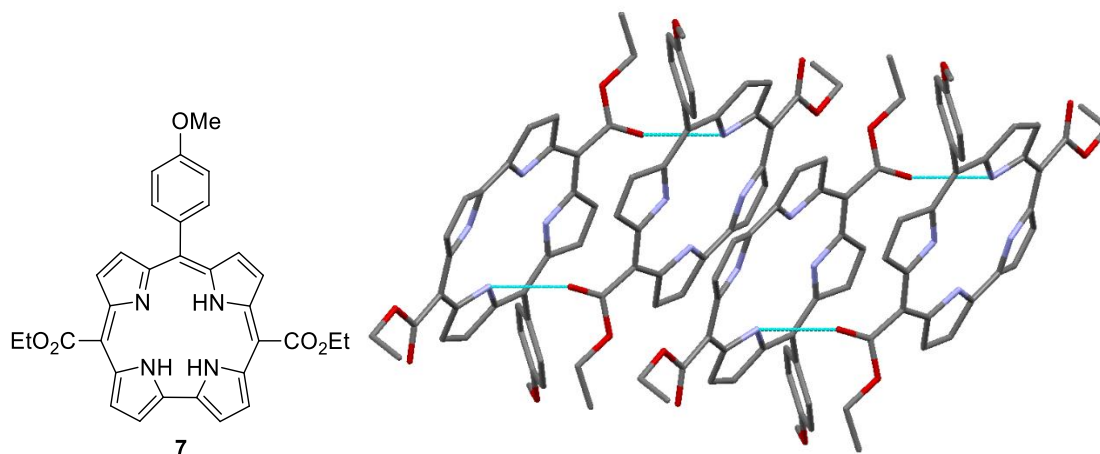


Rysunek 5. Struktura korolu **6** i struktura krystalograficzna z uwidocznionymi wiązaniami wodorowymi N-H...F-C.

Pierścienie pirolowe **A** i **B** związku **6** (**Rysunek 5**) są zasadniczo ortogonalne względem siebie, co jest niezwykłym zniekształceniem dla związku aromatycznego. Dodatkowo kąty dwuścienne wewnątrz otrzymanej cząsteczki są największe z pośród wszystkich znany przykładów wolnych zasad koroli.

W 2015 roku ukazała się obszerna praca Balabana,¹⁶ która skupiła się na zastąpieniu powszechnie stosowanych elektronoakceptorowych podstawników arylowych w korolu, znacznie mniejszymi grupami estrowymi. Zastosowana strategia zagwarantowała nie tylko zadowalającą stabilność otrzymanych koroli, ale też pozwoliła na skrócenie odległości pomiędzy poszczególnymi cząsteczkami związku w kryształach. Wszystkie otrzymane związki tworzyły kolumny, połączone poprzez oddziaływania typu N-H... π , π ... π lub międzycząsteczkowe wiązania wodorowe (**Rysunek 6**).

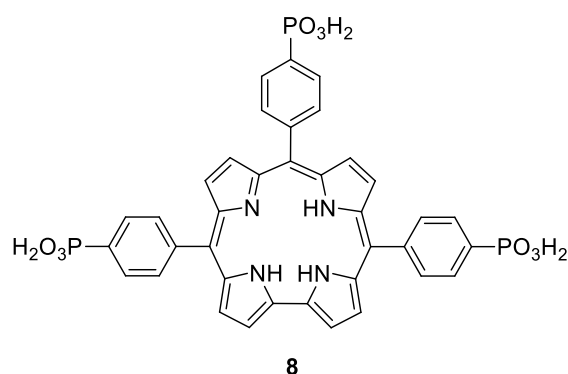
¹⁶ Canard, G.; Gao, D.; D'Aléo, A.; Giorgi, M.; Dang, F.-X.; Balaban, T. S. *Chem. Eur. J.* **2015**, *21*, 7760.



Rysunek 6. Przykład układu wiązań wodorowych w kryształach korolu **7**. Cząsteczki układają się w kolumny poprzez wiązania N-H...N i N-H...O=C pomiędzy sąsiednimi cząsteczkami.

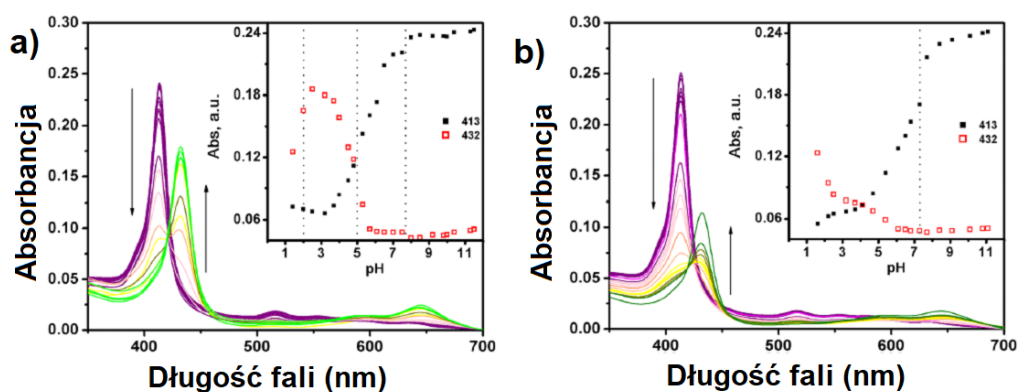
Charakter podstawnika znajdującego się w pozycji *mezo*-10, nie miał znacznego wpływu na właściwości fotofizyczne koroli. Dodatkowo, zaproponowana metoda syntezy pozwalała na otrzymanie docelowych związków z wydajnościami rzędu zaledwie kilku procent.

Paolesse i Purrello opierając się na swoich doświadczeniach z amfifilowymi korolami zbadali w 2016 roku właściwości nowego korolu **8** (Rysunek 7).¹¹ W celu analizy zależności jego trybu samoorganizacji od etapów protonowania przeprowadzili oni dwie serie pomiarów. W pierwszym eksperymencie zarejestrowano widma UV-Vis roztworów przygotowanych przy różnych wartościach pH, minimalizując efekt agregacji. Następnie wykonali powolne miareczkowanie roztworu związku **8** obniżając jego pH, co promowało proces samoorganizacji (Rysunek 8).



Rysunek 7. Forma obojętna korolu **8**.

W wyższym pH oba eksperymenty dały podobne wyniki. Pasma Soreta (413 nm) ulegało stopniowemu poszerzeniu, oraz przy 432 nm można było zauważyć obecność niewielkiego pasma od sprotonowanej cząsteczki korolu. Zmiany te przypisano protonowaniu grup fosfonianowych (pK_a 7.5–7.2). Wraz ze spadkiem pH dla pierwszej serii eksperymentów zaobserwowano szybki wzrost intensywności pasma przy 432 nm poprzez protonowanie atomu azotu rdzenia korolu (pK_a ~5.2). W przypadku powolnego miareczkowania, zauważono gwałtowny spadek absorbancji, co wskazuje, że agregacja korolu **8** następuje wkrótce po pierwszym protonowaniu grup fosfonianowych. Konsekwencją tego jest utrudnienie protonowania rdzenia makrocyklu. Dalsze obniżenie pH do wartości niższych niż 4, powoduje wzrost intensywności pasma przy 432 nm co potwierdza zarówno zmiana ładunku rdzenia **8** oraz rozpad agregatów (**Rysunek 8**).



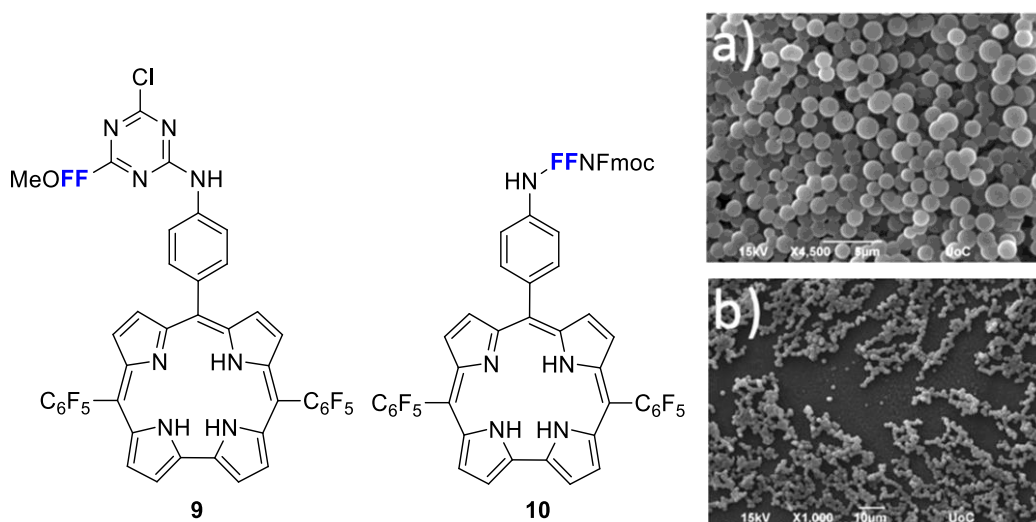
Rysunek 8. Widmo absorpcji. a) widma absorpcji roztworów **8** przy różnych pH. b) miareczkowanie roztworu **8**. Wstawki: absorbancja vs. pH roztworów korolu **8**.

Protonowanie rdzenia korolu **8** indukuje powstanie jednego ładunku dodatniego, który sprzyja rozpadowi zagregowanych cząsteczek w wyniku odpychania elektrostatycznego. Zjawisko to jest dowodem na to, że dalsze dodawanie kwasu umożliwia przejście z prowadzącej do agregacji ścieżki kinetycznej na termodynamiczną. Cecha ta odróżnia opisany korol od jego porfiryнового odpowiednika.

Praca Gryko i Coutsolelosa z 2016 roku skupia się na pochodnych **9** i **10** zawierających w swojej strukturze aminokwas (**Rysunek 9**).¹⁷ Połączenie danych z badań SEM, absorpcji i spektroskopii fluorescencyjnej wykazało, że obecność dipeptydu *L*-fenyloalaniny-*L*-fenyloalaniny (**FF**) odgrywa kluczową rolę w tworzeniu nanoagregatów,

¹⁷ Karikis, K.; Georgilis, E.; Charalambidis, G.; Petrou, A.; Vakuliuk, O.; Chatziioannou, T.; Raptaki, I.; Tsovolas, S.; Papakyriacou, I.; Mitraiki, A.; Gryko, D. T.; Coutsolelos, A. G. *Chem. Eur. J.* **2016**, *22*, 11245.

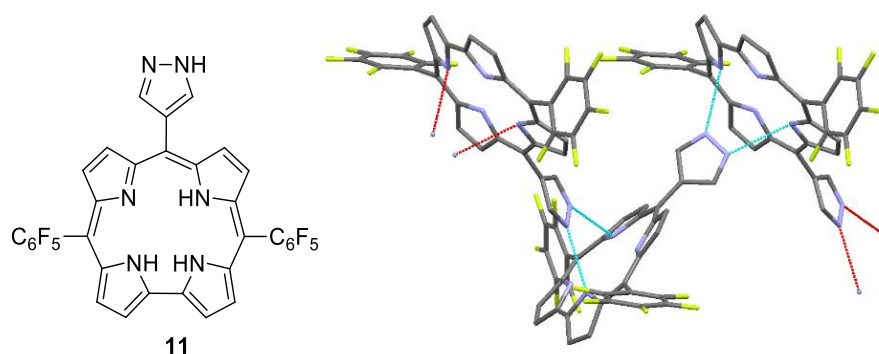
a także wpływa na ich wielkość. Wykazali oni, że skłonność do samoorganizacji biokoniugatów FF w tych rozpuszczalnikach skutkuje powstawaniem kulistych nanostruktur w HFIP/THF (**Rysunek 9**).



Rysunek 9. Struktury oraz wynik samoorganizacji: a) korolu **10** (skala 5 μm), b) korolu **9** (skala 10 μm).

Proces samoorganizacji był niezależny od sposobu przyłączenia *L*-fenyloalaniny-*L*-fenyloalaniny do rdzenia korolu. Zarówno wiązanie przez grupę $-\text{COOH}$ **9** jak i $-\text{NH}_2$ **10** znajdującą się na podstawniku fenylowym z pozycji *mezo*-10 makrocyklu prowadziło do otrzymania analogicznych nanostruktur. Opisane pochodne koroli charakteryzowało również przesunięcie batochromowe widma absorpcji, co zostało wyjaśnione tworzeniem agregatów już w niskich stężeniach, które są stosowane podczas pomiarów fotofizycznych.

Warto tu podkreślić, że zainteresowanie tematem samoorganizujących się koroli nie słabnie, a w badania nad nimi angażują się kolejne grupy badawcze. W 2020 roku już po skończeniu badań wchodzących w skład tej dysertacji ukazała się publikacja Grossa opisująca samoorganizację koroli posiadających ugrupowania pirazolowe **11** (**Rysunek 10**).¹²



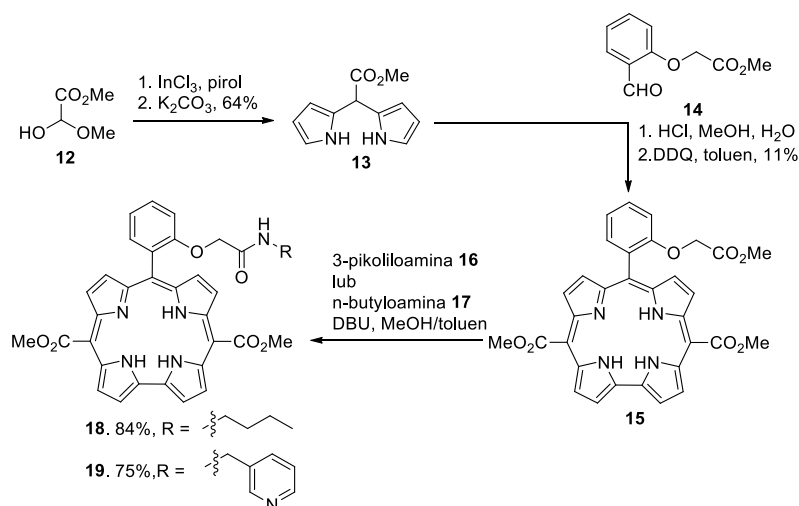
Rysunek 10. Łańcuchy korolu **11** w ciele stałym.

7.3. Wyniki własne

7.3.1. Wpływ podstawników *mezo* korolu

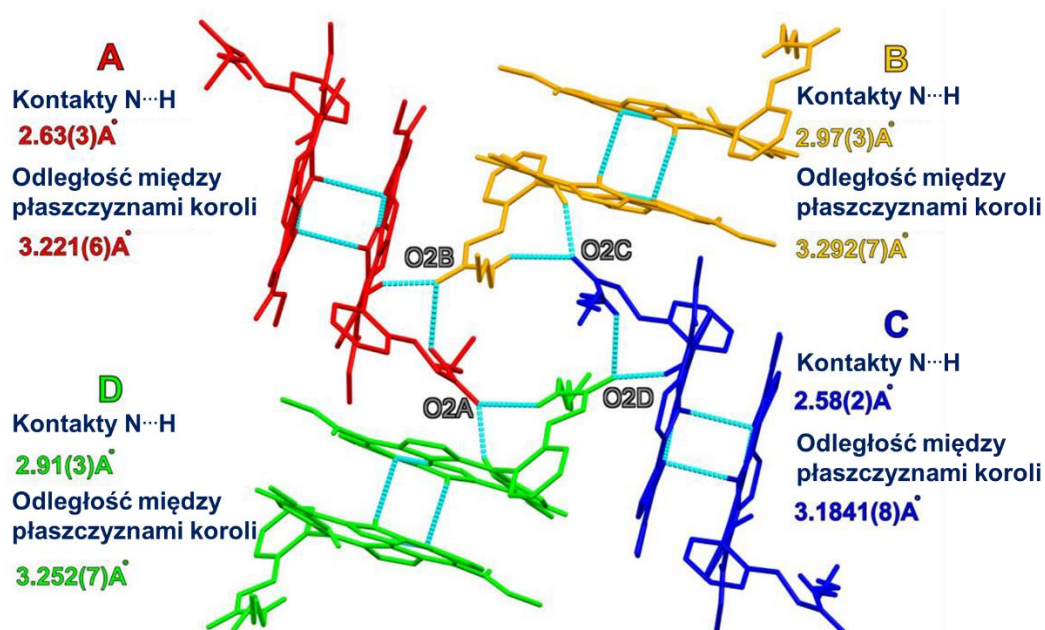
Swoje badania rozpocząłem od analizy wpływu struktury *mezo* podstawników korolu na jego zdolność do wytwarzania wewnątrz- i międzycząsteczkowych wiązań wodorowych. Dostępne literaturowo przykłady samoorganizujących się koroli zawierały ugrupowania pentafluorofenyłowe znajdujące się w pozycji *mezo* 5- i 15, które cechuje znaczna zawada steryczna. Pełnią one jednak kluczową rolę w zapewnieniu wysokiej stabilności cząsteczek dzięki ich właściwościom elektrono-akceptorowym.

Przy projektowaniu nowych struktur bazowałem na wcześniej zbadanym przeze mnie ugrupowaniu $-OCH_2CONHR$,¹³ które będąc w pozycji *orto* podstawnika *mezo*-fenyłowego, indukuje wytwarzania wewnątrz- i międzycząsteczkowych wiązań wodorowych zarówno w kryształach jak i w roztworze. Zastąpienie grup pentafluorofenyłowych znacznie mniejszymi podstawnikami estrowymi wymagało ode mnie opracowania nowych warunków syntezy. Niestety metody dostępne literaturowo pozwalały na otrzymanie pożądaných związków z wydajnościami sięgającymi zaledwie kilku procent.¹⁶ W związku z niezadowolającymi rezultatami postanowiłem przeprowadzić optymalizację opublikowanych w 2006 roku warunków syntezy koroli z wykorzystaniem układu rozpuszczalników woda metanol.¹⁵ Dziesięciokrotne zwiększenie stężenia substratów pozwoliło na otrzymanie koroli zawierających podstawniki estrowe z zadowalającą wydajnością (**Schemat 1**). Warto podkreślić, że aminoliza estru jest w tym przypadku całkowicie chemoselektywna, ze względu na obniżenie reaktywności grupy estrowej połączonej bezpośrednio z rdzeniem korolu. Jest to wywołane przez kombinację efektu elektronowego (bogaty w elektrony pierścień korolu osłabia polaryzację wiązania C=O) i sterycznego.



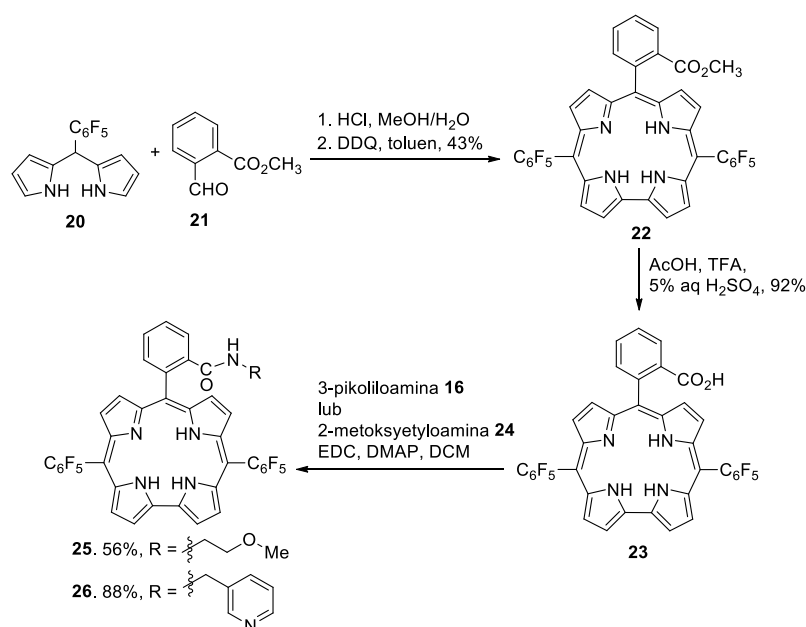
Schemat 1. Synteza koroli **18** i **19**.

Umożliwiło mi to otrzymanie nowej generacji koroli cechujących się znacznie niższą zawadą steryczną. W cieple stałym tworzyły one silnie związane tetrametry. Struktury te stabilizuje wytworzone wiązania wodorowe między tlenem z grupy amidowej, a grupami -CONH- i NH rdzenia sąsiedniego korolu **18**. Otrzymane agregaty tworzą centrosymetryczne dimery, poprzez parę wiązań wodorowych pomiędzy protonami NH w rdzeniu jednego z korolu wchodzącego w skład tetrameru, a sąsiadującymi atomami pirolu typu N pochodzącymi z drugiego agregatu. Skutkuje to wytworzeniem struktury drugorzędowej: silnie upakowanej warstwy dimerycznie połączonych tetramerów, która znajduje się w płaszczyźnie (111) sieci krystalicznej (**Rysunek 11**).



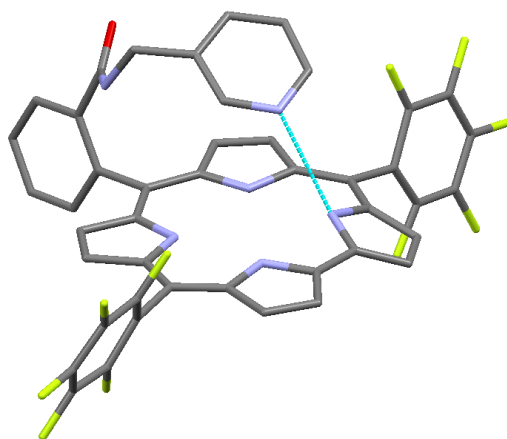
Rysunek 11. Upakowanie w kryształach korolu **18**: samo-organizacja w ciele stałym.

Podjąłem również próbę oceny wpływu długości i sztywności zastosowanego łącznika pomiędzy korolem, i akceptorem wiązań wodorowych na strukturę tworzonych agregatów. Pierwsza próba syntezy zaproponowanych cząsteczek **25** i **26** posiadających w swojej strukturze krótkie wiązanie pomiędzy ugrupowaniem amidowym, a korolem z wykorzystaniem aminolizy estrów nie pozwoliła na otrzymanie pożądaných cząsteczek. Rozwiązaniem okazało się przeprowadzenie hydrolizy wiązania estrowego, a następnie zastosowanie standardowej chemii peptydów. Pozwoliło to na uzyskanie pożądaných koroli **25** i **26** (**Schemat 2**) z wysokimi wydajnościami.



Schemat 2. Synteza koroli **25** i **26**.

W korolu **26** jeden z pierścieni pirolowych jest znacznie wychylony poza płaszczyznę makrocyklu. Odpowiada to za skierowanie grupy NH w stronę atomu azotu pirydyny łącznika z pozycji *mezo*-10 i utworzenie silnego wewnątrzcząsteczkowego wiązania wodorowego (**Rysunek 12**). Zachowanie to uniemożliwia wytwarzanie międzycząsteczkowych wiązań wodorowych co hamuje agregację korolu.



Rysunek 12. Struktura krystalograficzna korolu **26**: wewnątrzcząsteczkowe wiązanie wodorowe.

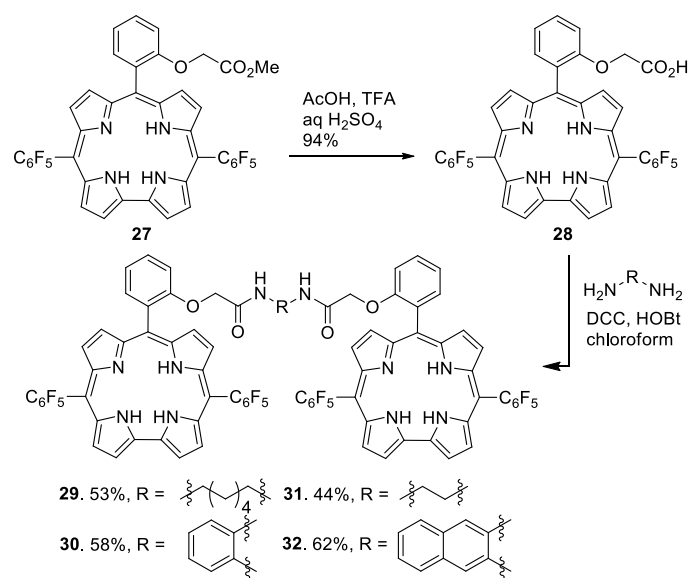
Dodatkowo dalsze innowacyjne badania z zastosowaniem techniki DOSY NMR, oparte na modelach opracowanych przez grupy Neufelda i Morrisona¹⁸ pozwoliły po raz pierwszy na precyzyjne określenie stopnia zorganizowania koroli w roztworze. Pomiar w zakresie stężeń 1–65 mM wykazały, że średnia masa cząsteczek związku **18** zwiększa się o 40%, podczas gdy masa korolu **26** pozostała bez zmian.

Dla zsyntezowanych koroli **18** i **19** zostały następnie zbadane parametry fotofizyczne we współpracy z zespołem dr Barbary Ventury (Bologna, Włochy). Niestety stężenia zastosowane podczas pomiarów absorpcji i emisji (10^{-6} M do 10^{-4} M) były niewystarczające, aby badane związki połączyły się w agregaty.

7.3.2. Połączone kowalencyjnie bis(amido-korole)

Zachęcony osiągnięciami opisanymi w poprzednim rozdziale postawiłem sobie kolejny ambitny cel. Postanowiłem przeanalizować czy zwiększenie ilości donorów i akceptorów wiązania wodorowego bezpośrednio przełoży się na zdolność cząsteczki do generowania bardziej skomplikowanych trójwymiarowych struktur. Zaprojektowałem serię koroli w których dwa pierścienie makrocyklu miały zostać połączone poprzez mostek amidowy (**Schemat 3**). Zastosowanie alifatycznych i aromatycznych diaminy pozwoliło by na modyfikację sztywności łącznika.

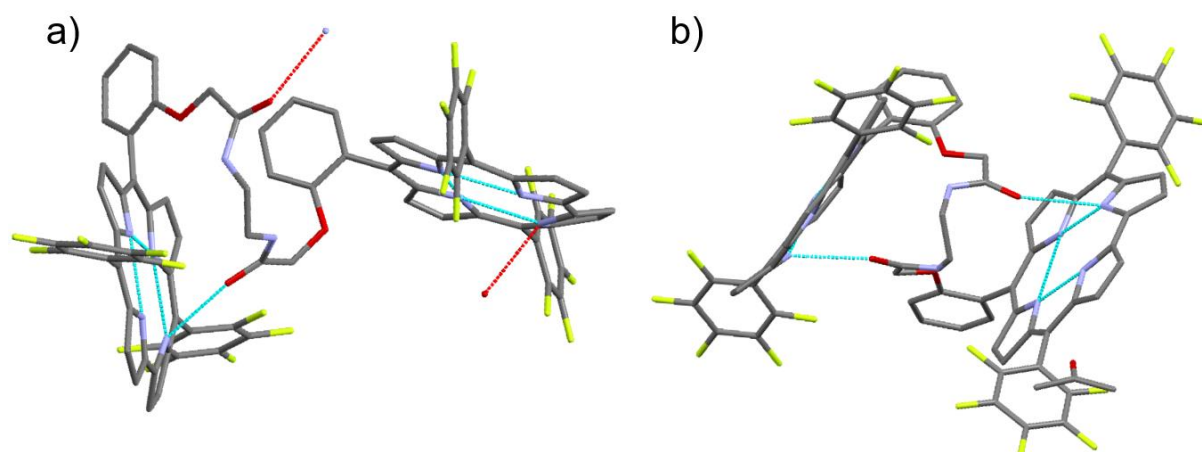
¹⁸ a) Evans, R.; Deng, Z.; Rogerson, A. K.; McLachlan, A. S.; Richards, J. J.; Nilsson, M.; Morris, G. A. *Angew. Chem.* **2013**, *125*, 3281. b) Neufeld, R.; Stalke, D. *Chem. Sci.* **2015**, *6*, 3354.



Schemat 3. Synteza kowalencyjnie połączonych bis(amido-koroli) **29-32**.

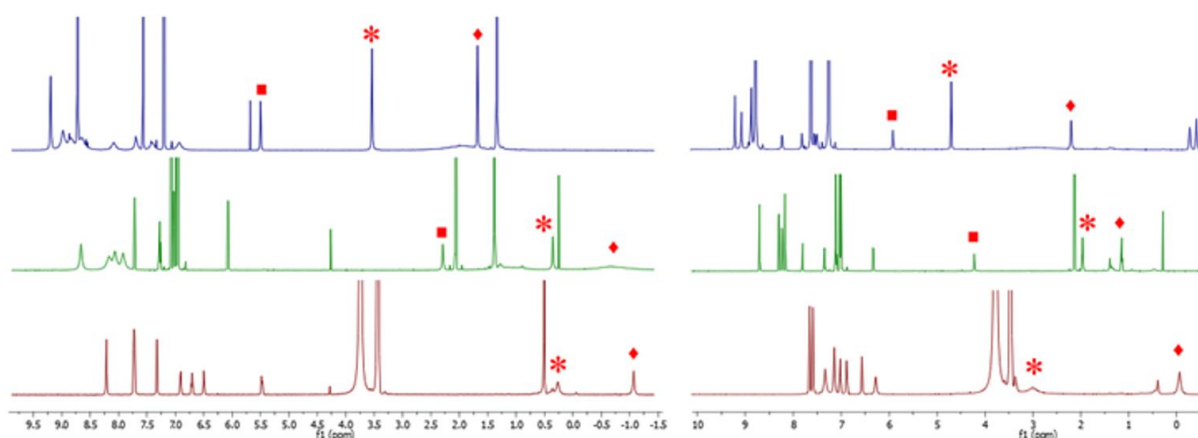
Podjąłem liczne próby syntezy zaprojektowanych barwników lecz procedury, które znajdowały zastosowanie w przypadku otrzymywania mono(amido-koroli), okazały się nieskuteczne. Bezpośrednia aminoliza korolu **27** w obecności 1,8-diazabicyklo(5.4.0)undek-7-enu (DBU) lub $\text{La}(\text{OTf})_3$ kończyła się powstaniem odpowiednich monoamidów z umiarkowaną wydajnością. Ostatecznie syntezę przeprowadziłem z wykorzystaniem hydrolizy estru i jego następczym sprzęgnięciem z odpowiednimi aminami z zastosowaniem klasycznych dla chemii peptydów odczynników sprzęgających (**Schemat 3**).

Analiza krystalograficzna otrzymanych bis(amido-koroli) wykazała, że cechuje je silna korelacja pomiędzy ulokowaniem wiązań wodorowych, a rodzajem rozpuszczalnika użytego w procesie krystalizacji (**Rysunek 13**).



Rysunek 13. Struktura krystalograficzna koroli **31**: a) krystalizacja z toluenu (międzycząsteczkowe wiązania wodorowe), b) krystalizacja z acetonu (wewnątrzcząsteczkowe wiązania wodorowe).

Wprowadzenie do sieci krystalicznej polarnych rozpuszczalników wymusza praktycznie równoległe ustawienie pierścieni koroli połączonych przez mostek -NHCH₂CH₂NH- (**31**) lub mostek zbudowany z 2,3-diaminonaftalenu (**32**). Indukuje to wytworzenie wewnątrzcząsteczkowych wiązań wodorowych pomiędzy grupami NHC=O···H-N pochodzących z dwóch różnych jednostek koroli. Solwatacja w toluenie powoduje zmianę układu wiązań - jedno z nich staje się międzycząsteczkowe dzięki czemu związek samoorganizuje tworząc „łańcuchy” (**Rysunek 13**). Warto zauważyć, że wewnątrzcząsteczkowe wiązania wodorowe zawsze powstają pomiędzy grupą funkcyjną -NHCO- znajdującą się dalej od pierścienia benzenowego obecnego w pozycji 10-*mezo*. Chociaż międzycząsteczkowe wiązania wodorowe odgrywają znaczącą rolę w sposobie organizacji przestrzennej koroli, są one dodatkowo wspierane poprzez występowanie wewnątrzcząsteczkowych wiązań wodorowych i słabych oddziaływań N-H···π między cząsteczkami rozpuszczalnika (toluen) a rdzeniami koroli. Mostki alifatyczne jak i ich aromatyczne odpowiedniki znajdują się bezpośrednio nad pierścieniem koroli, tak jak w przypadku mono(amido-koroli). W roztworze, analogicznie do ciała stałego, kluczowy wpływ na sposób wytwarzania wiązań wodorowych bis(amido-koroli) pełni rodzaj rozpuszczalnika. Porównując wpływ DMSO i pirydyny w stosunku do toluenu (sygnały ¹H NMR silnie są przesunięte w górę pola) zaobserwowałem zahamowanie procesu samoorganizacji, natomiast zastosowanie heksafluoroizopropanolu (HFIP) zaowocowało wzmocnieniem powstających wiązań wodorowych i znaczne przesłanianie diagnostycznych sygnałów (**Rysunek 14**).

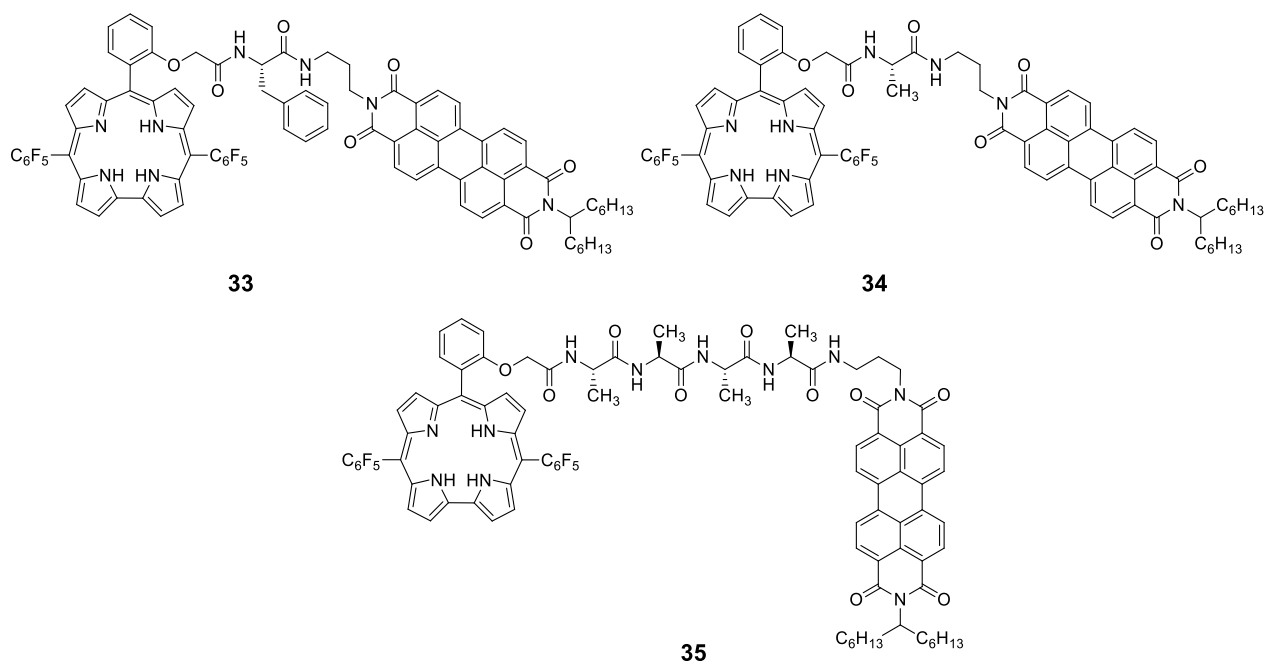


Rysunek 14. Porównanie położenia sygnałów $-\text{OCH}_2\text{C}(\text{O})-$ (*), $-\text{C}(\text{O})\text{NH}-$ (■) i $-\text{NHCH}_2-$ (◆) związku **29** (lewe widmo) i **31** (prawe widmo). Od góry do dołu: pirydyna, toluen i HFIP.

W trakcie mojej pracy wykazałem, że bis(amido-korole) mają zdolność do samoorganizacji zarówno w stanie stałym, jak i w roztworze. Proces ten zachodzi niezależnie od długości i charakteru chemicznego łącznika. W stanie stałym na sieć wiązań wodorowych silnie wpływa rozpuszczalnik użyty do krystalizacji, a wewnątrzcząsteczkowe wiązania wodorowe są zawsze tworzone przez grupę $-\text{NHCO}-$ umiejscowioną dalej od podstawnika 10-mezo-fenylowego. Silny wpływ natury rozpuszczalnika na wiązania wodorowe powoduje zmianę zarówno oddziaływań międzycząsteczkowych, jak i wewnątrzcząsteczkowych. Ma to z kolei odzwierciedlenie w zorganizowanej strukturze, prowadzi do zmian odległości, kątów między płaszczyznami koroli, a także do stopnia wypłaszczenia makrocyclicznych rdzeni związku. Pirydyna i DMSO łatwo tworzą wiązania wodorowe rozrywając międzycząsteczkowe wiązania wodorowe między grupą $-\text{CONH}-$ a „wewnętrzny” protonami koroli. Jest to odzwierciedlone zmianą przesunięć chemicznych sygnałów pochodzących od łącznika na widmach ^1H NMR. Natomiast oddziaływania HFIP z bis(amido-korolami) wzmacniają wiązania wodorowe co przybliży łącznik amidowy ku rdzeniu korolu, powodując znaczne przysłanianie sygnałów.

7.3.3. Przepływ elektronów przez układy typu donor-mostek-akceptor

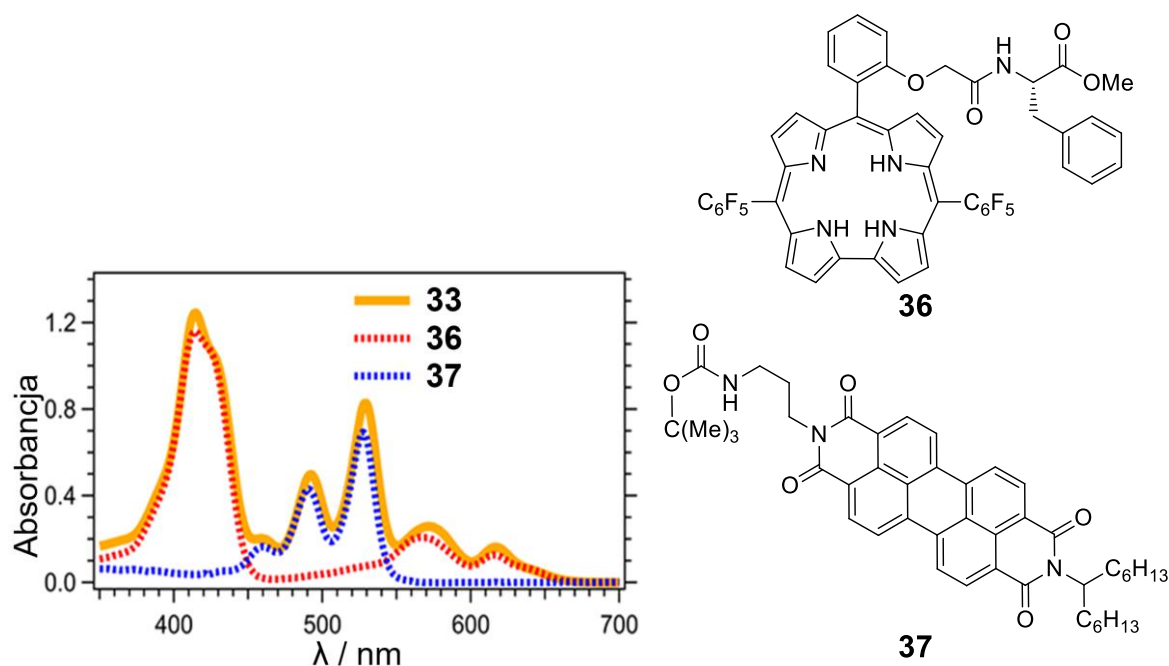
Zwieńczeniem mojej pracy było przeprowadzenie badań nad transferem elektronów (ET) i transferem dziur (HT) w zaawansowanych układach biomimetycznych. Zjawiska te zachodziły pomiędzy korolem będącym donorem elektronów, a akceptorem – perylenobisimidem połączonymi przez krótki łącznik zbudowany z aminokwasów (**Rysunek 15**).



Rysunek 15. Struktura układów bichromoforowych **33-35**.

Podczas projektowania tych innowacyjnych struktur opierałem się na czterech założeniach. (1) Zgodnie z wcześniejszymi badaniami *trans*-A₂B-podstawione korole zawierające grupę -OCH₂CONHR w podstawniku fenylowym znajdującym się w pozycji *mezo* mają skłonność do tworzenia wiązań wodorowych. (2) Dzięki dodatkowym wiązaniom wodorowym typu C=O⋯H-N w łączniku bazującym na aminokwasach może nastąpić zbliżenie się obu chromoforów przez ‘złożenie się’ cząsteczek. (3) Kolejnym założeniem była promowanie tworzenia się dodatkowych wewnątrzcząsteczkowych wiązań wodorowych dzięki obecności grupy C=O w PDI. (4) Kluczowy element uzyskałem z wcześniejszych badań prowadzonych przez L. Flamingi i D. T. Gryko. Było nim odkrycie możliwości przebiegu efektywnego przeniesienia elektronów pomiędzy korolem, a PDI.¹⁹ Połączenie korolu jako donora elektronów i PDI jako akceptora elektronów pozwala na selektywne foto-wzbudzenie akceptora w obszarze 460-530 nm. Korole w tym przedziale absorbują ≤ 10% światła. Donor może być selektywnie wzbudzony w jego paśmie Soreta między 390 a 440 nm lub przy długościach fal dłuższych niż 570 nm (**Rysunek 16**). Wzbudzenie donora indukuje transfer elektronów (ET) do LUMO akceptora, a wzbudzenie PDI indukuje transfer dziur (HT) do HOMO donora.

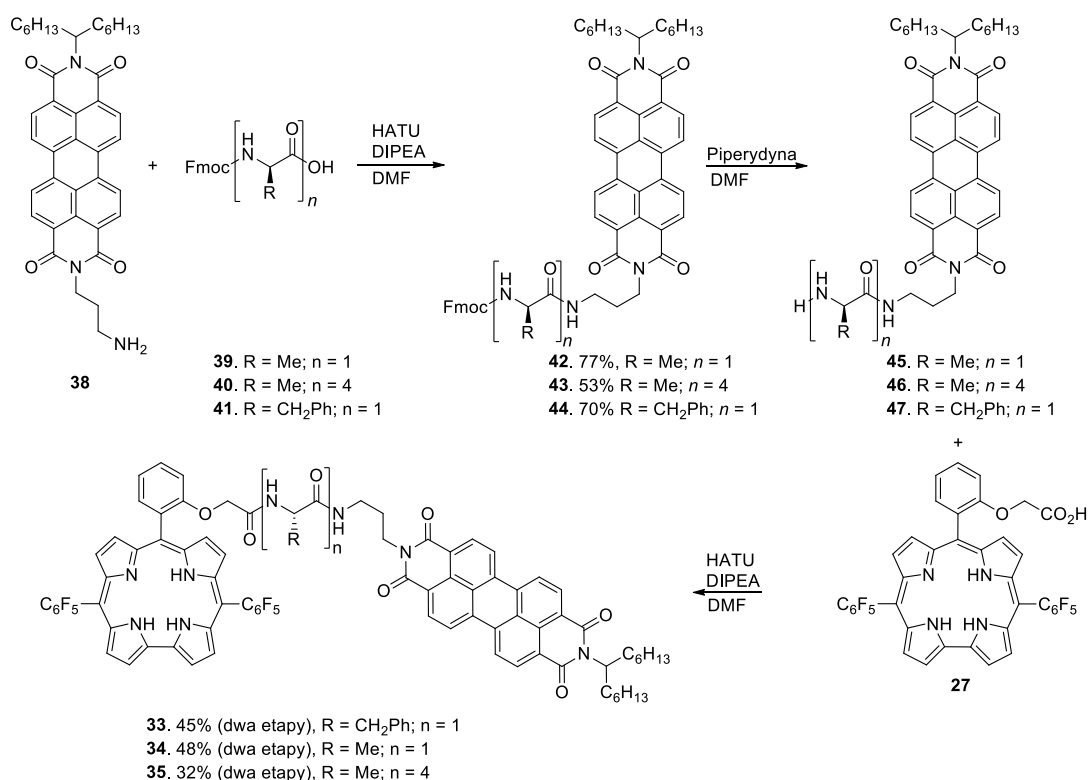
¹⁹ a) Flamingi, L.; Ventura, B.; Tasiar, M.; Becherer, T.; Langhals, H.; Gryko, D. T. *Chem. Eur. J.* **2008**, *14*, 169. b) Voloshchuk, R.; Gryko, D. T.; Chotkowski, M.; Ciuciu, A. I.; Flamingi, L. *Chem. Eur. J.* **2012**, *18*, 14845.



Rysunek 16. Widmo UV-Vis związku **33**, nałożone na widmo korolu **36** i PDI **37**.

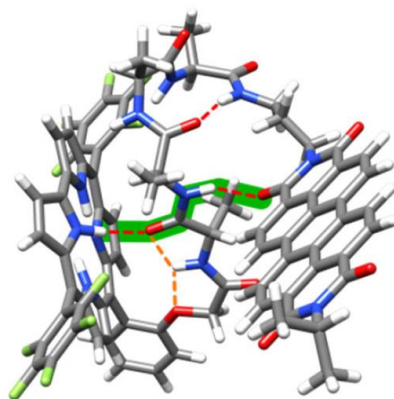
Przeprowadzona przeze mnie analiza retrosyntetyczna zaprojektowanych, złożonych układów dichromoforowych zawierających korole ujawnia wiele potencjalnych wyzwań. Synteza pochodnych tetrapiroli i następcza modyfikacja grup znajdujących się na peryferyjnych ich pierścienia umożliwia otrzymywanie nawet bardzo złożonych porfiryńoidów. Umiarkowana stabilność koroli ogranicza jednak liczbę możliwych przekształceń dla bloków budulcowych zawierających ten makrocykl. Alternatywną strategią jest przygotowanie skomplikowanych aldehydów, które po kondensacji z dipiranami dają złożone mieszaniny zawierające docelowe trans-A₂B-korole. Niska rozpuszczalność perylenobisimidu stanowi kolejne wyzwanie syntetyczne. Wprowadzenie całego krótkiego peptydu na jeden z atomów azotu PDI przyczyniłoby się do poprawienia rozpuszczalności, niestety jego obecność może spowodować niepożądaną na tym etapie samoorganizację związku (poprzez tworzenie międzycząsteczkowych wiązań wodorowych). Wytwarzanie agregatów miałoby negatywny wpływ na późniejsze reakcje kondensacji, co z kolei przełożyłoby się niekorzystnie na końcową wydajność. Biorąc pod uwagę złożoność aldehydów zawierających przyłączone poprzez mostek peptydowy PDI (**Rysunek 15**) strategia poprowadzenia jako ostatni krok kondensacji z dipiranami mogłaby się wydawać w tym przypadku nierozsądnym wyborem.

Spostrzeżenia te popchnęły mnie ku podejściu pośredniemu pomiędzy opisanymi strategiami (**Schemat 4**). Zaplanowana i przeprowadzana przeze mnie synteza rozpoczęła się od przygotowania aldehydu o złożoności pozwalającej na wydajne otrzymanie trans-A₂B-korolu podczas kondensacji i następczej hydrolizy. Równoległe postanowiłem zastosować peptydy *N*-zabezpieczone grupą 9-fluorenylometyloksykarbonylowa (Fmoc) i połączyć je z PDI. Strategia ta umożliwiła późniejsze łatwe sprzęgnięcie tych związków poprzez połączenie grupy karboksylowej donora z odbezpieczoną terminalną aminą akceptora. Przeprowadziłem sprzęganie mostków zabezpieczonych Fmoc **39-41** z aminą wywodzącą się od pochodnej PDI **38**, które doprowadziło do otrzymania pożądaných bloków budulcowych **42-44**. Kolejnym krokiem było zdjęcie zabezpieczenia Fmoc poprzez reakcję z piperydyną. Ostatnim i kluczowym etapem było sprzęganie otrzymanych bloków budulcowych w warunkach, które umożliwiały ich wydajne połączenie bez naruszania struktury pierścienia korolu. Finalna reakcja została przeprowadzona z zastosowaniem aktywacji grupy karboksylowej z wykorzystaniem HATU. Sprzęganie z wykorzystaniem takich warunków cechuje wysoka wydajność, krótki czas reakcji oraz brak niepożądaney epimeryzacji.



Schemat 4. Synteza układów dwuchromoforowych **33–35**.

Badania fotofizyczne zostały wykonane w zespole Valentina Vullev'a (University of California, Riverside, USA) i w zespole Harrego Gray'a (California Institute of Technology, Pasadena, USA). W badaniach tych aktywnie uczestniczyłem podczas odbywanego w Kalifornii stażu. Przeprowadziłem tam szereg pomiarów czasowo-rozdzielczych dla otrzymanych kompleksów typu DBA. Wykonane badania pokazały, że zarówno ET i HT przebiegają w skali pikosekundowej. Otrzymane wyniki były podobne dla wszystkich trzech koniugatów (**33-35**), pomimo znacznych różnic w odległości, mierzonej przez wiązania kowalencyjne, znajdujące się między donorem i akceptorem. Znaczna liczba węgli sp^3 pomiędzy chromoforami związku **35** wedle naszej najlepszej wiedzy powinna całkowicie uniemożliwić przeniesienie elektronów. Czasowo-rozdzielcze badania ewolucji absorpcji i emisji udowadniają, że zastąpienie łącznika tetrafenylalaninowego pojedynczą alaniną lub fenyloalaniną nie wpływa zasadniczo na kinetykę ET i HT. Obserwacje te sugerują, że przeniesienie elektronów nie przebiega w tych przypadkach poprzez wiązania kowalencyjne pomiędzy cząsteczką korolu i perylenobisimidu. Wyniki pomiarów wskazują, że przepływ ten musi zachodzić poprzez wewnątrzcząsteczkowe wiązania wodorowe. W przypadku otrzymanych związków, dzięki zastosowaniu elastycznego linkera zbudowanego z aminokwasów, mamy do czynienia z pofałdowaniem struktury kompleksu DBA i ustabilizowanie jej poprzez skomplikowaną sieć wiązań wodorowych (**Rysunek 17**).



Rysunek 17. Geometria związku **35**. Na zielono zaznaczono najkrótszą ścieżkę sprzężenia donor-akceptor.

Analiza widm NMR, dichroizmu kołowego i badań DFT wykazała, że wewnątrzcząsteczkowe wiązania wodorowe zbliżają donor i akceptor, tworząc architekturę „w kształcie skorpiona” (**Rysunek 17**), co odpowiada za niezwykle wysoką szybkość przeniesienia elektronów. Analogiczne zachowanie jest obserwowane w białkach, gdzie wewnątrzcząsteczkowe sieci wiązań wodorowych mogą skracać szlaki sprzężenia elektronów

donor-akceptor dzięki czemu efektywność i szybkość ET zostaje zwiększona. W roztworze barwnika **35** istnieją trzy wewnątrzcząsteczkowe wiązania wodorowe tj. (korol) $\text{NH}\cdots\text{O}=\text{C}-\text{NH}\cdots\text{O}=\text{C}$ (perylenebisimid) (**Rysunek 17**).

Utworzona w roztworach trójwymiarowa struktura zaobserwowana dla tych układów dichromoforowych nie ma precedensu w literaturze. Wynika to m.in. z kluczowości doboru obu chromoforów. Korol, który tworzy wewnątrzcząsteczkowe wiązanie wodorowe z $\text{C}=\text{O}$ pozycjonuje aminokwas lub krótki peptyd nad pierścieniem makrocyclicznym. Z kolei grupa karbonylowa perylenebisimidu tworząc wiązanie wodorowe z $\text{N}-\text{H}$ odpowiada za ułożenie PDI nad alifatycznym łącznikiem.

7.3.4. Podsumowanie

Za swoje najważniejsze osiągnięcie uważam zaprojektowanie, przeprowadzenie efektywnej syntezy oraz zbadanie właściwości fizykochemicznych układów dichromoforowych składających się z korolu, perylenebisimidu i łącznika aminokwasowego lub peptydowego. Wyjaśnienie czynników, które kontrolują szybkość przenoszenia elektronów na duże odległości, pozostaje wielkim wyzwaniem. Częściowo jest to spowodowane złożonością białek i innych struktur makrocząsteczkowych, które pośredniczą w takich procesach. Połączenie korolu z perylenebisimidem poprzez krótkie łączniki peptydowe, tworzy niewielkie biomimetyki, których zbadanie przyczynia się do zrozumienia dynamiki ET i HT w bardziej skomplikowanych układach. Krótkie peptydy, łączące donor i akceptor elektronów są zdolne do wytworzenia wiązań wodorowych, mogących zginać cząsteczkę na kształt fałd, tworząc dodatkowe szlaki dla ultraszybkiego przenoszenia elektronów. Praca ta stanowi nowy paradygmat w projektowaniu wydajnych systemów donorowo-akceptorowych do zastosowań w efektywnym transferze elektronów.

Udowodniłem również, że wybór rozpuszczalnika ma istotny wpływ na rodzaj wiązań wodorowych bis(amido-koroli) zarówno w roztworze, jak i w kryształach. W roztworze wewnątrzcząsteczkowe wiązania wodorowe można rozerwać polarnymi, aprotonowymi rozpuszczalnikami lub wzmocnić heksafluoroizopropanolem. Międzycząsteczkowe wiązania wodorowe z niepolarnymi rozpuszczalnikami i oddziaływania typu $\text{N}-\text{H}\cdots\pi$ stanowią dodatkowe czynniki mające wpływ na ostateczną konformację cząsteczek w kryształach.

Finalnie wykazałem, że krótka odległość pomiędzy resztą amidową a korolem ułatwia tworzenie wewnątrzcząsteczkowych wiązań wodorowych, zarówno w roztworze, jak i w kryształach. Jeśli łącznik jest elastyczny, silne oddziaływanie napędza supramolekularną oligomeryzację w stanie stałym i dimeryzację w roztworze w niepolarnych rozpuszczalnikach. Usunięcie podstawników o znacznej zawadzie sterycznej z pozycji *mezo* 5- i 15- powoduje

zmianę sposobu samoorganizacji. Korol posiadający dwie grupy $-CO_2Me$ tworzy struktury tetrameryczne w stanie stałym. Zmniejszenie swobody łącznika znajdującego się w pozycji *mezo*-10 hamuje procesy agregacji. Wyniki te wyjaśniają rolę podstawników w pozycjach *mezo* 5- i 15- oraz wpływ długości i sztywności linkera między korolem a grupą akceptorową znajdującą się w pozycji *mezo*-10 na tworzone wiązania wodorowego w cząsteczkach. Pozwalają one na projektowanie związków zdolnych do wytwarzania między- lub wewnątrzcząsteczkowych wiązań wodorowych i przewidywanie finalnej struktury otrzymywanych agregatów. Wykazałem również, że analiza DOSY NMR jest bardzo przydatną metodą do badania zjawisk agregacji nawet tak dużych makrocykli jak tetrapirole.

Prowadzone przeze mnie badania nad pochodnymi koroli przyczyniły się to do lepszego zrozumienia zależności między budową koroli, a ich zdolnością do tworzenia uporządkowanych struktur i właściwościami fizykochemicznymi. Realizacja tego projektu pozwoli kolejnym grupom badawczym na zrozumienie fundamentalnych zasad pozwalających na świadome projektowanie nowej generacji nowatorskich samoorganizujących się koroli. Dzięki możliwości precyzyjnego zaprojektowania ich właściwości zapewne znajdą one zastosowanie w technologiach przyszłości.

8. PUBLIKACJE ORYGINALNE

Hydrogen Bonds Involving Cavity NH Protons Drives Supramolecular Oligomerization of Amido-Corroles

Rafał Orłowski,^[a] Mariusz Tasiór,^[a] Olga Staszewska-Krajewska,^[a] Łukasz Dobrzycki,^[b] Wojciech Schilf,^[a] Barbara Ventura,^{*,[c]} Michał K. Cyrański,^{*,[b]} and Daniel T. Gryko^{*,[a]}

In memory of Teodor Silviu Balaban

Abstract: *trans*-A₂B-Corroles with amide substituents at different positions versus the macrocyclic core have been synthesized. Their self-organizing properties have been comprehensively evaluated both in solid-state and in solution. The rigid arrangement of the amide functionality with the corrole ring led to the formation of strong intramolecular interactions and precluded intermolecular interactions. Replacement of sterically hindered C₆F₅ substituents at positions 5 and 15 with smaller electron-withdrawing CO₂Me groups resulted in significant changes in the self-assembly pattern. With these substituents, tetramers formed in a crystalline

state, in which one of the H-pyrrole subunits is out of the corrole plane. This allows the N-H group to form a hydrogen bond with a neighboring carbonyl group of the *n*-butyl amide fragment. DOSY NMR studies showed that amido-corroles bearing the OCH₂CONH*n*Bu motif formed dimers in millimolar solutions in nonpolar solvents and the dimers existed in equilibrium with monomers. However, the corroles possessing *meso*-ester groups did not form dimers in polar tetrahydrofuran. Comprehensive optical studies allowed the absorption and emission features of the monomer corroles to be characterized in dilute solutions.

Introduction

Nature's ability to assemble individual molecules into more complex structures, such as light-harvesting photosynthetic units,^[1] has been the inspiration for many studies. Consequently, porphyrins and other tetrapyrroles that are structurally related to naturally occurring chlorophylls, have been intensively studied for their self-assembly capabilities.^[2–4] On the other hand, scaffolds based on corroles,^[5–8] which are analogues of porphyrins with one less carbon, are still much less studied in this regard. Recent reports have presented only a few cases of self-assembling corroles,^[9] such as corrole–amino acid conjugates,^[10] corrole amphiphilic sodium salts,^[11] as well as corroles bearing PO(OH)₂ functionalities.^[12]

Aromatic amides are intensively explored because they form an amazing variety of discrete architectures such as helices, tapes, and molecular electrets.^[13] With a notable exception of β -sheet foldamers developed by Huc and co-workers,^[14] the

formation of all other architectures rely on hydrogen bonds formed by secondary amides. While analyzing the possibility of self-organization among corroles, we concluded that these macrocycles provide another, completely different, yet even more interesting opportunity. A unique property of free-base corroles is the inherent acidity of the three cavity protons.^[5,15] The inner protons deviate significantly from the plane of the slightly distorted macrocycle, and are available for deprotonation or hydrogen bonding. We envisioned that corroles bearing appropriate functionalities at the periphery of the macrocycle ring would exhibit a tendency towards formation of hydrogen bonds and we very recently confirmed the existence of such an interaction.^[9a] We found that *trans*-A₂B-corroles bearing -OCH₂CONHR substituents at the *ortho*-position of the *meso*-phenyl substituent (Figure 1), undergo different self-organization patterns in the solid state, depending on the nature of the secondary amides.^[9a] The key element of this self-assembly is the hydrogen bond between the internal N-H and either the C=O or pyridine nitrogen atom in the case of a pyridine-substituted amide. Such behavior has never been observed among porphyrins or chlorins.

We believe that the unique mode of hydrogen bonding observed in the corroles described above opens entirely new possibilities for self-assembly as well as for spatial positioning of chromophores, and it would be of general benefit to further study the relationship between the molecular structure of amido-corroles and the arrangement of their aggregates.

The goal of this project was threefold: 1) To investigate the role of substituents in positions 5 and 15 of the corrole core and, in particular, whether contraction of electron-withdrawing groups would alter the aggregation pattern. Recent research has indicated that replacement of sterically hindered penta-

[a] R. Orłowski, Dr. M. Tasiór, Dr. O. Staszewska-Krajewska, Prof. W. Schilf, Prof. D. T. Gryko
Institute of Organic Chemistry PAS
44/52 Kasprzaka str., 01-224 Warsaw (Poland)
E-mail: dtgryko@icho.edu.pl

[b] Dr. Ł. Dobrzycki, Prof. M. K. Cyrański
Faculty of Chemistry, University of Warsaw
Pasteura 1, 02-093 Warsaw (Poland)
E-mail: mkc@chem.uw.edu.pl

[c] Dr. B. Ventura
Istituto ISOF-CNR, Via P. Gobetti 101, 40129 Bologna (Italy)
E-mail: barbara.ventura@isof.cnr.it

Supporting information and the ORCID identification number(s) for the author(s) of this article can be found under <https://doi.org/10.1002/chem.201701674>.

CHEMISTRY

A **European** Journal

Supporting Information

Hydrogen Bonds Involving Cavity NH Protons Drives Supramolecular Oligomerization of Amido-Corroles

Rafał Orłowski,^[a] Mariusz Tasior,^[a] Olga Staszewska-Krajewska,^[a] Łukasz Dobrzycki,^[b]
Wojciech Schilf,^[a] Barbara Ventura,^{*[c]} Michał K. Cyrański,^{*[b]} and Daniel T. Gryko^{*[a]}

chem_201701674_sm_miscellaneous_information.pdf

Author Contributions

R.O. Investigation: Lead; Visualization: Lead; Writing – original draft: Equal

M.T. Conceptualization: Supporting; Investigation: Equal; Supervision: Supporting; Writing – original draft: Supporting; Writing – review & editing: Equal

B.V. Formal analysis: Equal; Investigation: Equal; Visualization: Equal; Writing – original draft: Equal; Writing – review & editing: Equal

O.S. Conceptualization: Supporting; Investigation: Equal; Visualization: Equal

W.S. Writing – review & editing: Equal

M.C. Supervision: Equal; Writing – review & editing: Equal

L.D. Investigation: Equal; Writing – original draft: Equal.

Table of Contents

1. Crystallographic data	S3-S11
2. The diffusion-ordered NMR spectroscopy	S12-S22
3. Absorption and Emission spectroscopy	S23-S25
4. ¹ H NMR spectra for synthesized compounds	S26-S33
5. References	S34

1. Crystallographic data

The X-ray measurement of **9** was performed at 125(2) K on a Bruker D8 Venture Photon100 CMOS diffractometer equipped with a TRIUMPH monochromator and a MoK α fine focus sealed tube ($\lambda=0.71073$ Å). A total of 2030 frames were collected with Bruker APEX2 program.^[1] The frames were integrated with the Bruker SAINT software package^[2] using a narrow-frame algorithm. The integration of the data using a triclinic unit cell yielded a total of 183143 reflections to a maximum θ angle of 25.05° (0.84 Å resolution), of which 22802 were independent (average redundancy 8.032, completeness = 99.8%, $R_{int} = 4.08\%$, $R_{sig} = 2.38\%$) and 17527 (76.87%) were greater than $2\sigma(F^2)$. The final cell constants of $a = 17.480(5)$ Å, $b = 19.775(6)$ Å, $c = 22.254(6)$ Å, $\alpha = 113.331(7)^\circ$, $\beta = 103.102(7)^\circ$, $\gamma = 102.875(7)^\circ$, $V = 6446.(3)$ Å³, are based upon the refinement of the XYZ-centroids of 9665 reflections above $20 \sigma(I)$ with $6.166^\circ < 2\theta < 50.68^\circ$. Data were corrected for absorption effects using the multi-scan method (SADABS).^[3] The ratio of minimum to maximum apparent transmission was 0.952. The calculated minimum and maximum transmission coefficients (based on crystal size) are 0.9180 and 0.9730.

The structure was solved and refined using SHELXTL Software Package^[4] using the space group $P-1$, with $Z = 4$ for the formula unit, C₇₁H₆₇Cl₃N₁₀O₁₂. The final anisotropic full-matrix least-squares refinement on F^2 with 1857 variables converged at $R1 = 4.79\%$, for the observed data and $wR2 = 14.77\%$ for all data. The goodness-of-fit was 1.047. The largest peak in the final difference electron density synthesis was 0.496 e⁻/Å³ and the largest hole was -0.656 e⁻/Å³ with an RMS deviation of 0.055 e⁻/Å³. On the basis of the final model, the calculated density was 1.400 g/cm³ and $F(000)$, 2840 e⁻.

The investigated crystal contains in the asymmetric unit four corrole molecules and two chloroform species. Terminal -CH₂CH₃ part of aliphatic chain in the two corrole molecules are disordered over two sites. In the molecule D occupancy ratio of corresponding disordered fragments was refined to the value of 0.55(1):0.45(1), whereas in the molecule C this ratio was kept fixed at the level of 0.9:0.1. In addition two chloroform molecules are disordered with non-refined occupancy ratio yielding to

0.975:0.025 and 0.95:0.05. To preserve reasonable geometry of disordered moieties additional geometry restraints were used.

Checkcif report suggest additional B centering of the unit cell indicated as Alert type B what is due to smaller intensity of halve of the reflections. This, in respect of triclinic symmetry of the lattice would lead to halving of the unit cell volume and averaging out of the structure causing additional disorder. Thus the final refinement was based on the all stronger and weaker reflections giving the superstructure.

All non-hydrogen atoms were refined anisotropically, atoms of disordered fragments with occupancy equal to 0.1 or less. Most of hydrogen atoms were placed in calculated positions and refined within the riding model. Twenty hydrogen atoms of N-H groups engaged in hydrogen bonds were refined. Temperature factors of these H atoms were also refined. The temperature factors of all other hydrogen atoms were not refined and were set to be equal to either 1.2 or 1.5 times larger than U_{eq} of the corresponding heavy atom. The atomic scattering factors were taken from the International Tables.^[5]

All the crystal data and structure refinement parameters are presented in Table S1. Numbering scheme and atomic displacement parameters, for each molecule separately, are presented in Figure S1 a), b), c) and d). Packing diagram of **9** is presented in Figure S2 a).

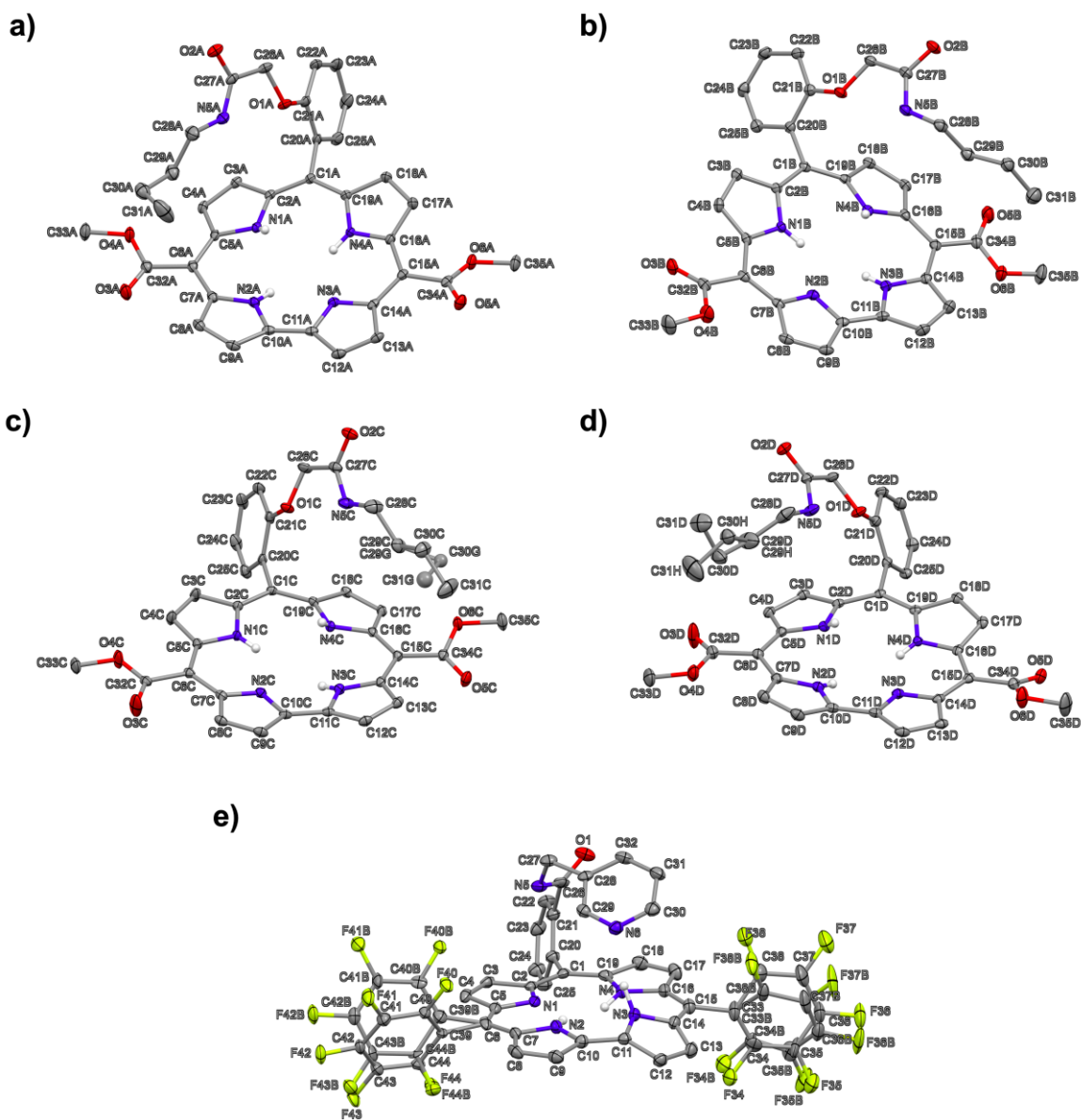


Figure S1. Numbering scheme and atomic displacement parameters for **9** – molecule **A a), B b), C c), D d)** and for **16 e)**. Thermal ellipsoid plot drawn at the 50% probability level.

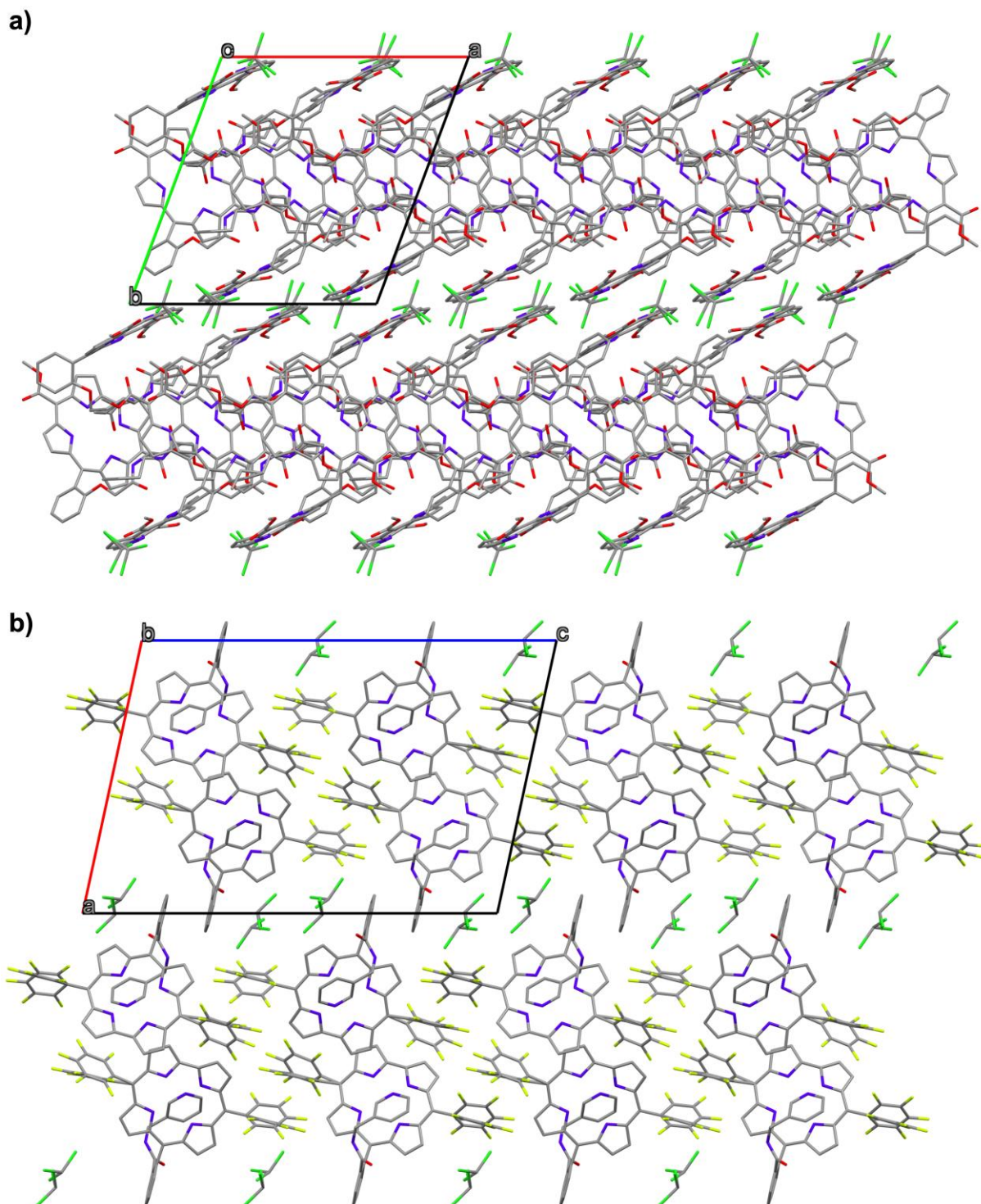


Figure S2. Packing diagram of **9** – view along [001] direction **a)** and **16** - view along [010] direction **b)**.

Detailed parameters of hydrogen bonds for each molecule in the crystal of **9** are given in Table S1.

To illustrate the uniqueness of this compound, comparisons with other known cases of meso-ester corroles reported by Balaban and co-workers^[6] should be conducted. Due to the presence of an aryl group at the 10-*meso* position and low steric hindrance of the 4-methoxy group located at the phenyl substituent, 5,15-diethoxycarbonyl-10-(4-methoxyphenyl)corrole (**18**) can be considered as a model compound suitable for such comparisons (Table S1). The χ_1 and χ_2 torsion angles of **9** were closer to either 0° or 180° (indicating coplanarity of these groups with corrole moiety) due to the decreased steric hindrance, however, in the model compound **18** and all the other reported meso-ester corroles, the two carbonyl groups were tilted towards the upper part of corrole. They were also involved in the formation of strong hydrogen bonds between the carbonyl oxygen and corrole core, forming dimers. This result was different from compound **9**, where the methyl ester groups did not participate in the formation of any strong hydrogen bonds. Moreover, the correlation between χ_3 and the distance between the $\text{NH}\cdots\text{N}'$ should be taken into account. The increasing strength of the π - π interaction of adjacent corrole rings, which is reflected in a decrease in intermolecular distances, imposed a perpendicular arrangement of the 10-*meso* phenyl substituent. The intriguing conformation of the 5,15-*meso*-ester substituents should be emphasized. Within the assembled units, they adopted two out of three possible arrangements, with both methyl groups tilted towards the direct pyrrole-pyrrole bond or facing the methine bridge. The *trans*-isomers were not present in the crystal structure. Furthermore, the OCH_2CONH group at the *ortho* position of the *meso*-phenyl substituent is positioned on the left or right face of corrole with the absolute value of the torsion angles χ_3 varying between 62.4° and 76.0° (Table S1). The angle χ_3 obtained for **9** indicates that analyzed molecules are enantiomers. Because the structure is centrosymmetric the same amount of left and right-handed stereoisomers is present in the unit cell, of course. Nevertheless, all the molecules constituting the asymmetric part of the unit cell of the crystal structure of **9** can be overlaid, but every second inverted – all the fifteen atoms of the inner

corrole ring (eleven C and four N atoms) were fitted using LSQ procedure.^[7] The overlay is presented in Figure S3a with different colors introduced to differentiate each molecule. As it can be seen the corrole moieties almost ideally match, including positions of pyrrole H atoms, with some deviations observed for χ_3 angles only. Because all molecules have the same chirality, all these angle values from the Table S1 are positive for the overlaid molecules.

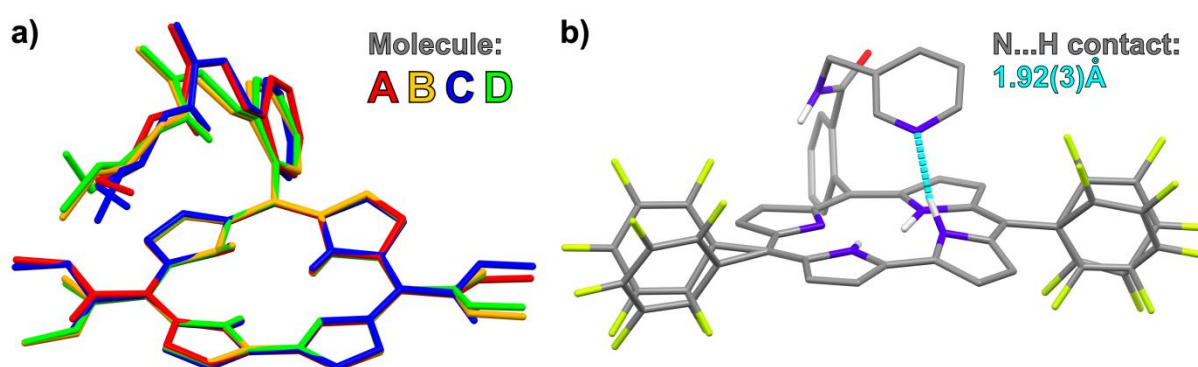


Figure S3. a) Overlay of the molecules of **9**; b) molecular structure of **16** presenting interaction of the pyridine nitrogen atom with the H atom of the corrole ring.

Table S1. Hydrogen bonds (HB) and selected geometrical parameters for molecules in **9** compared with corrole **18** (structure JUHROV).^[14]

	Carbonyl oxygen hydrogen bond length [Å]		Direct core to core HB length [Å]	Direct core to core HB angle [°]	χ_1 [°]	χ_2 [°]	χ_3 [°]
9A	$\text{CO}_A \cdots \text{HN}_D$ 2.07(3)	$\text{CO}_A \cdots \text{HNCO}_D$ 2.48(3)	$\text{NH}_A \cdots \text{N}_A$ 2.63(3)	$\text{NH}_A \cdots \text{N}_A$ 137(2)	179.5	157.1	73.4
9B	$\text{CO}_B \cdots \text{HN}_A$ 2.07(3)	$\text{CO}_B \cdots \text{HNCO}_A$ 2.67(3)	$\text{NH}_B \cdots \text{N}_B$ 2.97(3)	$\text{NH}_B \cdots \text{N}_B$ 142(2)	3.6	14.8	-62.4
9C	$\text{CO}_C \cdots \text{HN}_B$ 2.08(2)	$\text{CO}_C \cdots \text{HNCO}_B$ 2.55(3)	$\text{NH}_C \cdots \text{N}_C$ 2.58(2)	$\text{NH}_C \cdots \text{N}_C$ 133(2)	-167.5	178.1	-76.0
9D	$\text{CO}_D \cdots \text{HN}_C$ 2.08(2)	$\text{CO}_D \cdots \text{HNCO}_C$ 2.51(3)	$\text{NH}_D \cdots \text{N}_D$ 2.91(3)	$\text{NH}_D \cdots \text{N}_D$ 140(2)	3.0	-21.9	66.4
18	EtOCO \cdots HN' 1.99		$\text{NH} \cdots \text{N}'$ 2.36	$\text{NH} \cdots \text{N}'$ 141	-10.0	24.0	60.7

The X-ray measurement of **16** was performed at 125(2) K on a Bruker D8 Venture Photon100 CMOS diffractometer equipped with a TRIUMPH monochromator and a MoK α fine focus sealed tube ($\lambda=0.71073$ Å). A total of 1740 frames were collected with Bruker APEX2 program.^[1] The frames were integrated with the Bruker SAINT software package^[2] using a narrow-frame algorithm. The integration of the data using a monoclinic unit cell yielded a total of 7288 reflections to a maximum θ angle of 25.05° (0.84 Å resolution), of which 7288 were independent (average redundancy 1.000, completeness = 98.7%, $R_{sig} = 6.52\%$) and 5828 (79.97%) were greater than $2\sigma(F^2)$. The final cell constants of $a=19.2301(11)$ Å, $b=7.7079(4)$ Å, $c=28.5647(16)$ Å, $\beta=102.2505(16)^\circ$, $V=4137.6(4)$ Å³, are based upon the refinement of the XYZ-centroids of 9051 reflections above $20 \sigma(I)$ with $6.009^\circ < 2\theta < 48.20^\circ$. Data were corrected for absorption effects using the multi-scan method (TWINABS).^[3] The ratio of minimum to maximum apparent transmission was 0.740. The calculated minimum and maximum transmission coefficients (based on crystal size) are 0.876 and 0.991. The structure was solved and refined using SHELXTL Software Package^[4] using the space group $P2_1/c$, with $Z = 4$ for the formula unit, C₄₅H₂₃Cl₃F₁₀N₆O. The final anisotropic full-matrix least-squares refinement on F^2 with 829 variables converged at $R1 = 6.98\%$, for the observed data and $wR2 = 18.08\%$ for all data. The goodness-of-fit was 1.082. The largest peak in the final difference electron density synthesis was 0.356 e⁻/Å³ and the largest hole was -0.293 e⁻/Å³ with an RMS deviation of 0.074 e⁻/Å³. On the basis of the final model, the calculated density was 1.541 g/cm³ and $F(000)$, 1936 e⁻.

The investigated crystal was twinned and the data integration and scaling was based on two twin components. The structure refinement was performed on unmerged reflections data in HKLF5 format giving ratio of twin fractions equal to 0.535(2):0.465(2).

The structure contains CHCl₃ solvent molecule disordered over two sites with refined occupancy ratio equal to 0.620(3):0.380(3). This effect is associated with disorder of two F-substituted phenyl rings in the **16** molecule [see Figure S1 e)]. These phenyl rings are also disordered over two position with refined occupancy ratio yielding

S9

0.620(3):0.380(3). To preserve reasonable geometry of disordered moieties additional geometry restraints were used.

All non-hydrogen atoms were refined anisotropically. Most of hydrogen atoms were placed in calculated positions and refined within the riding model. Four hydrogen atoms of N-H groups engaged in hydrogen bonds were refined, however with restrained N-H distances to be close to 1Å. Temperature factors of three of these H atoms were refined. The temperature factors of all other hydrogen atoms were not refined and were set to be equal to either 1.2 or 1.5 times larger than U_{eq} of the corresponding heavy atom. The atomic scattering factors were taken from the International Tables.^[5]

All the crystal data and structure refinement parameters are presented in Table S1. Numbering scheme and atomic displacement parameters are presented in Figure S1 e). Packing diagram of **16** is presented in Figure S2 b).

Table S2. Crystal data and structure refinement parameters for **9** and **16**.

Identification code	9	16
Formula	C ₇₁ H ₆₇ Cl ₃ N ₁₀ O ₁₂	C ₄₅ H ₂₃ Cl ₃ F ₁₀ N ₆ O
M _x / g·mol ⁻¹	1358.69	960.04
T/ K	125(2)	130(2)
λ/ Å	0.71073	0.71073
Crystal size/ mm	0.127×0.130×0.404	0.028×0.170×0.437
Space group	P -1	P2 ₁ /c
Unit cell dimensions	a = 17.480(5) Å c = 22.254(6) Å b = 19.775(6) Å α = 113.331(7)° β = 103.102(7)° γ = 102.875(7)°	a = 19.2301(11) Å b = 7.7079(4) Å c = 28.5647(16) Å β = 102.2505(16)°
V/ Å ³ , Z	6446.(3), 4	4137.6(4), 4
D _x / g·cm ⁻³	1.400	1.541
μ/ mm ⁻¹	0.216	0.312
F(000)	2840	1936
θ _{min} , θ _{max}	2.89, 25.05°	2.89, 25.05°
Index ranges	-20 ≤ h ≤ 20 -23 ≤ k ≤ 23 -26 ≤ l ≤ 26	-22 ≤ h ≤ 22 0 ≤ k ≤ 9 0 ≤ l ≤ 33
Reflections	183143/ 22802	62303/ 7288

collected/ Independent	($R_{int} = 0.0408$)	($R_{int} = 0.1265$)
Completeness	99.8%	98.7%
Absorption correction	multi-scan	multi-scan
T_{max}, T_{min}	0.973, 0.918	0.9910, 0.8760
Refinement method	Full-matrix LSQ on F^2	Full-matrix LSQ on F^2
Data / restraints / parameters	22802 / 33 / 1857	7288 / 138 / 829
Goof on F^2	1.047	1.082
Final R indices	17527 data; $>2\sigma(I)$ $R1 = 0.0479$, $wR2 =$ 0.1298 all data $R1 = 0.0670$, $wR2 =$ 0.1477	5828 data; $>2\sigma(I)$ $R1 = 0.0698$, $wR2 =$ 0.1658 all data $R1 = 0.0933$, $wR2 =$ 0.1808
Extinction coefficient	0.0002(1)	0.0092(11)
ρ_{max}, ρ_{min}	0.496, -0.656 eÅ ⁻³	0.356, -0.293 eÅ ⁻³

2. The diffusion-ordered NMR spectroscopy

The relationship between the diffusion coefficient and molecular weight can be determined in various ways, which are based on equation $D=K*MW^\alpha$, wherein K and α are determined for each solvent using model compounds^[8] or by applying internal reference substances.^[9] The lowest estimation error of 9% was declared in Neufeld-Stalke's method. In this approach, an external reference is used, which eliminates almost all instrumental errors and viscosity variations. Moreover, in this method, it is also possible to use the solvent as the reference.

For the investigated corroles, both methods have their advantages and disadvantages. The Evan-Morris method seems to be more effective for bigger compounds than is the Neufeld-Stalke approach, but does not consider viscosity changes and molecular shapes, and was established based on a limited number of model compounds. An error in molecular weight determination by this method did not exceeded 30% for 44 model compounds studied in 5 different solvents. The Neufeld-Stalke method exploits external references and takes into account molecular shape with three different classifications (spheres, ellipsoids, and discs). The disadvantage of this method, from our point of view, is low molecular weight of model compounds, which only in two cases exceeded 600 Da. This lack of data with large molecules can hamper the measurement's accuracy for compounds with higher mass.

¹H DOSY NMR measurements were also performed for compounds **6** and **9**. The presence of polar methyl ester groups on the 5 and 15 *meso* positions made their solubility in non-polar media too low to conduct the experiments in toluene, hence we change the solvent to THF (Tables S6 – S7, ESI). Since the molecular weights of corroles **6** and **9** were close to 600, the Neufeld-Stalke method could also be applied (Table S8 – S9, ESI), with shape approximations based on two models - *DSE* (dissipated spheres and ellipsoids) and *merge* (with the calibration curves averaged from all three shape classifications).

Relative diffusion constants for the Evans-Morris model were calculated according to the Equation S1.

$$\frac{D_{tol,dil}}{D_{tol}} = \frac{D_{x,rel}}{D_x}$$

Equation S1. $D_{tol,dil}$ - diffusion coefficient for toluene in diluted probe; D_{tol} - diffusion coefficient for toluene in given sample; $D_{x,rel}$ – relative diffusion coefficient for given solute; D_x – diffusion coefficient for given solute

Table S3. The Evan-Morris method measurement data for corrole 1 (MW=795 Da) in toluene.

Sample concentration	1 mM	2 mM	8 mM	19 mM	38 mM
Sample weight	0.5 mg	1 mg	3 mg	7.5 mg	15 mg
$D_{tol} [10^{-10}m^2 s^{-1}]$	20.97	20.95	20.79	20.35	20.02
$D_x [10^{-10}m^2 s^{-1}]$	6.02	5.99	6.01	5.85	5.72
$D_{x,rel} [10^{-10}m^2 s^{-1}]$	6.02	6.00	6.06	6.03	5.99
M_{det} [Da]	921	928	907	917	931

Table S4. The Evan-Morris method measurement data for corrole 2 (MW=836 Da) in toluene.

Sample concentration	1 mM	2 mM	9 mM	18 mM	36 mM	65 mM
Sample weight	0.5 mg	1 mg	3.7 mg	7.5 mg	15 mg	27 mg
$D_{tol} [10^{-10}m^2 s^{-1}]$	21.19	21.01	20.90	20.49	20.22	19.26
$D_x [10^{-10}m^2 s^{-1}]$	6.16	5.97	5.79	5.52	5.22	4.92
$D_{x,rel} [10^{-10}m^2 s^{-1}]$	6.16	6.02	5.87	5.71	5.47	5.41
M_{det} [Da]	875	921	974	1036	1140	1169

Table S5. Reverse calculations based on the Evan-Morris model for compound **2**. Values given in bold represents the lowest error for given concentration. $MW_{err}=[1-MW_{det}/MW]*100\%$, where MW_{det} is the experimentally determined and MW is the calculated molecular weight.

	M_{det}	Calculations error [%]					
		1 mM	2 mM	9 mM	18 mM	36 mM	65 mM
MW = 835 Da	875	5	5	13	19	25	30
1.1*MW (919 Da)	921	10	0	8	15	21	26
1.2*MW (1002 Da)	974	17	6	3	10	17	22
1.3*MW (1086 Da)	1036	24	13	3	5	11	17
1.4*MW (1169 Da)	1140	37	24	14	5	2	9
1.5*MW (1253 Da)	1169	40	27	17	8	0	7

Table S6. The Evan-Morris method measurement data for corrole **6** (MW=579 Da) in THF.

Sample concentration	2 mM	3 mM	12 mM	24 mM	35 mM
Sample weight	0.5 mg	1 mg	3.5 mg	7 mg	10 mg
$D_{THF}[10^{-10}m^2 s^{-1}]$	25.48	25.42	25.07	24.33	23.67
$D_x[10^{-10}m^2 s^{-1}]$	7.62	7.59	7.43	7.21	6.84
$D_{x,rel}[10^{-10}m^2 s^{-1}]$	7.62	7.61	7.55	7.55	7.36
M_{det} [Da]	774	776	790	790	836

Table S7. The Evan-Morris method measurement data for corrole **9** (MW=620 Da) in THF.

Sample concentration	2 mM	3 mM	12 mM	24 mM	48 mM
Sample weight	0.5 mg	1 mg	3.7 mg	7.5 mg	15 mg
D_{THF} [$10^{-10}m^2 s^{-1}$]	25.65	25.73	25.18	24.76	23.94
D_x [$10^{-10}m^2 s^{-1}$]	7.53	7.57	7.28	7.08	6.74
$D_{x,rel}$ [$10^{-10}m^2 s^{-1}$]	7.53	7.55	7.42	7.33	7.22
M_{det} [Da]	795	790	821	844	873

Table S8. The Neufeld-Stalke method measurement data for corrole **6** (MW=579 Da) in THF; comparison with data obtained *via* the Evan-Morris model. Values in brackets are the calculation errors.

Sample concentration	2 mM	3 mM	12 mM	24 mM	35 mM
Sample weight	0.5 mg	1 mg	3.5 mg	7 mg	10 mg
DSE [Da]	609 (5)	611(6)	618(7)	619(7)	646(12)
$Merge$ [Da]	596(3)	597(3)	604(5)	604(5)	630(9)
M_{det} [Da]	774 (34)	776 (34)	790 (37)	790 (37)	836 (45)

Table S9. The Neufeld-Stalke method measurement data for corrole **9** (MW=620 Da) in THF; comparison with data obtained *via* the Evan-Morris model. Values in brackets are the calculation errors.

Sample concentration	2 mM	3 mM	12 mM	24 mM	48 mM
Sample weight	0.5 mg	1 mg	3.7 mg	7.5 mg	15 mg
DSE [Da]	629 (2)	626 (1)	645 (4)	658 (6)	675 (9)
$Merge$ [Da]	614 (1)	612 (1)	629 (2)	641 (4)	658 (6)
M_{det} [Da]	795 (28)	790 (28)	821 (33)	844 (36)	873 (41)

Table S10. Comparison between the measurements' results for corrole **2** (MW=836 Da) in THF and toluene *via* the Evan-Morris method.

Sample weight	1 mg	15 mg
THF; M_{det} [Da]	1013	1066
Toluene; M_{det} [Da]	921	1140

Table S11. The Evan-Morris method measurement data for corrole **16** (MW=841 Da) in toluene.

Sample concentration	1 mM	2 mM	15 mM	30 mM
Sample weight	0.5 mg	1 mg	6.2 mg	12.5 mg
D_{tol} [$10^{-10}m^2 s^{-1}$]	21.35	21.03	20.58	20.09
D_x [$10^{-10}m^2 s^{-1}$]	6.24	6.09	5.90	5.73
$D_{x,rel}$ [$10^{-10}m^2 s^{-1}$]	6.24	6.18	6.12	6.09
M_{det} [Da]	851	869	888	898

Table S12. Morris method measurement data for corrole **17** (MW=822 Da) in toluene.

Sample concentration	1 mM	2 mM	17 mM	37 mM
Sample weight	0.5 mg	1 mg	7 mg	15 mg
D_{tol} [$10^{-10}m^2 s^{-1}$]	21.14	21.22	20.37	20.01
D_x [$10^{-10}m^2 s^{-1}$]	6.21	6.19	5.85	5.78
$D_{x,rel}$ [$10^{-10}m^2 s^{-1}$]	6.21	6.17	6.07	6.11
M_{det} [Da]	860	872	904	891

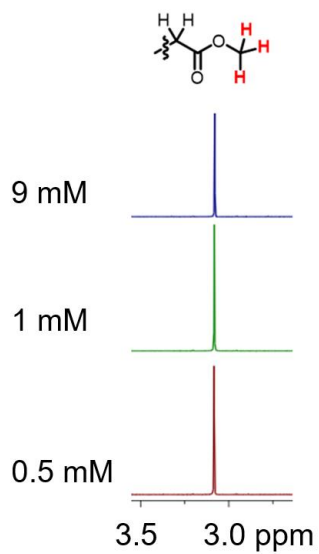


Figure S4. Concentration-dependent ^1H NMR spectra of corrole **1** in toluene at 25 $^\circ\text{C}$.

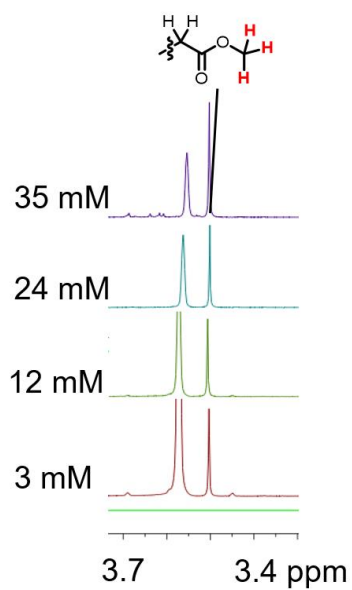


Figure S5. Concentration-dependent ^1H NMR spectra of corrole **6** in THF at 25 $^\circ\text{C}$.

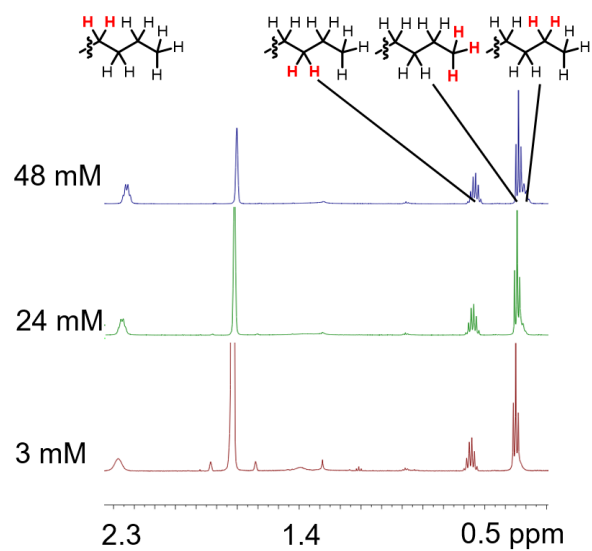


Figure S6. Concentration-dependent ^1H NMR spectra of corrole **9** in THF at 25 $^\circ\text{C}$.

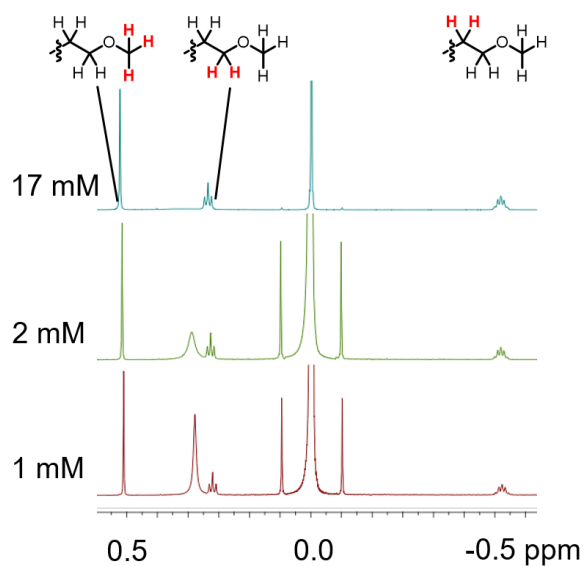


Figure S7. Concentration-dependent ^1H NMR spectra of corrole **16** in toluene at 25 $^\circ\text{C}$.

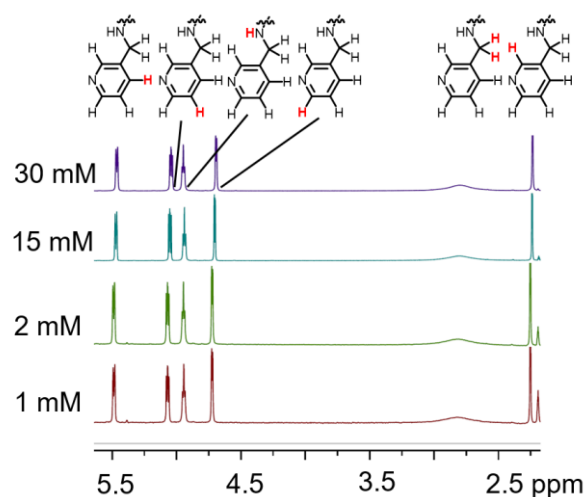


Figure S8. Concentration-dependent ^1H NMR spectra of corrole **17** in toluene at 25 $^\circ\text{C}$.

The dimerization constant of corrole **2** was calculated according to the Equation S2. Values of a and b were determined from DOSY NMR data.

$$K_a = \frac{b(b+1)}{C_o a^2}$$

Equation S2. K_a - dimerization constant; C_o - initial concentration; a – mole fraction of monomers; b – mole fraction of dimers.

Table S13. The dimerization constant of corrole **2** calculated for each concentration.

Sample concentration [mM]	1	2	9	18	36	65
K_a [mol^{-1}]	45.3	58.3	31.3	28.6	34.2	23.9

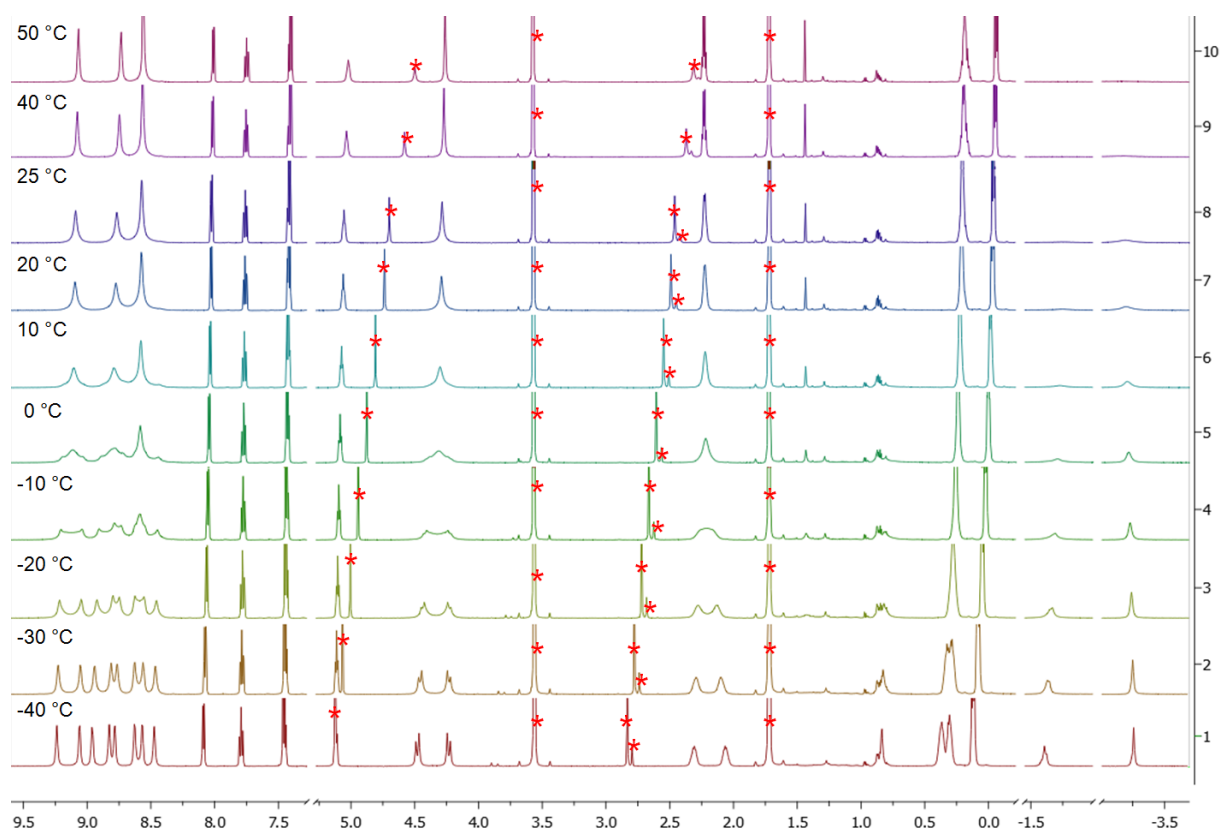


Figure S9. The temperature dependent ^1H NMR spectrum of **2** in THF. Solvent residual signals and impurities are marked with * symbol.

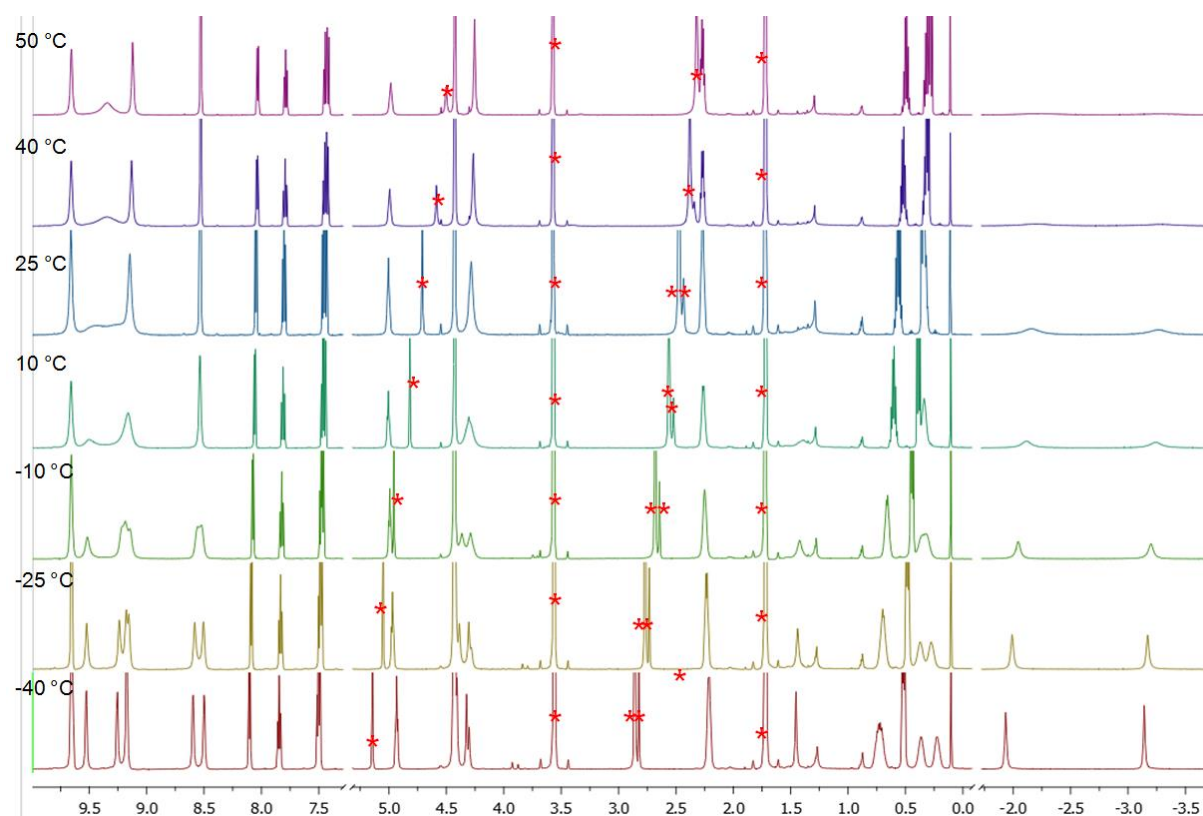


Figure S10. The temperature dependent ¹H NMR spectrum of **9** in THF. Solvent residual signals and impurities are marked with * symbol.

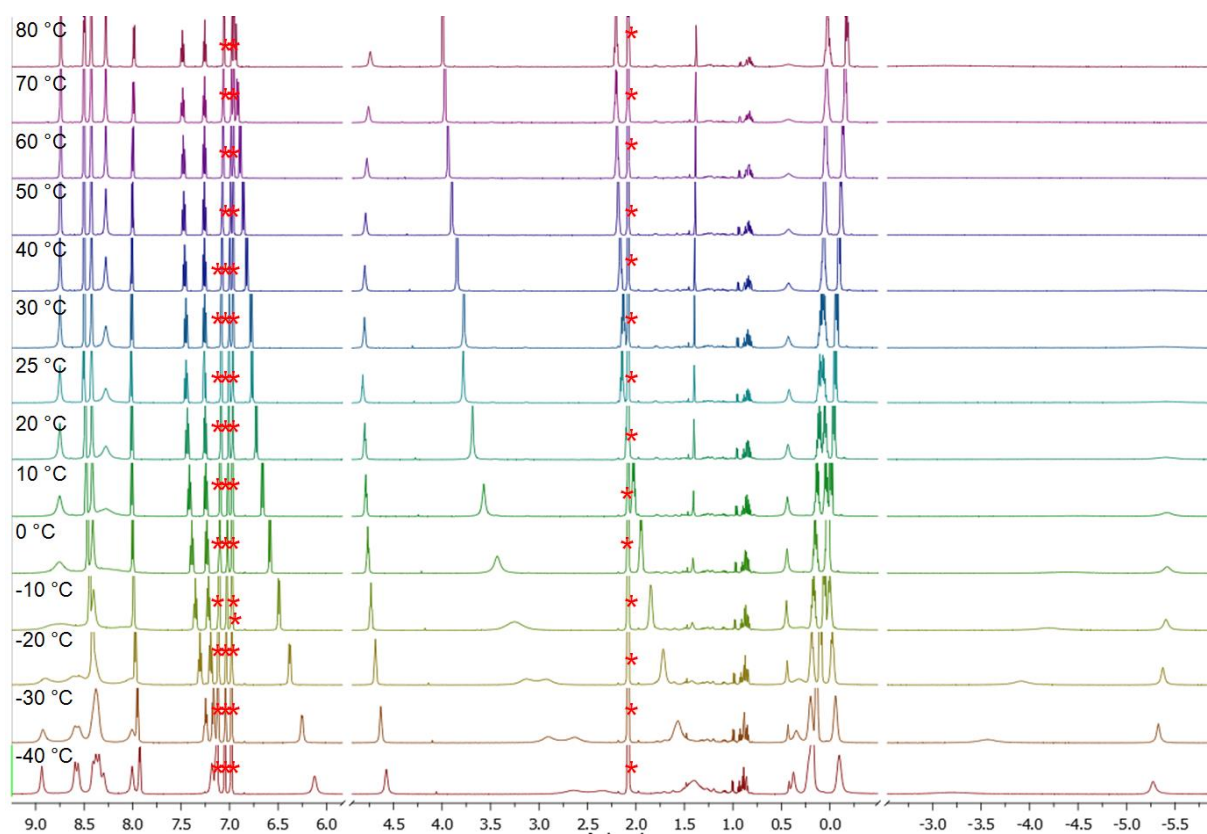


Figure S11. The temperature dependent ¹H NMR spectrum of **2** in toluene. Solvent residual signals are marked with * symbol.

3. Absorption and Emission spectroscopy

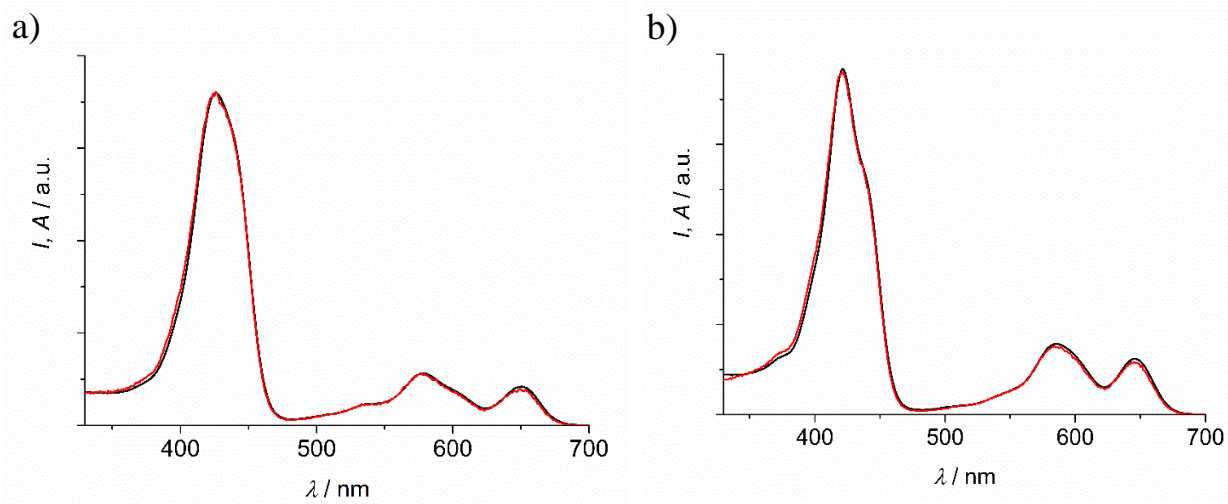


Figure S12. Excitation spectra (red) and arbitrarily scaled absorption spectra (black) of a) **9** and b) **10** in TOL. $\lambda_{\text{em}} = 720$ nm.

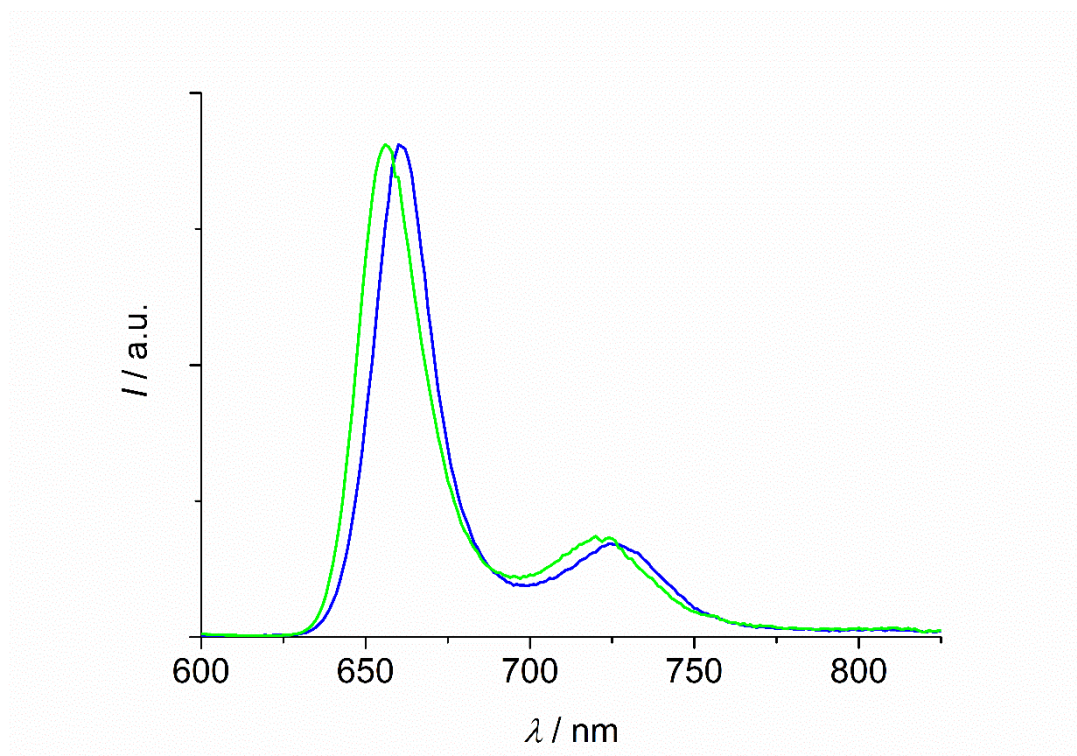


Figure S13. Normalized corrected emission spectra of **9** (blue) and **10** (green) in TOL glassy matrices at 77 K. $\lambda_{\text{exc}} = 580$ nm.

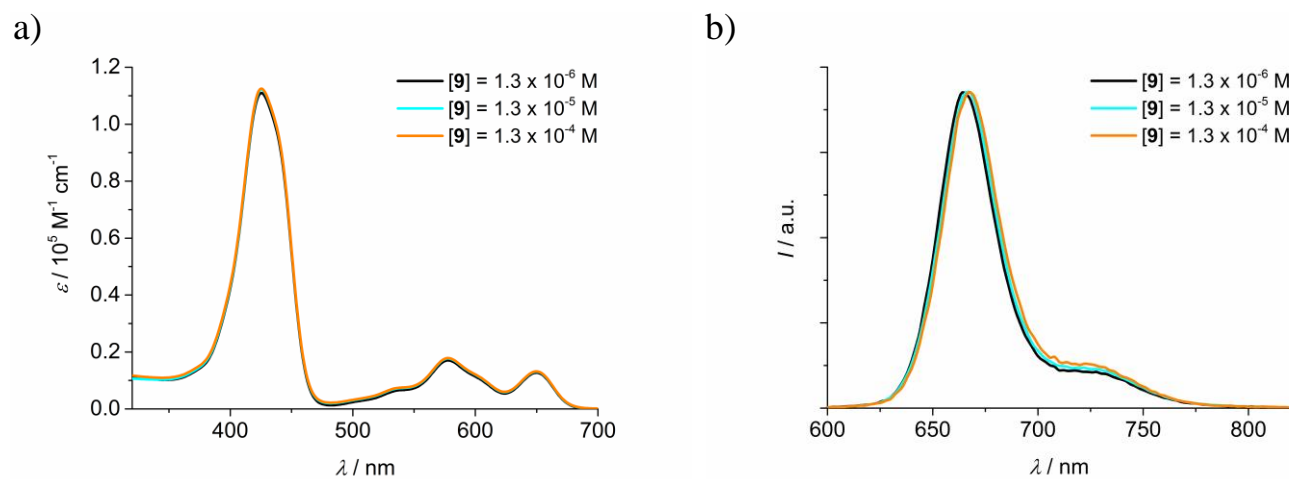


Figure S14. Absorption a) and normalized emission b) spectra of **9** in TOL at the indicated concentrations. $\lambda_{\text{exc}} = 580$ nm.

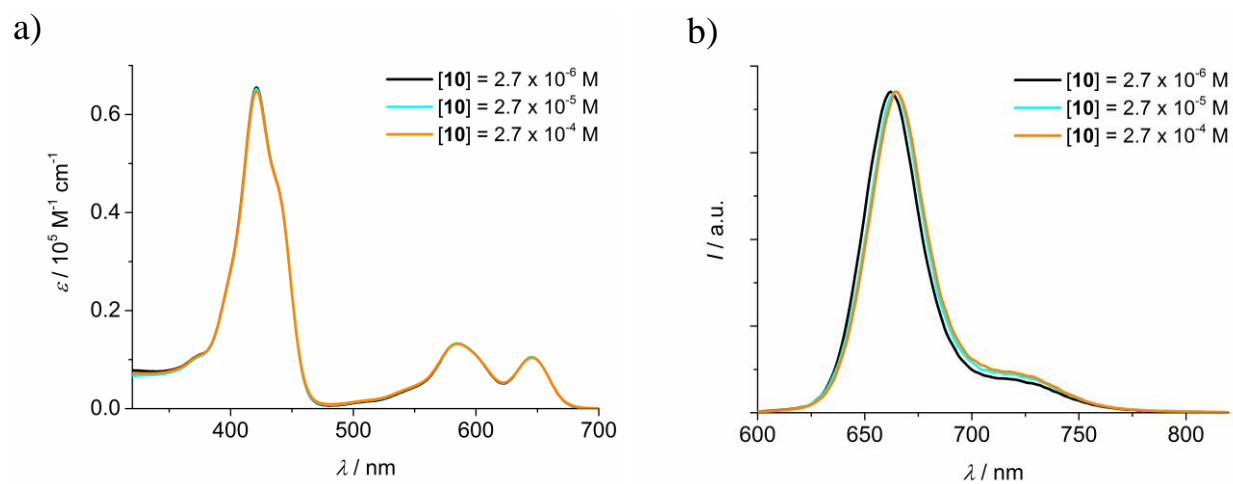
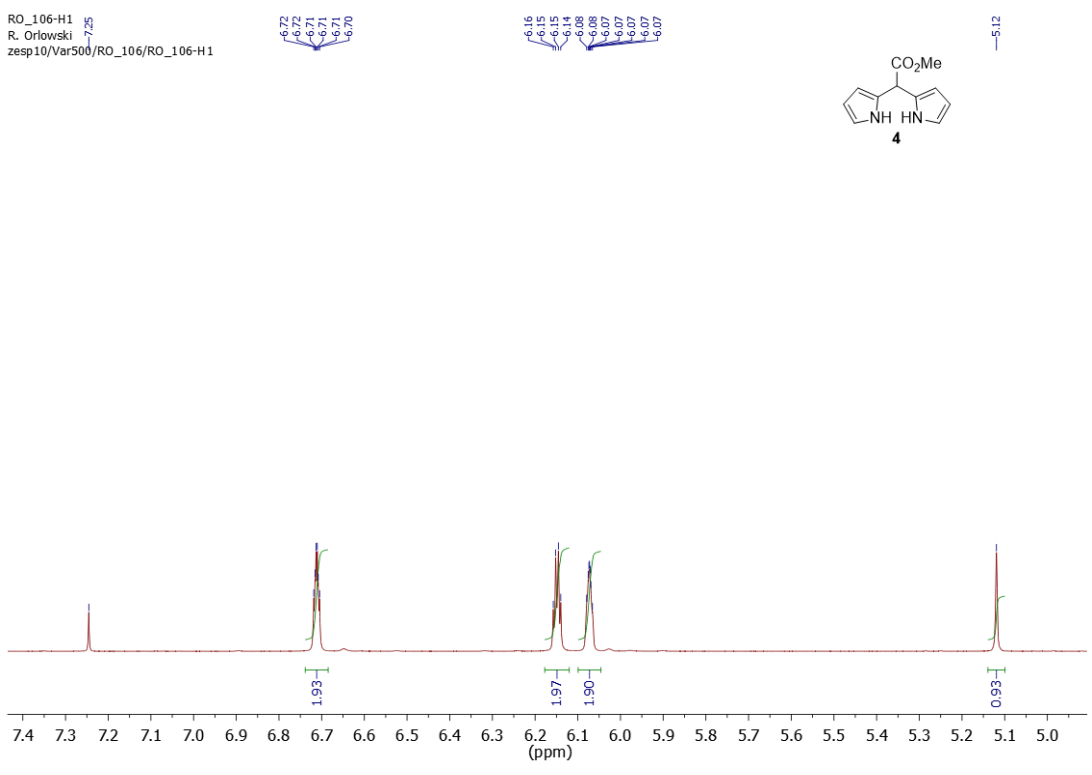
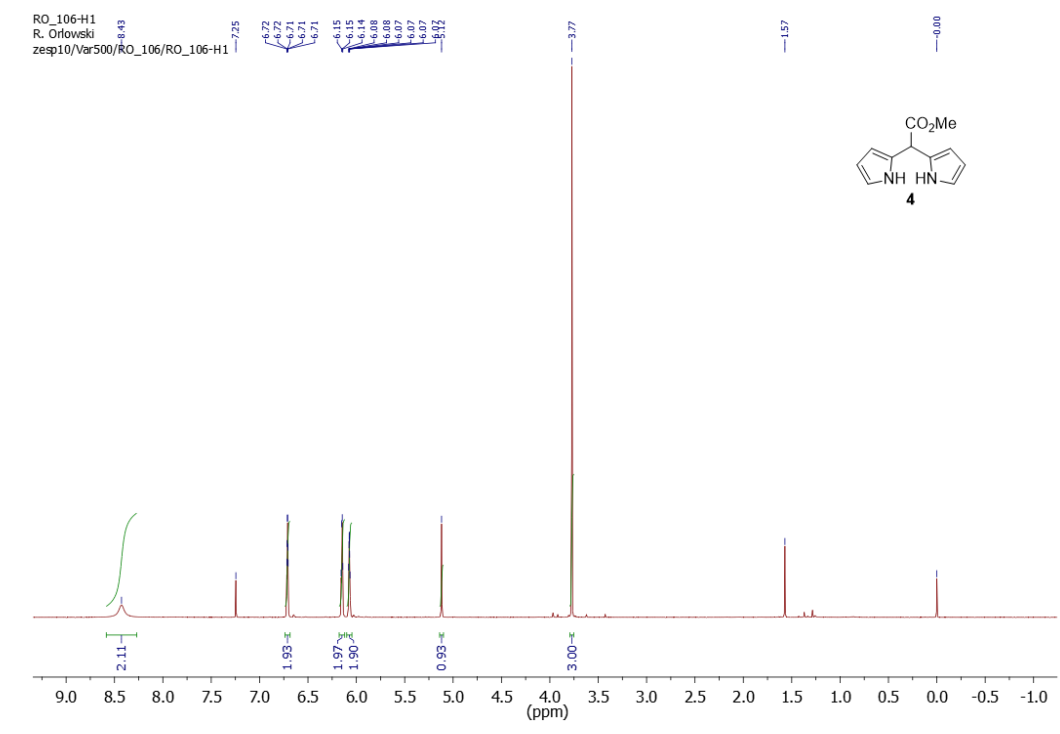


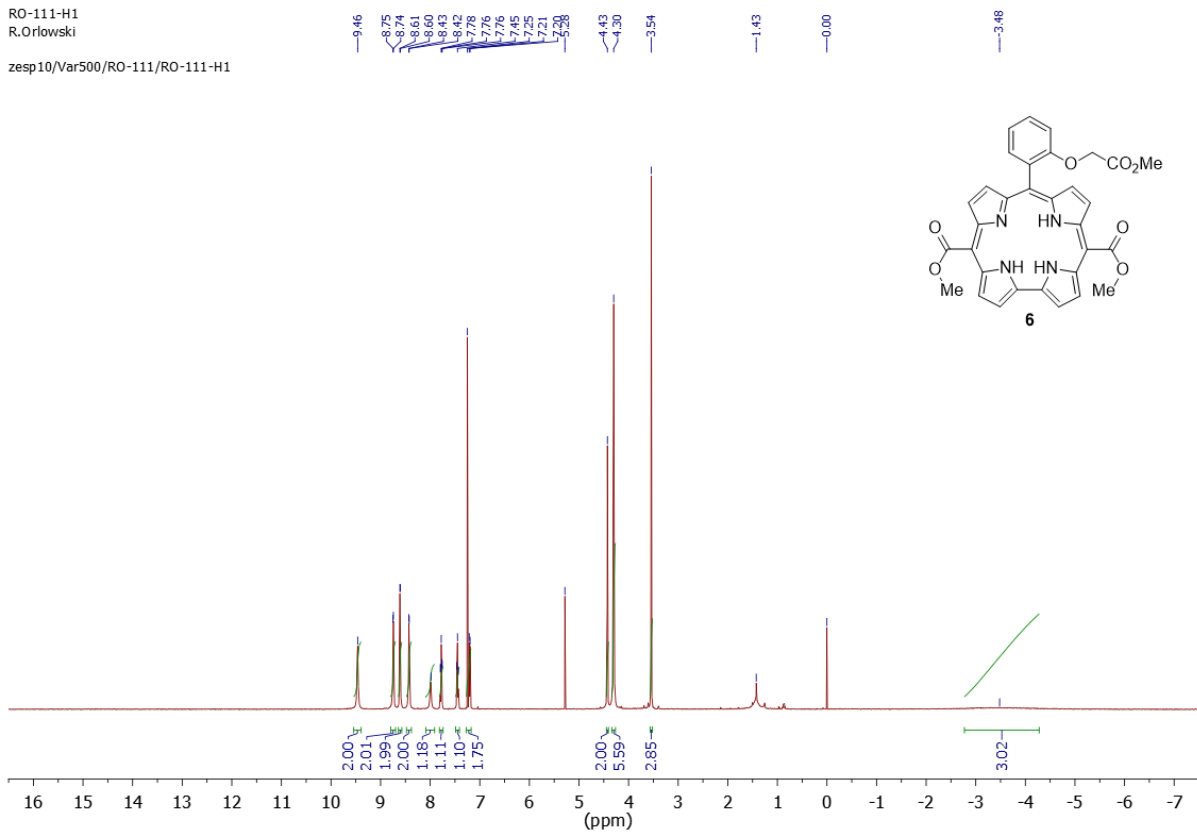
Figure S15. Absorption a) and normalized emission b) spectra of **10** in TOL at the indicated concentrations. $\lambda_{\text{exc}} = 580 \text{ nm}$.

4. ¹H NMR spectra for synthesized compounds



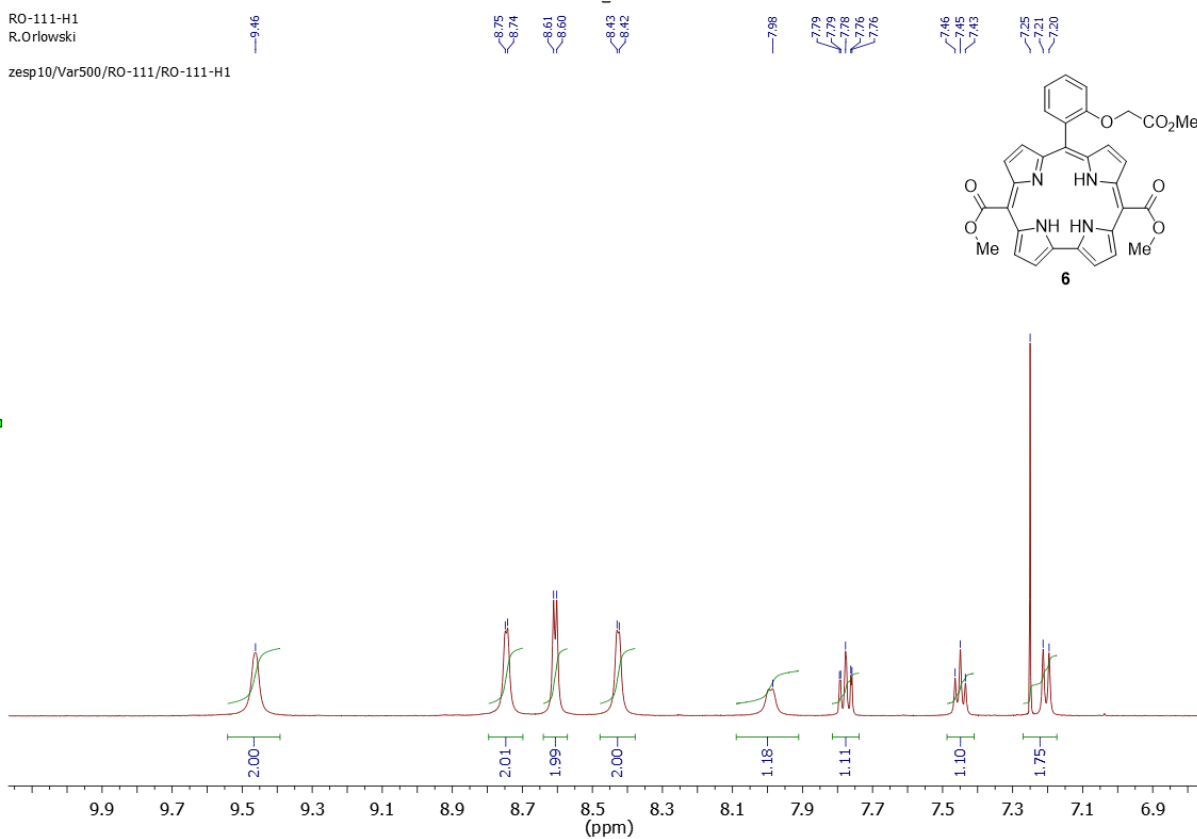
RO-111-H1
R.Orlowski

zesp10/Var500/RO-111/RO-111-H1

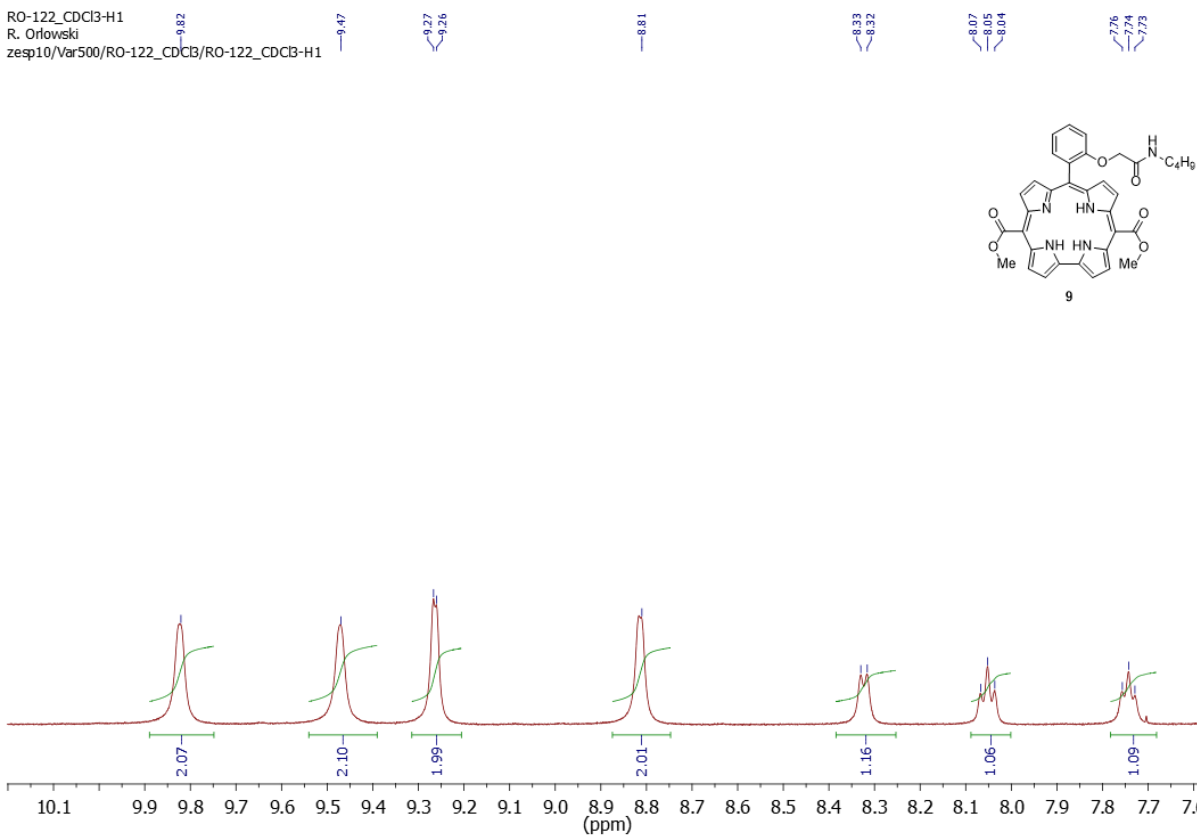
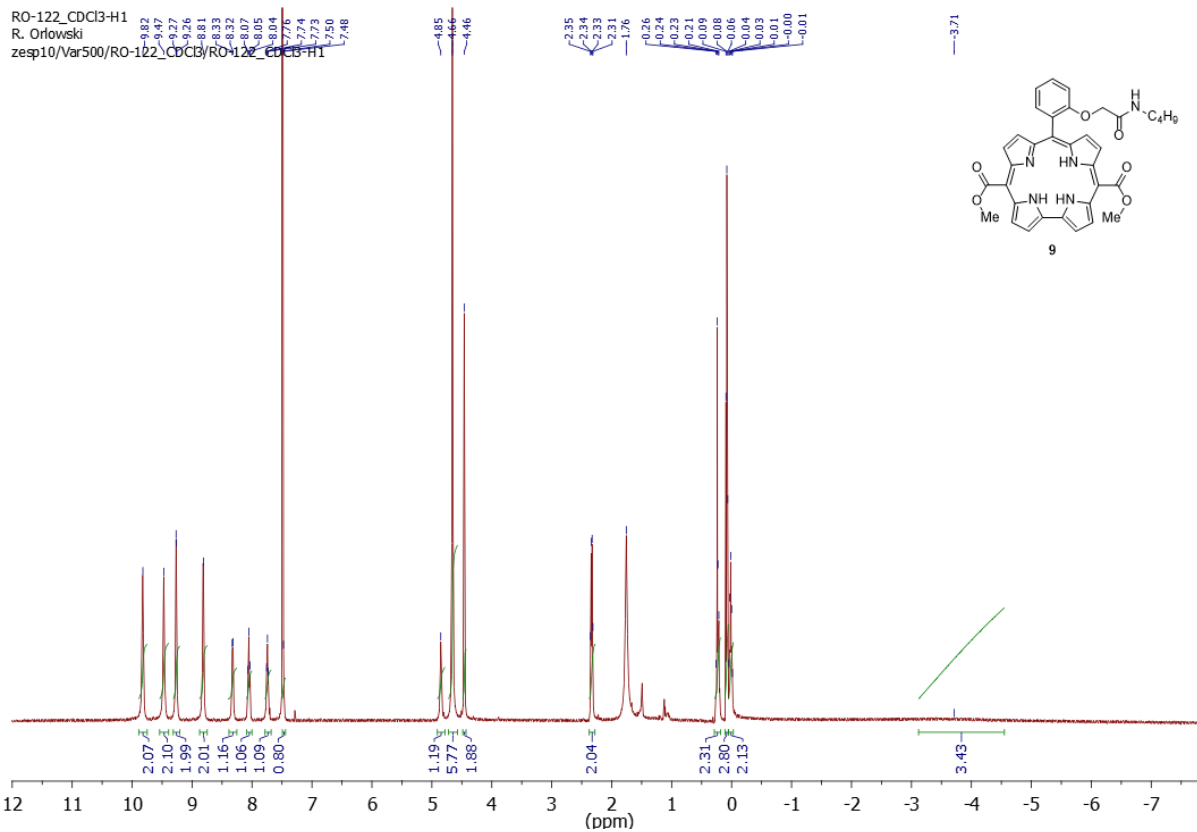


RO-111-H1
R.Orlowski

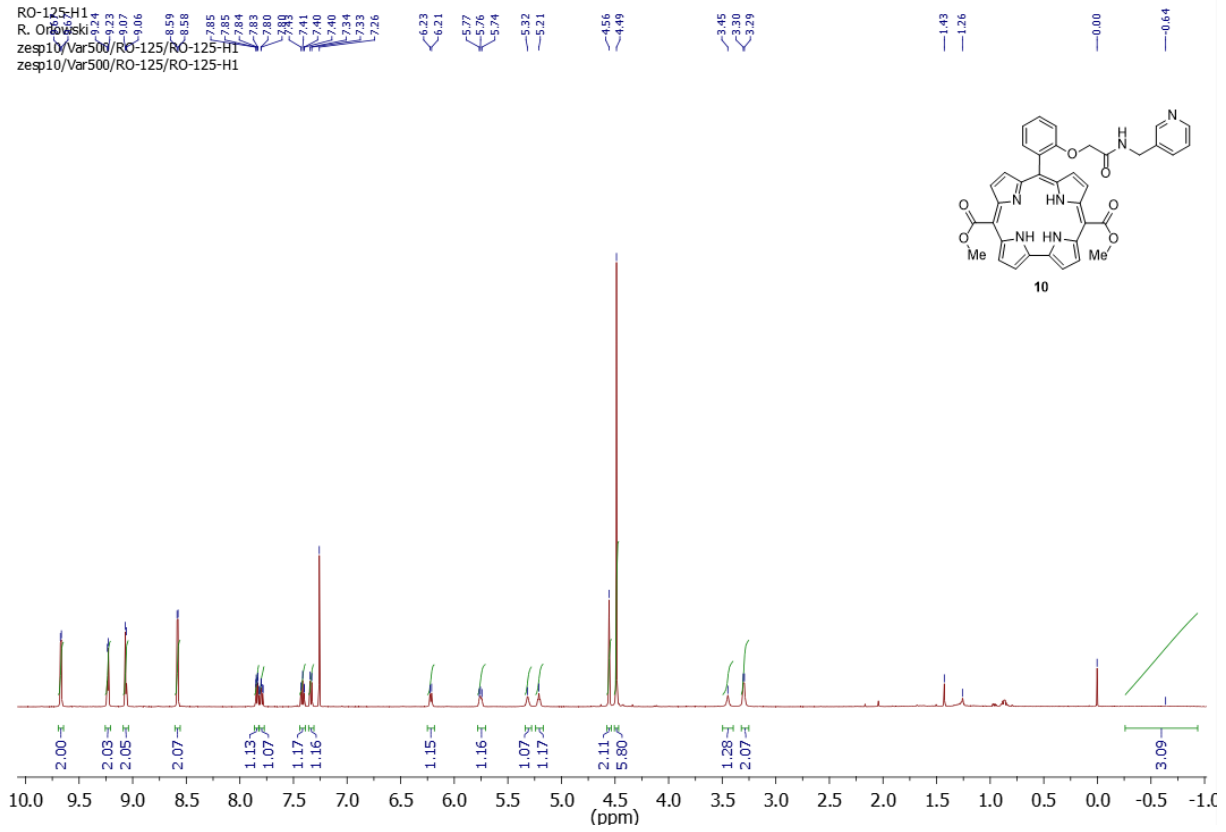
zesp10/Var500/RO-111/RO-111-H1



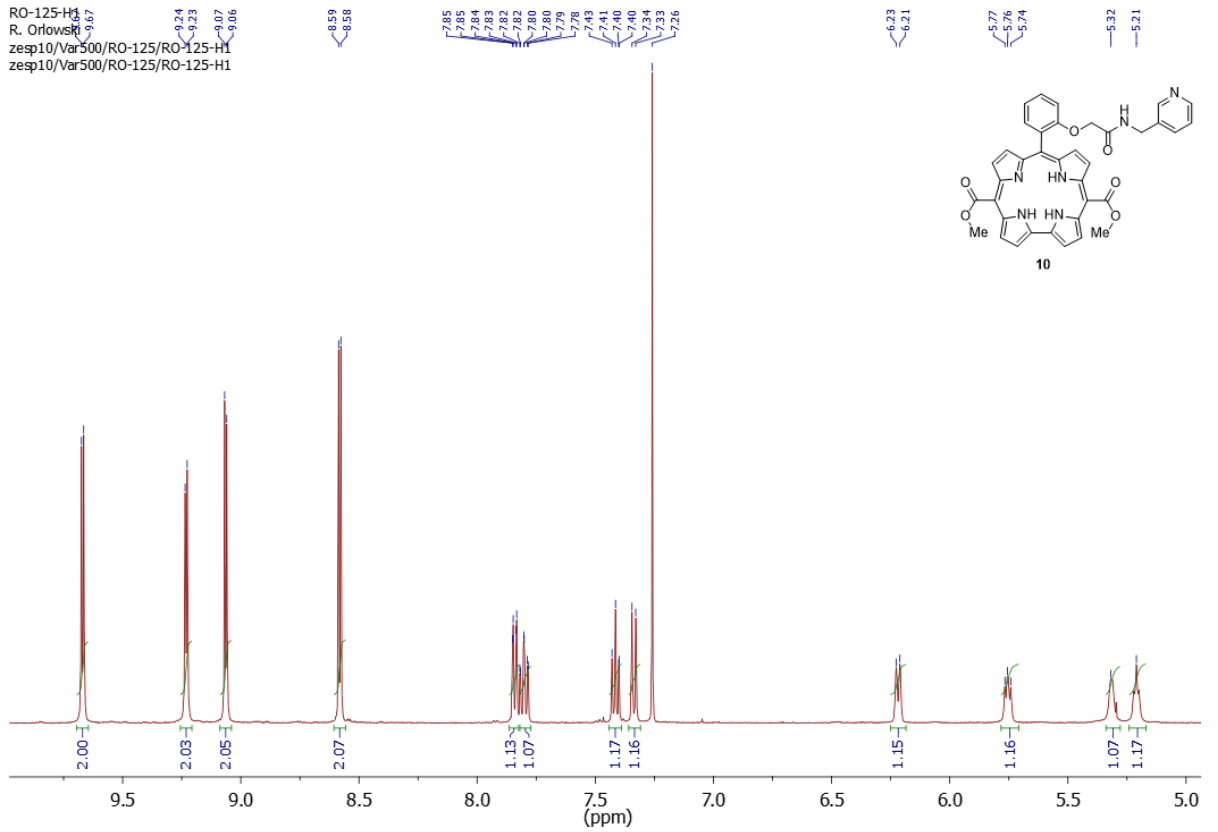
S27



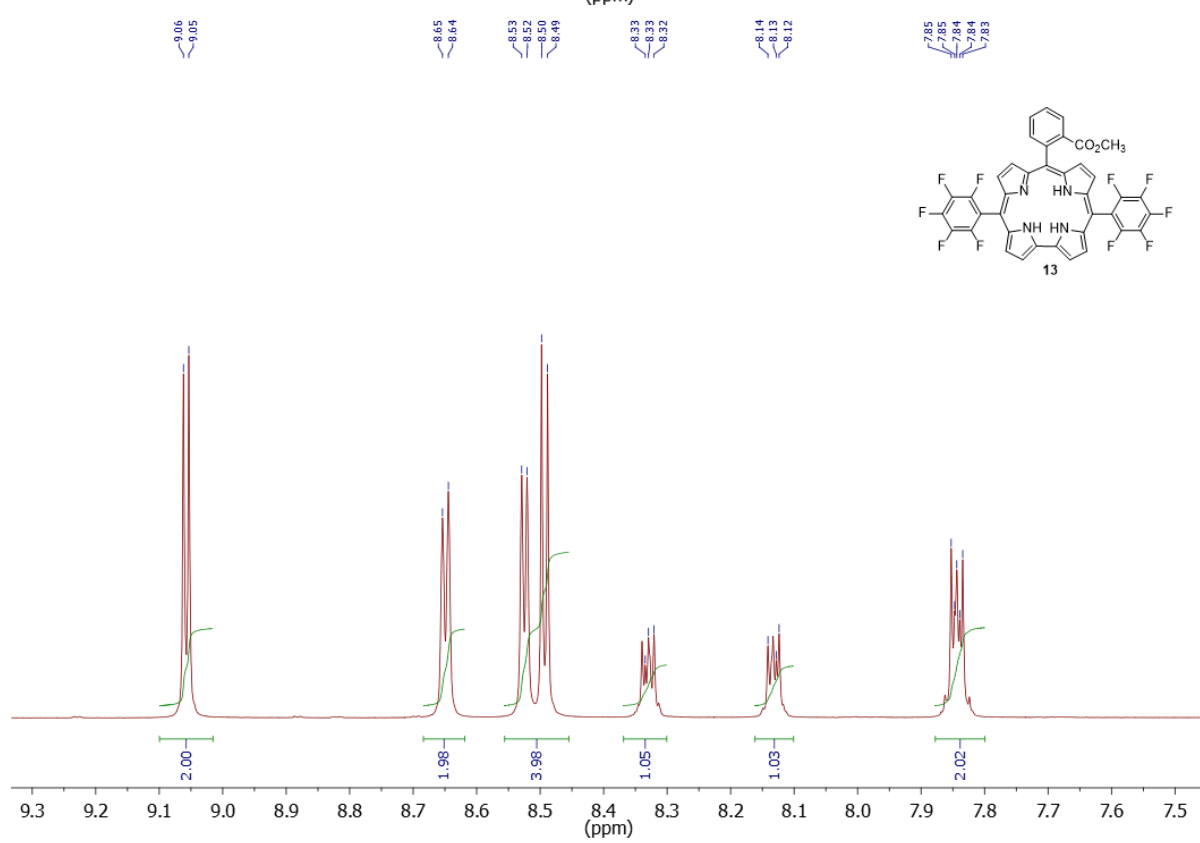
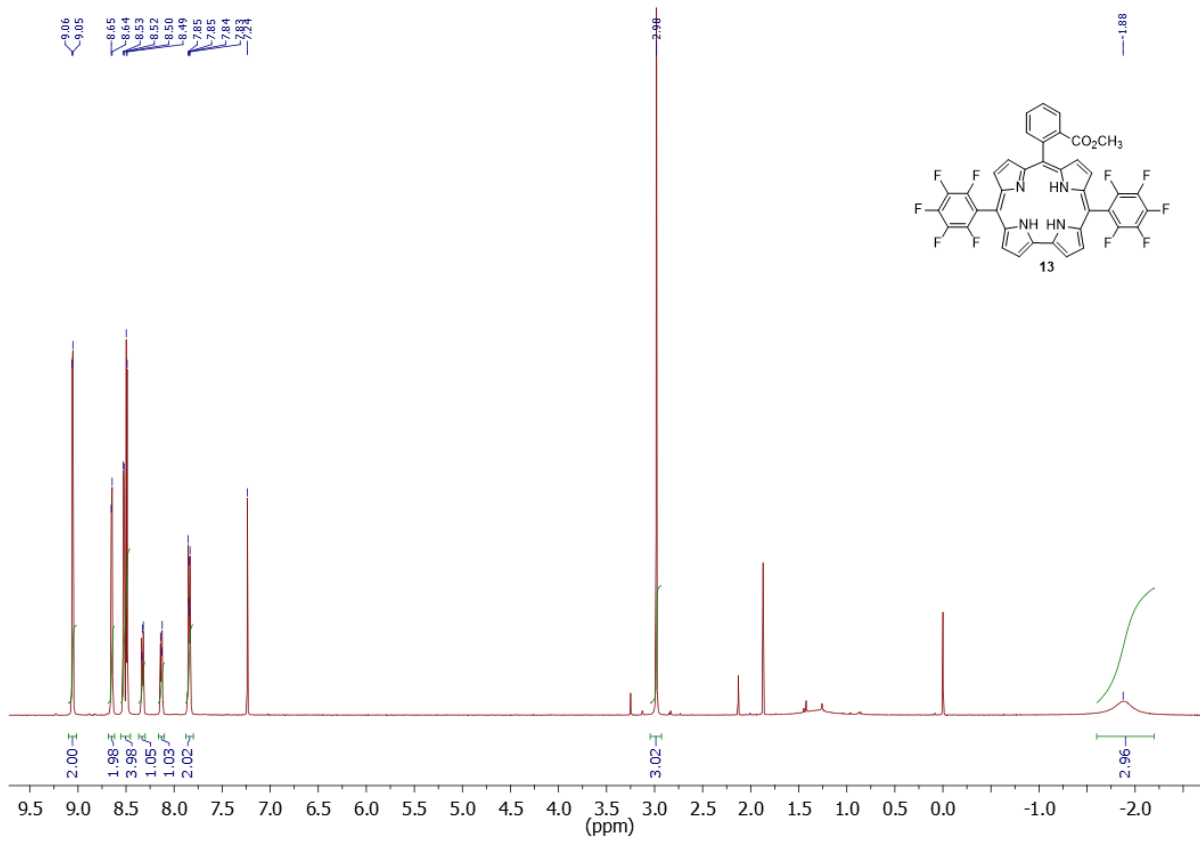
RO-125-H1
R. Orłowski
zesp10/Var500/RO-125/RO-125-H1
zesp10/Var500/RO-125/RO-125-H1

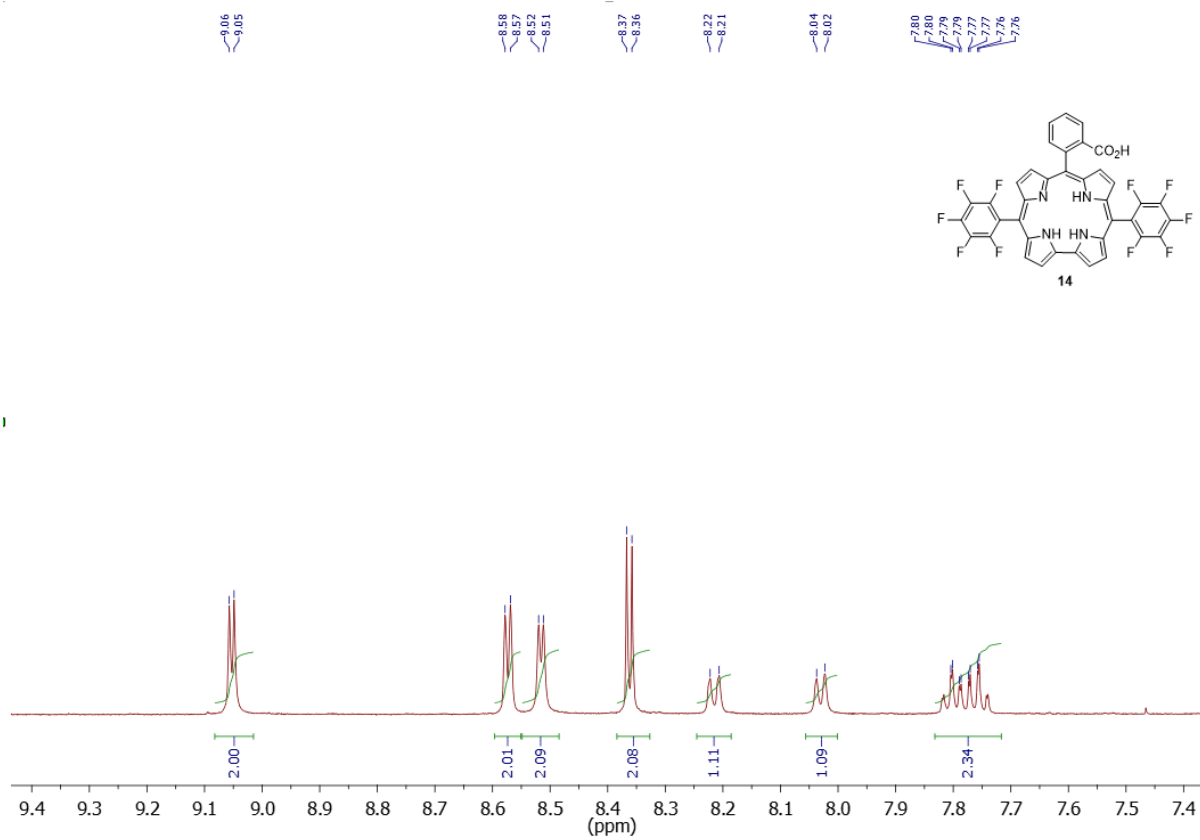
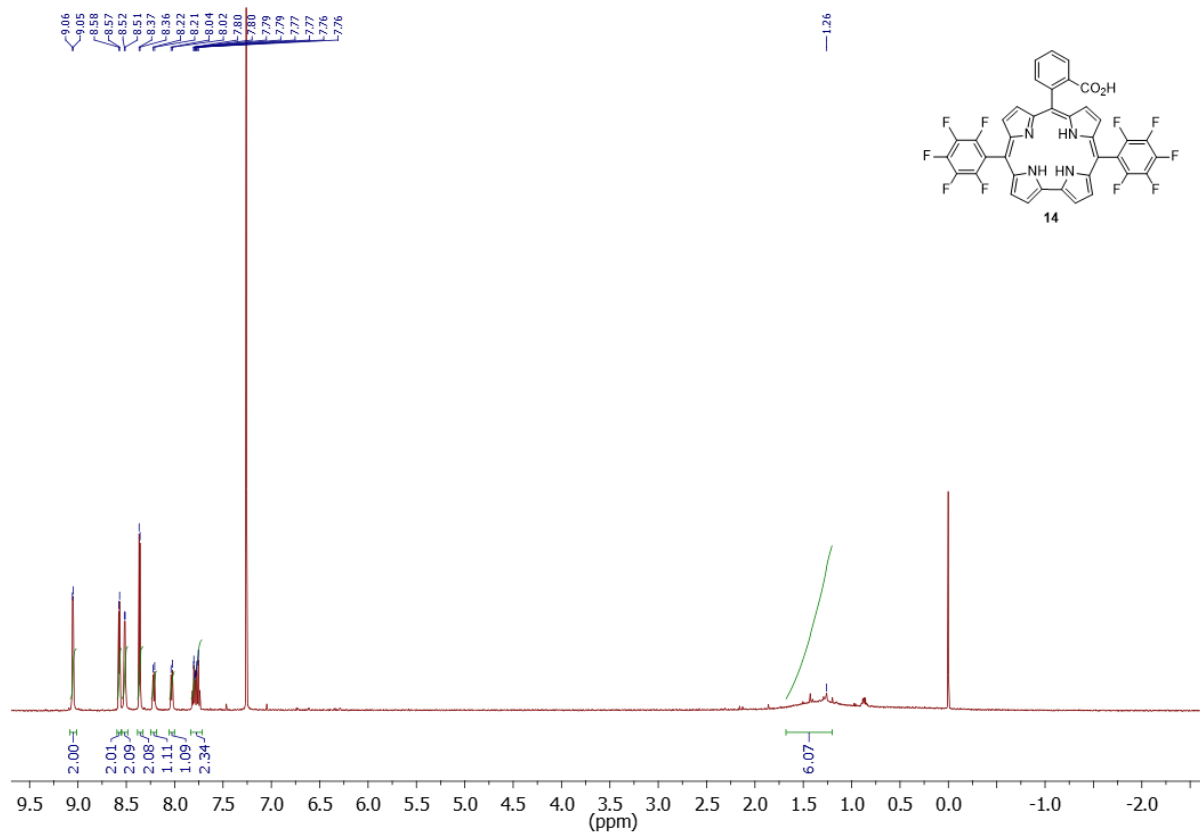


RO-125-H1
R. Orłowski
zesp10/Var500/RO-125/RO-125-H1
zesp10/Var500/RO-125/RO-125-H1

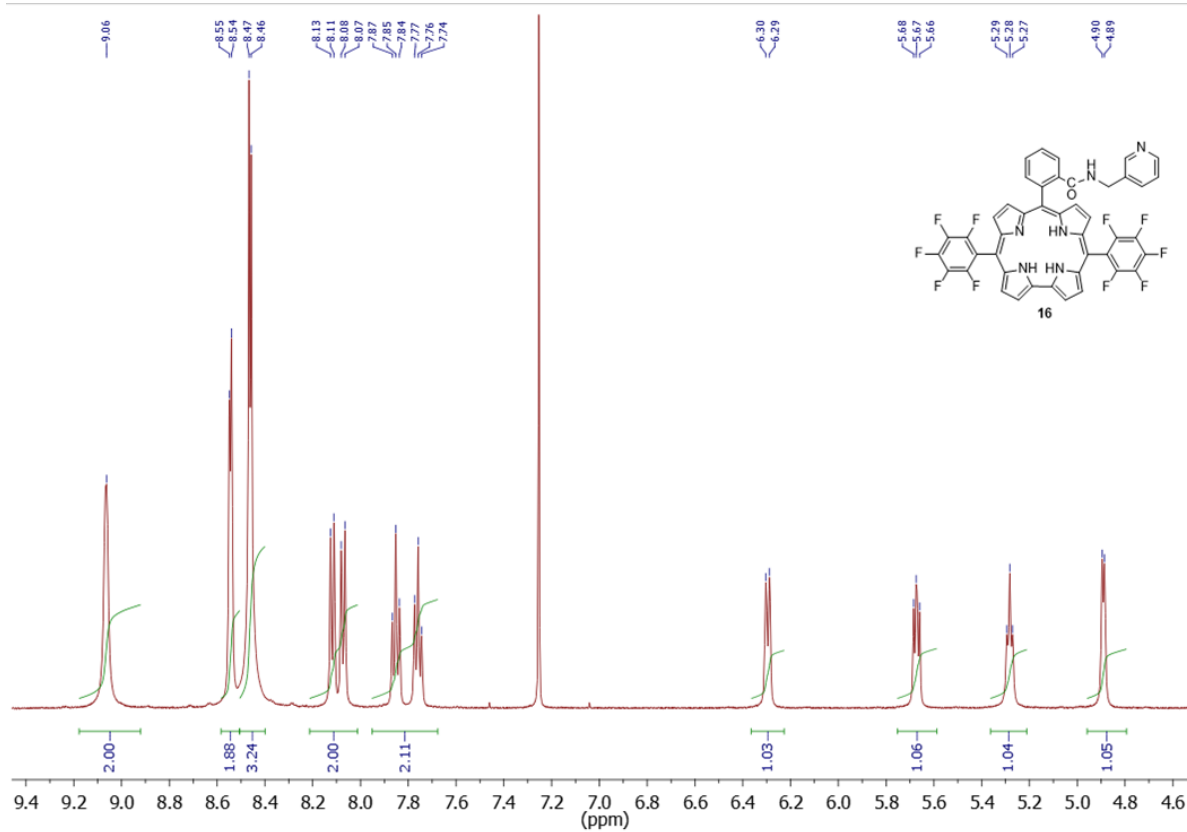
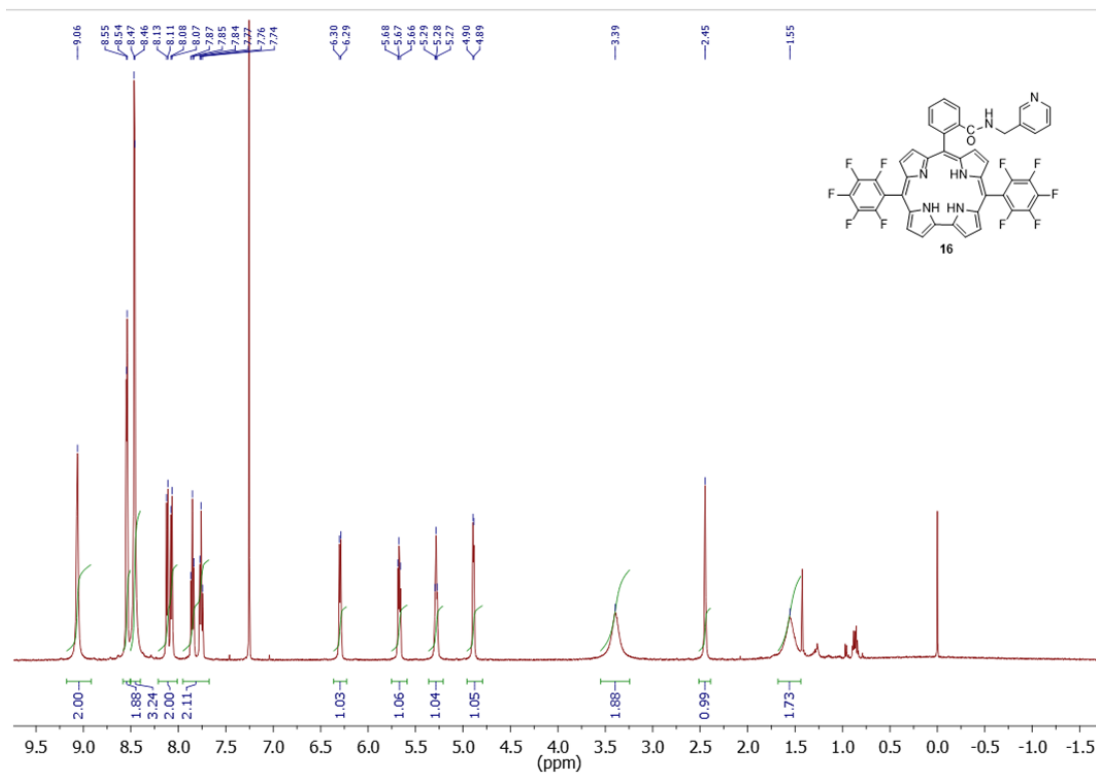


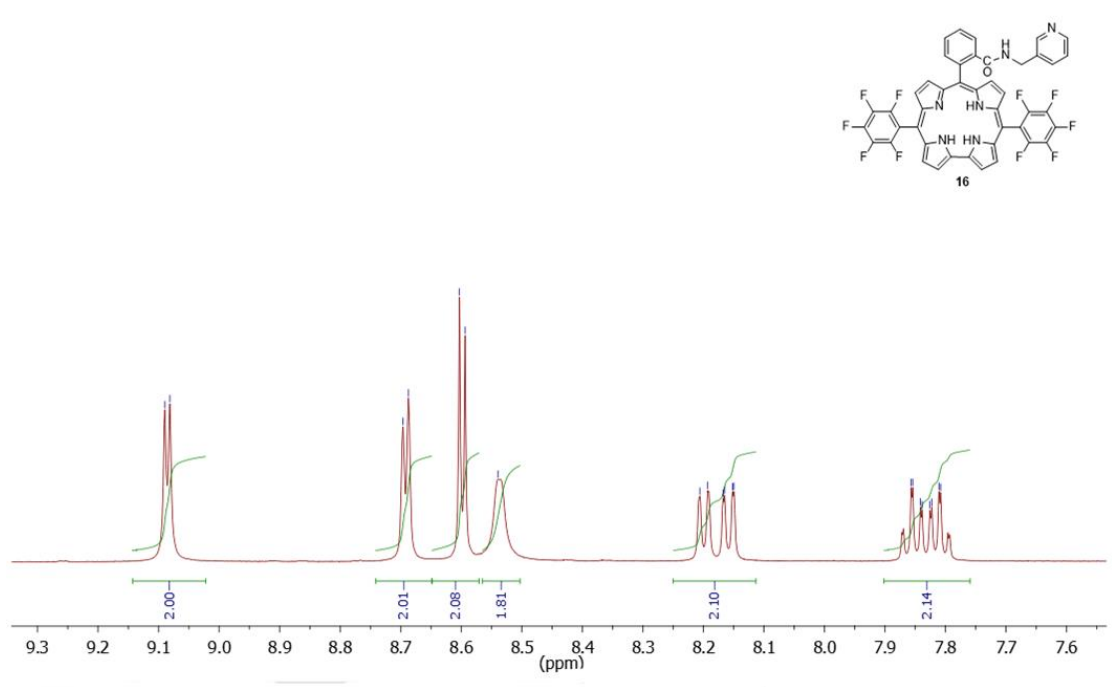
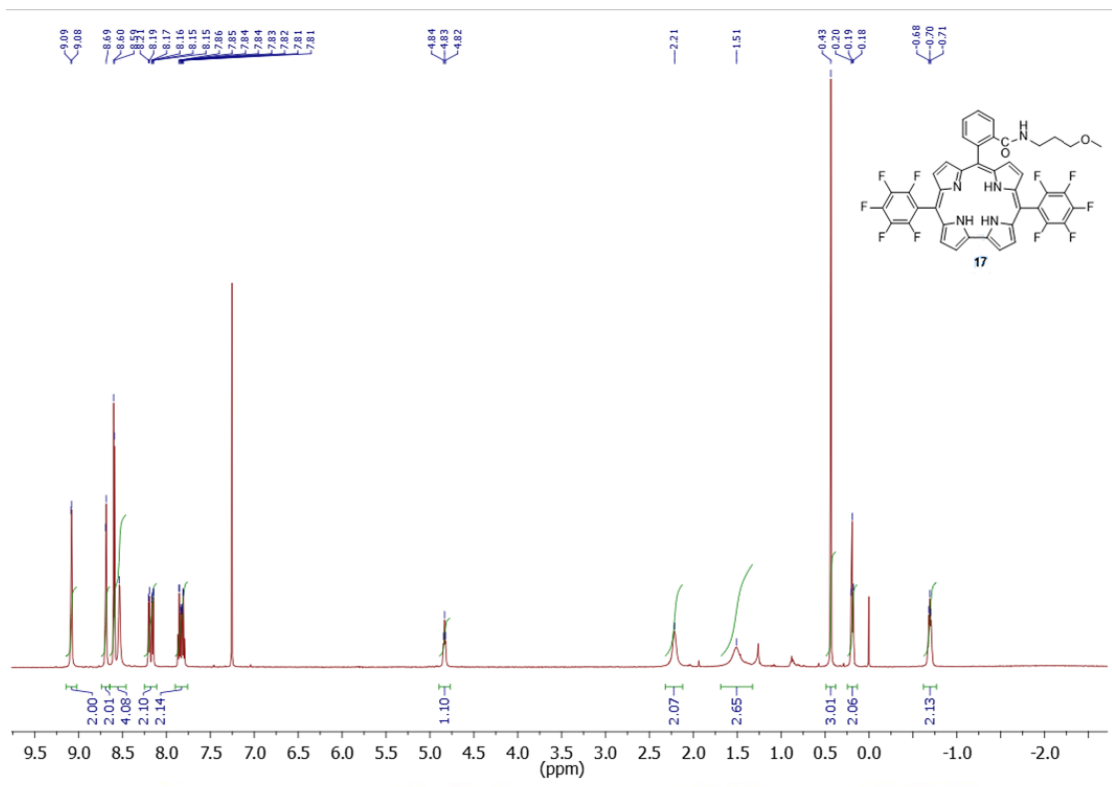
S29





S31





5. References

- [1] APEX2, Bruker AXS Inc., Madison, Wisconsin, USA, **2013**.
- [2] SAINT, Bruker AXS Inc., Madison, Wisconsin, USA, **2013**.
- [3] TWINABS, Bruker AXS Inc., Madison, Wisconsin, USA, **2012**.
- [4] G. M. Sheldrick, *Acta Crystallogr.* **1990**, *A46*, 467–473; G. M. Sheldrick, *Acta Crystallogr.* **2008**, *A64*, 112–122.
- [5] *International Tables for Crystallography*, Ed. A. J. C. Wilson, Kluwer: Dordrecht, **1992**, Vol.C.
- [6] G. Canard, D. Gao, A. D'Aléo, M. Giorgi, F.–X. Dang, T. S. Balaban, *Chem. Eur. J.* **2015**, *21*, 7760–7771.
- [7] C. F. Macrae, I. J. Bruno, J. A. Chisholm, P. R. Edgington, P. McCabe, E. Pidcock, L. Rodriguez-Monge, R. Taylor, J. van de Streek, P. A. Wood, *J. Appl. Cryst.* **2008**, *41*, 466–470.
- [8] R. Neufeld, D. Stalke, *Chem. Sci.* **2015**, *6*, 3354–3364.
- [9] D. Li, I. Keresztes, R. Hopson, P. G. Williard, *Acc. Chem. Res.* **2008**, *42*, 270–280.

Corroles

Covalently Linked Bis(Amido-Corroles): Inter- and Intramolecular Hydrogen-Bond-Driven Supramolecular Assembly

Rafał Orłowski,^[a] Grzegorz Cichowicz,^[b] Olga Staszewska-Krajewska,^[a] Wojciech Schilf,^[a] Michał K. Cyrański,^{*,[b]} and Daniel T. Gryko^{*,[a]}

Abstract: Four bis-corroles linked by diamide bridges were synthesized through peptide-type coupling of a *trans*-A₂B-corrole acid with aliphatic and aromatic diamines. In the solid state, the hydrogen-bond pattern in these bis-corroles is strongly affected by the type of solvent used in the crystallization process. Although intramolecular hydrogen bonds play a decisive role, they are supported by intermolecular hydrogen bonds and weak N–H... π interactions between molecules of toluene and the corrole cores. In an analogy to mono(amido-corroles), both in crystalline state and in solutions, the aliphatic or aromatic bridge is located directly above the corrole ring. When either ethylenediamine or 2,3-diaminonaphthalene are used as linkers, incorporation of

polar solvents into the crystalline lattice causes a roughly parallel orientation of the corrole rings. At the same time, both NHCO...NH corrole hydrogen bonds are intramolecular. In contrast, solvation in toluene causes a distortion with one of the hydrogen bonds being intermolecular. Interestingly, intramolecular hydrogen bonds are always formed between the –NHCO– functionality located further from the benzene ring present at the position 10-*meso*. In solution, the hydrogen-bonds pattern of the bis(amido-corroles) is strongly affected by the type of the solvent. Compared with toluene (strongly high-field shifted signals), DMSO and pyridine disrupt self-assembly, whereas hexafluoroisopropanol strengthens intramolecular hydrogen bonds.

Introduction

The synthetic design of effective, functional analogues of naturally occurring light-harvesting systems, polished through billions of years of evolution, is a driving force of many research groups.^[1] During recent years, many examples of non-discrete porphyrin-based aggregates, formed through hydrogen bonding, π -stacking, metal–ligand, or hydrophobic interactions have been proposed for this purpose.^[2,3] Corroles^[4–7] are younger and less symmetrical analogues of porphyrins, a feature which is reflected in a markedly lower activity in the study of their self-assembly processes. Some noteworthy instances of self-assembling corroles^[8] include octabromo corroles,^[9] corroles bearing PO(OH)₂ functionalities,^[10] amphiphilic corrole-sodium salts,^[11] along with corrole amino acid conjugates.^[12]

The presence of multiple secondary amide groups in organic molecules has been proven to be a robust way of increasing the propensity for said molecule to self-assemble into reprodu-

cible secondary structures. This is strongly related to the ability of –NHCO– to act simultaneously as hydrogen-bond donor and acceptor. These structures include helices,^[13] zig-zags,^[14] antiparallel β -strands,^[15] tapes,^[16] macrocycles,^[17] cryptands,^[18] capsules,^[19] Janus-dendrimers,^[20] and molecular electrets.^[21] Clearly, this ability has been utilized by nature to form three-dimensional peptide and protein secondary structures.^[22] Although the propensity of –NHCO– groups to form strong hydrogen bonds has been known for a long time, chemists continue to reinvent it by revealing new type of structures every once in a while.^[23]

Corrole-NH protons have been shown to act as hydrogen-bond donors to exogenous acceptors.^[8] To further investigate this ability, we decided to synthesize a range of corrole dimers linked by secondary amide functionalities. The nature of the linker, with regard to its length and rigidity, is expected to play a crucial role in the hydrogen-bonding interactions between the cavity NH and oxygen atoms of the amide groups and hence have a strong impact on the relative orientations of the corrole units.

The goals of this project were to investigate these interactions by: 1) studying the impact of the length and rigidity of the bridge between amide functionalities and 2) to evaluate the influence that the solvent character has on the intramolecular hydrogen bond.

[a] R. Orłowski, Dr. O. Staszewska-Krajewska, Dr. W. Schilf, Prof. Dr. D. T. Gryko
Institute of Organic Chemistry, Polish Academy of Sciences
44/52 Kasprzaka str., 01224 Warsaw (Poland)
E-mail: dtgryko@icho.edu.pl

[b] G. Cichowicz, Prof. M. K. Cyrański
Faculty of Chemistry, University of Warsaw
Pasteura 1, 02093 Warsaw (Poland)
E-mail: mkc@chem.uw.edu.pl

Supporting information and the ORCID identification number(s) for the author(s) of this article can be found under:
<https://doi.org/10.1002/chem.201901254>

CHEMISTRY

A **European** Journal

Supporting Information

Covalently Linked Bis(Amido-Corroles): Inter- and Intramolecular Hydrogen-Bond-Driven Supramolecular Assembly

Rafał Orłowski,^[a] Grzegorz Cichowicz,^[b] Olga Staszewska-Krajewska,^[a] Wojciech Schilf,^[a]
Michał K. Cyrański,^{*[b]} and Daniel T. Gryko^{*[a]}

chem_201901254_sm_miscellaneous_information.pdf

Author Contributions

R.O. Investigation: Lead; Writing - Original Draft: Equal; Writing - Review & Editing: Supporting

G.C. Investigation: Equal; Writing - Original Draft: Equal

O.S. Investigation: Equal; Writing - Original Draft: Supporting

W.S. Supervision: Equal; Writing - Review & Editing: Supporting

M.C. Supervision: Equal; Writing - Original Draft: Supporting; Writing - Review & Editing: Equal

D.G. Conceptualization: Lead; Supervision: Lead; Writing - Original Draft: Supporting; Writing - Review & Editing: Lead.

Table of Contents

1. Crystallographic data	S3-S18
2. The diffusion-ordered NMR spectroscopy	S19-S22
3. ¹ H NMR spectra for synthesized compounds	S23-S27
4. References	S28

1. Crystallographic data

Name	5A	5B	6A	6B
CDS Number	1902360	1902361	1902363	1902362
Formula	C101H64F20N10O4	C170.80H101.60F40N20O11.60	C101.10H61.20F20N10O5.60	C91.40H45.40C110.20F20N10O4
M_x/ g/mol	1861.62	3379.51	1885.60	2089.17
T/ K	100(2)	130(2)	100(2)	100(2)
λ/ Å	1.54178	0.71073	1.54178	1.54178
Crystal size/ mm	0.096×0.199×0.419	0.126×0.189×0.651	0.096×0.199×0.4190	0.096×0.199×0.4190
Crystal system	monoclinic	monoclinic	monoclinic	monoclinic
Space group	Cc	$P2_1/c$	$P2_1/n$	$C2/c$
Unit cell dimensions	$a = 35.1706(11)$ Å $b = 14.7705(4)$ Å $c = 17.6404(5)$ Å $\beta = 112.6040(10)^\circ$	$a = 13.4562(5)$ Å $b = 41.2178(18)$ Å $c = 14.4855(6)$ Å $\beta = 109.123(2)^\circ$	$a = 14.6853(6)$ Å $b = 36.5435(14)$ Å $c = 15.6611(6)$ Å $\beta = 92.353(2)^\circ$	$a = 28.5787(11)$ Å $b = 13.7778(5)$ Å $c = 23.2051(9)$ Å $\beta = 105.932(2)^\circ$
V/ Å³	8460.0(4)	7590.8(5)	8397.5(6)	8786.1(6)
Z, D_x/ g/cm³	4, 1.462	2, 1.479	4, 1.491	4, 1.579
μ/ mm⁻¹	1.042	0.128	1.073	3.861
$F(000)$	3808	3438	3850	4197
θ_{min}, θ_{max}	2.71, 66.50°	2.18, 25.05	2.42, 66.50	3.22, 66.49
Index range	$-41 \leq h \leq 41$, $-17 \leq k \leq 17$, $-19 \leq l \leq 20$	$-16 \leq h \leq 16$, $-49 \leq k \leq 49$, $-17 \leq l \leq 17$	$-17 \leq h \leq 17$, $-43 \leq k \leq 43$, $-18 \leq l \leq 18$	$-33 \leq h \leq 33$, $-16 \leq k \leq 16$, $-27 \leq l \leq 27$
Reflections collected	65753/14554	81323/13410	109837/14804	98711/7740
/independent	[$R_{int} = 0.0626$]	[$R_{int} = 0.0335$]	[$R_{int} = 0.0334$]	[$R_{int} = 0.0674$]
Completeness	99.9%	99.9%	100.0	99.9%
Absorption correction	multi-scan	multi-scan	multi-scan	multi-scan
T_{max}, T_{min}	0.9320 and 0.6690	0.9840, 0.9210	0.8810, 0.5300	0.7400, 0.4650
Structure solution technique	direct methods	direct methods	direct methods	direct methods
Refinement method	Full-matrix LSQ on F^2	Full-matrix LSQ on F^2	Full-matrix LSQ on F^2	Full-matrix LSQ on F^2
Data / restraints / parameters	14554 / 142 / 1304	13410 / 180 / 1229	14804 / 686 / 1807	7740 / 34 / 680
Goodness-of-fit on F^2	1.053	1.114	1.041	1.041
Final R indices	12288 data; $I > 2\sigma(I)$ $R1 = 0.0421$, $wR2 = 0.0925$ all data $R1 = 0.0547$ $wR2 = 0.0991$	11294 data; $I > 2\sigma(I)$ $R1 = 0.0474$, $wR2 = 0.1121$ all data $R1 = 0.0588$ $wR2 = 0.1178$	12553 data; $I > 2\sigma(I)$ $R1 = 0.0664$, $wR2 = 0.1749$ all data $R1 = 0.0763$ $wR2 = 0.1845$	6320 data; $I > 2\sigma(I)$ $R1 = 0.0531$, $wR2 = 0.1404$ all data $R1 = 0.0664$ $wR2 = 0.1513$
Absolute structure parameter	Refined as racemic twin	-	-	-
ρ_{max}, ρ_{min}/ eÅ⁻³	0.277, -0.242	0.471, -0.274	0.469, -0.347	0.721, -0.642

Table S1. Crystal data and structure refinement parameters for all structures.

The X-ray measurements of **5A**, **6A** and **6B** were performed at 100(2) K D8 VENTURE PHOTON 100 CMOS system equipped with a mirror monochromator and a CuK α INCOATEC I μ S micro-focus source ($\lambda = 1.54178 \text{ \AA}$) whereas measurement of **5B** was performed on a Bruker D8 VENTURE PHOTON 100 CMOS diffractometer equipped with a TRIUMPH monochromator and a MoK α fine focus sealed tube ($\lambda = 0.71073 \text{ \AA}$). All data for all crystals were collected with Bruker APEX2 program [1]. The frames were integrated with the Bruker SAINT software package [2] using a narrow-frame algorithm. Data were corrected for absorption effects using the multi-scan method (SADABS) [3]. All structures were solved and refined using the Bruker SHELXTL Software Package [4]. All non-hydrogen atoms with occupation higher than 0.5 were refined anisotropically. Most of hydrogen atoms in all crystal structures were placed in calculated positions and refined within the riding model. Hydrogen atoms bonded to N-pyrrole atoms were placed based on density map. The temperature factors of all other hydrogen atoms were not refined and were set to be either 1.2 or 1.5 times larger than U_{eq} of the corresponding heavy atom. The atomic scattering factors were taken from the International Tables [5]. Molecular graphics was prepared using program Mercury CSD 3.9 [6]. Thermal ellipsoids parameters are presented at 50% probability level. Crystal data and the structure refinement parameters are presented in **Table SII**. All hydrogen-bonds parameters for each structures are presented in **Tables S2-S4**. All structures are disordered with description provided below.

5A The specimen of **5A** was refined as racemic two-component twin with ratio of 50:50. Disordered molecules of toluene adopt occupancy ratio of 0.68:0.42 for D and F parts, and 0.72:0.28 for E and G, respectively. .

5B One of molecules of acetone is disordered over two sites D and F with occupancy 0.82:0.18. The occupancy of the second one is nonstoichiometric and divided over three parts E, G and H with fixed occupancy 0.5, 0.2, 0.1, respectively. . In corrole the disorder involves (i) the C₆F₅ substituents, which adopt two positions with occupancy ratio 0.89:0.11 , and (ii) one of the amide groups with occupancy of sites of 0.7:0.3.

6A The molecule of corrole is highly disordered over two sites, for subunit A (A and I) and linker with occupancy 0.81:0.19, and with occupancy 0.78:0.22 for subunit B (B and J parts). Apart for that, one ring C₆F₅ (C36A>F46A, C36I>F46I) has different occupancy with ratio of 0.90:0.10. One of the molecule of toluene adopts two positions, D and E with occupancy 0.6:0.4 respectively. The rest of solvents molecules within the structure are in nonstoichiometric content. The molecule of toluene H has fixed occupancy of 0.3, both molecules of methanol K and M adopts occupancy of 0.2. The molecule of acetone F was refined anisotropically with

occupancy of 0.6. Two remaining one, G and L have fixed occupancy values of 0.4 and 0.2, respectively.

6B One of the molecule of trichloromethane is divided over five sites D, E, F, G, H with occupancy of 0.17, 0.21, 0.18, 0.14, 0.20, respectively. All values sum to nonstoichiometric value of 0.9.

LSQ method was applied to fit planes for the six atoms of each toluene ring (using Mercury CSD [6]) or corrole (obtained during the last refinement process in Bruker SHELXTL Software Package [4]). The results of analysis are presented on **Figures S11-S13**.

	Donor-H	Acceptor-H	Donor-Acceptor	Angle
C3A-H3A...F56A	0.95	2.57	3.496(5)	164.2
C7A-H7A...F54A	0.95	2.43	3.120(5)	129.7
C12A-H12A...O34B	0.95	2.64	3.484(5)	148.9
N21A-H1NA...O34B	0.90(3)	1.95(3)	2.772(4)	152.(4)
N22A-H2NA...N21A	0.88(3)	2.29(5)	2.762(5)	114.(4)
N22A-H2NA...N23A	0.88(3)	2.41(5)	2.900(4)	116.(4)
N24A-H4NA...N23A	0.86(3)	1.94(4)	2.635(5)	137.(4)
C7B-H7B...F54B	0.95	2.45	3.195(5)	135.4
C18B-H18B...F56A	0.95	2.32	3.253(5)	167.5
N21B-H1NB...O34A	0.88(3)	1.86(3)	2.727(4)	169.(4)
N22B-H2NB...N21B	0.89(3)	2.29(4)	2.753(5)	112.(3)
N22B-H2NB...N23B	0.89(3)	2.30(4)	2.900(5)	125.(3)
N24B-H4NB...N23B	0.90(3)	1.90(4)	2.631(5)	137.(4)

Table S2 Hydrogen bond distances and angles for **5A**

	Donor-H	Acceptor-H	Donor-Acceptor	Angle
C2A-H2AA...F57B	0.95	2.54	3.386(3)	148.1
C8A-H8A...F43A	0.95	2.34	3.194(3)	149.2
C13A-H13A...F55B	0.95	2.63	3.330(3)	130.5
C17A-H17A...O34A	0.95	2.65	3.580(3)	165.2
C18A-H18A...F53B	0.95	2.54	3.446(3)	160.0
N21A-H1NA...O34B	0.941(17)	1.864(19)	2.759(2)	158.(2)
N22A-H2NA...N21A	0.934(17)	2.27(3)	2.742(3)	110.9(19)
N22A-H2NA...N23A	0.934(17)	2.28(2)	2.913(3)	125.(2)
N24A-H4NA...N23A	0.924(17)	1.85(2)	2.619(3)	140.(2)
C32A-H32E...F56A	0.99	2.62	3.366(3)	132.6
C7B-H7B...F44B	0.95	2.46	3.316(3)	149.1
C7B-H7B...F44C	0.95	2.41	3.350(19)	169.1
C8B-H8B...F45A	0.95	2.56	3.424(3)	151.1
N21B-H1NB...O34A	0.917(17)	1.988(18)	2.885(2)	166.(3)
N22B-H2NB...N21B	0.921(16)	2.29(2)	2.763(3)	111.1(18)
N22B-H2NB...N23B	0.921(16)	2.29(2)	2.895(3)	123.0(19)
N24B-H4NB...N23B	0.937(17)	1.87(2)	2.631(2)	136.(2)
C27B-H27B...F42A	0.95	2.5	3.352(3)	150.0
C1G-H1G2...F55B	0.98	2.61	3.46(2)	145.9

Table S3 Hydrogen bond distances and angles for **5B**

	Donor-H	Acceptor-H	Donor-Acceptor	Angle
C2A-H2AA...F57B	0.95	2.54	3.386(3)	148.1
C8A-H8A...F43A	0.95	2.34	3.194(3)	149.2
C13A-H13A...F55B	0.95	2.63	3.330(3)	130.5

C2'-H2'...F54I	0.95	2.6	3.31(3)	131.4
N23A-H3NA...N22A	0.91(2)	2.51(6)	2.994(7)	113.(5)
N23A-H3NA...N24A	0.91(2)	1.99(5)	2.602(10)	123.(5)
C2I-H2I...F56J	0.95	2.46	3.03(4)	118.3
C3I-H3I...F56J	0.95	2.62	3.08(5)	110.2
C17I-H17I...F42J	0.95	2.56	3.42(4)	151.5
N21I-H1NI...N22I	0.88	1.97	2.66(4)	134.3
N22I-H2NI...N21I	0.88	2.13	2.66(4)	118.1
N22I-H2NI...N23I	0.88	2.46	2.98(4)	118.3
N23I-H3NI...N22I	0.88	2.46	2.98(4)	118.9
N23I-H3NI...N24I	0.88	1.97	2.63(5)	129.7
C32A-H32A...F44A	0.99	2.52	3.492(4)	166.4
C32A-H32B...N23B	0.99	2.7	3.587(10)	149.6
C13B-H13B...O1F	0.95	2.43	3.364(7)	167.0
N21B-H1NB...O34A	0.899(19)	1.896(17)	2.782(8)	168.(3)
N22B-H2NB...N21B	0.91(2)	2.23(5)	2.810(18)	121.(4)
N22B-H2NB...N23B	0.91(2)	2.36(4)	2.975(10)	124.(4)
N24B-H4NB...N23B	0.908(19)	1.88(3)	2.634(10)	139.(3)
C27B-H27B...F43A	0.95	2.35	3.239(8)	154.9
C3J-H3J...O34J	0.95	2.61	3.36(3)	135.6
N21J-H1NJ...O34A	0.91(2)	1.896(17)	2.78(2)	163.(4)
N22J-H2NJ...N21J	0.88	2.19	2.67(7)	113.4
N22J-H2NJ...N23J	0.88	2.19	2.73(4)	119.1
N24J-H4NJ...N23J	0.88	1.88	2.55(4)	131.2
C27J-H27J...F43I	0.95	1.93	2.73(4)	139.5
O1G-H1G...N23J	0.98	2.54	3.29(4)	132.5
C1G-H1G...F42I	0.98	2.56	3.33(2)	135.7

Table S4 Hydrogen bond distances and angles for **6A**

	Donor-H	Acceptor-H	Donor-Acceptor	Angle
C2-H2...Cl4D	0.95	2.93	3.767(11)	147.1
C2-H2...Cl4E	0.95	2.95	3.738(8)	141.0
C2A-H2A...F57A	0.95	2.45	3.242(3)	140.2
C3A-H3A...Cl4C	0.95	2.89	3.842(3)	178.3
C7A-H7A...Cl3G	0.95	2.93	3.849(7)	162.0
C8A-H8A...F56A	0.95	2.63	3.308(3)	128.9
N21A-H1NA...O34A	0.914(18)	1.91(2)	2.809(3)	168.(3)
N22A-H2NA...N21A	0.902(18)	2.28(3)	2.755(3)	113.(3)
N22A-H2NA...N23A	0.902(18)	2.34(3)	2.933(3)	123.(3)
N24A-H4NA...N23A	0.917(19)	1.91(3)	2.632(3)	134.(3)
C32A-H32A...N23A	0.99	2.57	3.449(4)	148.2
C1C-H1C...Cl2C	1.0	2.94	3.586(4)	123.0
C1D-H1D...F42A	1.0	2.56	3.293(15)	129.6
C1E-H1E...F42A	1.0	2.45	3.258(17)	137.8
C1F-H1F...F42A	1.0	2.12	2.903(8)	133.7
C1F-H1F...Cl2C	1.0	2.84	3.684(9)	142.6
C1G-H1G...F42A	1.0	2.41	2.903(8)	109.7
C1G-H1G...Cl2C	1.0	2.77	3.684(9)	152.2
C1H-H1H...F42A	1.0	2.37	3.170(15)	136.0

Table S5 Hydrogen bond distances and angles for **6B**

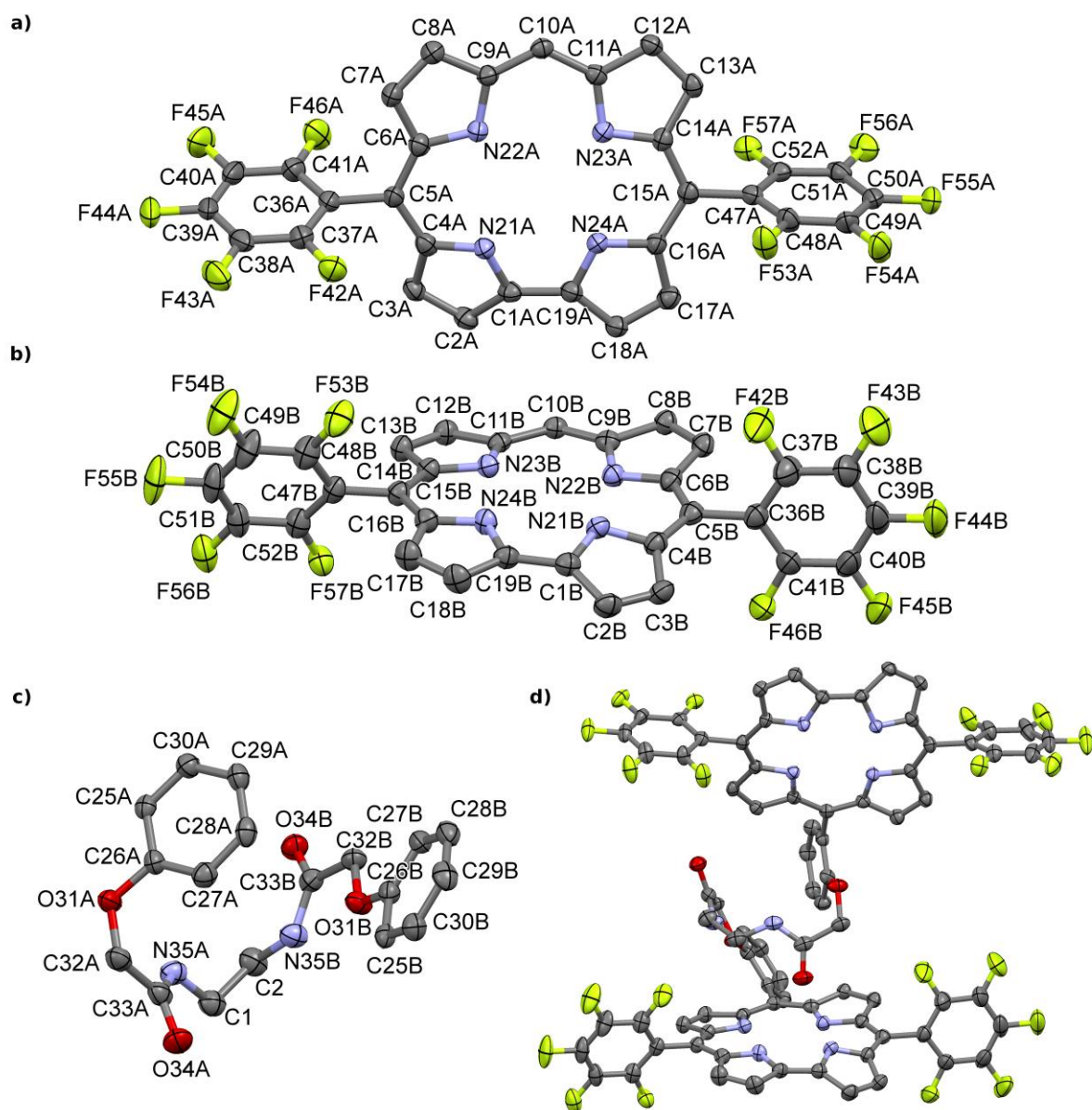


Figure S1 Numbering scheme and thermal ellipsoid at 50% probability level for molecules of **5** in **5A**: **a)** subunit (A), **b)** subunit (B), **c)** linker, **d)** whole molecule.

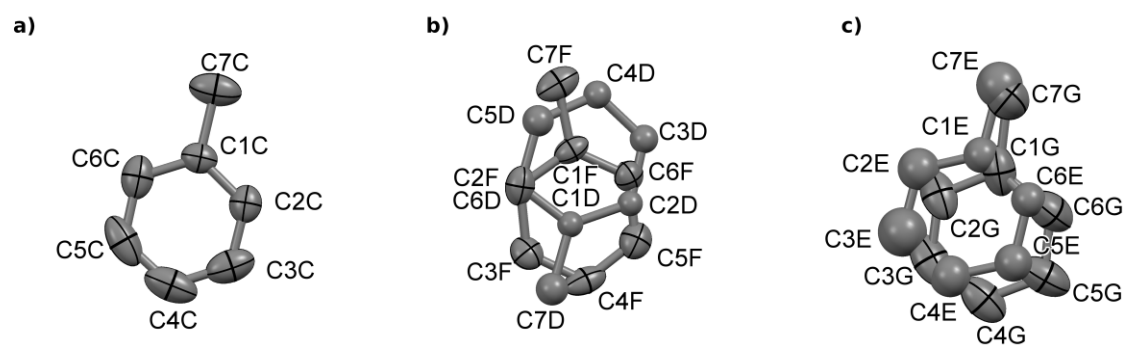


Figure S2 Numbering scheme and thermal ellipsoid at 50% probability level for molecules of toluene in **5A**: **a)** C, **b)** D and F, **c)** G and E.

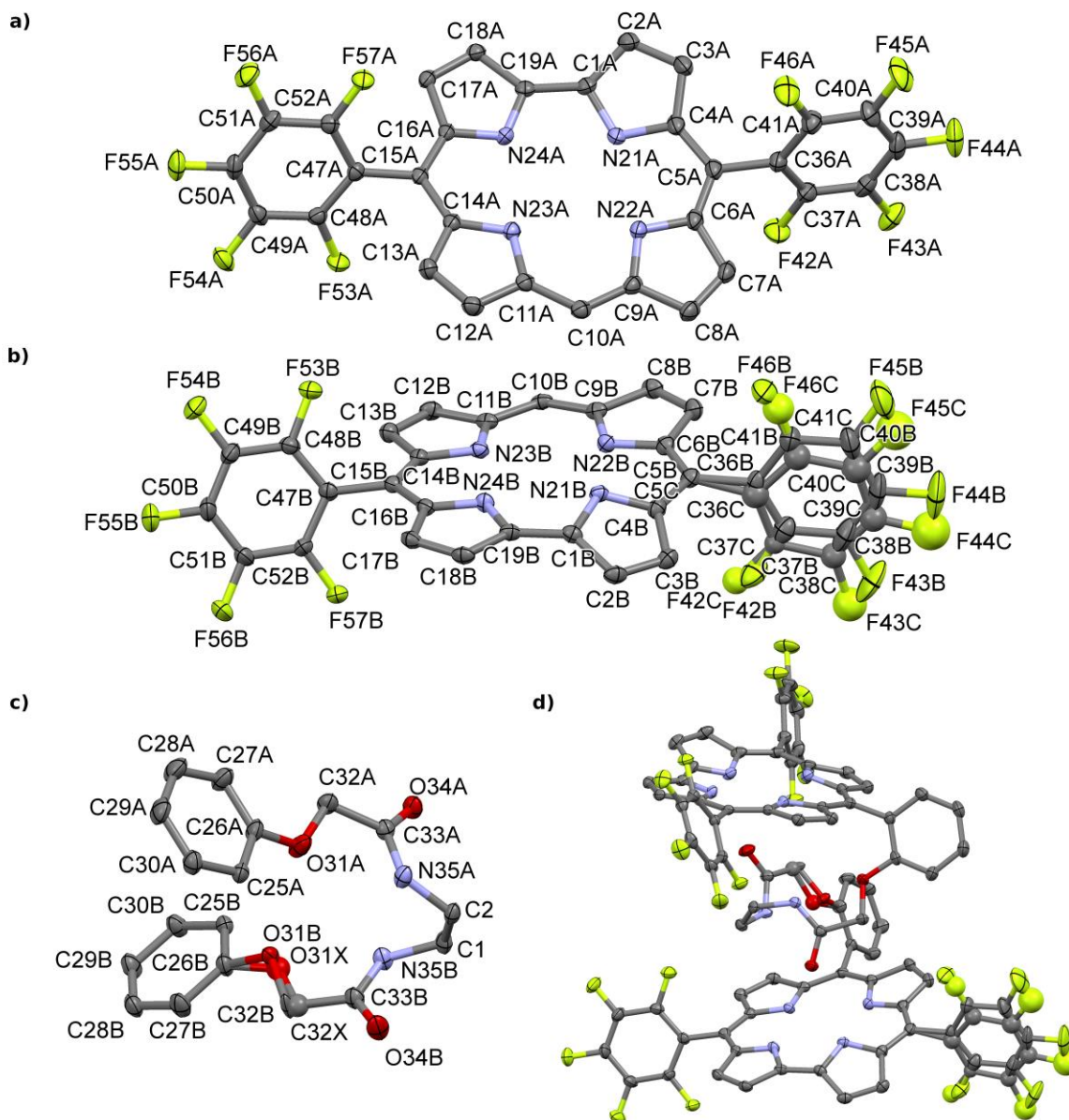


Figure S3 Numbering scheme and thermal ellipsoid at 50% probability level for molecules of **5** in **5B**: **a)** subunit (A), **b)** subunit (B), **c)** linker, **d)** whole molecule.

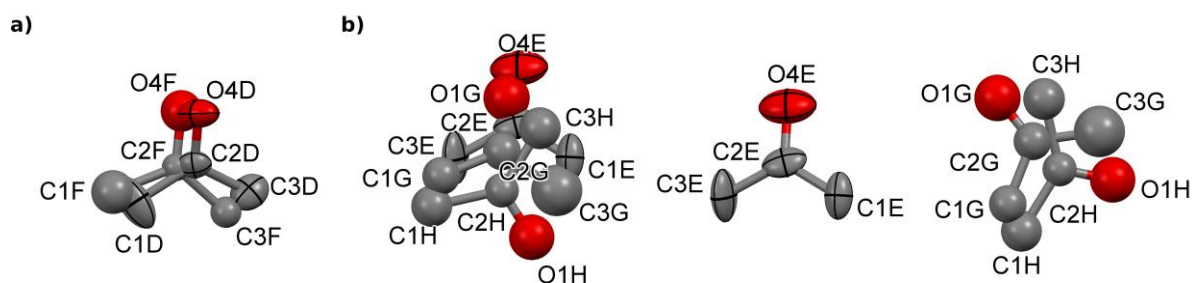


Figure S4 Numbering scheme and thermal ellipsoid at 50% probability level for molecules of acetone in **5B** **a)** D and F, **b)** E, H, G.

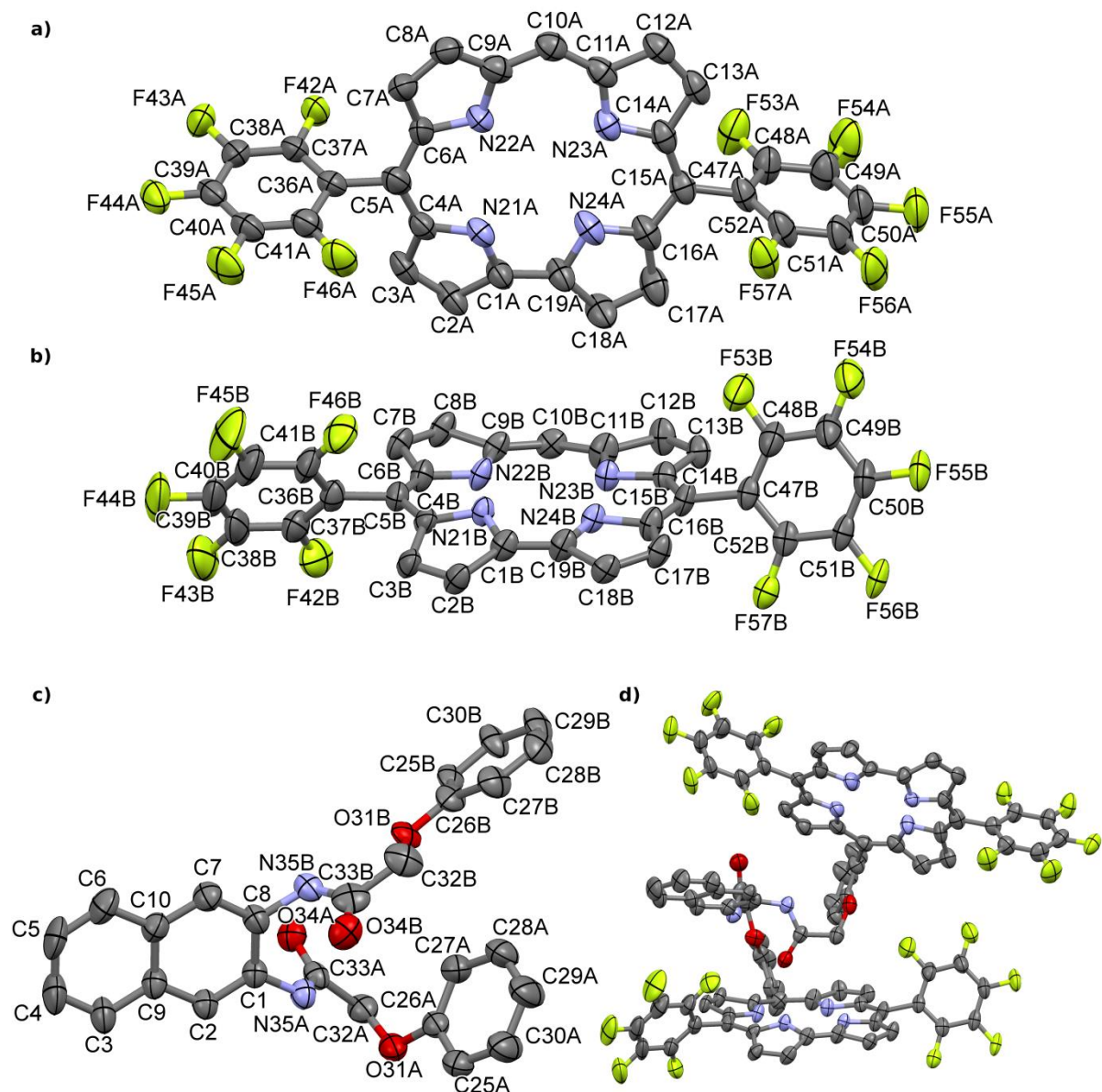


Figure S5 Numbering scheme and thermal ellipsoid at 50% probability level for molecules of **6** (component with higher occupancy) in **6A**: **a)** subunit (A), **b)** subunit (B), **c)** linker, **d)** whole molecule.

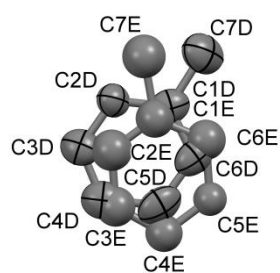


Figure S6 Numbering scheme and thermal ellipsoid at 50% probability level for molecule of toluene D and E.

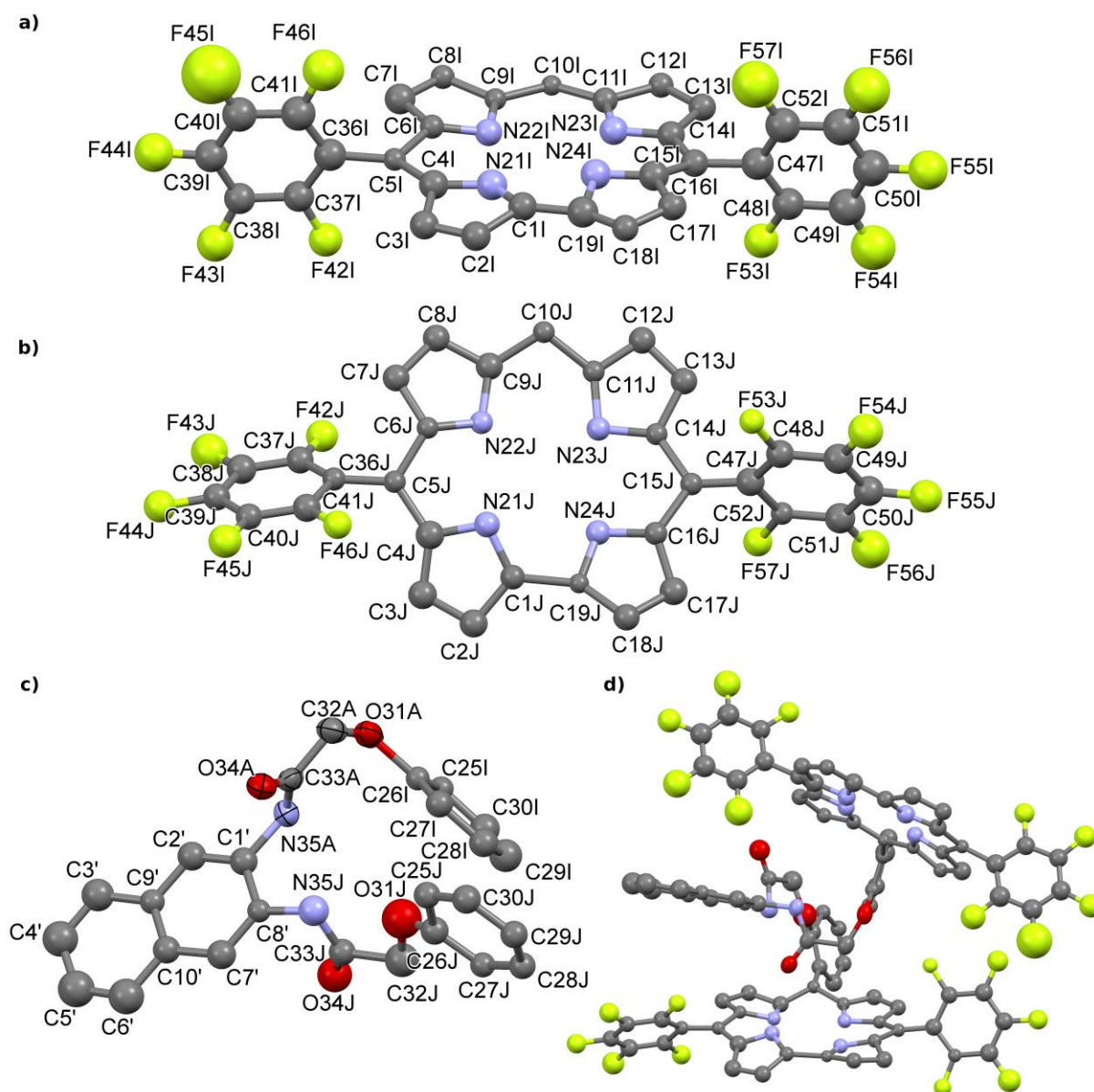


Figure S7 Numbering scheme and thermal ellipsoid at 50% probability level for molecules of **6** (component with lower occupancy) in **6A**: **a)** subunit (A), **b)** subunit (B), **c)** linker, **d)** whole molecule.

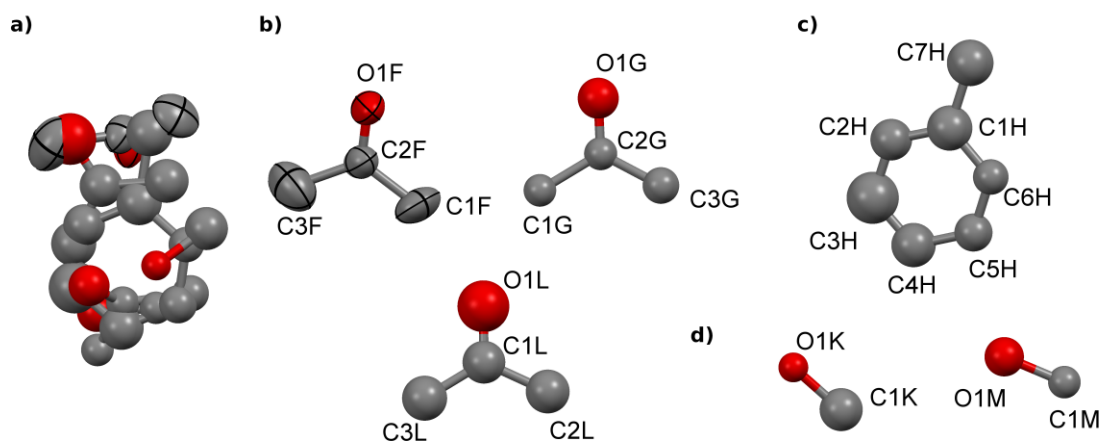


Figure S8 Numbering scheme and thermal ellipsoid at 50% probability level for molecules of acetone, toluene and methanol in **6A** **a)** all molecules, **b)** acetone, F, G and L, **c)** toluene, H, **d)** methanol, K and M.

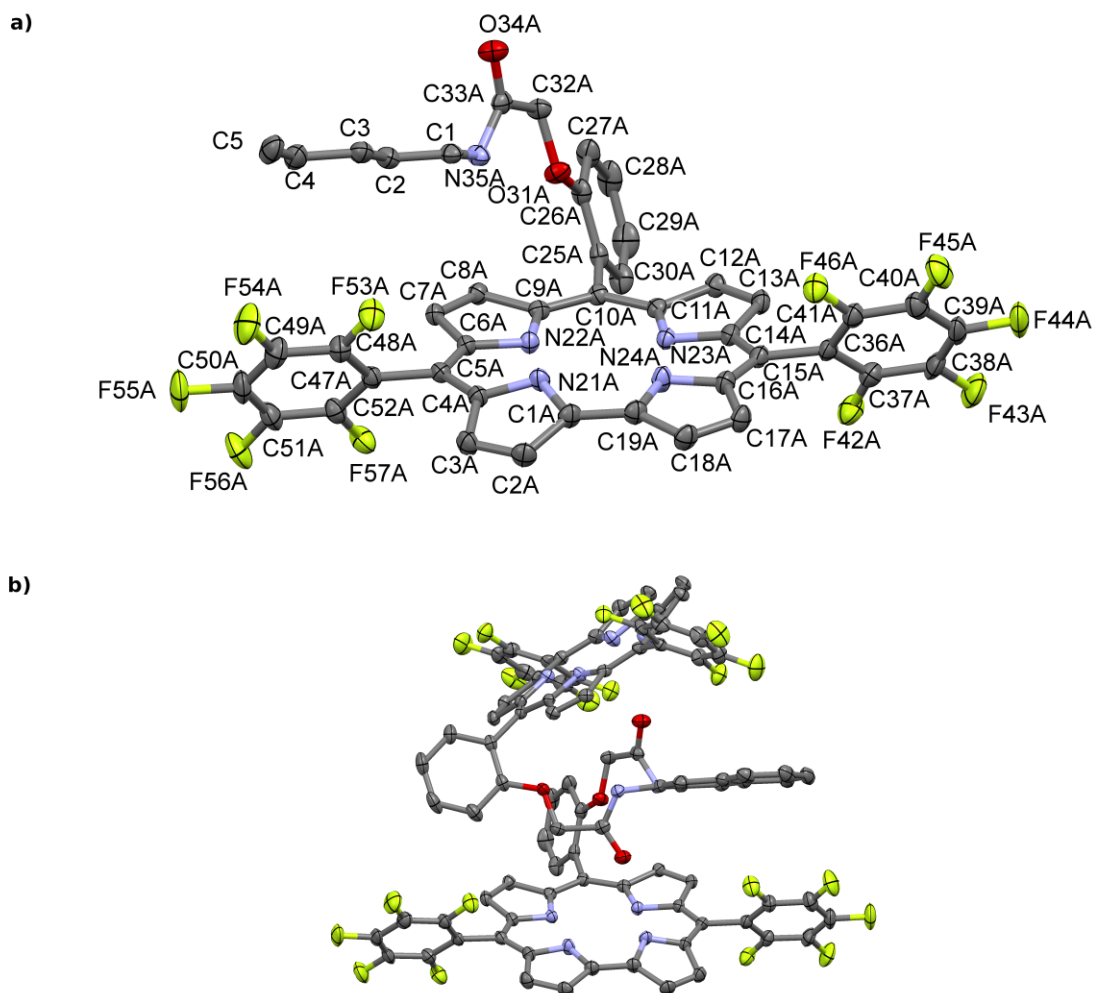


Figure S9 Numbering scheme and thermal ellipsoid at 50% probability level for molecules of **6** in **6B**: **a)** subunit (A) with linker, **b)** whole molecule.

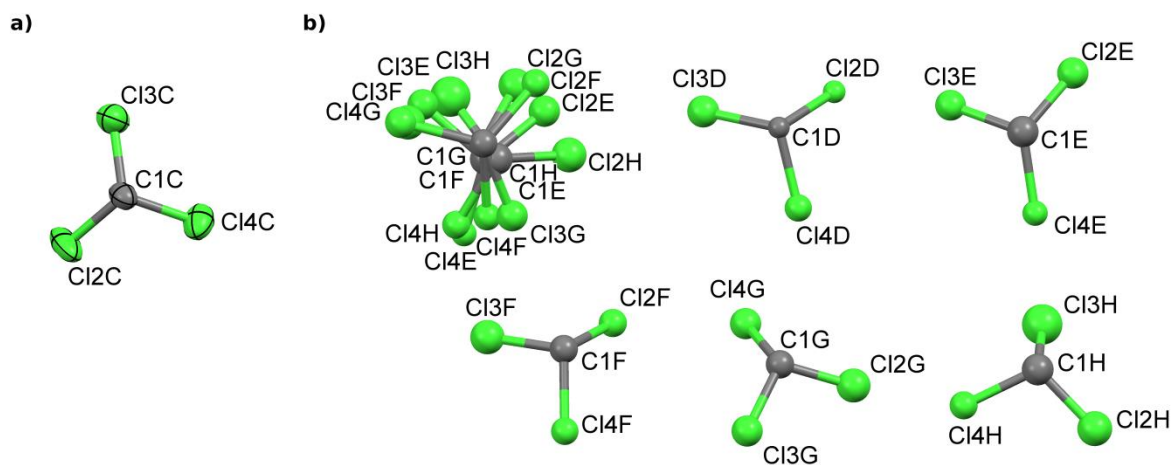


Figure S10 Numbering scheme and thermal ellipsoid at 50% probability level for molecules of trichloromethane in **6B** a) C, b) D, E, F, G and H.

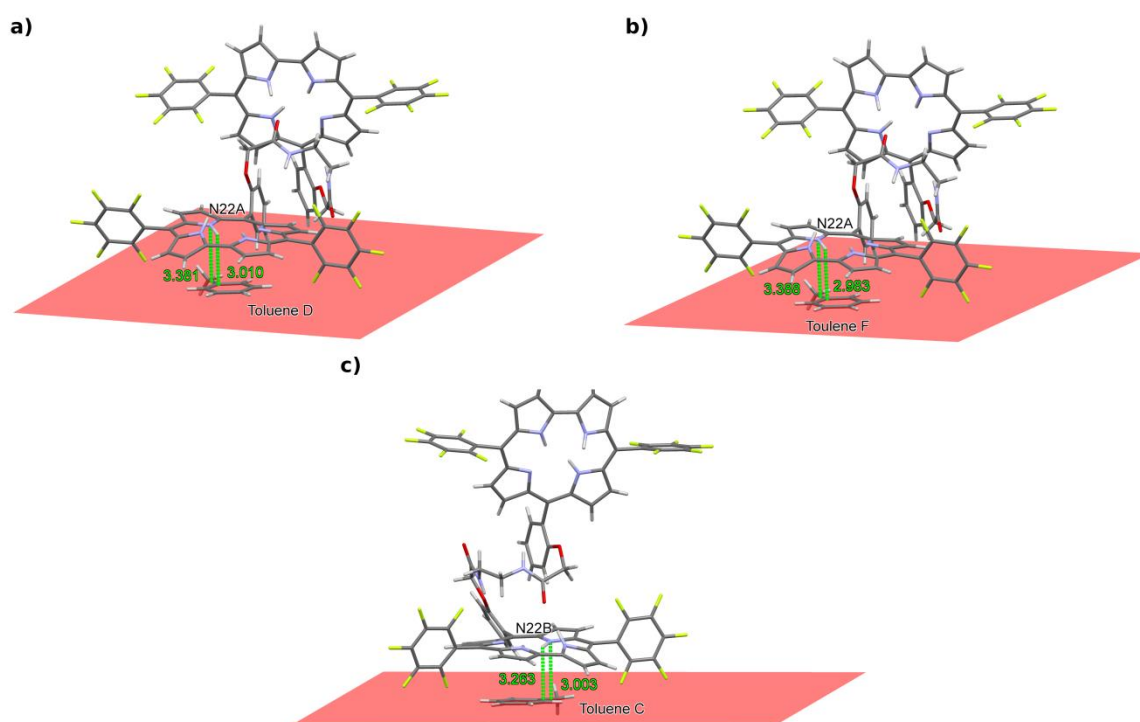


Figure S11 Estimated distances between pyrrole N, H atoms and fitted planes to toluene molecules in **5A** a) D, b) F, c) C.

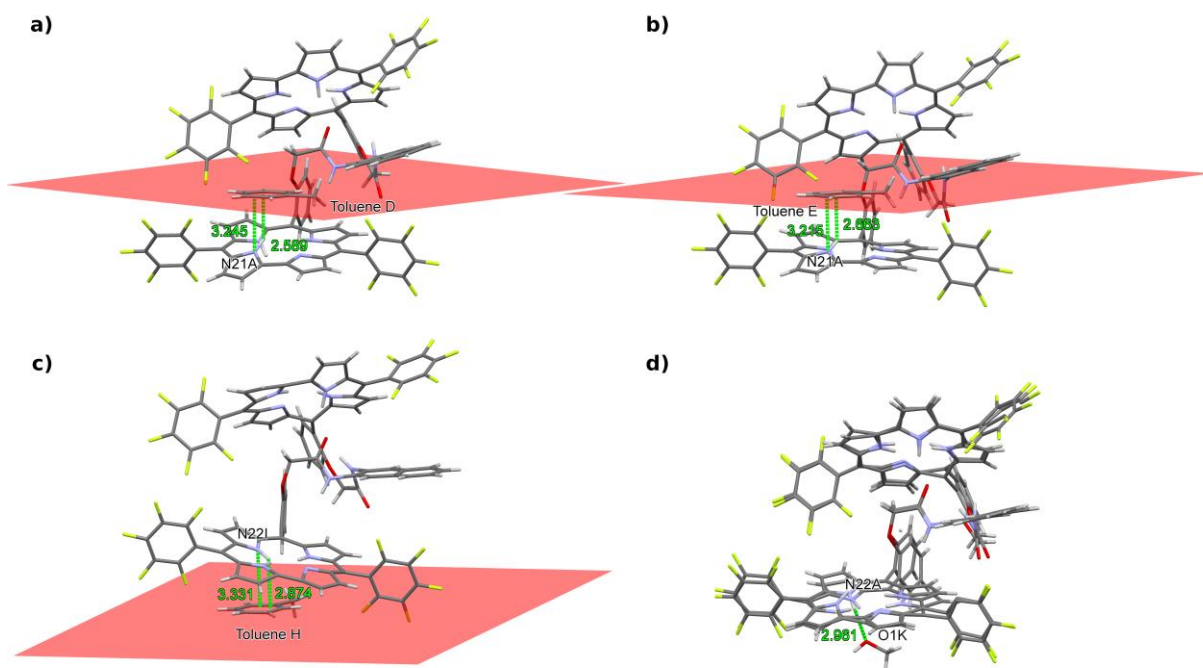


Figure S12 Estimated distances between pyrrole N, H atoms and fitted planes to toluene molecules in **5A** a) D, b) F, c) C d) Estimated distances between pyrrole N atom and methanol K.

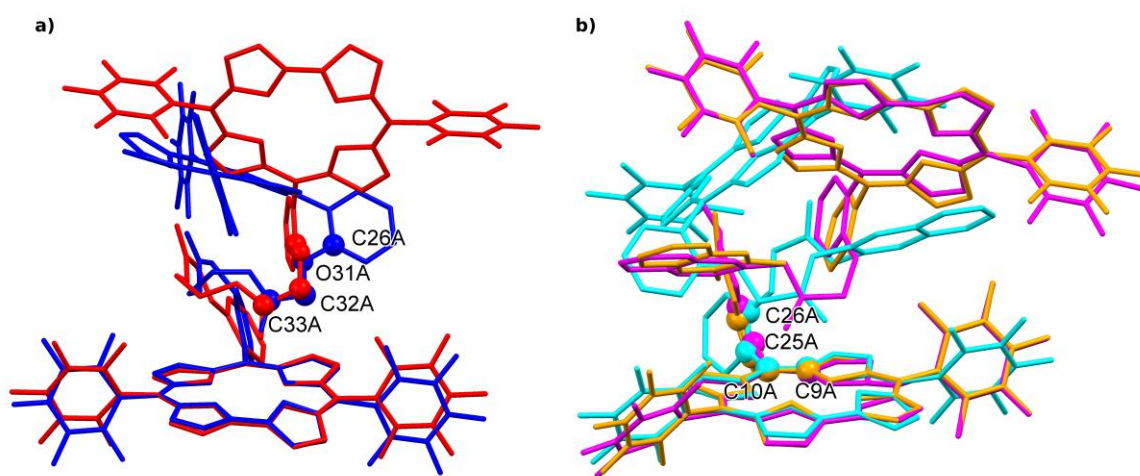


Figure S13 Definition of torsion angles a) Φ - for atoms C33A-C32A-O31A-C26A, b) Θ - for atoms C9A-C10A-C25A-C26A.

For each corrole moiety (atoms C1-C19 and N21-N24) least-squares planes (x,y,z in crystal coordinates) and deviations from them were calculated during the refinement procedure in Bruker SHELXTL Software Package [4]. Obtained parameters for structures **5A**, **5B**, **6A**, **6B** are presented below.

5A - Subunit (A)

$$21.8717 (0.0100) x - 3.5072 (0.0049) y + 7.9365 (0.0057) z = 11.6840 (0.0040)$$

Deviations for atoms:

- * 0.0827 (0.0037) C1A
- * -0.4777 (0.0037) C2A
- * -0.5169 (0.0036) C3A
- * 0.0225 (0.0036) C4A
- * 0.0670 (0.0036) C5A
- * 0.1007 (0.0036) C6A
- * 0.2023 (0.0037) C7A
- * 0.1082 (0.0037) C8A
- * -0.0200 (0.0036) C9A
- * -0.1278 (0.0035) C10A
- * -0.1248 (0.0035) C11A
- * -0.2548 (0.0033) C12A
- * -0.1856 (0.0034) C13A
- * -0.0128 (0.0035) C14A
- * 0.0776 (0.0034) C15A
- * 0.1778 (0.0036) C16A
- * 0.0237 (0.0037) C17A
- * -0.0056 (0.0037) C18A
- * 0.1506 (0.0037) C19A
- * 0.4007 (0.0032) N21A
- * 0.0012 (0.0032) N22A
- * 0.0248 (0.0030) N23A
- * 0.2860 (0.0032) N24A

Rms deviation of fitted atoms = 0.2091

5A - Subunit (B)

$$32.3415 (0.0056) x + 3.6395 (0.0055) y - 11.2198 (0.0053) z = 18.8613 (0.0057)$$

Deviations for atoms:

- * -0.0140 (0.0038) C1B
- * 0.4950 (0.0040) C2B
- * 0.5098 (0.0039) C3B
- * 0.0316 (0.0038) C4B
- * -0.0688 (0.0037) C5B
- * -0.1186 (0.0037) C6B
- * -0.3010 (0.0037) C7B
- * -0.2132 (0.0036) C8B
- * 0.0045 (0.0035) C9B
- * 0.1185 (0.0035) C10B
- * 0.1530 (0.0035) C11B
- * 0.3808 (0.0038) C12B
- * 0.2644 (0.0038) C13B
- * -0.0001 (0.0037) C14B
- * -0.1535 (0.0038) C15B
- * -0.2312 (0.0039) C16B
- * -0.1532 (0.0042) C17B
- * -0.0516 (0.0042) C18B
- * -0.1052 (0.0040) C19B
- * -0.2897 (0.0034) N21B
- * 0.0425 (0.0032) N22B

- * -0.0541 (0.0031) N23B
- * -0.2463 (0.0034) N24B

Rms deviation of fitted atoms = 0.2262

5B - Subunit (A)

$$2.9803 (0.0026) x - 1.0024 (0.0082) y + 12.2911 (0.0016) z = 5.7609 (0.0029)$$

Deviations for atoms:

- * 0.1350 (0.0021) C1A
- * -0.3086 (0.0022) C2A
- * -0.4294 (0.0022) C3A
- * -0.0553 (0.0021) C4A
- * -0.0682 (0.0021) C5A
- * -0.0209 (0.0021) C6A
- * 0.1876 (0.0021) C7A
- * 0.2320 (0.0021) C8A
- * 0.0354 (0.0021) C9A
- * 0.0411 (0.0020) C10A
- * -0.0618 (0.0020) C11A
- * -0.1602 (0.0020) C12A
- * -0.2070 (0.0020) C13A
- * -0.1041 (0.0019) C14A
- * -0.0288 (0.0019) C15A
- * 0.0929 (0.0019) C16A
- * 0.0772 (0.0019) C17A
- * 0.1227 (0.0020) C18A
- * 0.1834 (0.0020) C19A
- * 0.3107 (0.0019) N21A
- * -0.1180 (0.0018) N22A
- * -0.0426 (0.0017) N23A
- * 0.1870 (0.0018) N24A

Rms deviation of fitted atoms = 0.1735

5B - Subunit (B)

$$3.1204 (0.0026) x + 16.2104 (0.0075) y + 11.0761 (0.0019) z = 18.6846 (0.0020)$$

Deviations for atoms:

- * -0.0804 (0.0020) C1B
- * 0.5180 (0.0020) C2B
- * 0.5762 (0.0021) C3B
- * 0.0238 (0.0020) C4B
- * -0.0235 (0.0020) C5B_a
- * -0.1010 (0.0020) C6B
- * -0.2469 (0.0021) C7B
- * -0.2075 (0.0020) C8B
- * -0.0285 (0.0020) C9B
- * 0.0858 (0.0020) C10B
- * 0.1540 (0.0020) C11B
- * 0.2491 (0.0020) C12B
- * 0.2004 (0.0020) C13B
- * 0.0753 (0.0020) C14B
- * -0.0250 (0.0019) C15B
- * -0.1450 (0.0020) C16B
- * -0.1634 (0.0019) C17B
- * -0.1610 (0.0020) C18B
- * -0.1620 (0.0020) C19B
- * -0.3951 (0.0018) N21B
- * -0.0057 (0.0018) N22B
- * 0.0554 (0.0017) N23B
- * -0.1930 (0.0018) N24B

Rms deviation of fitted atoms = 0.2245

6A - Subunit (A) – main component

- 9.6460 (0.0106) x + 16.0219 (0.0390) y - 9.1770 (0.0129) z = 0.7162 (0.0304)

Deviations for atoms:

* 0.1036 (0.0121) C1A_a
* -0.3596 (0.0074) C2A_a
* -0.4128 (0.0090) C3A_a
* 0.0007 (0.0202) C4A_a
* 0.0067 (0.0165) C5A_a
* -0.0249 (0.0087) C6A_a
* 0.2381 (0.0177) C7A_a
* 0.2528 (0.0078) C8A_a
* -0.0356 (0.0077) C9A_a
* -0.0792 (0.0064) C10A_a
* -0.1095 (0.0060) C11A_a
* -0.1451 (0.0058) C12A_a
* -0.1086 (0.0055) C13A_a
* -0.0410 (0.0072) C14A_a
* 0.0177 (0.0068) C15A_a
* 0.0789 (0.0121) C16A_a
* 0.0587 (0.0102) C17A_a
* 0.0909 (0.0092) C18A_a
* 0.1691 (0.0076) C19A_a
* 0.3651 (0.0057) N21A_a
* -0.1762 (0.0086) N22A_a
* -0.0575 (0.0050) N23A_a
* 0.1676 (0.0140) N24A_a

Rms deviation of fitted atoms = 0.1780

6A - Subunit (B) – main component

1.1644 (0.0176) x + 4.6966 (0.0450) y + 15.4175 (0.0034) z = 4.5123 (0.0289)

Deviations for atoms:

* 0.0942 (0.0185) C1B_a
* -0.3937 (0.0122) C2B_a
* -0.3592 (0.0134) C3B_a
* 0.0983 (0.0196) C4B_a
* 0.1493 (0.0154) C5B_a
* 0.0415 (0.0142) C6B_a
* 0.2066 (0.0118) C7B_a
* 0.0907 (0.0102) C8B_a
* -0.0696 (0.0084) C9B_a
* -0.2489 (0.0084) C10B_a
* -0.1380 (0.0133) C11B_a
* -0.0653 (0.0091) C12B_a
* 0.0218 (0.0076) C13B_a
* 0.0289 (0.0079) C14B_a
* 0.0708 (0.0119) C15B_a
* 0.0541 (0.0187) C16B_a
* 0.0260 (0.0114) C17B_a
* -0.0012 (0.0134) C18B_a
* 0.0607 (0.0150) C19B_a
* 0.3545 (0.0150) N21B_a
* -0.0894 (0.0098) N22B_a
* -0.0768 (0.0092) N23B_a
* 0.1447 (0.0071) N24B_a

Rms deviation of fitted atoms = 0.1670

6A - Subunit (A) – secondary component

- 8.9730 (0.0459) x + 15.6870 (0.1684) y - 10.0149 (0.0495) z = 0.0619 (0.1302)

Deviations for atoms:

* 0.0697 (0.0521) C1I_b
* -0.2115 (0.0363) C2I_b
* -0.3079 (0.0444) C3I_b
* -0.0179 (0.0871) C4I_b
* -0.0425 (0.0554) C5I_b
* 0.1204 (0.0338) C6I_b
* 0.3361 (0.0852) C7I_b
* 0.1753 (0.0297) C8I_b
* -0.0726 (0.0287) C9I_b
* -0.0517 (0.0227) C10I_b
* -0.0873 (0.0255) C11I_b
* -0.0567 (0.0249) C12I_b
* -0.0897 (0.0262) C13I_b
* -0.1197 (0.0321) C14I_b
* -0.0897 (0.0326) C15I_b
* 0.2320 (0.0617) C16I_b
* 0.2094 (0.0478) C17I_b
* 0.1095 (0.0339) C18I_b
* -0.0517 (0.0389) C19I_b
* -0.0137 (0.0284) N21I_b
* -0.1654 (0.0385) N22I_b
* -0.1160 (0.0249) N23I_b
* 0.2417 (0.0616) N24I_b

Rms deviation of fitted atoms = 0.1568

6A - Subunit (B) – secondary component

1.4083 (0.0457) x + 4.2030 (0.1306) y + 15.4098 (0.0091) z = 4.1374 (0.0826)

Deviations for atoms:

* 0.0587 (0.0564) C1J_b
* -0.2979 (0.0252) C2J_b
* -0.3562 (0.0311) C3J_b
* 0.0209 (0.0707) C4J_b
* 0.1002 (0.0435) C5J_b
* 0.1873 (0.0366) C6J_b
* 0.1056 (0.0360) C7J_b
* 0.0011 (0.0303) C8J_b
* -0.1712 (0.0310) C9J_b
* 0.2492 (0.0224) C10J_b
* -0.0685 (0.0353) C11J_b
* -0.1224 (0.0268) C12J_b
* -0.0956 (0.0250) C13J_b
* -0.1375 (0.0210) C14J_b
* 0.1046 (0.0320) C15J_b
* 0.1743 (0.0502) C16J_b
* 0.0917 (0.0216) C17J_b
* 0.0551 (0.0299) C18J_b
* 0.0671 (0.0366) C19J_b
* 0.4064 (0.0471) N21J_b
* -0.1536 (0.0274) N22J_b
* -0.1539 (0.0306) N23J_b
* -0.0653 (0.0227) N24J_b

Rms deviation of fitted atoms = 0.1731

6B - Subunit (A)

$$24.3251 (0.0039) x + 4.7499 (0.0033) y + 3.4106 (0.0059) z = 13.4964 (0.0024)$$

Deviations for atoms:

- * 0.1115 (0.0028) C1A
- * -0.3088 (0.0028) C2A
- * -0.3269 (0.0028) C3A
- * 0.0852 (0.0027) C4A
- * 0.0833 (0.0025) C5A
- * 0.0320 (0.0025) C6A
- * 0.1488 (0.0024) C7A
- * 0.0731 (0.0024) C8A
- * -0.0788 (0.0024) C9A
- * -0.0978 (0.0024) C10A
- * -0.1360 (0.0024) C11A
- * -0.0157 (0.0025) C12A
- * 0.0376 (0.0025) C13A
- * -0.0495 (0.0025) C14A
- * 0.0598 (0.0026) C15A
- * 0.1066 (0.0027) C16A
- * -0.0535 (0.0027) C17A
- * -0.0721 (0.0028) C18A
- * 0.1040 (0.0028) C19A
- * 0.3790 (0.0024) N21A
- * -0.1325 (0.0022) N22A
- * -0.1758 (0.0022) N23A
- * 0.2264 (0.0025) N24A

Rms deviation of fitted atoms = 0.1578

2. The NMR spectroscopy

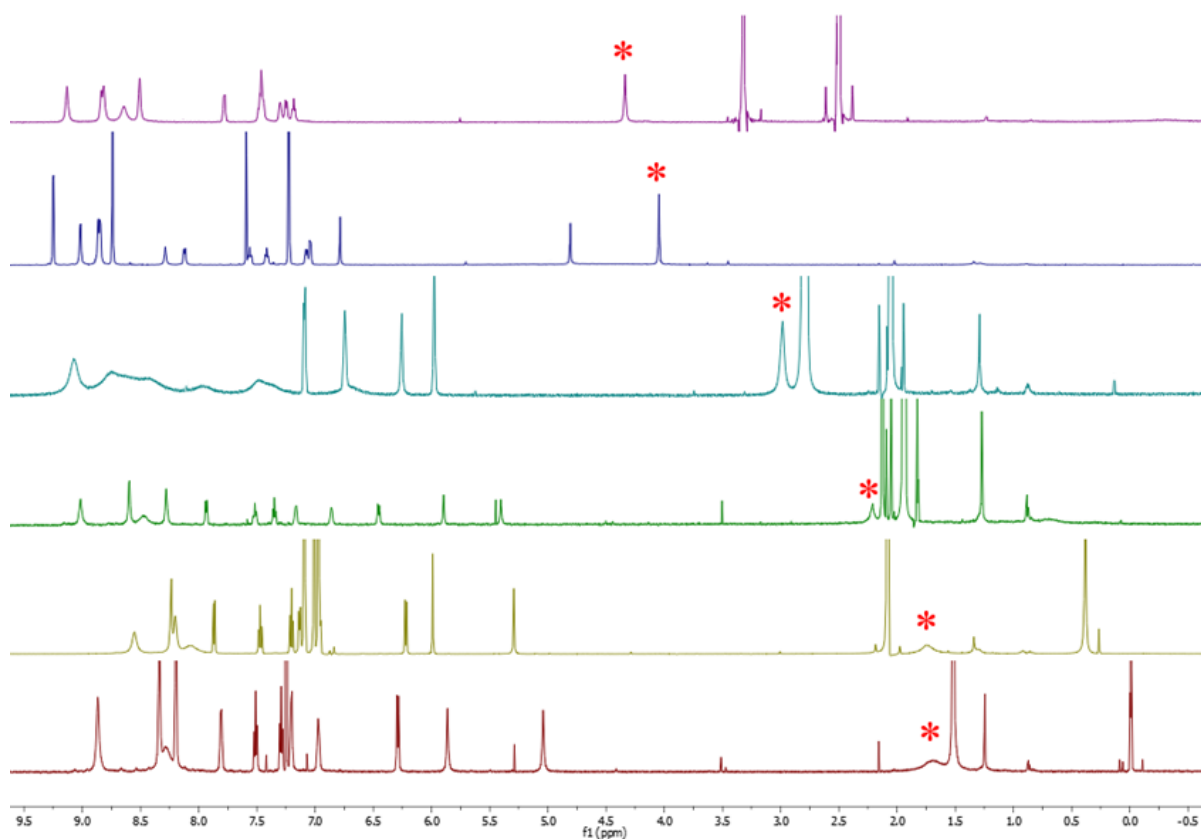


Figure S14. Position of $-\text{OCH}_2\text{C}(\text{O})-$ signals (*) in **6**. From top to bottom: DMSO, pyridine, acetone, acetonitrile, toluene and chloroform.

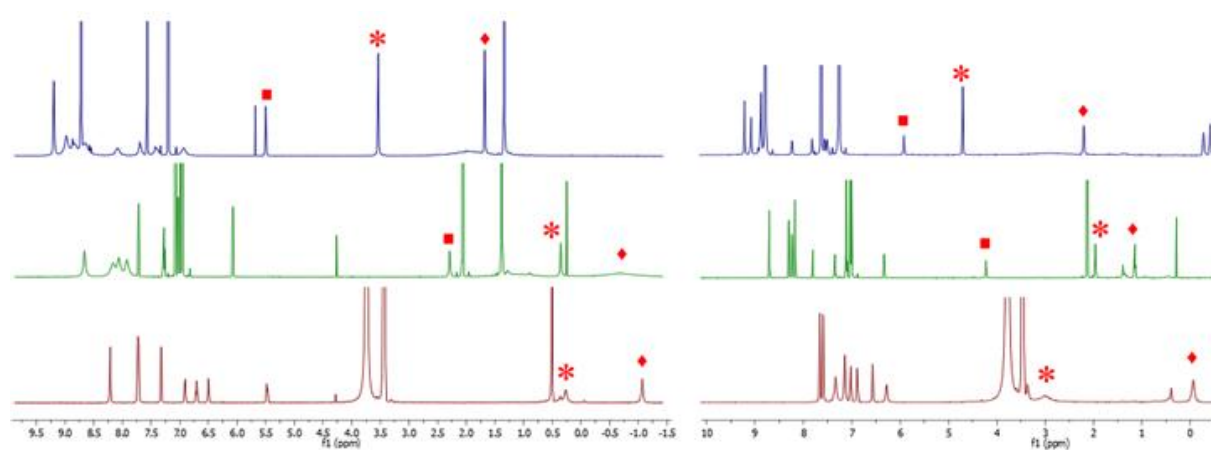


Figure S15. Comparison of $-\text{OCH}_2\text{C}(\text{O})-$ (*), $-\text{C}(\text{O})\text{NH}-$ (■) and $-\text{NHCH}_2-$ (◆) signals positions in **5** (left spectrum) and **3** (right spectrum). From top to bottom: pyridine, toluene and HFIP.

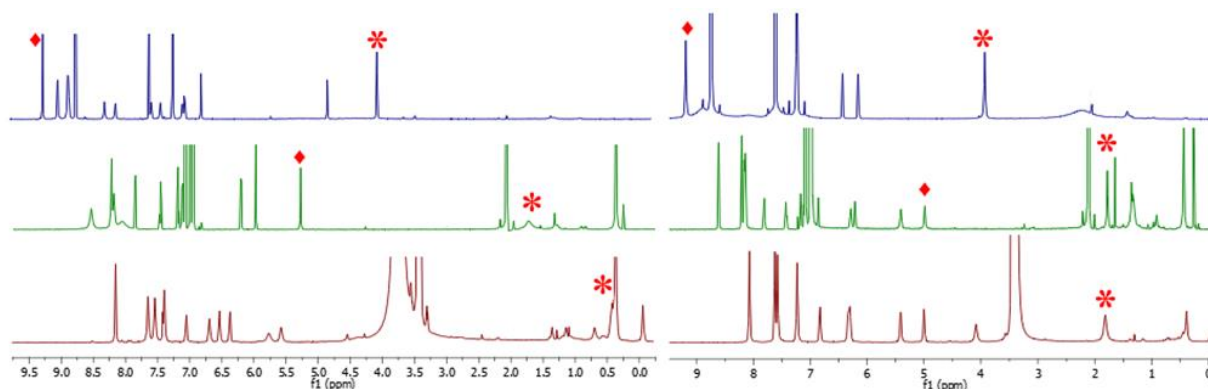


Figure S16. Comparison of $-\text{OCH}_2\text{C}(\text{O})-$ (*) and $-\text{C}(\text{O})\text{NH}-$ (■) signals positions in **6** (left spectrum) and **4** (right spectrum). From top to bottom: pyridine, toluene and HFIP.

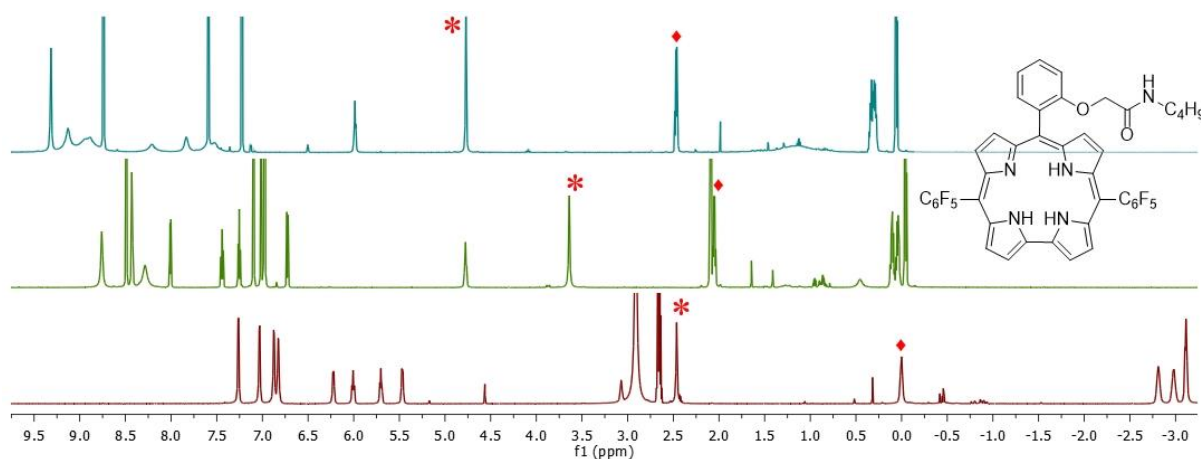


Figure S17. Comparison of $-\text{OCH}_2\text{C}(\text{O})-$ (*) and $-\text{NHCH}_2-$ (◆) signals positions in 10-[2-(N-Butylcarbamoylmethoxy)phenyl]-5,15-bis(pentafluorophenyl)corrole. From top to bottom: pyridine, toluene and HFIP.

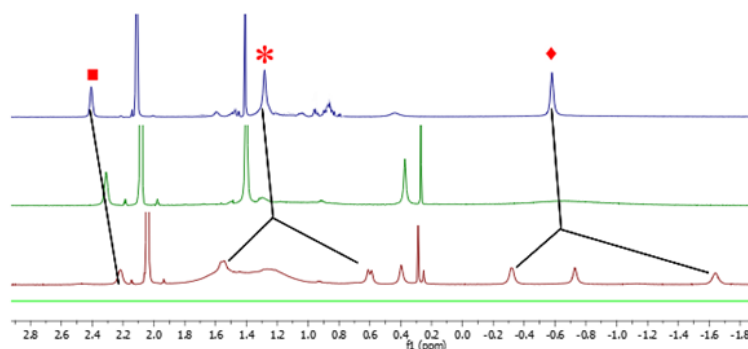


Figure S18. Position of $-\text{C}(\text{O})\text{NH}-$ (■) signals and split of $-\text{OCH}_2\text{C}(\text{O})-$ (*) and $-\text{NHCH}_2-$ (◆) signals in **5**. From top to bottom: 80 °C, 25 °C and -40 °C.

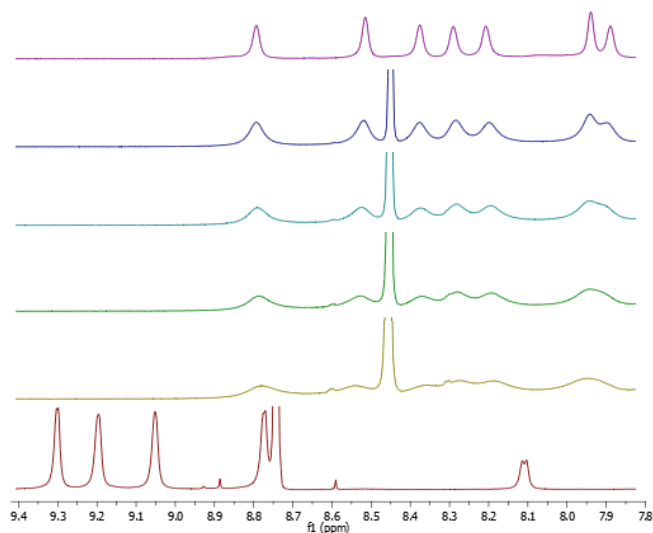


Figure S19. ¹H NMR spectra of **5**. From top to bottom: toluene; toluene and 1 eq. pyridine, toluene and 2 eq. pyridine, toluene and 3 eq. pyridine, toluene and 5 eq. pyridine, pyridine.

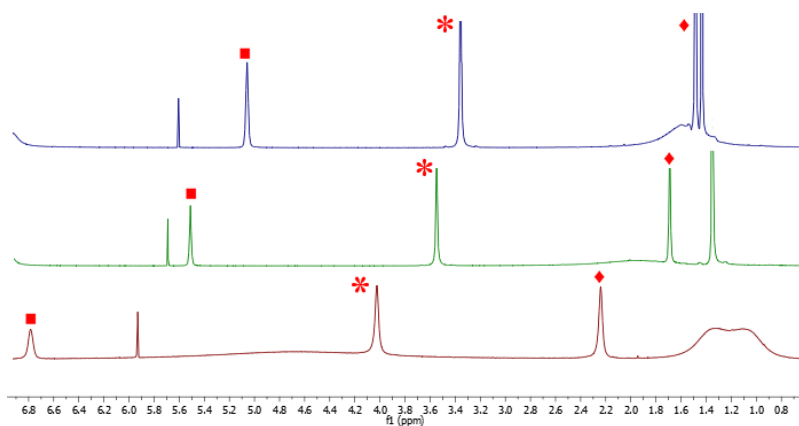


Figure S20. Influence of temperature on **5** spectrum on $-\text{OCH}_2\text{C}(\text{O})-$ (*), $-\text{C}(\text{O})\text{NH}-$ (■) and $-\text{NHCH}_2-$ (◆) signals in pyridine. From top to bottom: 80 °C, 25 °C and -40 °C.

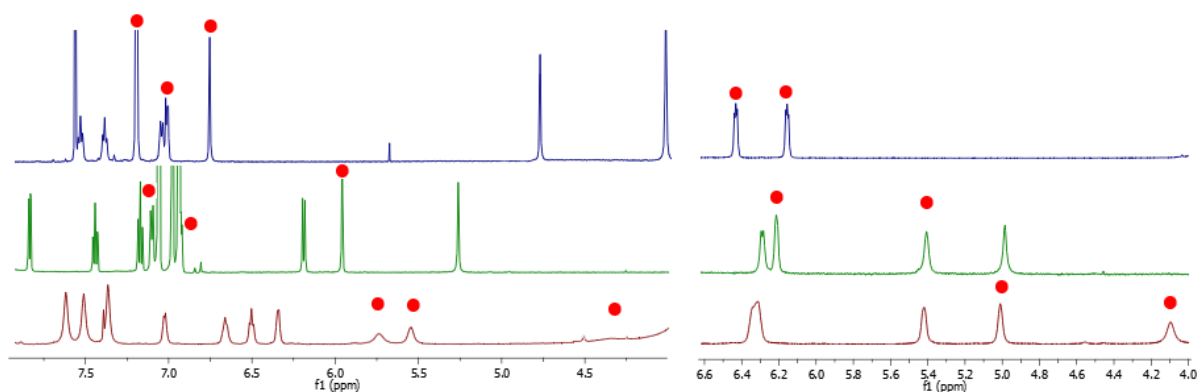
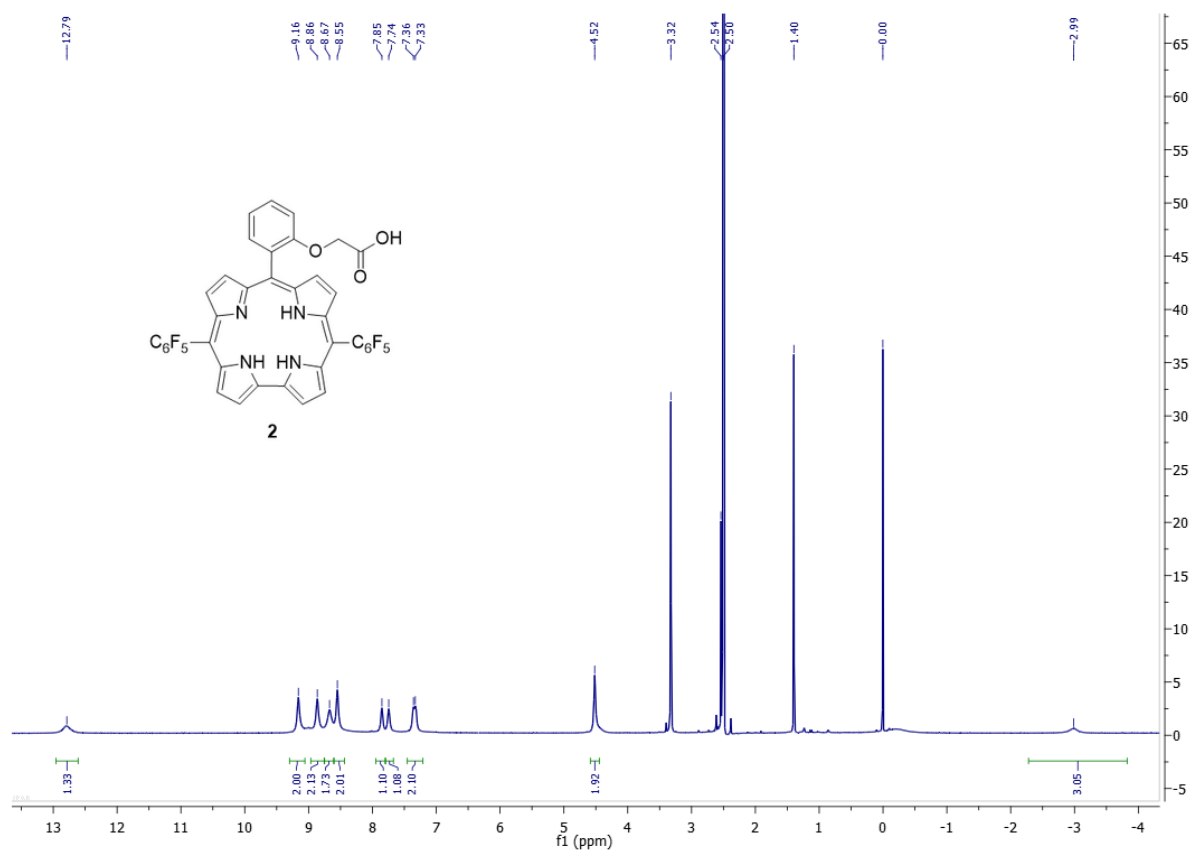
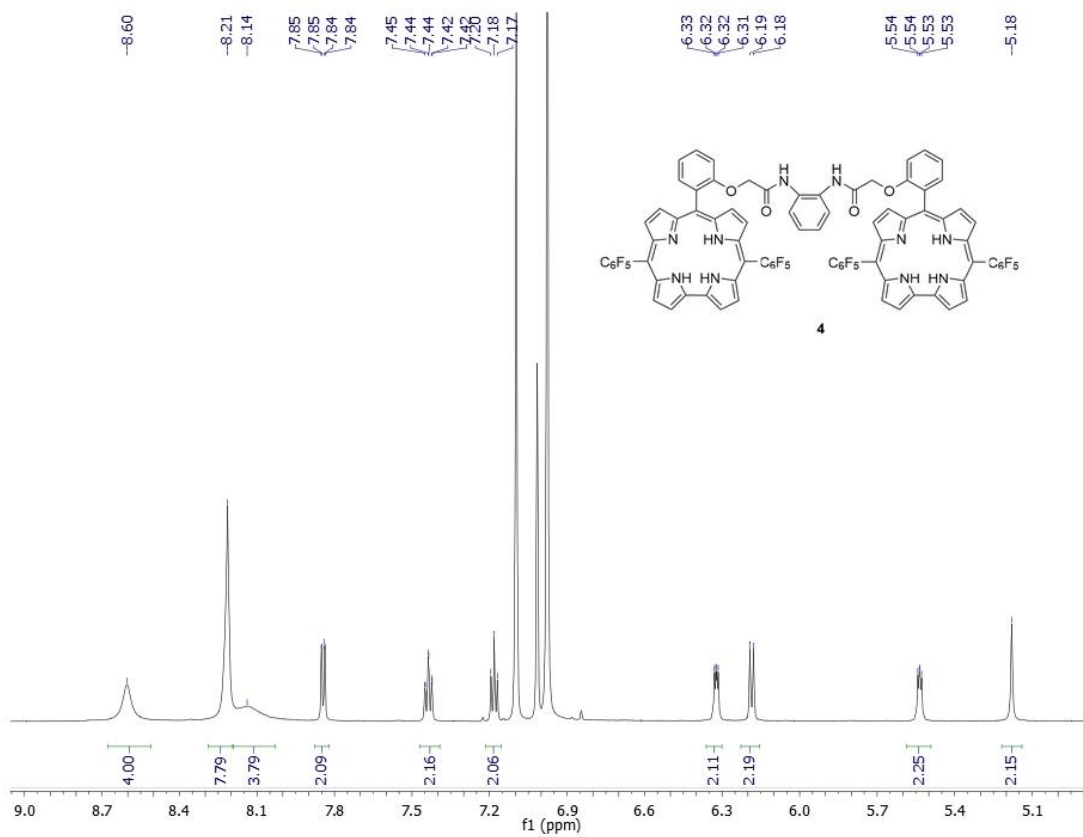
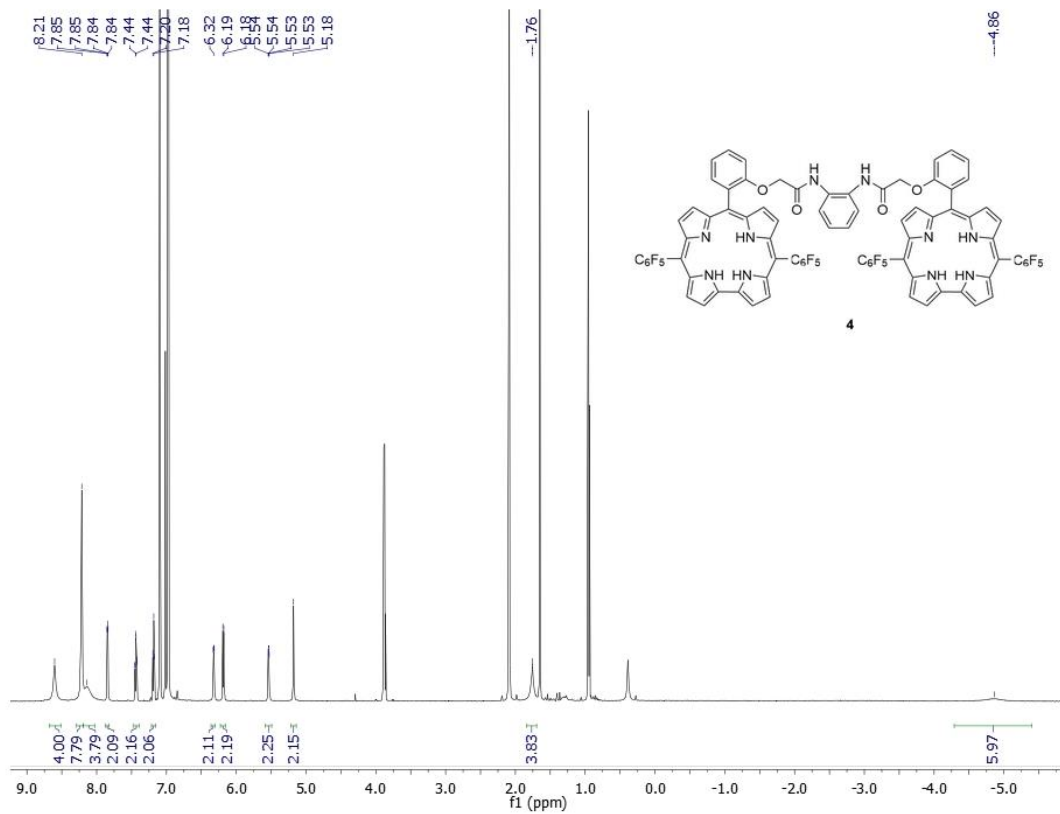


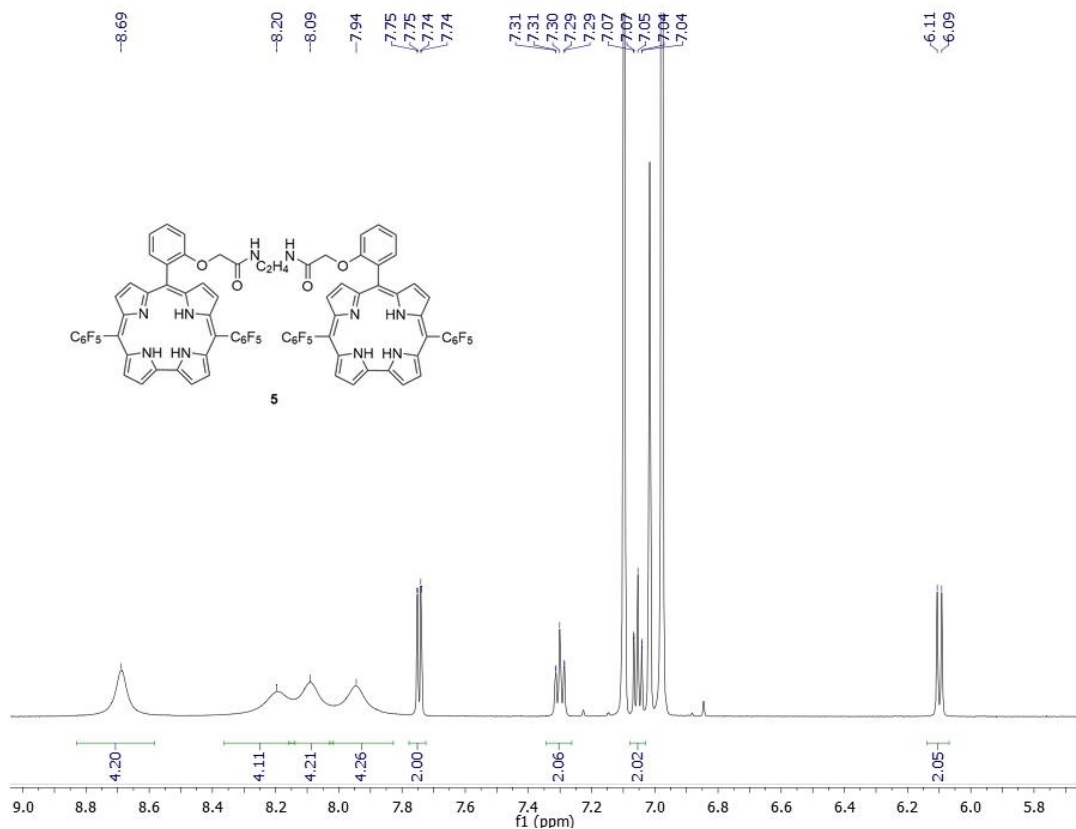
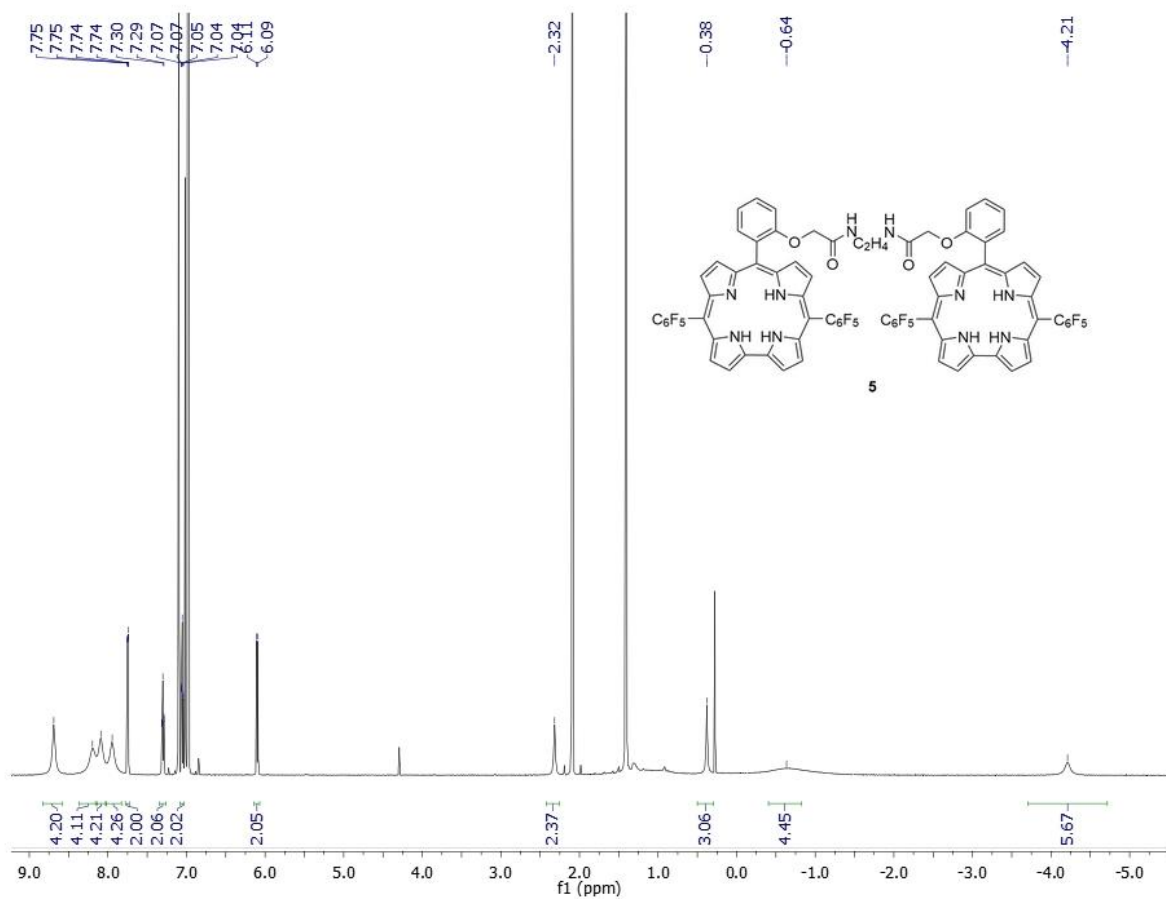
Figure S21. The aromatic signals positions in **6** (left spectrum) and **4** (right spectrum). From top to bottom: pyridine, toluene and HFIP.

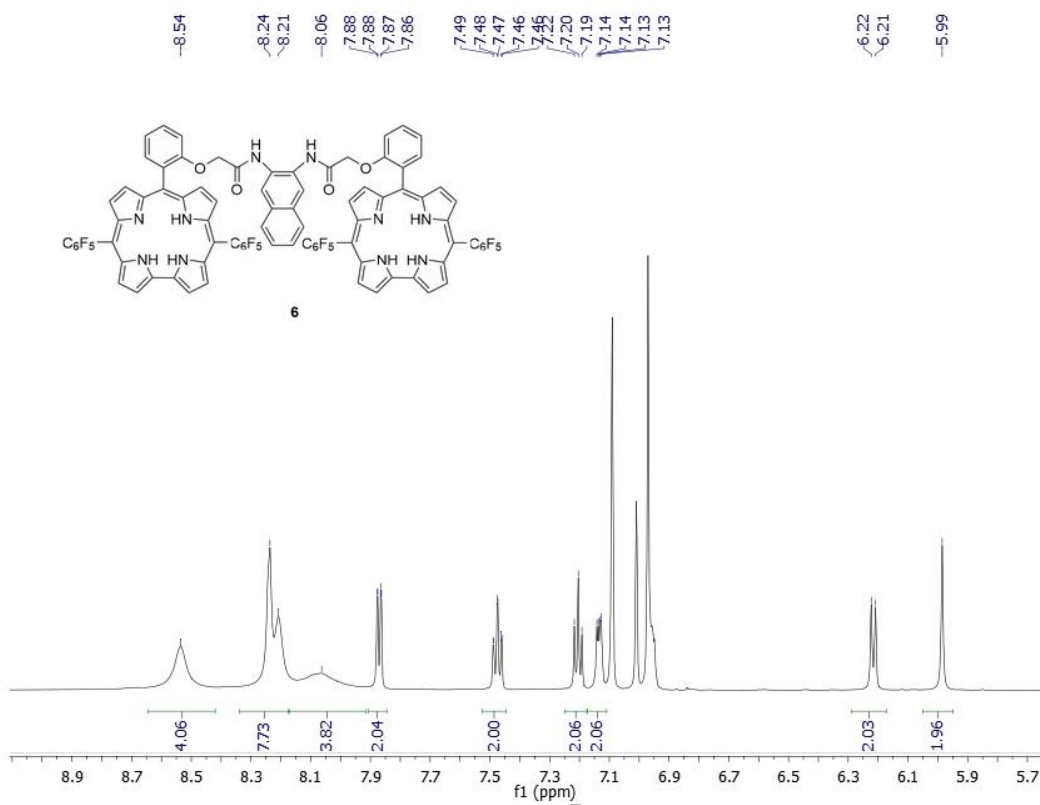
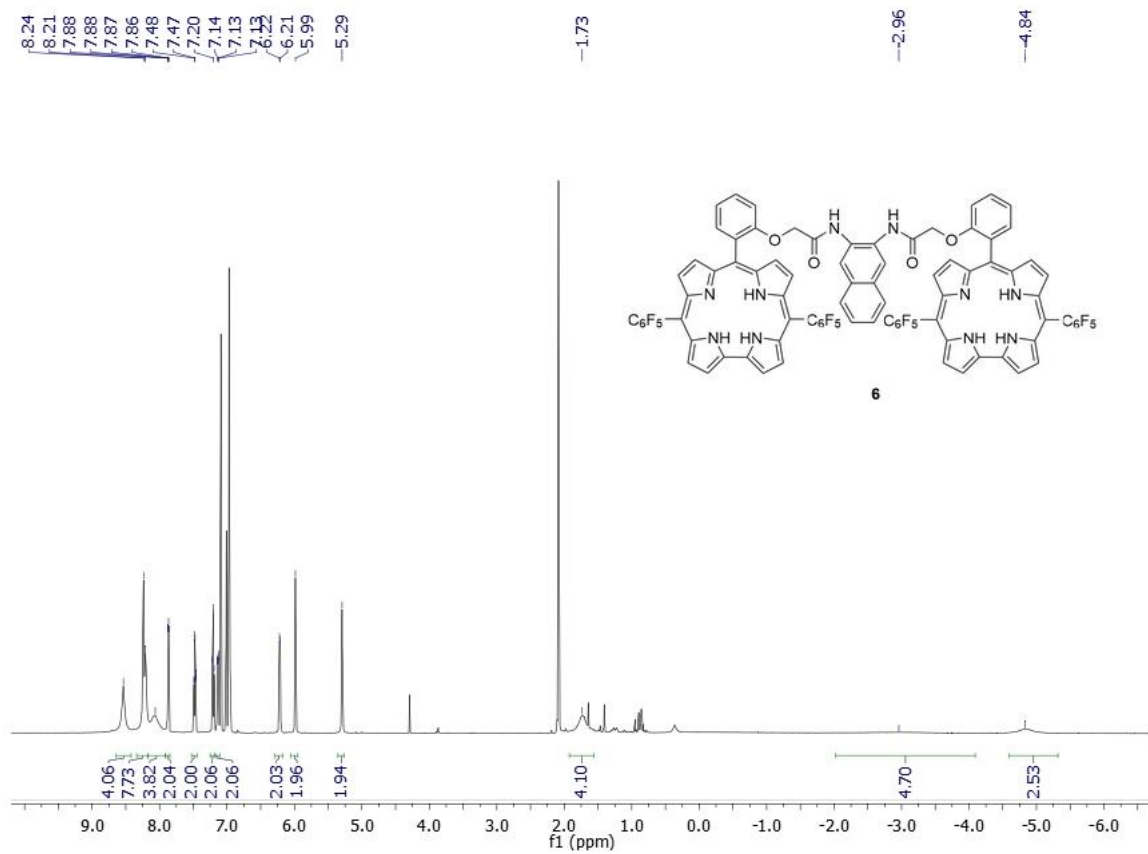
Figure S22

3. ¹H NMR spectra for synthesized compounds









5. References

- [1] APEX2,. Bruker AXS Inc., Madison, Wisconsin, USA, **2013**.
- [2] SAINT,. Bruker AXS Inc., Madison, Wisconsin, USA, **2013**.
- [3] SADABS,. Bruker AXS Inc., Madison, Wisconsin, USA, **2012**.
- [4] G. M. Sheldrick, *Acta Crystallogr.* **1990**, A46, 467-473; Sheldrick, G. M. *Acta Cryst.*, **2008**, A64, 112–122.
- [5] *International Tables for Crystallography*, Ed. A. J. C. Wilson, Kluwer: Dordrecht, **1992**, Vol.C.
- [6] C. F. Macrae, I. J. Bruno, J. A. Chisholm, P. R. Edgington, P. McCabe, E. Pidcock, L. Rodriguez-Monge, R. Taylor, J. van de Streek and P. A. Wood, *J. Appl. Cryst.*, **2008**, 41, 466-470.



Role of intramolecular hydrogen bonds in promoting electron flow through amino acid and oligopeptide conjugates

Rafał Orłowski^{a,1}, John A. Clark^{b,1}, James B. Derr^c, Eli M. Espinoza^{d,2}, Maximilian F. Mayther^d, Olga Staszewska-Krajewska^a, Jay R. Winkler^e, Hanna Jędrzejewska^a, Agnieszka Szumna^a, Harry B. Gray^{e,3}, Valentine I. Vullev^{b,c,d,3}, and Daniel T. Gryko^{a,3}

^aInstitute of Organic Chemistry, Polish Academy of Sciences, 01-224 Warsaw, Poland; ^bDepartment of Bioengineering, University of California, Riverside, CA 92521; ^cDepartment of Biochemistry, University of California, Riverside, CA 92521; ^dDepartment of Chemistry, University of California, Riverside, CA 92521; and ^eDivision of Chemistry and Chemical Engineering, California Institute of Technology, Pasadena, CA 91125

Contributed by Harry B. Gray, January 17, 2021 (sent for review December 28, 2020; reviewed by David N. Beratan and David I. Schuster)

Elucidating the factors that control charge transfer rates in relatively flexible conjugates is of importance for understanding energy flows in biology as well as assisting the design and construction of electronic devices. Here, we report ultrafast electron transfer (ET) and hole transfer (HT) between a corrole (Cor) donor linked to a perylene-diimide (PDI) acceptor by a tetrameric alanine (Ala)₄. Selective photoexcitation of the donor and acceptor triggers subpicosecond and picosecond ET and HT. Replacement of the (Ala)₄ linker with either a single alanine or phenylalanine does not substantially affect the ET and HT kinetics. We infer that electronic coupling in these reactions is not mediated by tetrapeptide backbone nor by direct donor–acceptor interactions. Employing a combination of NMR, circular dichroism, and computational studies, we show that intramolecular hydrogen bonding brings the donor and the acceptor into proximity in a “scorpion-shaped” molecular architecture, thereby accounting for the unusually high ET and HT rates. Photoinduced charge transfer relies on a (Cor)NH⁺···O=C–NH⁺···O=C(PDI) electronic-coupling pathway involving two pivotal hydrogen bonds and a central amide group as a mediator. Our work provides guidelines for construction of effective donor–acceptor assemblies linked by long flexible bridges as well as insights into structural motifs for mediating ET and HT in proteins.

charge transfer | hydrogen bonding | corrole | folding | perylene diimide

Many vital biological processes, including photosynthesis (1, 2), enzyme catalysis (3–5), and DNA repair (6–9), rely on electron transfer (ET) through proteins and nucleic acids (10–12). As the redox centers and chromophores mediating charge transfer (CT) are normally separated by relatively long molecular distances (>1 nm), the rates of ET and hole transfer (HT) depend critically on the media between donors and acceptors. It follows that the folding of biopolymer backbones plays a key role in governing CT properties.

Owing to the complexities of studying ET processes in biomacromolecules, model systems composed of donor and acceptor units located at the termini of oligomeric bridges have been employed to gain insight into the factors that control the redox behavior of biological systems. The evolution of biomimetic and bioinspired molecular devices also has become a major driving force for such studies (13). Despite the inherent flexibility of natural biomolecular oligomers, rigid bridges are common for the myriad of synthetic CT systems (10, 14–19). The difficulty in accounting for conformational dynamics has plagued interpretations of CT through peptides (20–22) and foldamers (23–25).

Long-range ET through covalent bonds in donor–bridge–acceptor (DBA) complexes has been the subject of numerous investigations over the last 40 years (10–12, 26). Of particular interest has been work on rigidly linked donor–acceptor units in Ru-modified proteins that has provided experimentally validated

tunneling timetables for interpretation and prediction of ET rates in structurally characterized DBA systems (10). Theoretical work by Beratan and others (27) has shed light on the factors that control these couplings both in small molecular DBA complexes and Ru-proteins.

Less well understood are couplings through solvents and other noncovalent molecular assemblies, most especially those in DBA complexes that feature B-group hydrogen-bond interactions (28, 29). In work reported here, we employ amino acids and an oligopeptide as bridges in corrole (Cor)–peptide–perylene-diimide (PDI) DBA conjugates in order to elucidate the role of hydrogen bonds in mediating biomimetic ET reactions. Specifically, we focus attention on a tetrapeptide bridging group, (Ala)₄, which if extended would separate D and A and greatly diminish through-bond coupling. For comparison purposes, we also have investigated related DBA systems, one with a single alanine (Ala), another with phenylalanine (Phe) (Fig. 1). Varying the number of bridging residues between one and four does not drastically alter the excited-state dynamics of the DBA conjugates. Here, we show that intramolecular hydrogen bonding opens efficient DBA electronic coupling pathways for these CT reactions.

Significance

Long-range electron transfer pervades biology, chemistry, and engineering, as it is critical for life-sustaining processes, chemical transformations, energy conversion, as well as electronic and photonic technologies. Elucidating the factors that control the rates of long-range electron transfer remains an outstanding challenge, owing in part to the complexity of proteins and other macromolecular structures that mediate such processes. We have found that short peptides linking electron donors and acceptors can assume folds with intramolecular hydrogen bond interactions that provide electronic-coupling pathways for ultrafast charge transfer. Our work will assist designs of donor–acceptor systems for efficient energy conversion and storage.

Author contributions: R.O., V.I.V., and D.T.G. designed research; R.O., J.A.C., J.B.D., E.M.E., M.F.M., O.S.-K., and H.J. performed research; J.R.W., A.S., H.B.G., V.I.V., and D.T.G. analyzed data; and R.O., J.A.C., J.R.W., H.B.G., V.I.V., and D.T.G. wrote the paper.

Reviewers: D.N.B., Duke University; and D.I.S., New York University.

The authors declare no competing interest.

Published under the [PNAS license](#).

¹R.O. and J.A.C. contributed equally to this work.

²Present address: College of Bioengineering, University of California, Berkeley, CA 94720.

³To whom correspondence may be addressed. Email: hbgray@caltech.edu, vullev@ucr.edu, or dtgryko@icho.edu.pl.

This article contains supporting information online at <https://www.pnas.org/lookup/suppl/doi:10.1073/pnas.2026462118/-DCSupplemental>.

Published March 11, 2021.

Supporting information for:

Role of intramolecular hydrogen bonds in promoting electron flow through amino-acid and oligopeptide conjugates

Rafał Orłowski^{a,=}, John A. Clark^{b,=}, James B. Derr^c, Eli M. Espinoza^{d,#}, Maximilian F. Mayther^d, Olga Staszewska-Krajewska^a, Jay R. Winkler^e, Hanna Jędrzejewska,^a Agnieszka Szumna,^a Harry B. Gray^{e,*}, Valentine I. Vullev^{b,c,d,f,*}, Daniel T. Gryko^{a,*}

^a Institute of Organic Chemistry, Polish Academy of Sciences, Kasprzaka 44/52, 01-224 Warsaw (Poland)

^b Department of Bioengineering, University of California, Riverside, CA 92521 (USA)

^c Department of Biochemistry, University of California, Riverside, CA 92521 (USA)

^d Department of Chemistry, University of California, Riverside, CA 92521 (USA)

^e Division of Chemistry and Chemical Engineering, California Institute of Technology, 1200 E California Blvd, Pasadena, CA 91125 (USA)

^f Materials Science & Engineering Program, University of California, Riverside, CA 92521 (USA)

⁼ Authors have equal contributions to the work presented in this publication.

[#] Present address: College of Bioengineering, University of California, Berkeley, CA 94720 (USA)

* Daniel T. Gryko , Valentine I. Vullev, Harry B. Gray

Email: dtgryko@icho.edu.pl, vullev@ucr.edu, hbgray@caltech.edu

Table of Contents

- 1. Synthetic procedures S3-S5**
- 2. NMR spectra S6-S17**
- 3. Electrochemical analysis S18**
- 4. Steady-state optical spectroscopy S18-S19**
- 5. Time-resolved optical spectroscopy S19-S24**
- 6. Computational analysis S25-S62**
- 7. References S63**

1. Synthetic procedures

All the reactions were carried out in flame-dried glassware in argon atmosphere. Required chemicals were purchased from Sigma-Aldrich and used without further purification. Fmoc-protected tetra-*L*-alanine was bought from ChinaPeptides and used as received. DMF was dried using solvent purification system. The reaction progress was monitored by thin layer chromatography (TLC, aluminum plates coated with silica gel, Merck 60, F-254) and visualized via UV lamp. The ¹H, ¹³C NMR spectra were measured at temperature 298 K in CDCl₃ (if not otherwise stated) solutions with a Varian vnmrs-600, using tetramethylsilane (TMS) as internal standard. The structures of the compounds studied were confirmed by 2D NMR spectra: COSY, ¹H–¹³C HSQC, ¹H–¹³C HMBC, ROESY. Due to the compound dynamics values given with the “u” appendix are averaged from two signals. Perylene bisimide derivatives **1**, **15** and corrole **8** were synthesized according to the reported procedures.^(1,2)

General procedure for compounds **5-7**: Perylene **1** (101 mg, 0.192 mmol), HATU (73 mg, 0.192 mmol), DIPEA (50 μ l, 0.288 mmol) were dissolved in dry DMF (18 mL) and stirred for 30 minutes under argon atmosphere. Subsequently corresponding amino-acid (0.192 mmol) was added and the resulting solution was stirred for 2h. After concentration *in vacuo* the purification of each compound is described as follows.

Compound **5**: Following the general procedure perylene **1** was reacted with aminoacid **2**. The crude reaction mixture was purified by column chromatography (silica, 2% MeOH:DCM) and crystalized from diethyl ether giving red crystals of **5** (77% yield).

¹H NMR (600 MHz, CDCl₃) δ (ppm): 8.58 – 8.47 (bs, 2H), 8.40 (d, *J* = 7.8 Hz, 2H), 8.34 (d, *J* = 8.0 Hz, 2H), 8.27 (d, *J* = 8.0 Hz, 2H), 7.67 – 7.62 (m, 2H), 7.57 (d, *J* = 7.5 Hz, 2H), 7.35 – 7.22 (m, 4H), 7.01 – 6.96 (bs, 1H), 5.61 (bs, 1H), 5.20 – 5.12 (m, 1H), 4.45 – 4.27 (m, 3H), 4.25 – 4.12 (m, 3H), 3.38 – 3.30 (m, 2H), 2.29 – 2.19 (m, 2H), 2.03 – 1.96 (m, 2H), 1.93 – 1.84 (m, 2H), 1.49 (d, *J* = 7.0 Hz, 3H), 1.40 – 1.18 (m, 16H), 0.82 (t, *J* = 6.9 Hz, 6H);

¹³C NMR (150 MHz, CDCl₃) δ (ppm): 172.3, 163.8u, 163.5, 155.9, 143.8u, 141.2, 134.6, 133.7, 131.3, 131.2u, 129.3, 129.1, 127.6, 127.0, 126.0, 125.9, 125.1, 123.7u, 123.0, 122.7, 122.5, 119.9, 67.1, 54.9, 50.8, 47.1, 37.7, 36.4, 32.4, 31.8, 29.2, 27.8, 27.0, 22.6, 19.0, 14.0;

TOF MS ES-. Mass 945.4203. Calculated for C₅₈, H₅₈, N₄, O₇, Na: 945.4203.

Compound **6**: Following the general procedure perylene **1** was reacted with aminoacid **3**. The crude reaction mixture was purified by column chromatography (silica, 5% MeOH:DCM) and crystalized from diethyl ether giving red crystals of **6** (53% yield).

¹H NMR (600 MHz, DMF-d₆) δ (ppm): 8.81 – 8.77 (m, 2H), 8.74 - 8.71 (m, 2H), 8.56 – 8.47 (m, 2H), 8.43 – 8.38 (m, 2H), 8.29 (d, *J* = 6.7 Hz, 1H), 8.11 (d, *J* = 8.5 Hz, 1H), 8.04 – 7.99 (m, 1H), 7.92 – 7.87 (m, 1H), 7.80 -7.75 (m, 2H), 7.70 – 7.63 (m, 3H), 7.36 – 7.22 (m, 4H), 5.24 – 5.15 (m, 1H), 4.41 – 4.13 (m, 9H), 3.37 – 3.27 (m, 2H), 2.38 – 2.30 (m, 2H), 2.00 – 1.85 (m, 4H), 1.45 – 1.17 (m, 28H), 0.82 (t, *J* = 6.9 Hz, 6H);

¹³C NMR (150 MHz, DMF-d₆) selected signals δ (ppm): 173.6, 172.9, 172.6, 172.4, 164.2u, 163.4, 156.8, 144.4, 141.3, 134.6, 131.4u, 131.2, 128.0, 127.4, 125.7, 124.3, 124.3, 120.3, 66.7, 54.3, 51.4, 49.6, 49.6, 49.6, 47.4, 38.5, 37.4, 32.6, 32.0, 29.5, 28.6, 27.2, 22.8, 18.1, 18.0, 17.6, 17.5, 13.9;

TOF MS ES+. Mass 1158.5310. Calculated for C₆₇, H₇₃, N₇, O₁₀, Na: 1158.5317.

Compound **7**: Following the general procedure perylene **1** was reacted with aminoacid **4**. The crude reaction mixture was purified by column chromatography (silica, 1% MeOH:DCM) and crystalized from diethyl ether giving red crystals of **7** (70% yield).

^1H NMR (600 MHz, CDCl_3) δ (ppm): 8.67 – 8.56 (bs, 2H), 8.54 - 8.48 (m, 4H), 8.45 (d, J = 8.1 Hz, 2H), 7.69 (d, J = 7.7 Hz, 2H), 7.58 – 7.52 (m, 2H), 7.39 -7.26 (m, 8H), 7.24 – 7.20 (m, 1H), 6.76 – 6.70 (bs, 1H), 5.56 – 5.47 (bs, 1H), 5.21 – 5.13 (m, 1H), 4.53 – 4.45 (m, 1H), 4.40 – 4.32 (m, 2H), 4.19 (dd, J = 7.2, 7.2 Hz, 1H), 4.06 – 3.98 (m, 1H), 3.96 – 3.85 (m, 1H), 3.35 – 3.04 (m, 4H), 2.28 – 2.19 (m, 2H), 1.93 – 1.75 (m, 4H), 1.40 – 1.16 (m, 16H), 0.82 (t, J = 6.9 Hz, 6H);

^{13}C NMR (150 MHz, CDCl_3) δ (ppm): 170.5, 163.9u, 163.7, 163.5, 155.9, 143.8u, 141.2u, 136.6, 134.9, 134.1, 131.6, 131.4u, 129.4, 128.7, 127.7, 127.1, 127.0, 126.3, 126.2, 125.1u, 124.1, 123.4, 123.2, 122.9, 122.6, 119.9, 67.1, 56.6, 54.8, 47.1, 39.0, 37.5, 36.1, 32.4, 31.7, 29.2, 27.8, 26.9, 22.6, 14.0.

TOF MS ES+. Mass 1021.4516. Calculated for C_{64} , H_{62} , N_4 , O_7 , Na: 1021.4516.

General deprotection procedure: Corresponding compounds **5-7** (0.100 mmol) were dissolved in 2 ml of 20% piperidine in DMF solution and stirred for 30 minutes. Each reaction mixture was concentrated *in vacuo* and used without further purification due to the limited stability.

Compound **8**: Following the general procedure crude product was washed diethyl ether giving **8** as red solid.

TOF MS ES+. Mass 701,3700. Calculated for C_{43} , H_{49} , N_4 , O_5 : 701,3703.

Compound **9**: Following the general procedure crude product was washed diethyl ether giving **9** as red solid.

TOF MS ES+. Mass 914,4824. Calculated for C_{52} , H_{64} , N_7 , O_8 : 914,4816.

Compound **10**: Following the general procedure crude product was washed diethyl ether giving **10** as red solid.

TOF MS ES+. Mass 777,4006. Calculated for C_{49} , H_{53} , N_4 , O_5 : 777,4016.

General procedure for corrole-perylene conjugates **12-14**. Corrole **11** (50 mg, 0.064 mmol), HATU (24 mg, 0.064 mmol), DIPEA (17 μl , 0.096 mmol) were dissolved in dry DMF (18 mL) and stirred for 30 minutes under argon atmosphere. Subsequently corresponding perylene derivative (0.064 mmol) was added and the resulting solution was stirred for 2h. After concentration *in vacuo* the purification of each compound is described as follows.

Cor-Ala-PDI: Following the general procedure corrole **11** was reacted with perylene-aminoacid conjugate **8**. The crude reaction mixture was purified by column chromatography (silica DCVC, ethyl acetate) and crystalized from diethyl ether giving dark red crystals of **Cor-Ala-PDI** (2 steps, 48% yield).

^1H NMR (600 MHz, CDCl_3) δ (ppm): 8.97 – 8.90 (bs, 2H), 8.68 - 8.55 (m, 4H), 8.55 – 8.47 (m, 6H), 8.42 – 8.35 (m, 4H), 8.29 – 8.24 (bs, 1H), 7.79 – 7.85 (m, 1H), 7.54 -7.48 (m, 1H), 7.18 – 7.14 (m, 1H), 5.31 – 5.25 (bs, 1H), 5.21 – 5.13 (m, 1H), 4.29 (d, J = 14.4 Hz, 1H), 4.14 (d, J = 14.4 Hz, 1H), 4.09 – 4.00 (bs, 1H), 3.42 – 3.33 (m, 1H), 3.30 – 3.22 (m, 1H), 3.01 – 2.93 (m, 1H), 2.29 – 2.15 (m, 2H), 1.91 – 1.88 (m, 2H), 1.38 – 1.14 (m, 16H), 0.81 (t, J = 6.9 Hz, 6H), 0.66 – 0.48 (bs, 2H), 0.43 – 0.11 (m, 2H), -0.50 - -0.85 (bs, 3H);

^{13}C NMR (125 MHz, CDCl_3) δ (ppm): 168.5, 166.2, 164.5, 163.4, 157.5, 147.1u, 144.9, 138.8, 136.8, 135.0, 134.0, 131.5, 131.4u, 130.9, 130.1, 129.5, 129.1, 126.3, 126.2, 123.5, 123.3, 122.8, 122.3, 121.4, 116.1, 114.3, 112.7, 107.6, 67.6, 46.0, 36.5, 33.9, 32.4, 31.7, 29.7, 29.2, 26.9, 25.6, 22.6, 17.2, 14.0;

TOF MS ES-. Mass 1461.4538. Calculated for C_{82} , H_{64} , N_8 , O_7 , F10: 1461.4538.

Cor-(Ala)₄-PDI: Following the general procedure corrole **11** was reacted with perylene-aminoacid conjugate **9**. The crude reaction mixture was purified by column chromatography (silica DCVC, 2% methanol:ethyl acetate) and crystalized from diethyl ether giving dark red crystals of **Cor-(Ala)₄-PDI** (2 steps, 32%).

¹H NMR (600 MHz, CDCl₃) δ (ppm): 9.21 – 8.92 (m, 2H), 8.67 – 8.10 (m, 15H), 7.78 – 7.68 (m, 1H), 7.54 – 7.44 (m, 1H), 7.36 – 7.09 (m, 2H), 6.95 – 6.75 (m, 1H), 5.99 – 5.77 (m, 1H), 5.71 – 5.46 (m, 1H), 5.20 – 5.07 (m, 1H), 4.50 – 4.01 (m, 6H), 4.00 – 3.82 (m, 1H), 3.43 – 3.07 (m, 2H), 3.03 – 2.87 (m, 1H), 2.30 – 1.78 (m, 6H), 1.39 – 0.99 (m, 22H), 0.81 (t, *J* = 6.9 Hz, 6H), -0.33 – -0.89 (m, 4H), -0.96 – -1.37 (m, 3H);

¹³C NMR (150 MHz, CDCl₃) selected signals δ (ppm): (171.8, 169.7, 163.7, 157.5, 146.9, 145.1, 136.9 z C13 NMR), 134.1u, 131.5, 131.3, 130.8, 130.2, 126.5, 125.1, 122.9, 122.7, 121.4, 112.5, 67.3, 54.8, 49.3, 48.6, 46.5, 45.6, 37.6, 36.3, 32.4, 31.8, 29.2, 27.8, 26.9, 22.6, 19.5, 17.8, 17.8, 17.2, 14.0;

TOF MS ES+. Mass 1698.5737. Calculated for C₉₁, H₇₉, N₁₁, O₁₀, F₁₀, Na: 1698.5749.

Cor-Phe-PDI: Following the general procedure corrole **11** was reacted with perylene-aminoacid conjugate **10**. The crude reaction mixture was purified by column chromatography (silica DCVC, 50% ethyl acetate:Hexane) and crystalized from diethyl ether giving dark red crystals of **Cor-Phe-PDI** (2 steps, 45%).

¹H NMR (600 MHz, CDCl₃) δ (ppm): 9.20 – 9.13 (bs, 1H), 8.95 – 8.88 (bs, 1H), 8.70 – 8.45 (m, 7H), 8.40 – 8.17 (m, 8H), 7.79 – 7.73 (m, 1H), 7.55 – 7.48 (m, 1H), 7.16 – 7.10 (m, 1H), 6.84 – 6.72 (m, 3H), 5.39 – 5.21 (bs, 2H), 5.21 – 5.13 (m, 1H), 4.97 – 4.90 (m, 1H), 4.28 (d, *J* = 14.4 Hz, 1H), 4.12 (d, *J* = 14.4 Hz, 1H), 3.98 – 3.86 (bs, 1H), 3.07 – 2.95 (m, 2H), 2.29 – 2.19 (m, 2H), 2.16 – 2.06 (m, 1H), 1.93 – 1.82 (m, 2H), 1.67 – 1.58 (bs, 1H), 1.49 – 1.40 (bs, 1H), 1.39 – 1.16 (m, 16H), 0.82 (t, *J* = 6.9 Hz, 6H), 0.68 – 0.52 (bs, 1H), 0.45 – 0.13 (m, 2H), -0.45 – -0.58 (bs, 1H);

¹³C NMR (125 MHz, CDCl₃) δ (ppm): 166.4, 165.9, 163.9u, 163.3, 157.4, 146.9u, 145.2u, 142.3, 140.7, 138.6, 136.9, 135.1, 134.6, 133.8, 131.5u, 131.2, 130.8u, 130.1, 129.3, 128.8, 128.2, 127.9, 126.1, 125.9, 123.7u, 123.1, 122.5, 122.0, 121.3, 116.2, 116.0, 114.4u, 112.3, 107.5, 67.2, 54.8, 52.3, 36.1, 33.6, 32.4, 31.7, 29.7, 29.2, 26.9, 25.6, 22.6, 14.0;

TOF MS ES+. Mass 1539.5142. Calculated for C₈₈, H₆₉, N₈, O₇, F₁₀: 1539.5130.

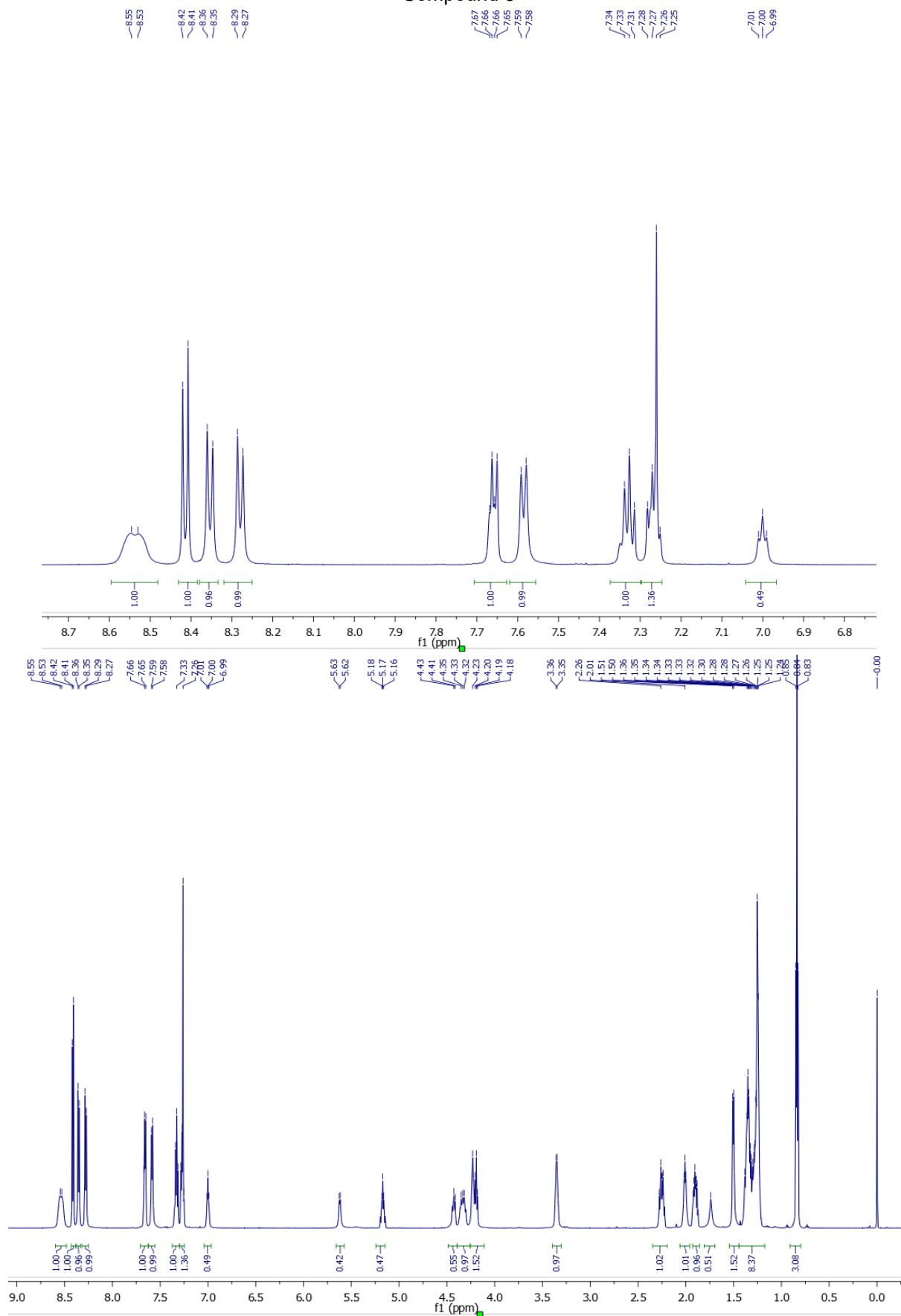
Cor-Phe: Following the general procedure corrole **11** was reacted with *L*-Phenylalanine Methyl Ester. The crude reaction mixture was purified by column chromatography (silica, 1% methanol:DCM) and crystalized from diethyl ether giving dark red crystals of **Cor-Phe** (62% yield).

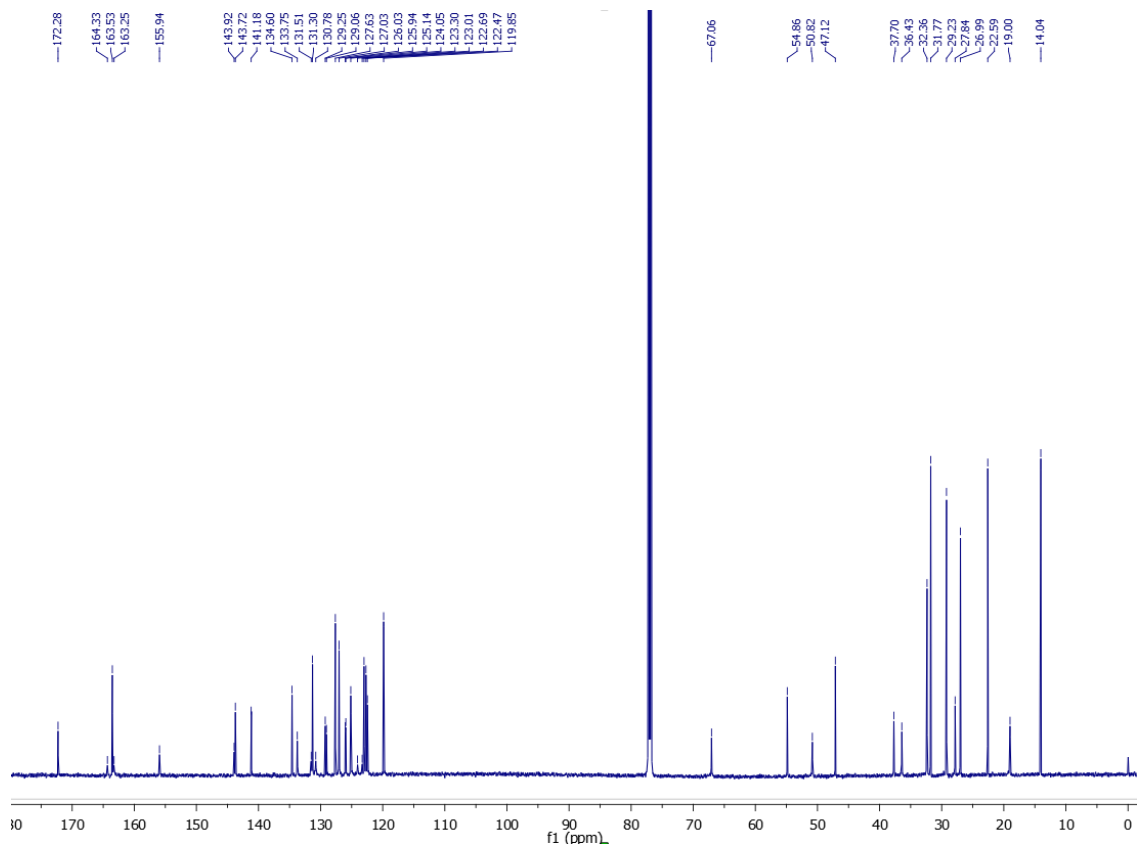
¹H NMR (600 MHz, DMF-d₆) δ (ppm): 9.36 – 9.17 (m, 2H), 9.13 – 8.54 (m, 4H), 8.72 – 8.53 (m, 2H), 8.14 – 8.07 (m, 1H), 7.85 – 7.76 (m, 1H), 7.52 – 7.45 (m, 1H), 7.44 – 7.37 (m, 1H), 6.72 – 6.04 (m, 4H), 5.99 – 5.57 (m, 2H), 4.58 – 4.36 (m, 2H), 4.06 – 3.96 (m, 1H), 3.29 – 3.03 (bs, 3H), 2.17 – 1.97 (m, 1H), 1.90 – 1.32 (m, 1H).

TOF MS ES-. Mass 940,1959. Calculated for C₄₉, H₂₈, N₅, O₄, F₁₀: 940.1982.

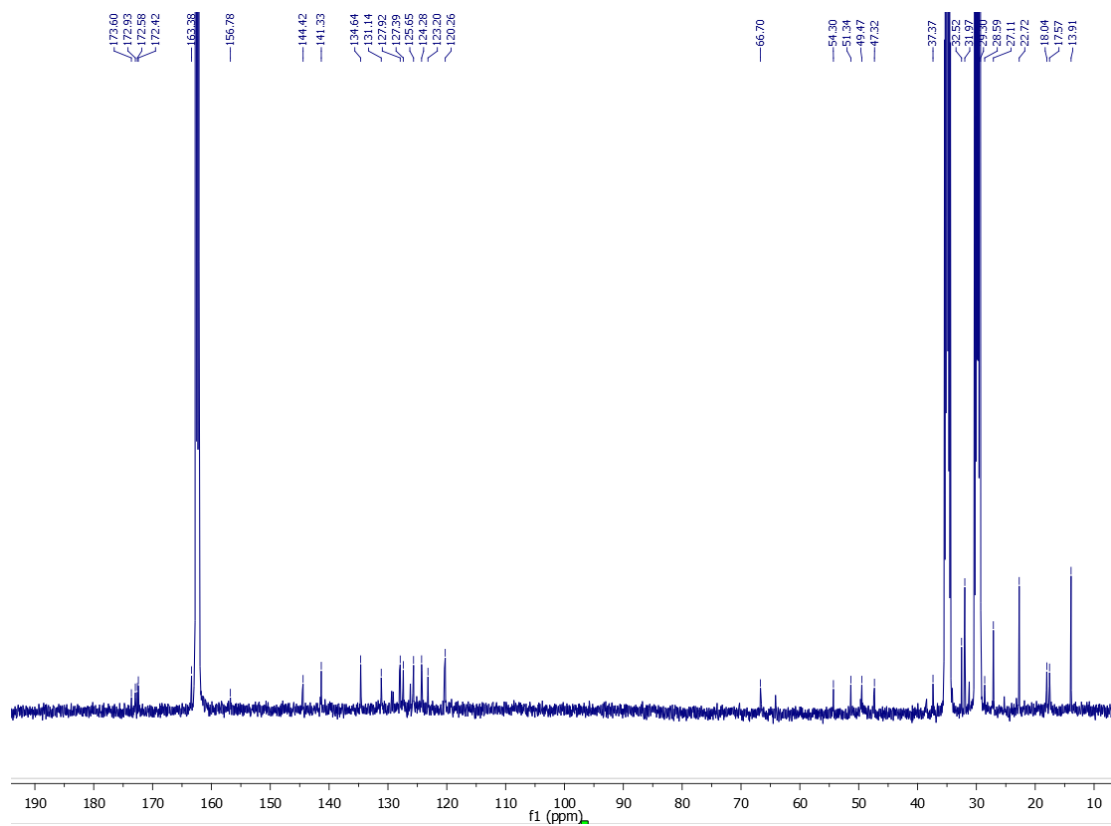
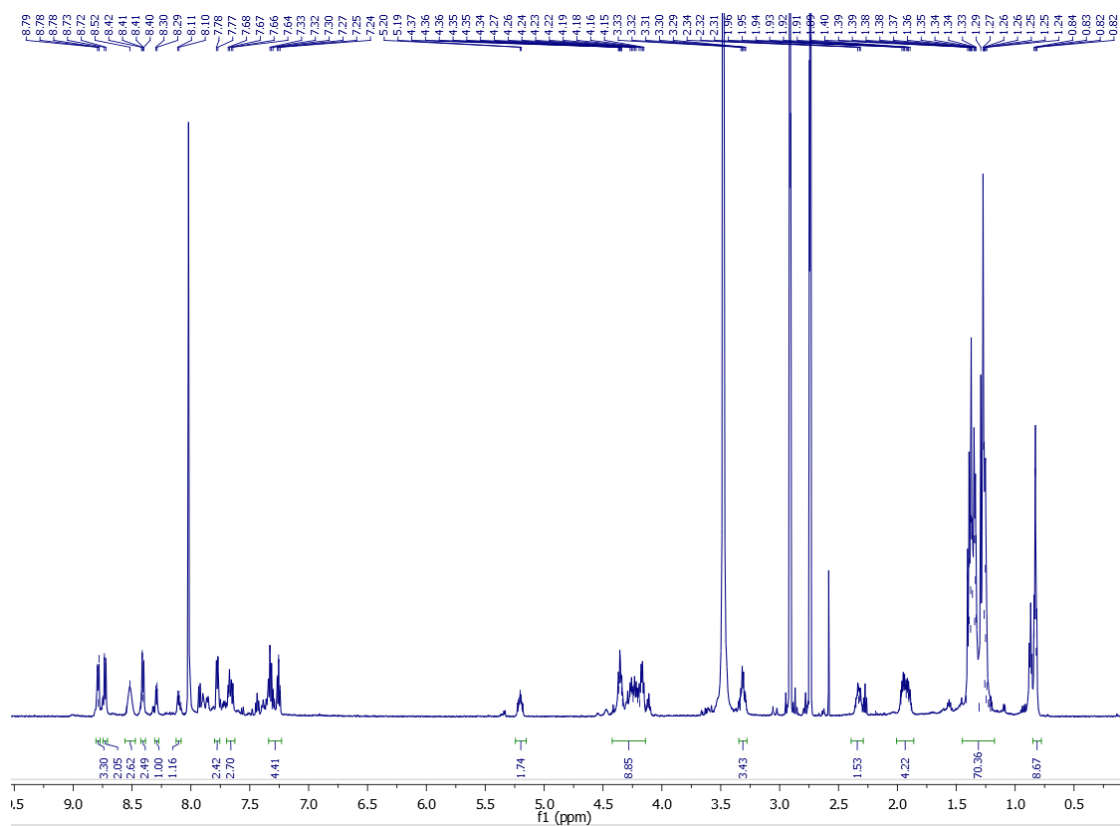
2. NMR spectra

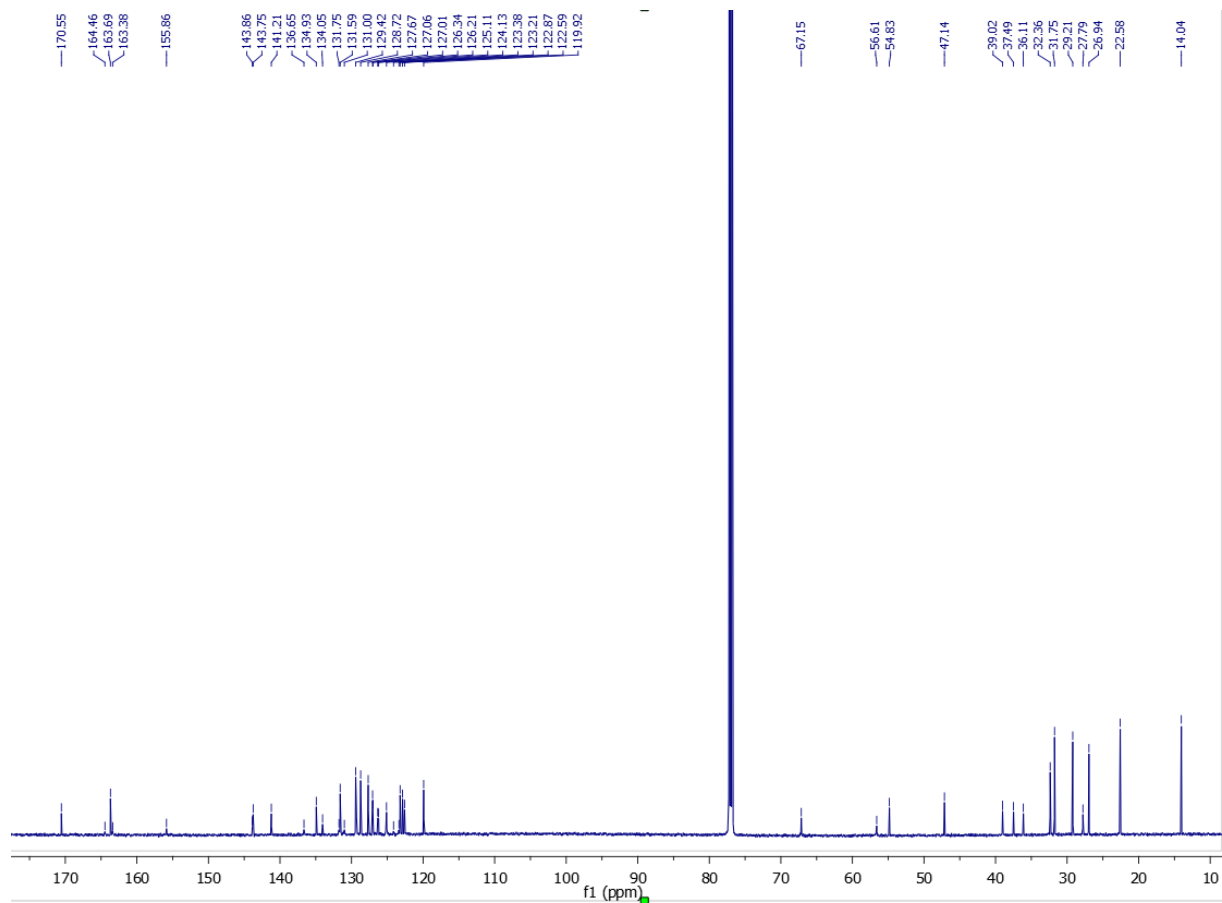
Compound 5

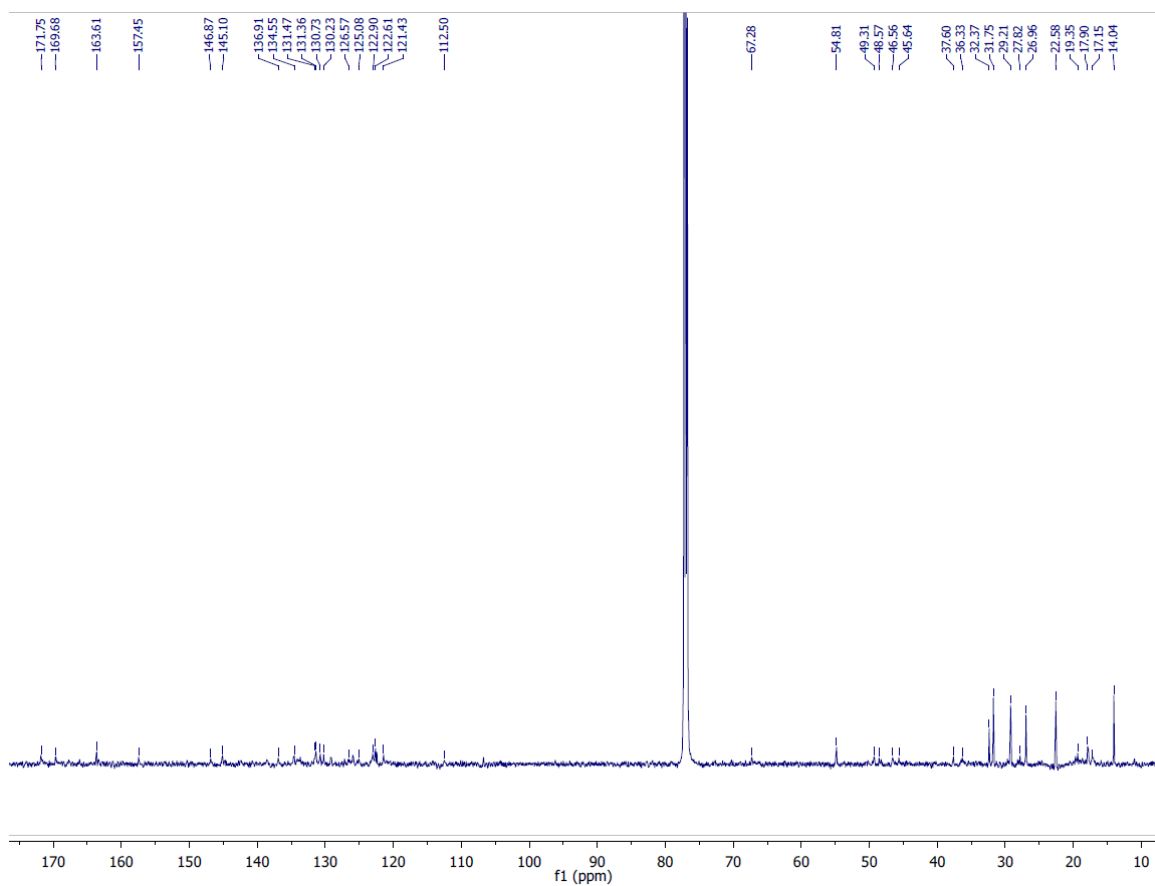




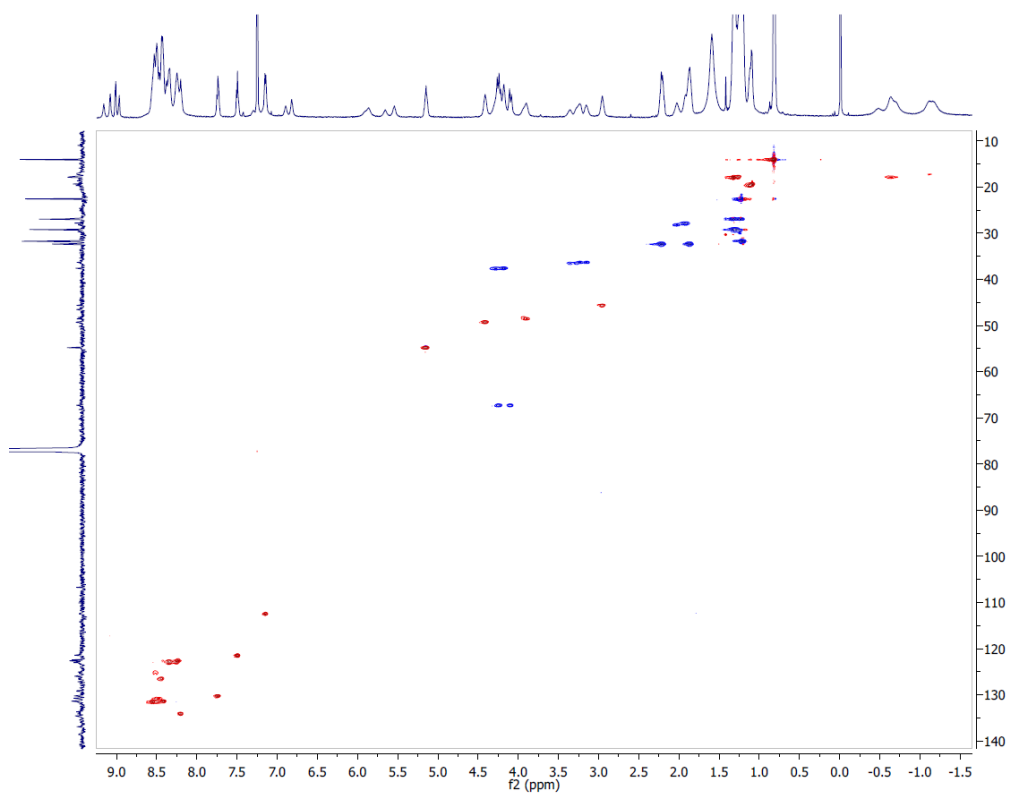
Compound 6



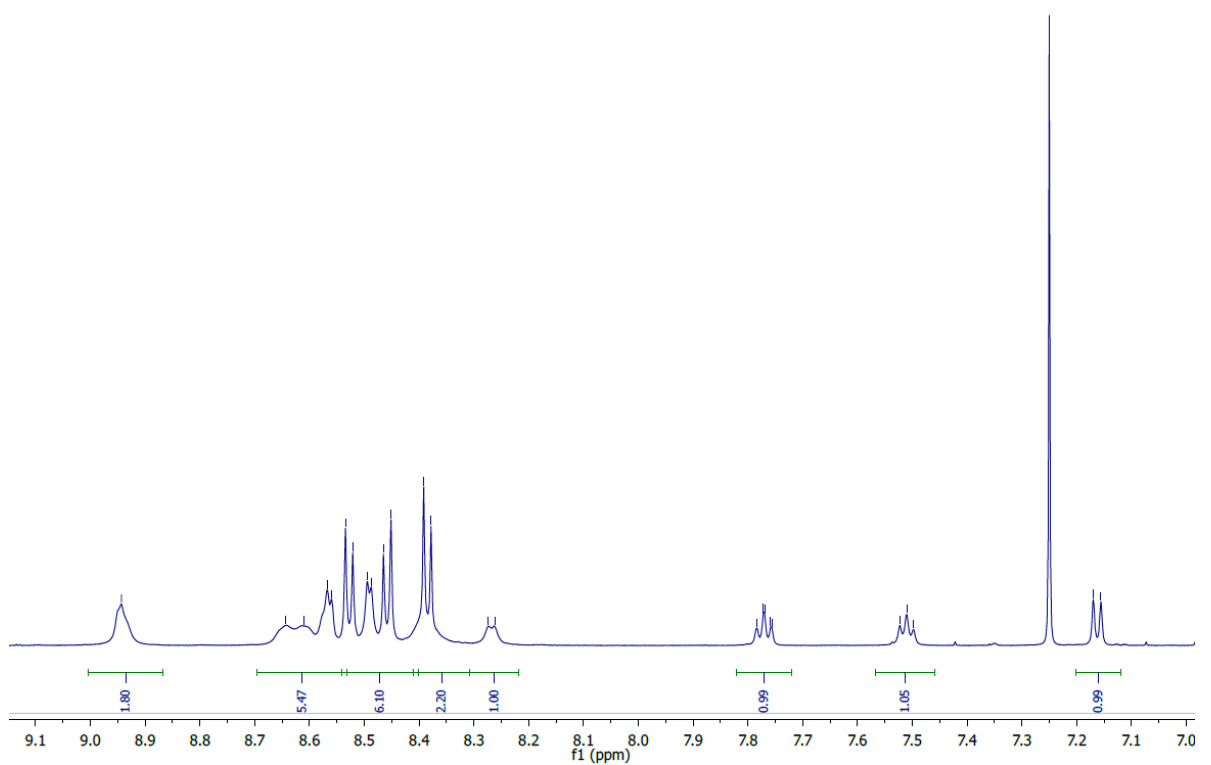
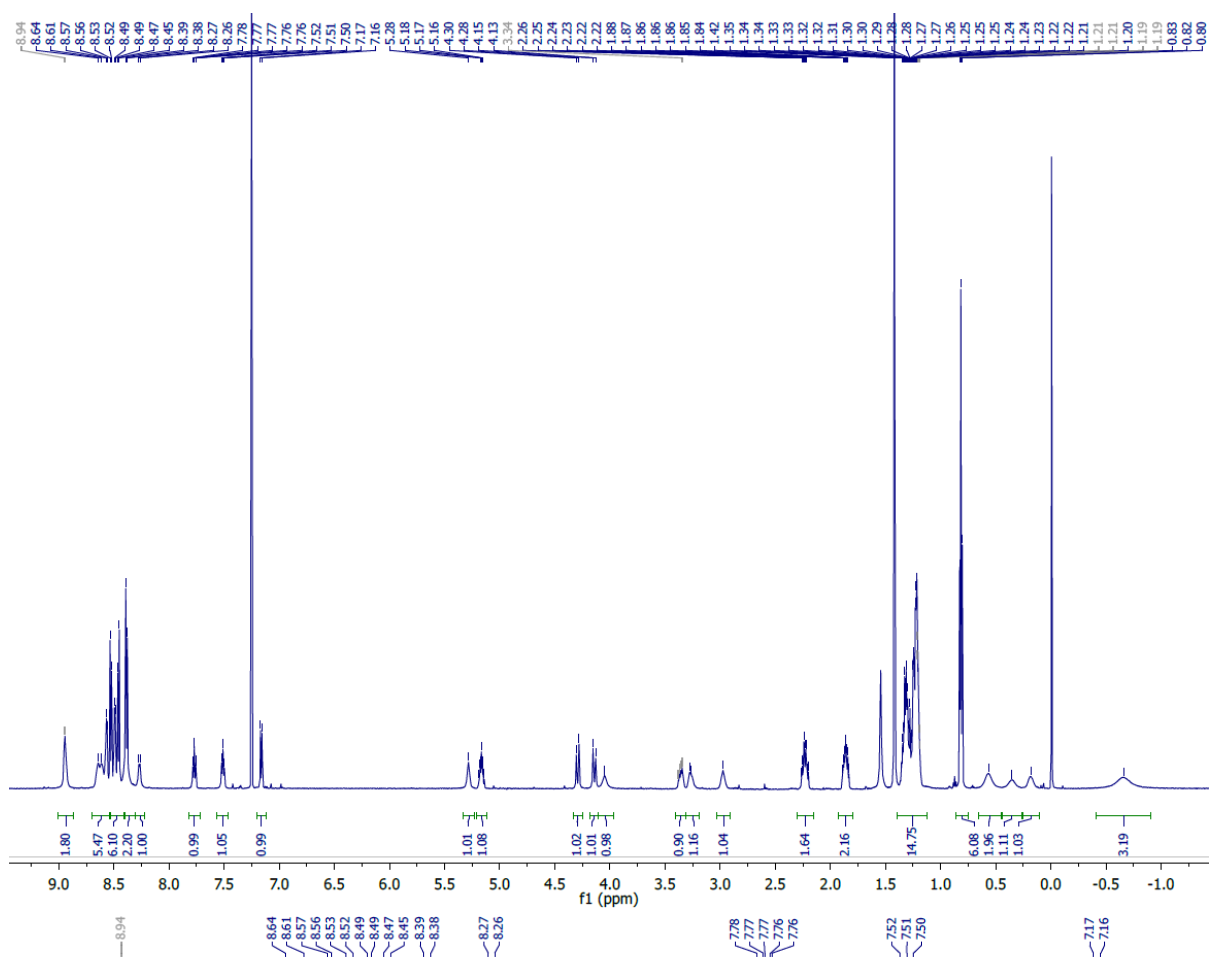


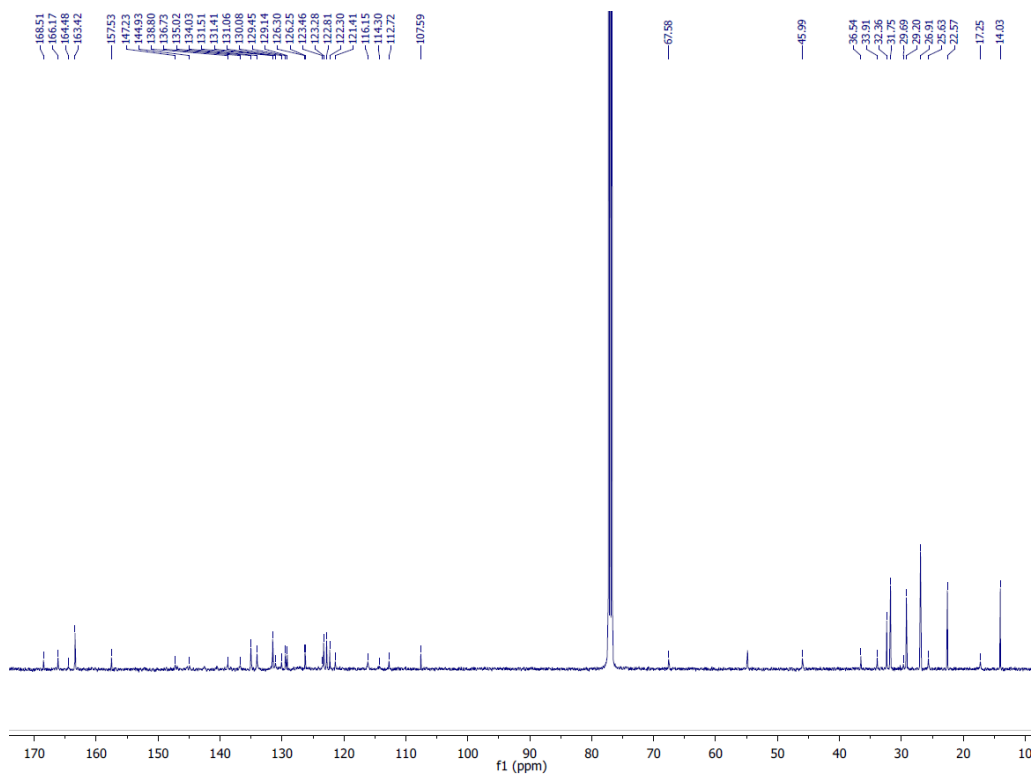


^1H - ^{13}C HSQC

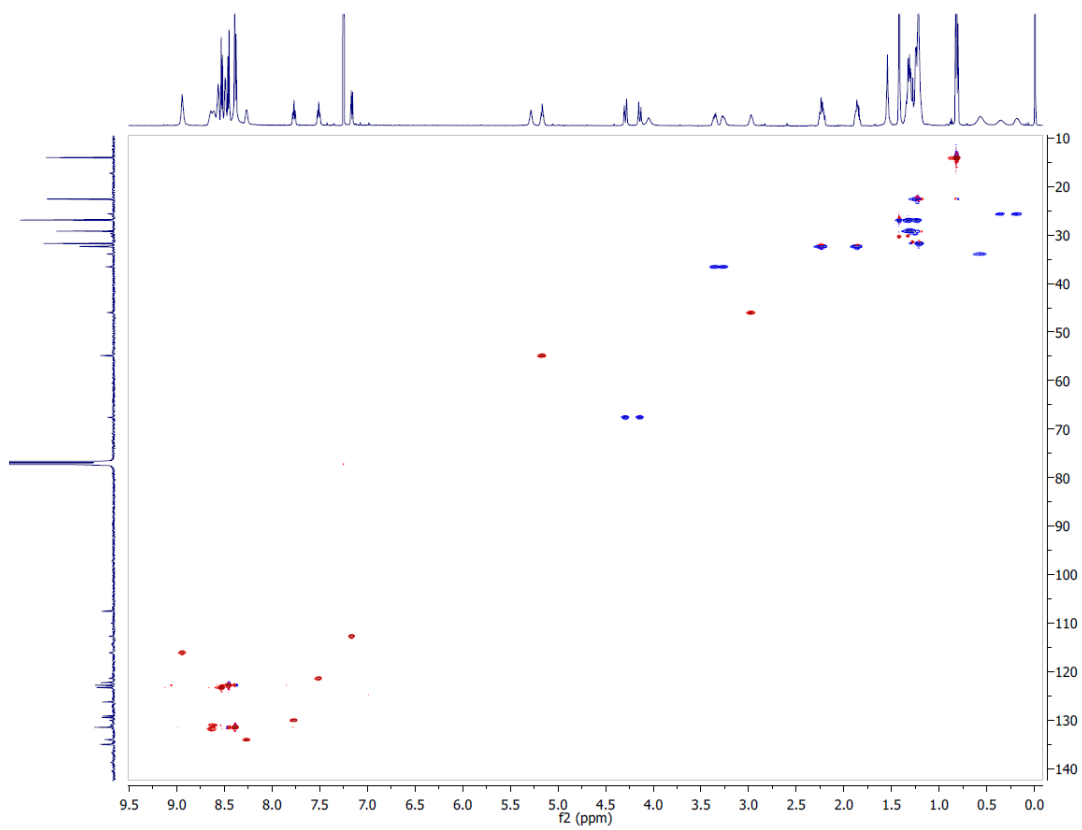


Cor-Ala-PDI

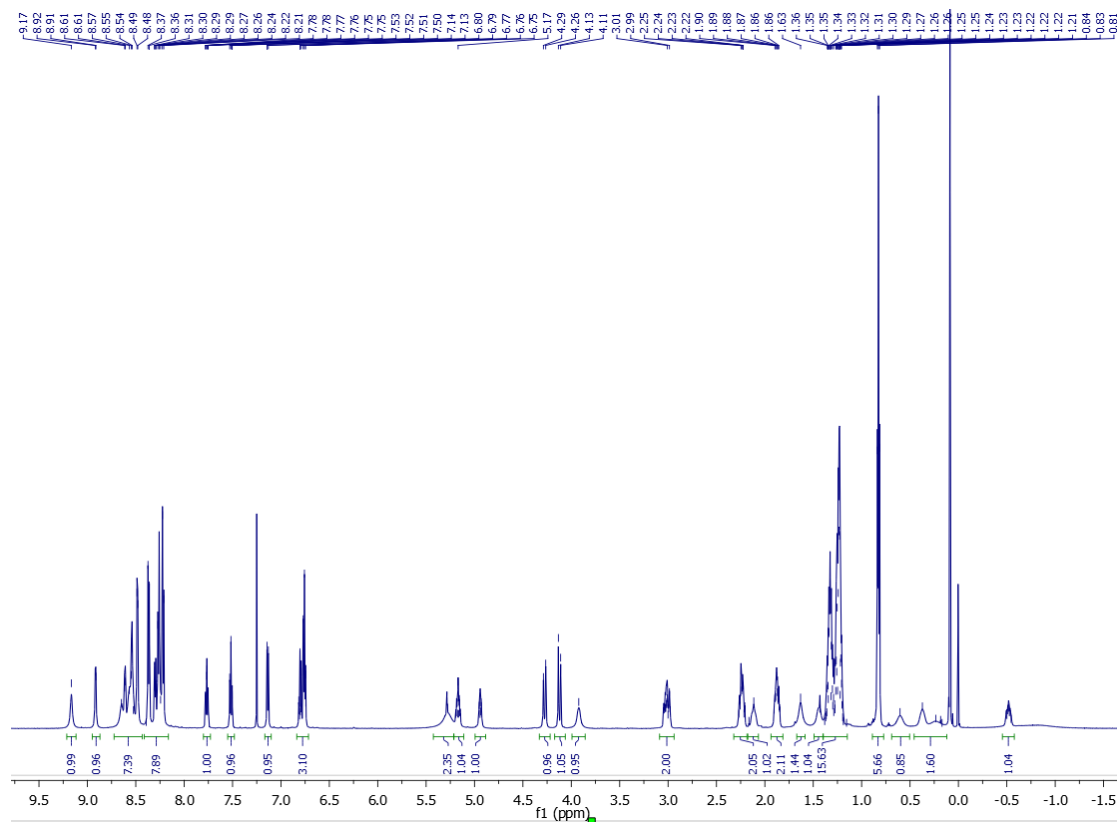
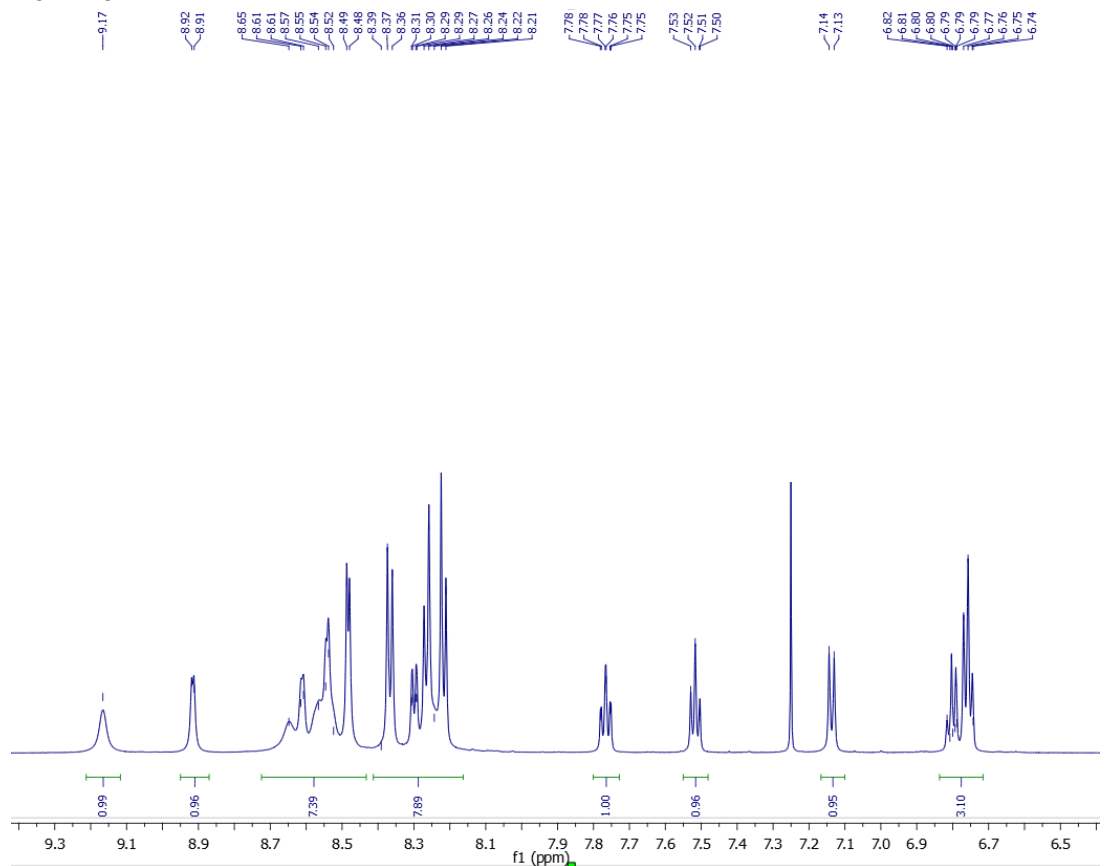


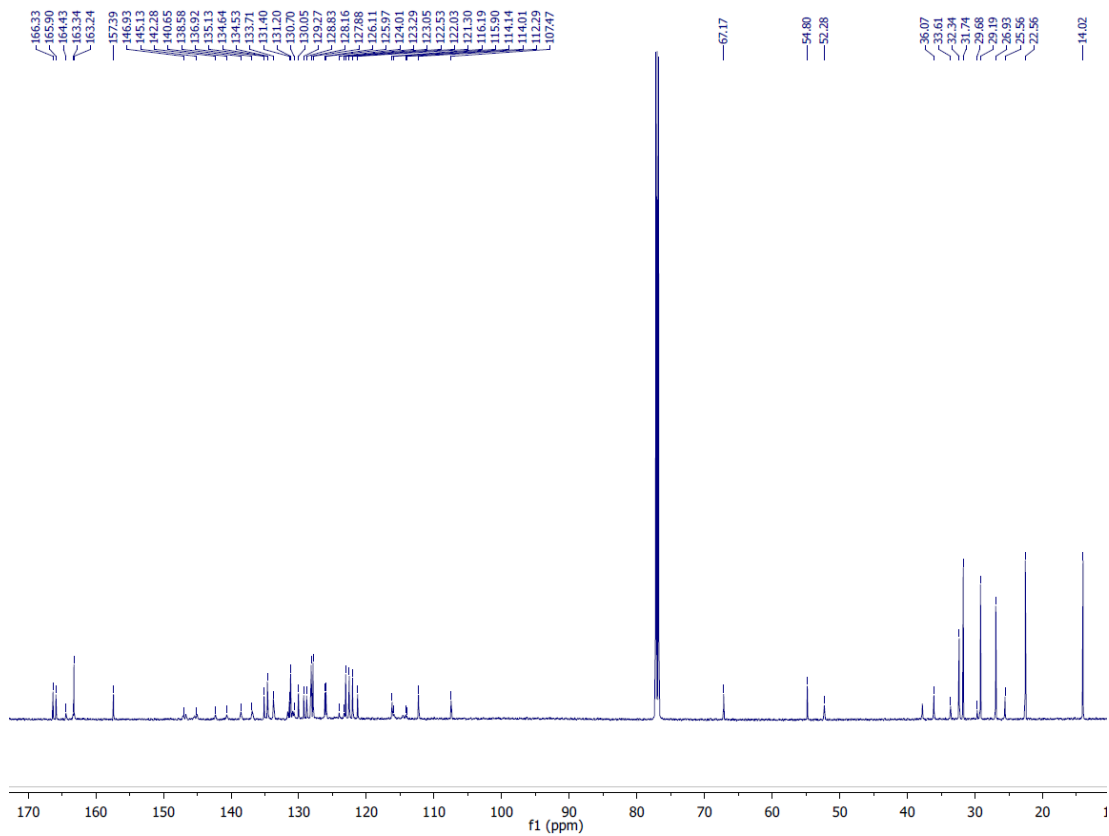


¹H-¹³C HSQC

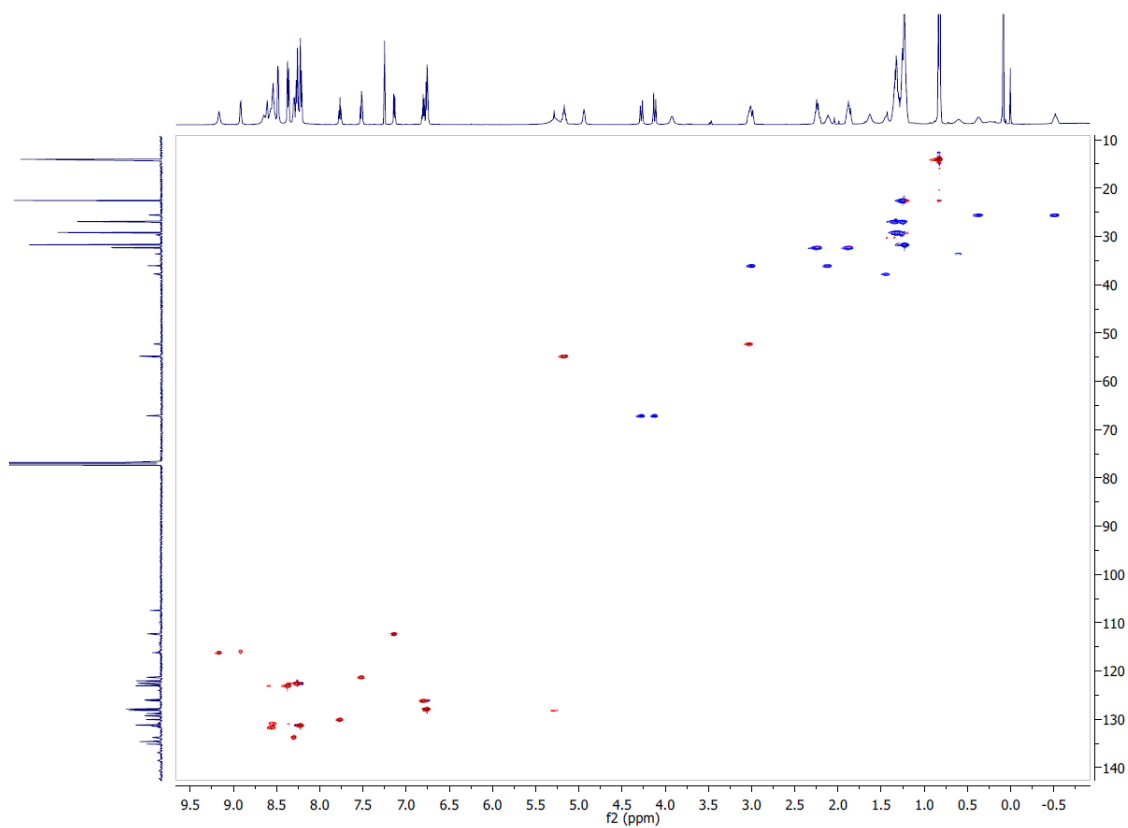


Cor-Phe-PDI

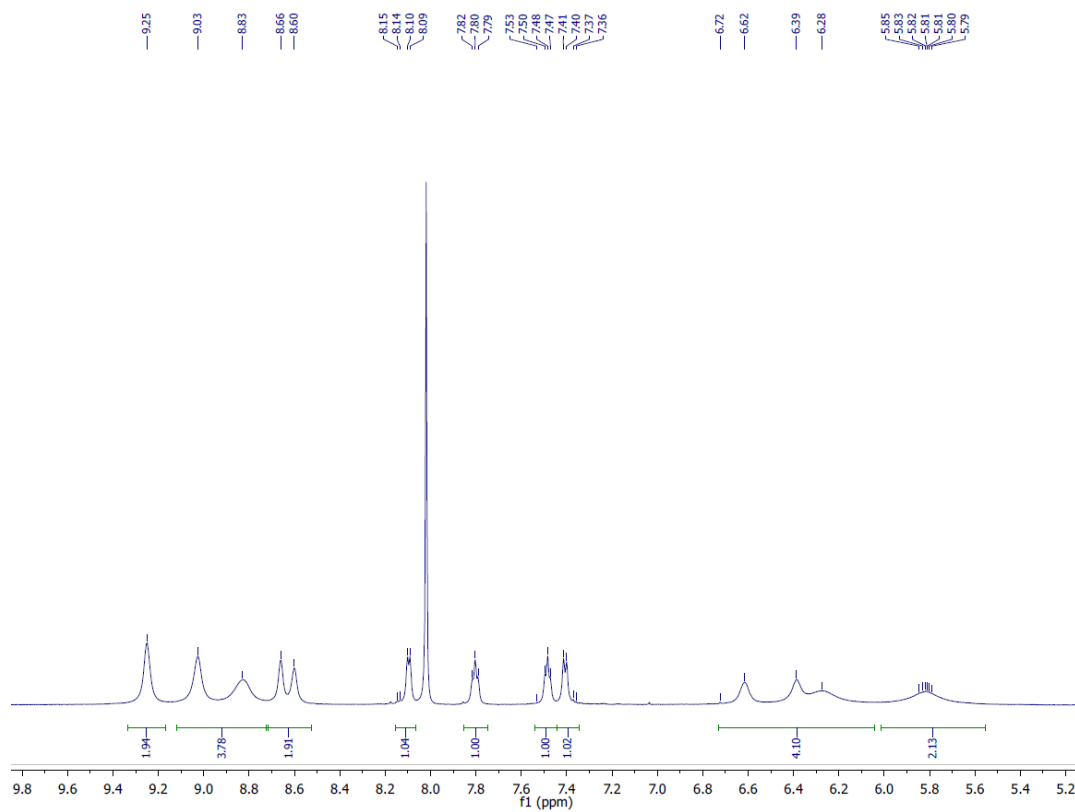
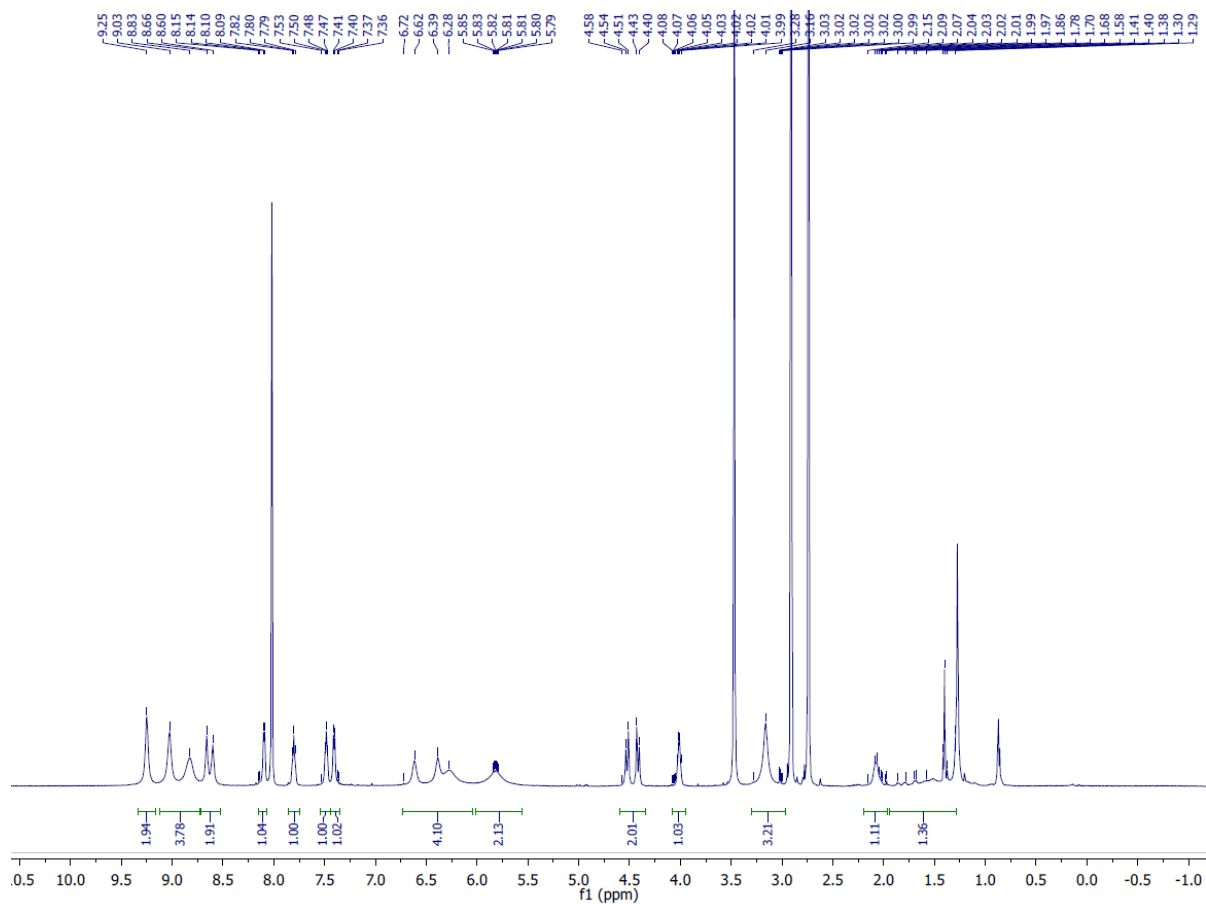




^1H - ^{13}C HSQC



Cor-Phe



3. Electrochemical analysis

3.1. Cyclic voltammetry (CV). CV measurements were performed using three-electrode cells powered by: (1) Bio-Logic SP-50 potentiostat (Lambda System, Warsaw, Poland); and (2) Reference 600 potentiostat-galvanostat (Gamry Instruments, Warminster, PA, USA). We utilized a glassy carbon working electrode for Cor oxidation and a platinum working electrode for PDI reduction, along with platinum counter electrodes. A high-impedance Ag/AgCl (3.0 M NaCl) electrode and an SCE electrode, connected to the cell via an electrolyte bridge containing 100 mM (*n*-C₄H₉)₄NPF₆ in acetonitrile (MeCN), served as references. Anhydrous MeCN, benzonitrile and dichloromethane were employed with different concentrations, C_{el} , of a supporting electrolyte (N(C₄H₉)₄PF₆), ranging from 25 mM to 200 mM with 25-mM increments. Immediately before and immediately after each set of measurements for a solvent with different C_{el} , we record the CVs of ferrocene in acetonitrile in the presence of 100 mM N(C₄H₉)₄PF₆ in order to correct should potential drifts of the reference electrodes occur.^(3, 4) Prior to each measurement, the sample was purged with argon. These experiments were carried out at room temperature at a scan rate of 100 mV·s⁻¹. For each sample, we recorded a triplicate of measurements.

3.2. Voltammogram analysis. The mean of the cathodic and anodic peak potentials provides estimates for the half-wave potentials, $E^{(1/2)}$, from voltammograms that show chemical reversibility and even partial reversibility.⁽⁴⁾ The zero values of the first derivatives of the voltammograms provide estimates for the peak potentials, i.e., the potentials where $\partial I/\partial E = 0$, while $\partial E/\partial t = \text{constant}$ ⁽⁵⁾. For irreversible oxidation and reduction, the potentials at the inflection points of the anodic and cathodic waves, respectively, extracted from the zero values of the second derivatives of the voltammograms, provide estimates for $E^{(1/2)}$, i.e., the potentials where $\partial^2 I/\partial E^2 = 0$, while $\partial E/\partial t = \text{constant}$ ^(4, 5). The dependence of $E^{(1/2)}$ on the electrolyte concentration, C_{el} , allows extrapolating to $C_{el} = 0$ and estimating the values of the reduction potentials for neat solvent, $E_0^{(1/2)}$ (Figure 5b).^(3,4) For each solvent, we estimate $\Delta E_0^{(1/2)} = E_0^{(1/2)}_{\text{Cor}^+|\text{Cor}} - E_0^{(1/2)}_{\text{PDI}|\text{PDI}^-}$. The linear dependence of $\Delta E_0^{(1/2)}$ on the inverse of the relative dielectric constants, ϵ^{-1} (eq. 3b), yields $\Delta E_0^{(1/2)}$ for toluene ($\epsilon^{-1} = 0.42$) and S_{1/r}, which we use for estimating the CT driving forces (eq. 3a) and the medium reorganization energy (Figure 5d).

4. Steady-state optical spectroscopy

4.1. Absorption and emission. The optical absorption spectra were recorded using a Varian Cary 50 UV-vis and Jasco V-660 UV-vis-NIR spectrophotometer. Fluorescence measurements were conducted with a Horiba Jobin Yvon Fluorolog-3-22 spectrofluorometer. All samples were purged with argon prior to measurement. The absorbance at the excitation wavelengths was kept within the range between 0.1 and 0.2 for measurements of the emission quantum yields. 10-[2-(N-butylcarbamoylmethoxy)phenyl]-5,15-bis(pentafluorophenyl)corrol ($\phi_f = 0.134$, for MeOH) was used as a standard.⁽⁵⁾

4.2. Estimating the inner reorganization energy (λ_v). The fluorescence spectra of **PDI** and **Cor** in toluene (T = 295 K) were modeled using a semiclassical Franck-Condon expression with one classical distortion and one quantum mechanical distorting mode.^(6, 7) The vibrational frequencies of the distorting mode were assumed to be identical in the ground and excited electronic states. The classical-mode distortion was represented by a Gaussian function with FWHM (cm^{-1}) $\approx [2274 \times \lambda_{\text{classical}} (\text{cm}^{-1})]^{1/2}$. The energy maximum of the Gaussian for the transition from the quantum mechanical vibrationally unexcited ground electronic state to the quantum mechanical vibrationally unexcited luminescent electronic state is defined as the parameter E_{00} . Distortions in the quantum mechanical vibrational mode of frequency ν are described by the Huang-Rhys parameter, S . The model parameters derived for **PDI** are: $E_{00} = 18475 \text{ cm}^{-1}$; $h\nu = 1270 \text{ cm}^{-1}$; $S = 0.82$; $\lambda_{\text{classical}} = 300 \text{ cm}^{-1}$ (**Figure S1**). The model parameters derived for **Cor** are: $E_{00} = 15250 \text{ cm}^{-1}$; $h\nu = 1250 \text{ cm}^{-1}$; $S = 0.32$; $\lambda_{\text{classical}} = 350 \text{ cm}^{-1}$ (**Figure S1**). The estimated upper limit to the inner-sphere reorganization is $\lambda_{\text{inner}} \leq (S \times h\nu) + \lambda_{\text{classical}}$: $\lambda_{\text{inner}}(\text{PDI}) \leq 0.17 \text{ eV}$; $\lambda_{\text{inner}}(\text{Cor}) \leq 0.09 \text{ eV}$.

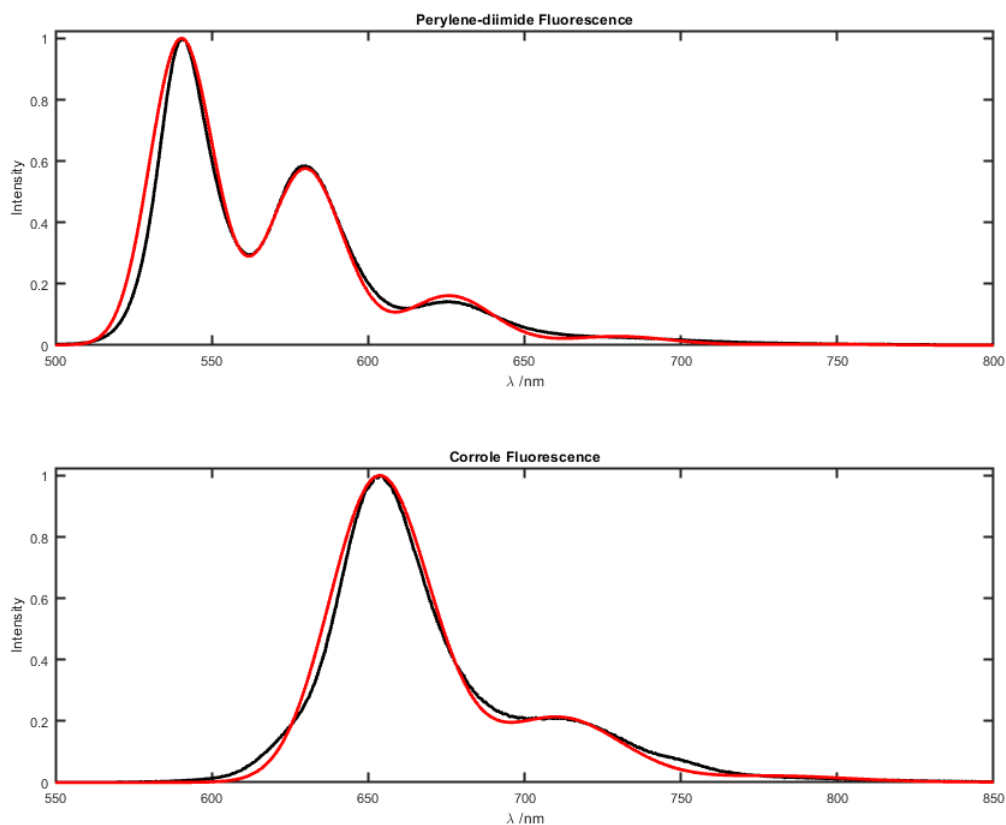


Figure S1. Measured (black) and modeled (red) fluorescence spectra of **PDI** and **Cor**. See text for model parameters.

4.3. Circular dichroism. The ECD spectra of for **Cor-(Ala)₄-PDI**, **Cor-Ala-PDI**, and **Cor-Phe-PDI** were recorded between 700 and 280 nm at room temperature in spectroscopic grade toluene with concentrations in the range from 5.94×10^{-5} to 6.83×10^{-5} M in a 0.1-cm quartz cell.

5. Time-resolved optical spectroscopy

5.1. Time-resolved fluorescence spectroscopy. The 1064-nm output of a passively mode-locked Nd:YAG laser (Spectra Physics Vanguard) was regeneratively amplified (Continuum) and frequency tripled using KDP crystals to produce 355-nm excitation pulses (~10 ps, 10 Hz). Luminescence was collected 90° from the excitation, passed through a polarizer oriented at the magic angle, then directed onto the entrance slit of a monochromator for wavelength selection. Fluorescence decays were measured using a streak camera (Hamamatsu C5680) in photon-counting mode, and data were collected with 1-, 10-, or 20-ns time windows. Instrument response time is ~1-2% of the time window. Samples were prepared in sealed 1 cm quartz cuvettes under Ar and were stirred during data acquisition.

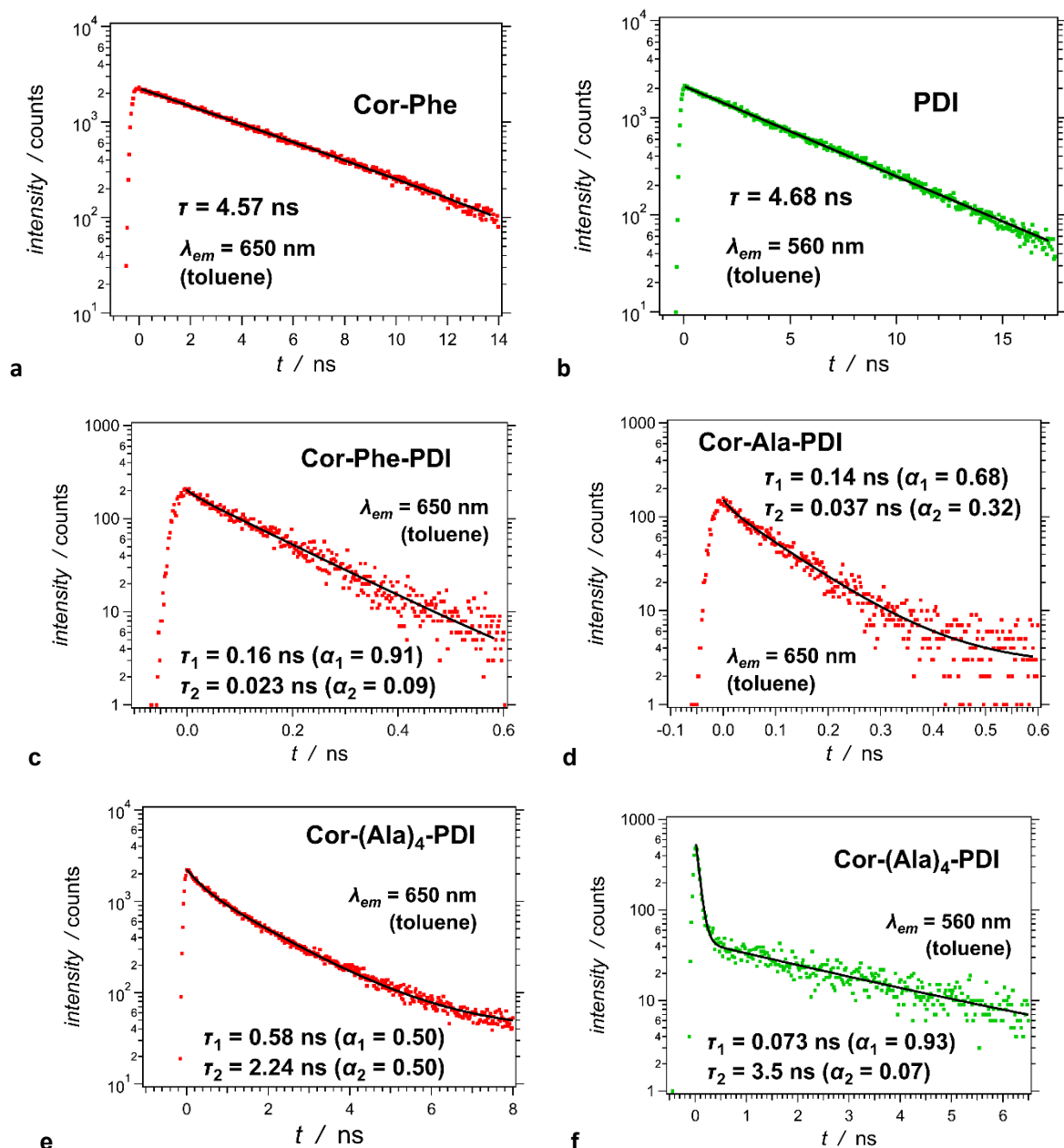


Figure S2. Emission decays with the corresponding exponential data fits (solid lines). Cor-Phe and PDI decays were adequately described by single-exponential functions. Biexponential functions were necessary to describe the decays of the Cor-PDI DBA conjugates. Time constants (τ_i) and amplitudes (α_i) for each phase are indicated in the plots.

5.2. Transient-absorption (TA) spectroscopy. A Helios pump-probe spectrometer (Ultrafast Systems, LLC, Florida, USA) was used to carry out TA measurements recorded in a transmission mode. 800-nm pulses (≥ 35 fs, 4.0 mJ per pulse, at 1 kHz) were generated by a SpitFire Pro 35F regenerative amplifier (Spectra Physics, Newport, CA, USA). The amplifier was pumped with an Empower 30 Q-switched laser ran at 20 W. A MaiTai SP oscillator provided the seed beam (55 nm bandwidth). The wavelength of the pump was tuned using an optical parametric amplifier, OPA-800CU (Newport Corporation, Newport, CA, USA), equipped with harmonic generators. Responses from pure solvents were used for the chirp correction of the TA data. The data analysis was carried out using Surface Explorer (Ultrafast Systems, LLC, Florida, USA) and IgorPro v. 8 (WaveMetrics, Inc., Lake Oswego, OR, USA).⁽⁸⁻¹⁰⁾

Steady-state optical absorption spectra reveal that when exciting the DBA conjugates at 400 to 430 nm, the electron donor, Cor, absorbs more than 95% of the light. When exciting the DBA conjugates at 460 to 470 nm, the electron acceptor, PDI, absorbs about 90% of the light. These results justify the use of 400 nm pump for selective excitation of the electron donor, and 465 nm pump for selective excitation of the electron acceptor.

5.3. Kinetic analysis. To analyze the TA dynamics, we use global fits employing sums of exponential functions:

$$\Delta A(\lambda, t) = B_{CT}(\lambda) \Delta A_{CT}(\lambda, t) + B_{LEC}(\lambda) \Delta A_{LEC}(\lambda, t) + B_{BC}(\lambda) \Delta A_{BC}(\lambda, t) + B_{LEP}(\lambda) \Delta A_{LEP}(\lambda, t) + B_{BP}(\lambda) \Delta A_{BP}(\lambda, t) \quad (S1)$$

Where each term, $B_i(\lambda) \Delta A_i(\lambda, t)$, represents species that have the same TA dynamics, with amplitudes from the signals scaled by $B_i(\lambda)$.

The charge-transfer (CT) term depicts the rise (via ET and HT) and the decay (via CR) of the TA of the radical ions:

$$\Delta A_{CT}(\lambda, t) = - \sum_{i=1}^p \alpha_i^{(HT)}(\lambda) e^{-k_i^{(HT)} t} - \sum_{i=1}^n \alpha_i^{(ET)}(\lambda) e^{-k_i^{(ET)} t} + \sum_{i=1}^w \alpha_i^{(CR)}(\lambda) e^{-k_i^{(CR)} t} \quad (S2a)$$

where $\sum_i \alpha_i^{(HT)} + \sum_i \alpha_i^{(ET)} = \sum_i \alpha_i^{(CR)}$. The terms in the first sum depict HT, $\text{Cor}\cdots^1\text{PDI}^* \rightarrow \text{Cor}^+\cdots\text{PDI}^-$, in the second sum – ET, $^1\text{Cor}^*\cdots\text{PDI} \rightarrow \text{Cor}^+\cdots\text{PDI}^-$, and in the third sum – CR, $\text{Cor}^+\cdots\text{PDI}^- \rightarrow \text{Cor}\cdots\text{PDI}$.

The term for the Cor locally excited state (LEC) describes the dynamics of $^1\text{Cor}^*$, that, in addition to the initial amplitude, $\Delta A_{LEC}(\lambda, 0) = \alpha_0^{(\text{Cor})}$, due to direct excitation of Cor, gets populated by EnT from $^1\text{PDI}^*$, $\text{Cor}\cdots^1\text{PDI}^* \rightarrow ^1\text{Cor}^*\cdots\text{PDI}$, and decays either directly to the ground state, $^1\text{Cor}^* \rightarrow \text{Cor}$, or via ET, $^1\text{Cor}^*\cdots\text{PDI} \rightarrow \text{Cor}^+\cdots\text{PDI}^- \rightarrow \text{Cor}\cdots\text{PDI}$:

$$\Delta A_{LEC}(\lambda, t) = - \sum_{i=1}^m \alpha_i^{(\text{EnT})}(\lambda) e^{-k_i^{(\text{EnT})} t} + \sum_{i=1}^h \alpha_i^{(\text{Cor})}(\lambda) e^{-k_i^{(\text{Cor})} t} \quad (S2b)$$

The first sum represents the EnT from $^1\text{PDI}^*$, and the second sum – the decay of $^1\text{Cor}^*$; also, $\sum_i \alpha_i^{(\text{EnT})} + \alpha_0^{(\text{Cor})} = \sum_i \alpha_i^{(\text{Cor})}$; and $\alpha_i^{(\text{EnT})} \propto \alpha_i^{(\text{PDI})} k_i^{(\text{EnT})} / (k_i^{(\text{EnT})} + k_i^{(\text{HT})} + k_0^{(\text{PDI})})$

The rate constants, $k_i^{(\text{Cor})}$, encompass all modes of deactivation of $^1\text{Cor}^*$, i.e., $k_i^{(\text{Cor})} = k_i^{(\text{ET})} + k_0^{(\text{Cor})}$, where $k_0^{(\text{Cor})}$ is cumulative for the pathways of $^1\text{Cor}^*$ deactivation that do not involve the PDI moiety, as obtained from the time-resolved fluorescence analysis of **Cor-Phe**, $k_0^{(\text{Cor})} = 2.2 \times 10^8 \text{ s}^{-1}$ (Figure S2a). The $\alpha_i^{(\text{ET})}$ preexponential amplitudes of eq. S2b relate to $\alpha_i^{(\text{Cor})}$ of eq. S2a, i.e., $\alpha_i^{(\text{ET})} \propto (k_i^{(\text{ET})} / k_i^{(\text{Cor})}) \alpha_i^{(\text{Cor})}$.

$\Delta A_{LEC}(\lambda, t)$ depicts the dynamics of the $^1\text{Cor}^*$ TA between about 450 and 545 nm, and also in the red and NIR spectral region. This function, eq. S2b, with negative amplitudes, $-\Delta A_{LEC}(\lambda, t)$, describes the stimulated emission (SE) of Cor in the TA spectra. In addition, for this analysis we multiply the fluorescence decay curves, recorded at 650 nm (Figure S2), by a negative constant for direct visual comparison with the SE TA traces.

The Cor bleach (BC) term describes the bleach enhancement (ΔA becoming more negative) and recovery (ΔA becoming more positive) originating, respectively, from the decrease and the increase in the ground-state absorption of Cor, which spreads throughout the visible region of the spectrum:

$$\Delta A_{BC}(\lambda, t) = \sum_{i=1}^m \alpha_i^{(\text{PDI})}(\lambda) e^{-(k_i^{(\text{EnT})} + k_i^{(\text{HT})}) t} - \left(\sum_{i=1}^w \alpha_i^{(\text{CR})}(\lambda) e^{-k_i^{(\text{CR})} t} + \left(\sum_{i=1}^n \alpha_i^{(\text{Cor})}(\lambda) \right) e^{-k_0^{(\text{Cor})} t} + \sum_{i=n+1}^h \alpha_i^{(\text{Cor})}(\lambda) e^{-k_i^{(\text{Cor})} t} \right) \quad (S2c)$$

[$n > h-1$] $\Rightarrow \alpha_i^{(\text{Cor})} = 0$

The first sum represents the EnT and HT from ${}^1\text{PDI}^*$ that lead to removal of the S_0 state of Cor, where $\alpha_i^{(PDI)} \propto \alpha_i^{(PDI)} (k_i^{(EnT)} + k_i^{(HT)}) / (k_i^{(EnT)} + k_i^{(HT)} + k_0^{(PDI)})$ (eq. S2d). The terms in the parentheses depict the deactivation of ${}^1\text{Cor}^*$ and Cor^* to ground state. The first sum in the parentheses shows the kinetics of the recovery of the Cor ground-state absorption from CR, as described in eq. S2a. The second sum encompasses the contributions from the inherent decay of ${}^1\text{Cor}^*$ that is parallel with the ET steps, where $\alpha_i^{(Cor)} \propto \alpha_i^{(Cor)} k_0^{(Cor)} / k_i$. The third term accounts for the deactivation of ${}^1\text{Cor}^*$ to Cor that does not involve accumulation of the CT state. Indeed, when CR is faster than ET, ${}^1\text{Cor}^* \cdots \text{PDI} \rightarrow \text{Cor}^* \cdots \text{PDI}^- \rightarrow \text{Cor} \cdots \text{PDI}$ becomes indiscernible from ${}^1\text{Cor}^* \cdots \text{PDI} \rightarrow \text{Cor} \cdots \text{PDI}$, with ET the rate limiting step of this ET-CR deactivation.

The term for the PDI locally excited state (LEP) describes the dynamics of the locally excited state of the electron acceptor, ${}^1\text{PDI}^*$, that decays via EnT and HT, as well as via the inherent deactivation pathways, observed in the absence of Cor, characterized with $k_0^{(PDI)}$:

$$\Delta A_{LEP}(\lambda, t) = \sum_{i=1}^m \alpha_i^{(PDI)}(\lambda) e^{-k_i^{(PDI)} t} \quad (\text{S2d})$$

Where $k_i^{(PDI)} = k_i^{(EnT)} + k_i^{(HT)} + k_0^{(PDI)}$, and $k_0^{(PDI)} = 2.1 \times 10^8 \text{ s}^{-1}$ (Figure S2b).

$\Delta A_{LEP}(\lambda, t)$ depicts the decay of the ${}^1\text{PDI}^*$ TA in the red and NIR spectral regions. The TA spectrum of ${}^1\text{PDI}^*$ overlaps with the TA spectrum of PDI^- . The differences in the shapes TA bands and the extinction coefficients are relatively small, Nevertheless, they are sufficient to allow for discerning the dynamics of the CT species from that of the LE state of PDI. This function (eq. S2d) with negative amplitudes, $-F_{LEP}(\lambda, t)$, describes the stimulated emission, SE of PDI, appearing between about 500 nm to 650 nm. In addition, for the analysis of **Cor-(Ala)₄-PDI**, with $\lambda_{ex} = 465 \text{ nm}$, we multiply the fluorescence decay curves, recorded at 560 nm (Figure S2f), by a negative constant for direct visual comparison with the SE TA traces.

The PDI bleach (BP) term describes the bleach recovery of the ground-state absorption of PDI, which extends to about 550 nm into the visible spectral region:

$$\Delta A_{BP}(\lambda, t) = - \sum_{i=1}^m \alpha_i^{(PDI)}(\lambda) e^{-k_i^{(EnT)} t} + \left(\sum_{i=1}^n \alpha_i^{(ET)}(\lambda) e^{-k_i^{(ET)} t} - \sum_{i=1}^w \alpha_i^{(CR)}(\lambda) e^{-k_i^{(CR)} t} \right) \quad (\text{S2e})$$

The first sum represents the bleach recovery from the deactivation of ${}^1\text{PDI}^*$ via EnT, and via the radiative and non-radiative decays that do not involve the Cor moiety; $\alpha_i^{(PDI)} \propto \alpha_i^{(PDI)} (k_i^{(EnT)} + k_0^{(PDI)}) / (k_i^{(EnT)} + k_i^{(HT)} + k_0^{(PDI)})$. The terms in the parentheses account for the CT processes, i.e., the PDI bleach enhancement resulting from ET, and the bleach recovery due to CR.

For excitation of the donor at 400 nm, we set $E_{LEP} = E_{BP} = 0$ (eq. S1), $\alpha_i^{(PDI)} = \alpha_i^{(PDI)} = \alpha_i^{(PDI)} = 0$, and $k_i^{(HT)} = k_i^{(EnT)} = k_0^{(PDI)} = 0$ (eq. S2). Global analysis employing this model (eq. S1 and S2) allows fitting the TA data and the fluorescence decays of **Cor-Ala-PDI** and **Cor-Phe-PDI** using five exponential components, i.e., $n = h = 3$ and $w = 2$, eq. S2 (Figure S3a,b, Table 1). Increasing the number of exponential terms yields rate constants, k_i , with closely similar values and no improvement of the fits. Still, the multiexponential outcomes from this analysis are consistent with the conformational heterogeneity of the conjugates that modulates not only the charge-separation (CS) but also the CR kinetics.

To attain good fits for **Cor-(Ala)₄-PDI**, the same global analysis, using eq. S1 and S2, resorts to five exponential components for the ${}^1\text{Cor}^*$ deactivation, i.e., $h = 5$ (eq. S2b,c). Four of the five components describe the kinetics of the formation of the CT state, i.e., $n = 4$ (eq. S2a,c). The fifth component depicts a direct deactivation of ${}^1\text{Cor}^*$ to ground state, corresponding to conformers that do not efficiently mediate ET, i.e., $k_5^{(ET)} \ll k_5^{(Cor)} \approx k_0^{(Cor)}$ (eq. S2, Figure S3c, Table 1). Biexponential decay of the CT state described well the CR dynamic, i.e., $w = 2$ (eq. S2) (Figure S3c, Table 1).

The three components describing the fastest ET, are similar for all three conjugates (Table 1). This feature suggests for close similarity between the donor-acceptor electronic-coupling pathways in the

three conjugates, regardless the length of the linker and the size of the side chains of the amino acids. The larger length of the flexible bridge in **Cor-(Ala)₄-PDI**, in comparison to that of the other two DBA conjugates, increases the degrees of freedom and leads to conformers that do not mediate ET as efficiently.

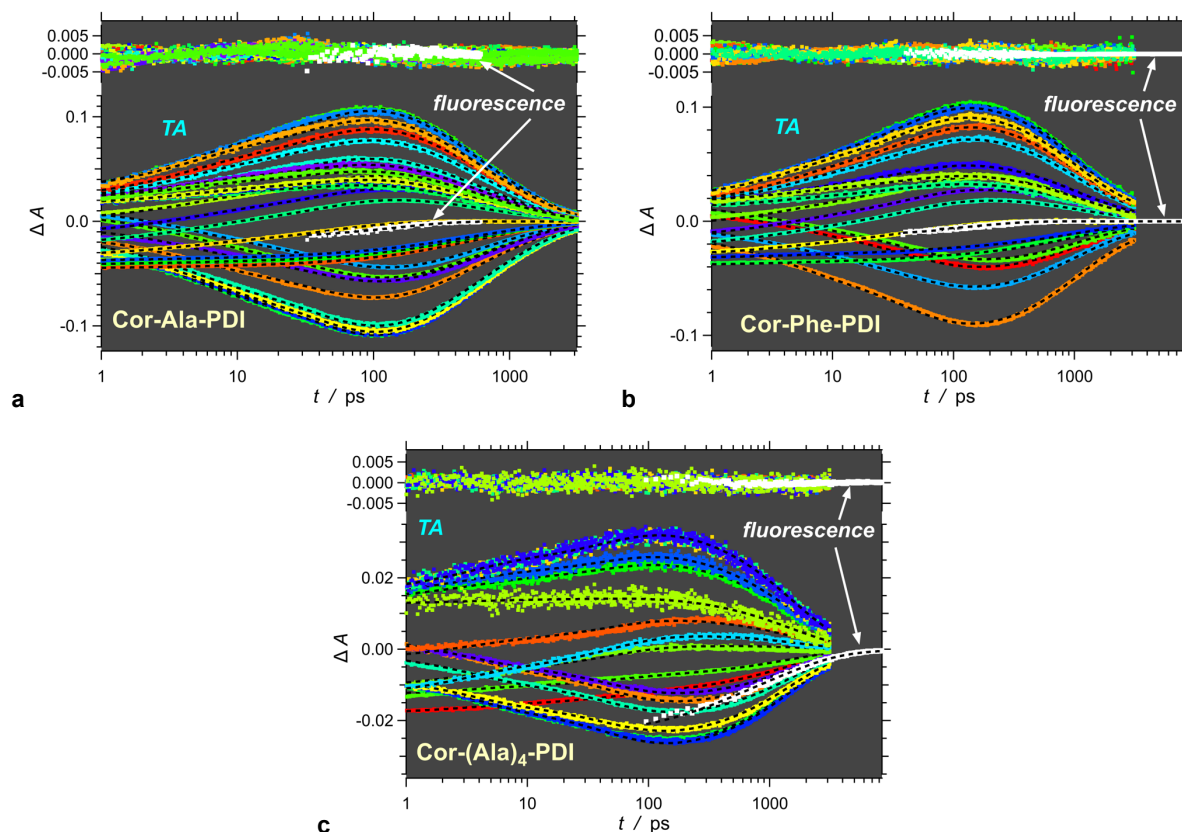


Figure S3. Global-fit analysis (using eq. 1 and 2) of TA and fluorescence-decay dynamics for the three conjugates ($\lambda_{\text{ex}} = 400 \text{ nm}$). The fluorescence decays of $^1\text{Cor}^*$ ($\lambda_{\text{fl}} = 650 \text{ nm}$) are displayed in white. The TA traces for different wavelengths, recorded between 490 and 800 nm, are shown in different colors. The black dashed lines represent the global fits. The residuals from the data fits are on top of the graphs.

Excitation of the acceptor at 465 nm leads to different dynamics in the picosecond time domain involving an initial fast decrease followed by an increase in the amplitude in the NIR spectral region, for example, which is consistent with the decays of $^1\text{PDI}^*$ to its ground state, followed by the growth of PDI^- (Figure 7d,h). The locally excited, LE, state of the electron acceptor, $^1\text{PDI}^*$, in the DBA conjugates has five principal pathways for deactivation: (i) radiative decay to ground state, i.e., via fluorescence; (ii) non-radiative direct decays to ground state via internal conversion, i.e., $^1\text{PDI}^* \rightarrow ^1\text{PDI}$; (iii) triplet formation via intersystem crossing; (iv) hole transfer, HT, to the electron donor, i.e., $\text{Cor}-^1\text{PDI}^* \rightarrow \text{Cor}^{+\bullet} \text{---} \text{PDI}^-$; and (v) resonance energy transfer, EnT, to the electron donor, i.e., $\text{Cor}\text{---}^1\text{PDI}^* \rightarrow ^1\text{Cor}^*\text{---}\text{PDI}$. The first three pathways are inherent for PDI and are described by a single rate constant, $k_0^{(\text{PDI})}$, determined from the excited-state lifetime of the chromophore in the absence of the electron donor, i.e., obtained from the optical emission decay of PDI (Figure S2b).

Because R_0 for EnT from PDI to Cor is 46 Å, which considerably exceeds the largest possible donor-acceptor distances in these DBA conjugates, it is reasonable to assume that it will dominate the excited state dynamics of PDI. Nevertheless, this estimate of R_0 assumes randomized orientation between the transition-dipole moments of Cor photoemission and PDI absorption. Conformers that lock orthogonal and close to orthogonal orientations between the transition dipole moments can suppress and even completely prevent EnT.

This model represented by eq. 1 and 2 leads to good global fits for the TA dynamics of the three DBA conjugates (Figure S4). For **Cor-(Ala)₄-PDI**, we also incorporated the fluorescence decay recorded at 560 nm, corresponding to the PDI emission (Figure S4c).

For the conjugates with short linkers, **Cor-Ala-PDI** and **Cor-Phe-PDI**, two exponential components can describe the PDI decay (depicting EnT and HT), i.e., $m = 2$, eq. S2 (Table 1). Similar to the results from the TA with selective excitation of the electron donor, three exponential terms describe the ¹Cor* decay dynamics, i.e., $n = 3$, and CR shows biexponential character, i.e., $w = 2$ (Table 1).

When exciting the electron acceptor in **Cor-(Ala)₄-PDI**, incorporating the fluorescence decay of PDI (monitored at 560 nm) along with the TA kinetics requires four exponential terms for describing the ¹PDI* dynamics, $m = 4$, eq. S2. The fourth component, however, does not have significant contribution, i.e., $k_4^{(PDI)} = 2.9 (\pm 0.3) \times 10^8 \text{ s}^{-1}$ and $\alpha_4^{(PDI)} = 2 \times 10^{-4}$. While this component is consistent with the long-lived PDI fluorescence of **Cor-(Ala)₄-PDI** (Figure S2f), it does not truly contribute to the TA dynamics (Table 1). Similar to the TA analysis with 400-nm excitation, five exponential terms can describe the ¹Cor* deactivation, $h = 5$ and $n = 4$, eq. S2 (Table 1). In this case, however, a monoexponential decay function can fit well the CR dynamics (Figure S4c, Table 1).

The absorption of the PDI transients, along with the PDI stimulated-emission, dominate the TA spectra of the three conjugates, which is another one of their characteristic. In the visible spectral region, the PDI transients have larger molar extinction coefficients than the Cor transients. PDI has considerably larger fluorescence quantum yields than Cor. Therefore, the absorption of the PDI transients, along with the PDI stimulated-emission, dominate the TA spectra of the three conjugates.

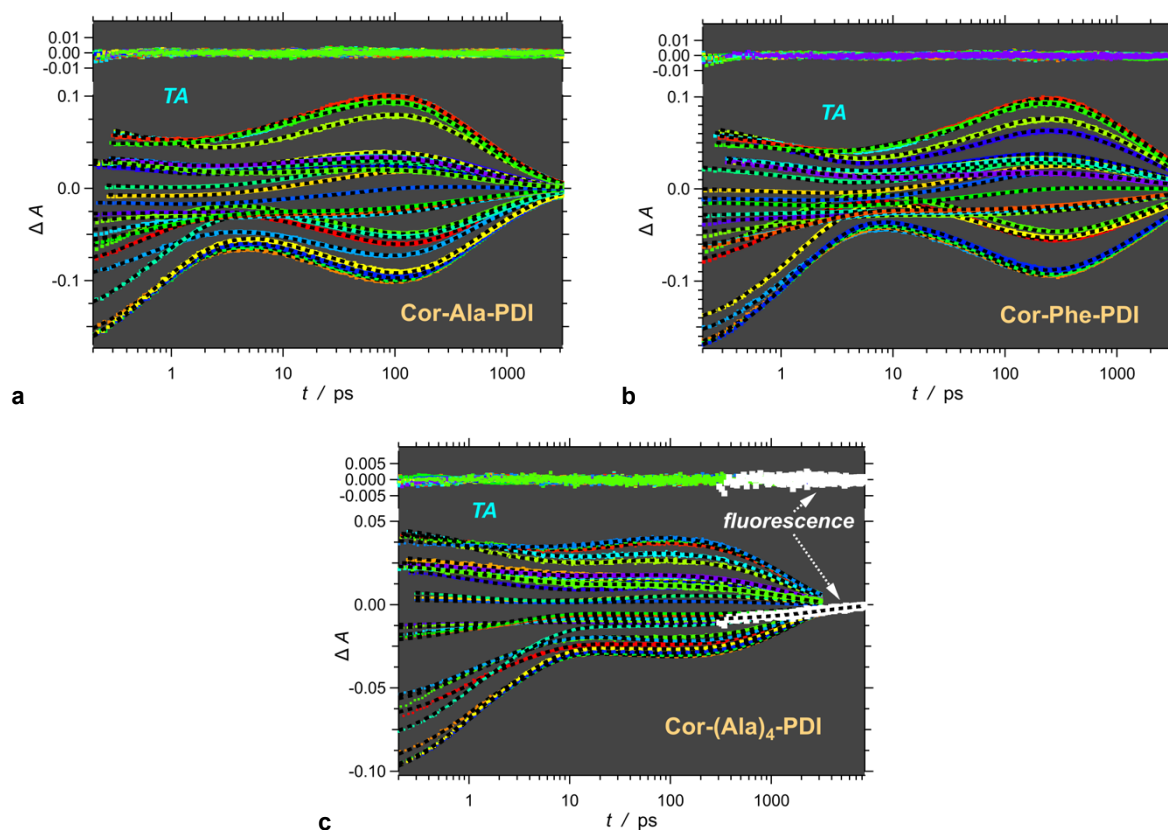


Figure S4. Global-fit analysis (using eq. 1 and 2) of TA dynamics for the three conjugates ($\lambda_{\text{ex}} = 465 \text{ nm}$). (c) For **Cor-(Ala)₄-PDI**, we also incorporate the fluorescence decays of ¹PDI* ($\lambda_{\text{fl}} = 560 \text{ nm}$), displayed in white, in the analysis. The TA traces for different wavelengths, recorded between 490 and 800 nm, are shown in different colors. The black dashed lines represent the global fits. The residuals from the data fits are on top of the graphs.

6. Computational analysis

All calculations were performed within the density functional theory (DFT) approach using Gaussian 09 program suite.⁽¹¹⁾ Geometry was optimized with the B3LYP functional, employing the 6-31G(d,p) basis set. Solvent effects were considered within the SCRF theory using the polarized continuum model (PCM) approach to model the interaction with the solvent. The structures were optimized in chloroform (for comparison with experimental NMR data) and in toluene (for comparison with ECD spectra). The results were highly similar. Excited electronic states were determined at the B3LYP/6-31G level by means of the time-dependent DFT (TD DFT) approach (100 excited states in each case). The ECD spectra were simulated by overlapping Gaussian functions for each transition where the width of the band at 1/e height is fixed at 0.1 eV. Aliphatic chains were shortened since their lengths have negligible influence on UV-VIS and ECD spectra.

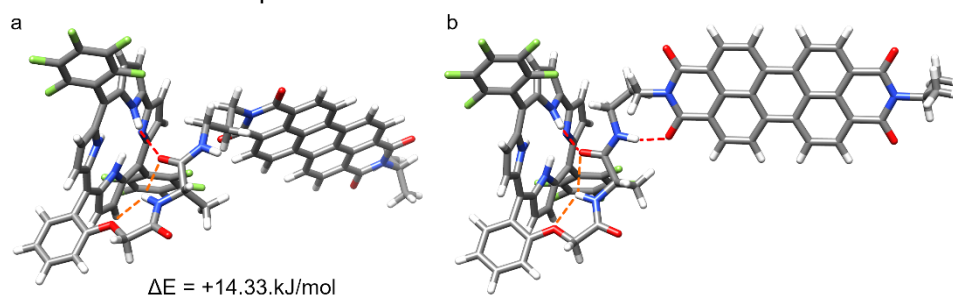


Figure S5. Structures of **Cor-Ala-PDI_{opt}** obtained by geometry optimization (DFT 6-31G(d,p) in chloroform): (a) **Cor-Ala-PDI_{opt}** without hydrogen bond to PDI; (b) **Cor-Ala-PDI_{opt}** with hydrogen bond to PDI.

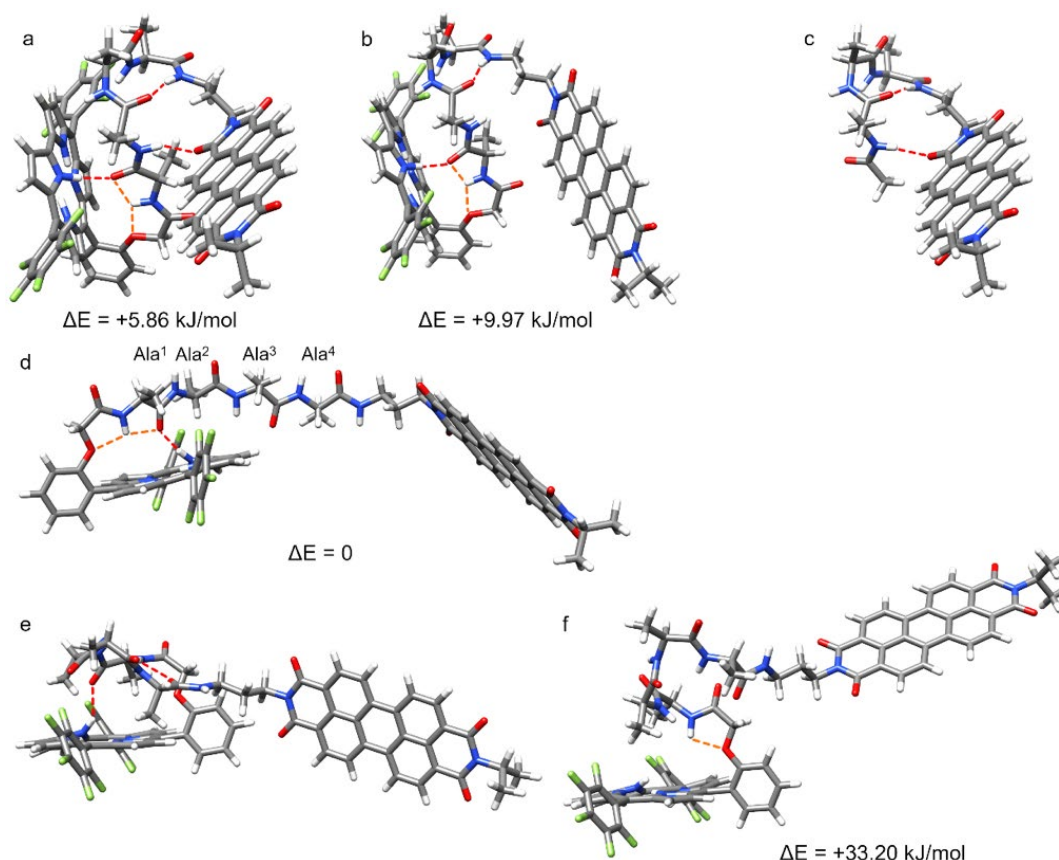


Figure S6. Structures of **Cor-(Ala)₄-PDI** obtained by geometry optimization (DFT 6-31G(d,p) in chloroform): (a) folded **Cor-(Ala)₄-PDI_{opt}** with hydrogen bond to PDI; (b) folded **Cor-(Ala)₄-PDI_{opt}** without hydrogen bond to PDI; (c) folded **(Ala)₄-PDI_{opt}** with hydrogen bond to PDI; (d) extended **Cor-(Ala)₄-PDI_{opt}**; (e) turn1,4-**Cor-(Ala)₄-PDI_{initial}**; (f) turn1,4-**Cor-(Ala)₄-PDI_{opt}**.

Atomic coordinates for all calculated geometries:

Cor-Ala-PDI_{opt} with hydrogen bond to PDI in chloroform

Energy total = -4733.31253682 a.u.

Symbol	X	Y	Z
C	-4.1504230	-0.6287080	-3.2054660
C	-4.0679930	-1.6059240	-4.2662100
H	-3.7214050	-1.4309010	-5.2763670
C	-4.5197870	-2.7876220	-3.7312200
H	-4.6225580	-3.7357360	-4.2421750
C	-4.8895460	-2.5057050	-2.3543600
C	-5.5765940	-3.3114920	-1.4152720
C	-6.0684290	-2.7867420	-0.1959950
C	-6.7753340	-3.4097480	0.8775570
H	-7.0663300	-4.4494770	0.9143190
C	-7.0158250	-2.4542320	1.8406660
H	-7.5440960	-2.5908770	2.7725350
C	-6.4653910	-1.2063480	1.3964220
C	-6.4764020	0.0258560	2.0964600
C	-6.0312490	1.2765620	1.6344010
C	-5.8550690	2.4765260	2.4020420
H	-6.0823280	2.5631010	3.4539970
C	-5.3171030	3.4470340	1.5922280
H	-5.0275860	4.4455920	1.8858040
C	-5.1310660	2.8999600	0.2829510
C	-4.5589880	3.4928530	-0.8613800
C	-4.2021280	2.7243160	-2.0044900
C	-4.0946660	3.0387740	-3.3865580
H	-4.2074440	4.0263820	-3.8114750
C	-3.9463310	1.8435940	-4.0924710
H	-3.9212750	1.7313210	-5.1675230
C	-3.9575760	0.7814570	-3.1567320
N	-4.6189290	-1.1996980	-2.0742000
N	-5.9164030	-1.4600270	0.1611060
N	-5.5992480	1.5936480	0.3587870
N	-4.0669290	1.3603910	-1.9132420
H	-3.7577420	0.8789350	-1.0668750
C	-6.9270840	-0.0323040	3.5269930
C	-6.0185510	-0.4568030	4.5221940
C	-6.4061840	-0.5235480	5.8629170
H	-5.7107760	-0.8572640	6.6242400
C	-7.7072780	-0.1581800	6.2215710
H	-8.0029450	-0.2129410	7.2650480
C	-8.6154810	0.2713460	5.2567240
H	-9.6240600	0.5562370	5.5382320
C	-8.2176350	0.3315650	3.9174990
H	-8.9160760	0.6644300	3.1553520
O	-4.7699570	-0.7826230	4.0704180
C	-3.7201960	-1.0574930	4.9853250
H	-3.6300050	-0.2654840	5.7395400
H	-3.8787500	-2.0094930	5.5063060
C	-2.3913280	-1.1419970	4.2318900
O	-1.3660660	-1.4414090	4.8461010
N	-2.4444320	-0.8558190	2.9166510
H	-3.3295650	-0.6145590	2.4862140
C	-5.8266480	-4.7425110	-1.7303350
C	-4.7691700	-5.6387990	-1.9342940
C	-4.9790580	-6.9786890	-2.2465970
C	-6.2782860	-7.4640200	-2.3599520
C	-7.3540370	-6.6036630	-2.1628010
C	-7.1197290	-5.2657340	-1.8591940
F	-3.4997470	-5.2202910	-1.8180580
F	-3.9400990	-7.8052360	-2.4270010
F	-6.4917840	-8.7499880	-2.6568180

F	-8.6067620	-7.0636680	-2.2820670
F	-8.1887450	-4.4698660	-1.7008880
C	-4.3376650	4.9555830	-0.8924650
C	-3.0795600	5.4976760	-1.1992710
C	-2.8507290	6.8683800	-1.2564360
C	-3.8941220	7.7525180	-0.9975340
C	-5.1557910	7.2545250	-0.6862270
C	-5.3646910	5.8794860	-0.6443330
F	-2.0305650	4.6888590	-1.4284350
F	-1.6307280	7.3418990	-1.5421920
F	-3.6849380	9.0716640	-1.0459480
F	-6.1664410	8.1012140	-0.4497870
F	-6.6068910	5.4523340	-0.3713770
C	-1.2725410	-0.8640550	2.0596810
H	-0.4330650	-0.4451290	2.6243590
C	-0.9006690	-2.2874830	1.6004180
H	-1.7131010	-2.7231480	1.0119380
H	0.0075740	-2.2734390	0.9911730
C	-1.5807160	0.0286680	0.8469270
N	-0.5075630	0.5393170	0.2244240
H	0.4222390	0.3771750	0.6082870
O	-2.7510950	0.2093320	0.4761520
N	3.0540300	2.0317720	-0.4823120
N	13.8172330	-1.6478850	0.5101800
O	3.7275570	3.5920930	-2.0131020
O	2.3676980	0.4050270	0.9649250
O	14.4604320	-0.0651670	-1.0164570
O	13.0971330	-3.2176780	2.0249990
C	4.0344650	2.6741520	-1.2613110
C	5.4222090	2.1869260	-1.1165360
C	5.7280710	1.1110160	-0.2481850
C	4.6921330	0.4874520	0.4899500
C	3.2968530	0.9469590	0.3584570
C	4.9898620	-0.5675330	1.3378260
H	4.1874940	-1.0368320	1.8954710
C	6.3056250	-1.0190460	1.4725300
H	6.4895900	-1.8444900	2.1480340
C	7.3595750	-0.4369180	0.7643430
C	7.0751880	0.6520530	-0.1202770
C	8.1046690	1.2925400	-0.8810010
C	7.7557240	2.3501290	-1.7240960
C	6.4352790	2.7923780	-1.8427500
H	6.1871890	3.6146780	-2.5042030
C	9.4897730	0.8174660	-0.7525170
C	10.5438140	1.3896720	-1.4677430
H	10.3613420	2.2123350	-2.1473640
C	11.8587380	0.9300790	-1.3384710
H	12.6612430	1.3887550	-1.9044990
C	12.1557040	-0.1189220	-0.4847070
C	11.1195810	-0.7287410	0.2598770
C	9.7732450	-0.2685500	0.1339850
C	8.7459640	-0.9071980	0.8972730
C	9.0984990	-1.9599590	1.7443530
C	10.4205030	-2.4018770	1.8616230
H	10.6703490	-3.2212040	2.5257260
C	11.4303710	-1.7992450	1.1299700
C	12.8225610	-2.2885170	1.2718560
C	13.5588040	-0.5874040	-0.3677580
C	1.6616610	2.5013140	-0.5890300
H	1.7071460	3.5292180	-0.9422430
C	0.8043940	1.6277670	-1.5367700
H	1.3092040	0.6721730	-1.7133840
H	0.7134210	2.1180220	-2.5099470
C	15.2199450	-2.1516860	0.6600560
H	15.1178580	-2.9494310	1.3944350
C	16.1497050	-1.0839620	1.2469390

H	15.7369620	-0.6772070	2.1753040
H	16.3182810	-0.2650230	0.5467430
C	15.7422120	-2.7700510	-0.6413840
H	15.8817470	-2.0177470	-1.4186960
H	15.0544830	-3.5374030	-1.0099410
H	8.5123040	2.8549440	-2.3110030
H	8.3444860	-2.4628690	2.3363990
C	-0.5968160	1.3494260	-0.9915070
H	17.1138710	-1.5454380	1.4828270
H	16.7059750	-3.2502760	-0.4445330
H	1.2514180	2.4991300	0.4220850
H	-1.1881810	0.8132130	-1.7398460
H	-1.1244060	2.2872410	-0.7783210
H	-5.7448700	1.0208460	-0.4576460
H	-0.7219010	-2.9120200	2.4784820
H	-5.3029470	-0.9036690	-0.4493020

Cor-Ala-PDI_{opt} with hydrogen bond to PDI in toluene

Energy total = -4733.30472140 a.u.

Symbol	X	Y	Z
C	-4.1588920	-0.6198330	-3.2043410
C	-4.0740420	-1.5978500	-4.2644740
H	-3.7256350	-1.4237970	-5.2741520
C	-4.5253940	-2.7790240	-3.7294170
H	-4.6259290	-3.7277470	-4.2395410
C	-4.8976710	-2.4962450	-2.3532440
C	-5.5837100	-3.3024070	-1.4145450
C	-6.0752590	-2.7785140	-0.1946390
C	-6.7831700	-3.4013270	0.8780480
H	-7.0771830	-4.4402110	0.9129530
C	-7.0216340	-2.4465960	1.8422960
H	-7.5504670	-2.5825380	2.7739140
C	-6.4687490	-1.1996910	1.3991420
C	-6.4781110	0.0323670	2.0998260
C	-6.0326740	1.2828870	1.6384410
C	-5.8576040	2.4827800	2.4063940
H	-6.0877810	2.5690130	3.4577190
C	-5.3180590	3.4529090	1.5976890
H	-5.0297410	4.4517060	1.8914570
C	-5.1298370	2.9062470	0.2884990
C	-4.5550970	3.4992590	-0.8542380
C	-4.2010760	2.7318100	-1.9993840
C	-4.0939680	3.0479790	-3.3807210
H	-4.2048730	4.0364330	-3.8041340
C	-3.9497540	1.8533350	-4.0887330
H	-3.9271400	1.7429510	-5.1640340
C	-3.9633440	0.7899760	-3.1550150
N	-4.6291470	-1.1898140	-2.0740840
N	-5.9204630	-1.4529860	0.1638700
N	-5.5994700	1.6006350	0.3633520
N	-4.0699580	1.3674760	-1.9105160
H	-3.7583720	0.8838540	-1.0659680
C	-6.9262290	-0.0269290	3.5310450
C	-6.0166870	-0.4571630	4.5230200
C	-6.4012960	-0.5254330	5.8644910
H	-5.7048980	-0.8636240	6.6230180
C	-7.6999820	-0.1559220	6.2273140
H	-7.9933820	-0.2119290	7.2714180
C	-8.6087800	0.2792070	5.2659100
H	-9.6155780	0.5672360	5.5506470
C	-8.2141300	0.3408530	3.9258200
H	-8.9129970	0.6778970	3.1659130
O	-4.7710750	-0.7858800	4.0670620
C	-3.7193150	-1.0709120	4.9760300

H	-3.6215670	-0.2832370	5.7340370
H	-3.8807220	-2.0247020	5.4930930
C	-2.3931230	-1.1592430	4.2170590
O	-1.3680690	-1.4656300	4.8254340
N	-2.4512130	-0.8670740	2.9023230
H	-3.3363690	-0.6205360	2.4751380
C	-5.8318380	-4.7338020	-1.7294420
C	-4.7725310	-5.6281920	-1.9336680
C	-4.9803310	-6.9687180	-2.2458780
C	-6.2789840	-7.4563940	-2.3583970
C	-7.3563730	-6.5978920	-2.1605020
C	-7.1243630	-5.2591520	-1.8572600
F	-3.5042820	-5.2076180	-1.8181050
F	-3.9402900	-7.7933900	-2.4268010
F	-6.4903440	-8.7426060	-2.6549660
F	-8.6079860	-7.0603730	-2.2786090
F	-8.1941890	-4.4656080	-1.6978610
C	-4.3274320	4.9609380	-0.8824270
C	-3.0666480	5.4978700	-1.1882980
C	-2.8312980	6.8677400	-1.2439630
C	-3.8706880	7.7565710	-0.9837130
C	-5.1347720	7.2638690	-0.6726860
C	-5.3503190	5.8894580	-0.6328630
F	-2.0210850	4.6847290	-1.4177850
F	-1.6091950	7.3357480	-1.5287320
F	-3.6553850	9.0746080	-1.0302630
F	-6.1410090	8.1148490	-0.4347870
F	-6.5939350	5.4679230	-0.3602710
C	-1.2815770	-0.8782040	2.0431960
H	-0.4390640	-0.4644120	2.6075270
C	-0.9153830	-2.3022710	1.5809370
H	-1.7300880	-2.7339790	0.9926730
H	-0.0076930	-2.2905890	0.9705550
C	-1.5885070	0.0175520	0.8327390
N	-0.5133810	0.5223670	0.2066640
H	0.4161750	0.3546300	0.5879670
O	-2.7577800	0.2070250	0.4657260
N	3.0486670	2.0148970	-0.4989870
N	13.8186630	-1.6424720	0.5214260
O	3.7245090	3.5785120	-2.0261410
O	2.3625430	0.3827080	0.9425710
O	14.4611730	-0.0571990	-1.0035270
O	13.0966030	-3.2124640	2.0356360
C	4.0301790	2.6605510	-1.2756360
C	5.4187010	2.1744720	-1.1278440
C	5.7245430	1.0984160	-0.2597710
C	4.6876590	0.4721230	0.4747050
C	3.2910850	0.9286660	0.3399450
C	4.9847230	-0.5828930	1.3224620
H	4.1804260	-1.0532460	1.8766430
C	6.3012110	-1.0314160	1.4606960
H	6.4853530	-1.8572380	2.1359040
C	7.3564910	-0.4466510	0.7566860
C	7.0723520	0.6421990	-0.1283140
C	8.1025460	1.2852920	-0.8860140
C	7.7529640	2.3424770	-1.7293340
C	6.4320120	2.7825240	-1.8511260
H	6.1818900	3.6048040	-2.5120160
C	9.4883350	0.8130550	-0.7539160
C	10.5435820	1.3870230	-1.4658510
H	10.3608000	2.2094550	-2.1459180
C	11.8593680	0.9304900	-1.3329920
H	12.6640920	1.3894520	-1.8958330
C	12.1556520	-0.1174910	-0.4782380
C	11.1186440	-0.7292830	0.2633830
C	9.7715450	-0.2723000	0.1334660

C	8.7437250	-0.9133330	0.8940270
C	9.0971670	-1.9645070	1.7426050
C	10.4199700	-2.4033850	1.8640340
H	10.6722230	-3.2215250	2.5288560
C	11.4297970	-1.7985860	1.1347080
C	12.8235170	-2.2852560	1.2812960
C	13.5606820	-0.5824270	-0.3573890
C	1.6561980	2.4842400	-0.6068490
H	1.7026850	3.5119620	-0.9608960
C	0.7982200	1.6111060	-1.5543530
H	1.3025470	0.6550650	-1.7307240
H	0.7079610	2.1015840	-2.5275420
C	15.2221380	-2.1430870	0.6752720
H	15.1194870	-2.9418270	1.4087110
C	16.1468420	-1.0723310	1.2647040
H	15.7318290	-0.6690460	2.1936040
H	16.3123690	-0.2517670	0.5656620
C	15.7496650	-2.7574450	-0.6259670
H	15.8873990	-2.0032740	-1.4017810
H	15.0663320	-3.5277130	-0.9966940
H	8.5104990	2.8487980	-2.3139420
H	8.3423560	-2.4684760	2.3329970
C	-0.6029280	1.3335250	-1.0081330
H	17.1128630	-1.5298270	1.5009640
H	16.7151210	-3.2339100	-0.4280230
H	1.2451630	2.4814370	0.4040770
H	-1.1959990	0.7992730	-1.7566500
H	-1.1295350	2.2718000	-0.7942030
H	-5.7373520	1.0252030	-0.4525120
H	-0.7375230	-2.9276180	2.4585750
H	-5.3052190	-0.8979220	-0.4461040

Cor-Ala-PDI_{opt} without hydrogen bond to PDI in chloroform
Energy total = -4733.30707714 a.u.

Symbol	X	Y	Z
C	2.1715570	-0.4470080	-2.5244940
C	0.9660820	-0.2877750	-3.3036370
H	0.5493370	-1.0056010	-3.9979630
C	0.4670710	0.9497900	-2.9810310
H	-0.4202710	1.4187300	-3.3841740
C	1.3913080	1.5362060	-2.0261370
C	1.4399550	2.8526860	-1.5069660
C	2.5587870	3.3300170	-0.7838320
C	2.8124370	4.5925370	-0.1659740
H	2.1360790	5.4349340	-0.1652450
C	4.0573290	4.5372890	0.4215470
H	4.5538780	5.3288400	0.9621940
C	4.6202580	3.2376480	0.1851710
C	5.8748390	2.7537840	0.6318810
C	6.4551540	1.5005940	0.3639100
C	7.6442160	0.9501620	0.9458260
H	8.2658750	1.4642470	1.6631190
C	7.8217680	-0.3279540	0.4740470
H	8.6024620	-1.0177140	0.7599450
C	6.7577100	-0.6349680	-0.4293660
C	6.5005480	-1.8278260	-1.1352440
C	5.2713990	-2.0468140	-1.8140870
C	4.9266540	-2.8317840	-2.9486280
H	5.5894980	-3.5220970	-3.4510750
C	3.6484290	-2.4586500	-3.3640030
H	3.1327100	-2.8069500	-4.2480210
C	3.1864880	-1.4435030	-2.4919910
N	2.3909980	0.6482780	-1.7629720
N	3.6798290	2.5555660	-0.5524060

N	5.9603690	0.5066180	-0.4658490
N	4.1696490	-1.2711170	-1.5448730
H	3.9816570	-0.8250870	-0.6504610
C	6.6469860	3.6508160	1.5554460
C	6.6206390	3.4142350	2.9474820
C	7.3439360	4.2276180	3.8243450
H	7.3268120	4.0432230	4.8919660
C	8.0910600	5.2945540	3.3169440
H	8.6481510	5.9240060	4.0044050
C	8.1236420	5.5493920	1.9481090
H	8.7062680	6.3765340	1.5556680
C	7.4050280	4.7233050	1.0790130
H	7.4317680	4.9047510	0.0086080
O	5.8523220	2.3550860	3.3484510
C	5.8768800	1.9337680	4.7030680
H	6.8925120	1.6669100	5.0205780
H	5.5051210	2.7173970	5.3751530
C	4.9792220	0.7112290	4.8870540
O	4.8866940	0.1982460	6.0037620
N	4.3239350	0.2808410	3.7908130
H	4.4596860	0.7401720	2.8973520
C	0.2936710	3.7672730	-1.7526380
C	-0.9938490	3.4554510	-1.2946970
C	-2.0928440	4.2704660	-1.5453040
C	-1.9266820	5.4524160	-2.2599340
C	-0.6606430	5.8019800	-2.7210770
C	0.4219720	4.9628900	-2.4713980
F	-1.2046150	2.3410920	-0.5811970
F	-3.3075150	3.9243410	-1.0903550
F	-2.9743640	6.2468500	-2.5021610
F	-0.4946260	6.9338680	-3.4186410
F	1.6159400	5.3303010	-2.9619460
C	7.5506220	-2.8682890	-1.2179530
C	7.2874120	-4.2005360	-0.8619140
C	8.2499140	-5.2007800	-0.9519350
C	9.5286780	-4.8887040	-1.4039510
C	9.8290000	-3.5789850	-1.7658580
C	8.8481290	-2.5958830	-1.6786850
F	6.0782500	-4.5469050	-0.3948680
F	7.9585690	-6.4574340	-0.5904450
F	10.4626380	-5.8408830	-1.4893030
F	11.0536140	-3.2763560	-2.2167100
F	9.1806650	-1.3572780	-2.0731400
C	3.3667900	-0.8085760	3.8388060
H	3.8119410	-1.6408620	4.3973360
C	2.0613040	-0.3815240	4.5419610
H	1.5766470	0.4265000	3.9865050
H	1.3602730	-1.2163730	4.6253290
C	3.0846830	-1.2589030	2.3940670
N	2.3828850	-2.4121280	2.2936800
H	2.1282630	-2.8800680	3.1529680
O	3.4500330	-0.5817340	1.4277990
N	-1.9790540	-2.7103180	-0.0455530
N	-13.1220230	-0.2479340	0.4488340
O	-1.5109280	-0.5020230	-0.3660980
O	-2.4510970	-4.9109020	0.3625330
O	-12.6079810	1.9687520	0.1800860
O	-13.5629370	-2.4854010	0.7277650
C	-2.3603090	-1.3672580	-0.1924980
C	-3.8057290	-1.0618050	-0.1253510
C	-4.7510140	-2.0932980	0.0903750
C	-4.3072360	-3.4296790	0.2487720
C	-2.8645930	-3.7664650	0.2001590
C	-5.2331560	-4.4381050	0.4574120
H	-4.8804650	-5.4559110	0.5793910
C	-6.6005410	-4.1485300	0.5081030

H	-7.2853680	-4.9708960	0.6712470
C	-7.0836230	-2.8469530	0.3587830
C	-6.1452780	-1.7863820	0.1515580
C	-6.5655880	-0.4261730	0.0039080
C	-5.5957660	0.5561200	-0.2085350
C	-4.2330780	0.2479150	-0.2737420
H	-3.4997570	1.0297310	-0.4384520
C	-7.9990710	-0.1090420	0.0814850
C	-8.4810200	1.1970780	-0.0271700
H	-7.7953300	2.0231560	-0.1661040
C	-9.8476340	1.4874800	0.0396340
H	-10.1990020	2.5092210	-0.0471600
C	-10.7743680	0.4734170	0.2158370
C	-10.3316460	-0.8643270	0.3349820
C	-8.9376670	-1.1714870	0.2742040
C	-8.5190830	-2.5328410	0.4080150
C	-9.4932850	-3.5182690	0.5824030
C	-10.8558660	-3.2073560	0.6346180
H	-11.5946040	-3.9888470	0.7701860
C	-11.2829790	-1.8950650	0.5149260
C	-12.7324450	-1.5943610	0.5748760
C	-12.2177780	0.8087310	0.2774870
C	-0.5351690	-3.0017020	-0.1214530
H	-0.1293520	-2.4039570	-0.9398130
C	0.1874060	-2.6606460	1.1869420
H	-0.2120270	-3.2838220	1.9965490
H	-0.0109490	-1.6151330	1.4386230
C	-14.5898870	0.0437460	0.5038000
H	-15.0321190	-0.9427450	0.6355510
C	-15.1031720	0.6211350	-0.8199020
H	-14.8305440	-0.0278980	-1.6577920
H	-14.7079300	1.6207760	-1.0041690
C	-14.9553860	0.8938830	1.7254760
H	-14.5545640	1.9051650	1.6475920
H	-14.5802960	0.4334940	2.6447090
H	-5.8830720	1.5928610	-0.3305780
H	-9.2086550	-4.5582250	0.6807030
C	1.7063300	-2.8551050	1.0772090
H	-16.1956300	0.6791610	-0.7821900
H	-16.0456590	0.9554210	1.8019430
H	-0.4396800	-4.0600690	-0.3621490
H	2.1085540	-2.2631960	0.2541660
H	1.9562820	-3.9049900	0.8885420
H	2.2997220	-0.0309080	5.5475500
H	5.2853430	0.6645810	-1.1982040
H	3.5910280	1.5645350	-0.8130500

Cor-Ala-PDI_{opt} without hydrogen bond to PDI in toluene

Energy total = -4733.29869576 a.u.

Symbol	X	Y	Z
C	2.6808860	-0.7866350	-2.5300080
C	1.4444940	-0.7234430	-3.2726980
H	1.0498710	-1.4856430	-3.9318080
C	0.8760900	0.4900490	-2.9650520
H	-0.0626150	0.8812750	-3.3315150
C	1.7919620	1.1583460	-2.0573390
C	1.7664550	2.4792770	-1.5525960
C	2.8571850	3.0408710	-0.8536580
C	3.0414400	4.3365450	-0.2811260
H	2.3213590	5.1415880	-0.3167510
C	4.2848830	4.3666370	0.3120580
H	4.7387900	5.2010150	0.8253540
C	4.9133830	3.0883920	0.1265100
C	6.1793510	2.6741300	0.6099700

C	6.8105500	1.4349310	0.4008220
C	7.9996400	0.9482570	1.0369910
H	8.5795790	1.5101390	1.7533060
C	8.2344990	-0.3386570	0.6191400
H	9.0284320	-0.9904180	0.9533000
C	7.2100570	-0.7162420	-0.3032810
C	7.0165880	-1.9428140	-0.9686830
C	5.8191170	-2.2327890	-1.6778790
C	5.5384390	-3.0783520	-2.7857500
H	6.2407060	-3.7657040	-3.2359330
C	4.2606130	-2.7725590	-3.2555280
H	3.7851670	-3.1798270	-4.1368450
C	3.7363710	-1.7383750	-2.4450890
N	2.8555710	0.3434020	-1.8091410
N	4.0166460	2.3364080	-0.5945460
N	6.3742650	0.3944110	-0.4050690
N	4.6827320	-1.4872220	-1.4792440
H	4.4468010	-0.9955060	-0.6221070
C	6.8893740	3.6266550	1.5279110
C	6.8017840	3.4422540	2.9256360
C	7.4636710	4.3049210	3.8034260
H	7.4057690	4.1562870	4.8752930
C	8.2081700	5.3708880	3.2897740
H	8.7182430	6.0390750	3.9772660
C	8.3000050	5.5748350	1.9154070
H	8.8808010	6.4015010	1.5192450
C	7.6439660	4.6982730	1.0458640
H	7.7164080	4.8400700	-0.0284230
O	6.0455940	2.3753420	3.3255770
C	5.8883890	2.0818760	4.7040700
H	6.8368200	1.7755470	5.1617170
H	5.5069410	2.9500470	5.2570820
C	4.8786000	0.9471330	4.8820120
O	4.6893060	0.4832820	6.0064910
N	4.2225830	0.5625570	3.7680150
H	4.5120980	0.9141410	2.8622160
C	0.5479320	3.3035830	-1.7809610
C	-0.6489370	3.0126180	-1.1154460
C	-1.8237780	3.7121240	-1.3742630
C	-1.8166730	4.7524120	-2.2988300
C	-0.6367300	5.0853830	-2.9581280
C	0.5226050	4.3596310	-2.6974020
F	-0.6827630	2.0471530	-0.1885720
F	-2.9630700	3.3973390	-0.7384550
F	-2.9401430	5.4339880	-2.5486740
F	-0.6284990	6.0868400	-3.8479910
F	1.6347650	4.6912490	-3.3692690
C	8.1030730	-2.9489820	-0.9726580
C	7.8728230	-4.2729820	-0.5659550
C	8.8714430	-5.2417520	-0.5819590
C	10.1531480	-4.9044690	-1.0076530
C	10.4210750	-3.6015950	-1.4175280
C	9.4048690	-2.6507520	-1.4047240
F	6.6620870	-4.6403050	-0.1218490
F	8.6116810	-6.4908500	-0.1748980
F	11.1206820	-5.8259240	-1.0219330
F	11.6486090	-3.2756840	-1.8424490
F	9.7075680	-1.4195210	-1.8422750
C	3.1917900	-0.4606520	3.7784670
H	3.5854880	-1.3549820	4.2819840
C	1.9418100	0.0176870	4.5408170
H	1.4613770	0.8492330	4.0176530
H	1.2089380	-0.7840860	4.6734830
C	2.9079230	-0.8326290	2.3044020
N	1.8202030	-1.6105710	2.1117770
H	1.2978630	-1.9018110	2.9252350

O	3.6377770	-0.4291470	1.3937360
N	-2.4018590	-1.9218390	-0.4173330
N	-13.6913210	-0.5191570	0.6417640
O	-2.2657800	0.0893220	-1.5009580
O	-2.5596280	-3.9311370	0.6575000
O	-13.4923910	1.5339480	-0.3567270
O	-13.8147680	-2.5910490	1.6276880
C	-2.9636520	-0.7441710	-0.9360590
C	-4.4240860	-0.5660800	-0.7622180
C	-5.2153620	-1.5794830	-0.1692040
C	-4.5975850	-2.7634160	0.3012650
C	-3.1307030	-2.9419030	0.2088060
C	-5.3687100	-3.7568570	0.8808030
H	-4.8796980	-4.6554590	1.2396740
C	-6.7526820	-3.5992760	1.0042690
H	-7.3144030	-4.4034150	1.4626570
C	-7.4046670	-2.4451430	0.5648270
C	-6.6271200	-1.4037830	-0.0346350
C	-7.2244390	-0.1880250	-0.4967270
C	-6.4002450	0.7928010	-1.0521410
C	-5.0201480	0.6097670	-1.1866730
H	-4.3977890	1.3915200	-1.6058750
C	-8.6777600	-0.0097430	-0.3639340
C	-9.3322290	1.1427390	-0.8037920
H	-8.7727200	1.9458960	-1.2667160
C	-10.7152700	1.3041040	-0.6688720
H	-11.2036510	2.2071920	-1.0168050
C	-11.4851690	0.3108200	-0.0875250
C	-10.8658560	-0.8755080	0.3695920
C	-9.4543980	-1.0511480	0.2353560
C	-8.8570570	-2.2639010	0.7032420
C	-9.6793240	-3.2356070	1.2775680
C	-11.0599080	-3.0525330	1.4070850
H	-11.6797280	-3.8192730	1.8575820
C	-11.6587470	-1.8863090	0.9607120
C	-13.1240070	-1.7184690	1.1120780
C	-12.9501850	0.5086850	0.0432700
C	-0.9382010	-2.0924540	-0.4984100
H	-0.5918510	-1.5290540	-1.3638210
C	-0.2466470	-1.6091800	0.7831330
H	-0.7362000	-2.0892250	1.6393240
H	-0.3779620	-0.5268860	0.8837000
C	-15.1716990	-0.3591220	0.7996060
H	-15.4691290	-1.2865640	1.2872670
C	-15.8819580	-0.2868750	-0.5565280
H	-15.6144990	-1.1452340	-1.1805940
H	-15.6361870	0.6304080	-1.0930170
C	-15.5209570	0.8028430	1.7361620
H	-15.2646790	1.7674150	1.2964920
H	-15.0004200	0.6997090	2.6932980
H	-6.8208920	1.7301260	-1.3939650
H	-9.2568680	-4.1644170	1.6398170
C	1.2504930	-1.9462770	0.8091090
H	-16.9640510	-0.3161820	-0.3933260
H	-16.5969700	0.7856430	1.9368190
H	-0.7507800	-3.1559860	-0.6540700
H	1.8000160	-1.3751030	0.0595340
H	1.4032050	-3.0133560	0.6015030
H	2.2469230	0.3476320	5.5347860
H	5.7204290	0.5037160	-1.1651600
H	3.9878720	1.3368300	-0.8270710

Cor-Phe-PDI_{opt} in chloroform

Energy total = -4964.36877585 a.u.

Symbol	X	Y	Z
C	-4.5655950	0.1064360	-3.4081390
C	-4.7068770	-0.7878710	-4.5340020
H	-4.4570610	-0.5695340	-5.5640700
C	-5.2179850	-1.9588120	-4.0290760
H	-5.4745260	-2.8505290	-4.5855750
C	-5.4000850	-1.7510560	-2.6024380
C	-6.0478070	-2.5619830	-1.6399790
C	-6.3363050	-2.0921820	-0.3358740
C	-6.9695280	-2.7303780	0.7743480
H	-7.3656690	-3.7354300	0.7749790
C	-6.9901370	-1.8372450	1.8239730
H	-7.4136820	-1.9984540	2.8041950
C	-6.3677480	-0.6163650	1.4004400
C	-6.1495980	0.5441130	2.1852450
C	-5.6158160	1.7743340	1.7623270
C	-5.1963300	2.8713880	2.5877550
H	-5.2798780	2.8886410	3.6639620
C	-4.6413040	3.8415210	1.7893310
H	-4.1933220	4.7683750	2.1171220
C	-4.6861930	3.3972070	0.4295080
C	-4.1810650	4.0197470	-0.7304510
C	-4.0614230	3.3233330	-1.9656470
C	-4.0777130	3.7469040	-3.3226350
H	-4.1131420	4.7751170	-3.6546620
C	-4.1650530	2.6109760	-4.1297320
H	-4.2792810	2.5941320	-5.2047510
C	-4.2006650	1.4775600	-3.2822320
N	-4.9667820	-0.5024550	-2.2708330
N	-6.0047120	-0.8191890	0.0888940
N	-5.3077720	2.1547520	0.4680950
N	-4.0902730	1.9508940	-1.9956350
H	-3.7456590	1.3614040	-1.2354200
C	-6.4162060	0.4080490	3.6562230
C	-5.4626950	-0.2378560	4.4753660
C	-5.6674460	-0.3644720	5.8512420
H	-4.9342570	-0.8627200	6.4750540
C	-6.8322900	0.1562680	6.4229440
H	-6.9877310	0.0541020	7.4928230
C	-7.7838070	0.7989330	5.6341060
H	-8.6863500	1.2031390	6.0809710
C	-7.5674550	0.9213430	4.2579930
H	-8.3002440	1.4236960	3.6333790
O	-4.3594530	-0.7100160	3.8215130
C	-3.2200340	-1.1608810	4.5383750
H	-2.9001150	-0.4242640	5.2849800
H	-3.4167490	-2.1097940	5.0527850
C	-2.0605380	-1.3790850	3.5622090
O	-0.9589860	-1.7107300	3.9958610
N	-2.3636170	-1.1870620	2.2590350
H	-3.2798400	-0.8236960	2.0253490
C	-6.4588380	-3.9411960	-2.0112990
C	-5.5114880	-4.9007710	-2.3918980
C	-5.8701990	-6.1934840	-2.7617850
C	-7.2114180	-6.5649470	-2.7532650
C	-8.1801510	-5.6395190	-2.3766930
C	-7.7982650	-4.3498800	-2.0184940
F	-4.2056600	-4.5926060	-2.3943240
F	-4.9338080	-7.0845130	-3.1135210
F	-7.5669320	-7.8052680	-3.1037150
F	-9.4734690	-5.9894960	-2.3761770
F	-8.7687800	-3.4856240	-1.6828190
C	-3.7704820	5.4405640	-0.6753190
C	-2.4892450	5.8444390	-1.0818220
C	-2.0832990	7.1744730	-1.0606660
C	-2.9651690	8.1564030	-0.6180900

C	-4.2435620	7.7955720	-0.2028340
C	-4.6316290	6.4598110	-0.2415520
F	-1.5891950	4.9310460	-1.4855780
F	-0.8462470	7.5129550	-1.4466510
F	-2.5854250	9.4375480	-0.5892930
F	-5.1003590	8.7381100	0.2114830
F	-5.8843480	6.1688740	0.1403380
C	-1.3955100	-1.2722560	1.1833480
H	-0.4022210	-1.3060790	1.6381090
C	-1.6074900	-2.5337080	0.2945090
H	-2.5863780	-2.4441170	-0.1881660
H	-0.8541220	-2.5068520	-0.5010390
C	-1.5658340	-0.0241730	0.3034830
N	-0.4436870	0.5089640	-0.2018390
H	0.4639220	0.1453520	0.0827770
O	-2.7044090	0.4065710	0.0655440
N	3.1687470	2.0709310	-0.1837670
N	13.9227030	-1.7572280	0.0699840
O	3.9072140	4.0960230	-0.9503370
O	2.4250750	0.0168890	0.4794940
O	14.6290650	0.2842360	-0.6937630
O	13.1410590	-3.7796500	0.8294480
C	4.1832110	2.9575250	-0.5902360
C	5.5687580	2.4440230	-0.5514530
C	5.8410630	1.1169960	-0.1393100
C	4.7733440	0.2637960	0.2330060
C	3.3796000	0.7451500	0.1921150
C	5.0383530	-1.0355980	0.6348650
H	4.2116910	-1.6778650	0.9160900
C	6.3523220	-1.5097900	0.6790630
H	6.5102250	-2.5308710	1.0015190
C	7.4371000	-0.7061370	0.3205390
C	7.1869380	0.6382430	-0.1026900
C	8.2492760	1.5154310	-0.4908670
C	7.9325870	2.8154960	-0.8913740
C	6.6132210	3.2757060	-0.9222430
H	6.3904000	4.2891840	-1.2359400
C	9.6334200	1.0214980	-0.4572230
C	10.7188600	1.8177090	-0.8285430
H	10.5628970	2.8372520	-1.1573650
C	12.0324630	1.3379900	-0.7927240
H	12.8598520	1.9735400	-1.0865310
C	12.2963410	0.0424980	-0.3809850
C	11.2278590	-0.7995530	0.0050190
C	9.8825820	-0.3205240	-0.0300040
C	8.8222920	-1.1965020	0.3626380
C	9.1423670	-2.4922850	0.7730800
C	10.4634560	-2.9510040	0.8054110
H	10.6880650	-3.9613240	1.1271520
C	11.5050240	-2.1208360	0.4256230
C	12.8954360	-2.6335770	0.4658380
C	13.6987950	-0.4412500	-0.3548110
C	1.7767090	2.5532220	-0.1854710
H	1.8243820	3.6390490	-0.1386770
C	0.9792570	2.0868390	-1.4261640
H	1.4898300	1.2394290	-1.8957850
H	0.9491170	2.8868350	-2.1710070
C	15.3232760	-2.2868490	0.1105490
H	15.1916340	-3.3053350	0.4731280
C	16.1876300	-1.5312310	1.1258560
H	15.7067460	-1.5157350	2.1087720
H	16.3791580	-0.5050490	0.8101580
C	15.9420900	-2.3583090	-1.2896980
H	16.1093520	-1.3650550	-1.7079560
H	15.2987000	-2.9254440	-1.9694450
H	8.7144790	3.5021990	-1.1893520

H	8.3626480	-3.1781010	1.0790860
C	-0.4536740	1.6739300	-1.0889250
H	17.1465160	-2.0488600	1.2297970
H	16.9038770	-2.8772220	-1.2271170
H	1.3159640	2.1844820	0.7323790
H	-0.9988200	1.4311990	-2.0073050
H	-0.9946440	2.4964150	-0.6075400
C	-1.5151120	-3.8376110	1.0537360
C	-0.2729140	-4.4415500	1.2937590
C	-2.6689350	-4.4643760	1.5433370
C	-0.1844130	-5.6381720	2.0051980
H	0.6321430	-3.9710110	0.9167730
C	-2.5845620	-5.6622240	2.2558650
H	-3.6398180	-4.0117160	1.3600350
C	-1.3414940	-6.2528330	2.4893340
H	0.7868770	-6.0927630	2.1784640
H	-3.4902390	-6.1354260	2.6247540
H	-1.2743660	-7.1861970	3.0406760
H	-5.6189990	1.6769710	-0.3628170
H	-5.4155900	-0.2767250	-0.5575320

Cor-Phe-PDI_{opt} in toluene

Energy total = -4964.36035494 a.u.

Symbol	X	Y	Z
C	-4.3376990	0.0055280	-3.4097330
C	-4.3132000	-0.9205090	-4.5189160
H	-4.0065740	-0.7015480	-5.5333750
C	-4.7529160	-2.1229040	-4.0215370
H	-4.8847180	-3.0458770	-4.5706070
C	-5.0602690	-1.9034500	-2.6182490
C	-5.6999850	-2.7493870	-1.6829040
C	-6.1212080	-2.2843780	-0.4141860
C	-6.7844150	-2.9542890	0.6587610
H	-7.1068150	-3.9853840	0.6475280
C	-6.9441040	-2.0529000	1.6892290
H	-7.4228930	-2.2328990	2.6402880
C	-6.3821640	-0.7958070	1.2901040
C	-6.2925470	0.3842870	2.0720740
C	-5.8323880	1.6473620	1.6612980
C	-5.5402810	2.7806540	2.4930560
H	-5.6811120	2.7999190	3.5631750
C	-5.0198860	3.7827800	1.7119220
H	-4.6605080	4.7438720	2.0498260
C	-4.9584190	3.3240580	0.3573200
C	-4.4322390	3.9699800	-0.7796830
C	-4.1888010	3.2715630	-1.9962340
C	-4.1461230	3.6764200	-3.3578030
H	-4.2369500	4.6947700	-3.7091660
C	-4.0908060	2.5272660	-4.1497630
H	-4.1300820	2.4893170	-5.2295820
C	-4.0969930	1.4048610	-3.2878650
N	-4.7681150	-0.6137420	-2.2902080
N	-5.9172600	-0.9848830	0.0097170
N	-5.4883670	2.0394400	0.3794990
N	-4.1132140	1.9012210	-2.0052520
H	-3.7751760	1.3490440	-1.2143290
C	-6.6106560	0.2338680	3.5306150
C	-5.6647330	-0.3831490	4.3814090
C	-5.9152680	-0.5243890	5.7481520
H	-5.1885010	-1.0013740	6.3957000
C	-7.1165920	-0.0458130	6.2796890
H	-7.3070580	-0.1590620	7.3428300
C	-8.0599630	0.5691320	5.4599990
H	-8.9911280	0.9403520	5.8757440

C	-7.7991650	0.7049710	4.0928960
H	-8.5261240	1.1842070	3.4438040
O	-4.5222620	-0.8103550	3.7670340
C	-3.3955070	-1.2304990	4.5214970
H	-3.1367720	-0.4983210	5.2957140
H	-3.5748550	-2.1976130	5.0080290
C	-2.1858870	-1.3780870	3.5927910
O	-1.0888360	-1.6541880	4.0706150
N	-2.4442910	-1.1907740	2.2779050
H	-3.3631480	-0.8603180	2.0091280
C	-5.9463150	-4.1719910	-2.0381930
C	-4.8797070	-5.0528920	-2.2583780
C	-5.0776810	-6.3865770	-2.6045530
C	-6.3739810	-6.8772240	-2.7346420
C	-7.4580330	-6.0316460	-2.5169560
C	-7.2352490	-4.6996480	-2.1785500
F	-3.6160340	-4.6251430	-2.1162540
F	-4.0336180	-7.2015330	-2.8015750
F	-6.5770140	-8.1566620	-3.0644780
F	-8.7060250	-6.5002850	-2.6477830
F	-8.3075740	-3.9155390	-1.9928010
C	-4.1198750	5.4150760	-0.7181750
C	-2.8446190	5.8978380	-1.0522140
C	-2.5274800	7.2518500	-1.0239700
C	-3.4962440	8.1779140	-0.6465740
C	-4.7714300	7.7382500	-0.3026960
C	-5.0696400	6.3794860	-0.3478910
F	-1.8649240	5.0414460	-1.3892370
F	-1.2940950	7.6674440	-1.3392570
F	-3.2025860	9.4810810	-0.6115430
F	-5.7093700	8.6267740	0.0494280
F	-6.3206160	6.0103010	-0.0360170
C	-1.4193700	-1.1865690	1.2533160
H	-0.4514150	-1.1713980	1.7615170
C	-1.4996210	-2.4310380	0.3206750
H	-2.4465540	-2.3868790	-0.2271390
H	-0.6982320	-2.3363960	-0.4217660
C	-1.6172010	0.0726420	0.3949380
N	-0.5026790	0.6422820	-0.0899670
H	0.4100380	0.2959320	0.1995800
O	-2.7628870	0.4773110	0.1483940
N	3.0957210	2.2263980	-0.0964160
N	13.8677750	-1.5595440	0.1063080
O	3.8210520	4.2461310	-0.8902610
O	2.3662930	0.1737030	0.5877180
O	14.5576080	0.4739770	-0.6942090
O	13.0991540	-3.5738880	0.9007740
C	4.1036910	3.1131440	-0.5217170
C	5.4916220	2.6038270	-0.4907330
C	5.7726470	1.2823510	-0.0670620
C	4.7111470	0.4294490	0.3233240
C	3.3144690	0.9045060	0.2880780
C	4.9841790	-0.8642660	0.7372580
H	4.1611450	-1.5052480	1.0320260
C	6.3004050	-1.3327300	0.7761810
H	6.4651760	-2.3496340	1.1087060
C	7.3795330	-0.5296080	0.3998730
C	7.1206490	0.8088320	-0.0369870
C	8.1762040	1.6853190	-0.4450840
C	7.8504070	2.9796560	-0.8566510
C	6.5292350	3.4352800	-0.8800240
H	6.2978440	4.4443900	-1.2018850
C	9.5623640	1.1963510	-0.4192730
C	10.6417840	1.9904280	-0.8119710
H	10.4787540	3.0049090	-1.1533290
C	11.9576100	1.5159130	-0.7824960

H	12.7813870	2.1485210	-1.0927240
C	12.2295670	0.2274540	-0.3552960
C	11.1676610	-0.6127100	0.0521850
C	9.8202830	-0.1390660	0.0231440
C	8.7670580	-1.0139020	0.4367840
C	9.0966440	-2.3024640	0.8619480
C	10.4198260	-2.7559330	0.8888500
H	10.6535690	-3.7605470	1.2220960
C	11.4540540	-1.9268930	0.4882930
C	12.8475180	-2.4347040	0.5235000
C	13.6352030	-0.2506260	-0.3357510
C	1.7024410	2.7055330	-0.0901440
H	1.7492550	3.7917760	-0.0486440
C	0.8964550	2.2330780	-1.3232970
H	1.4091270	1.3888820	-1.7967380
H	0.8551940	3.0326310	-2.0681420
C	15.2707050	-2.0834230	0.1418250
H	15.1459880	-3.0969210	0.5208990
C	16.1412450	-1.3079540	1.1367180
H	15.6706950	-1.2804160	2.1243950
H	16.3240270	-0.2857800	0.8032720
C	15.8764970	-2.1719440	-1.2631720
H	16.0339790	-1.1838380	-1.6971400
H	15.2302740	-2.7530670	-1.9283060
H	8.6274020	3.6656080	-1.1692660
H	8.3221310	-2.9867730	1.1845980
C	-0.5305840	1.8084110	-0.9745960
H	17.1039540	-1.8189090	1.2388550
H	16.8418610	-2.6844970	-1.2025180
H	1.2491040	2.3390920	0.8324010
H	-1.0799260	1.5610380	-1.8890760
H	-1.0761870	2.6269200	-0.4906080
C	-1.3797930	-3.7510770	1.0477840
C	-0.1327030	-4.2222630	1.4811940
C	-2.5150970	-4.5291480	1.3067350
C	-0.0225770	-5.4371790	2.1564220
H	0.7594380	-3.6316110	1.2866950
C	-2.4090060	-5.7467090	1.9821750
H	-3.4877960	-4.1783950	0.9726880
C	-1.1620760	-6.2044380	2.4092140
H	0.9524680	-5.7867120	2.4838800
H	-3.3004290	-6.3382050	2.1716020
H	-1.0771130	-7.1522490	2.9328480
H	-5.7095830	1.5280580	-0.4601400
H	-5.3280800	-0.4054440	-0.6031630

Extended Cor-(Ala)₄-PDI_{opt} in chloroform

Energy total = -5475.33678397 a.u.

Symbol	X	Y	Z
O	-9.9498730	-3.1250660	0.8974320
C	-3.6599530	0.0696750	-0.5576640
C	-2.3109830	-0.2699100	-0.2586800
H	-1.4968860	0.4375900	-0.1907550
C	-2.2587730	-1.6461390	-0.0574450
H	-1.3769890	-2.2292540	0.1674910
C	-3.5765650	-2.1681840	-0.2387560
C	-4.1422090	-3.4652570	-0.2940560
C	-5.4907280	-3.6894110	-0.6657550
C	-6.1760140	-4.9690100	-0.6273460
H	-5.7335760	-5.9180070	-0.3578940
C	-7.4744460	-4.7290150	-0.9584150
H	-8.2792070	-5.4468840	-1.0294890
C	-7.5900740	-3.3000390	-1.2111800
C	-8.8140070	-2.6459370	-1.5271080

C	-8.9766290	-1.2802170	-1.8031100
C	-10.1945480	-0.5413220	-1.9907800
H	-11.1822090	-0.9774990	-1.9759040
C	-9.8799760	0.7845440	-2.1528760
H	-10.5739640	1.6029880	-2.2776890
C	-8.4545090	0.9332610	-2.0657120
C	-7.6888920	2.1159140	-2.0948960
C	-6.3122730	2.1379970	-1.7414440
C	-5.2464670	3.0183920	-2.0528460
H	-5.3352260	3.9225880	-2.6384780
C	-4.0576790	2.4586960	-1.5729530
H	-3.0579720	2.8463160	-1.7076030
C	-4.3769140	1.2287450	-0.9600940
N	-4.3737310	-1.0924180	-0.4984720
H	-5.3529580	-1.2781720	-0.7493070
N	-6.3760310	-2.7009230	-1.0481740
N	-7.9633720	-0.3492460	-1.8816840
N	-5.7527670	1.0812530	-1.0519980
H	-6.2789310	0.5893870	-0.3227980
C	-10.0727120	-3.4553340	-1.4234420
C	-10.6290970	-3.6924140	-0.1458800
C	-11.7962460	-4.4461710	-0.0016820
H	-12.2215330	-4.6275280	0.9785020
C	-12.4238160	-4.9648730	-1.1388210
H	-13.3309780	-5.5501220	-1.0211200
C	-11.8978670	-4.7337620	-2.4074950
H	-12.3883610	-5.1361790	-3.2879740
C	-10.7270790	-3.9798990	-2.5397100
H	-10.3041760	-3.7971590	-3.5232260
C	-3.2778220	-4.6150970	0.0793870
C	-2.7477690	-4.7332200	1.3705740
C	-1.9235840	-5.7910920	1.7420260
C	-1.6090790	-6.7768430	0.8110970
C	-2.1207770	-6.6942800	-0.4805770
C	-2.9375650	-5.6229570	-0.8309480
F	-3.0449440	-3.8162610	2.3058570
F	-1.4419340	-5.8728220	2.9894130
F	-0.8198780	-7.7990380	1.1568630
F	-1.8122140	-7.6364520	-1.3815940
F	-3.3932080	-5.5735110	-2.0914810
C	-8.3278070	3.3866850	-2.5085320
C	-8.2973100	4.5209090	-1.6826590
C	-8.8694490	5.7318610	-2.0582990
C	-9.5063480	5.8398310	-3.2913730
C	-9.5607090	4.7356520	-4.1367340
C	-8.9725030	3.5368230	-3.7451570
F	-7.7186040	4.4594270	-0.4719310
F	-8.8252560	6.7879180	-1.2353340
F	-10.0634740	6.9971100	-3.6609880
F	-10.1613810	4.8383450	-5.3295140
F	-9.0265790	2.5102580	-4.6070510
C	-10.3652050	-3.3469060	2.2353090
H	-10.3641910	-4.4155060	2.4832880
H	-11.3747200	-2.9554790	2.4141440
C	-9.4085920	-2.6386190	3.1961820
O	-9.5913610	-2.7337090	4.4106050
N	-8.4095560	-1.9373920	2.6234180
H	-8.3359160	-1.8920920	1.6136730
C	-7.4276880	-1.2007920	3.3971710
H	-7.9310630	-0.7923640	4.2799480
C	-6.9071320	-0.0529930	2.5193340
O	-7.0192150	-0.1022880	1.2863620
N	-6.3093260	0.9567220	3.1798790
H	-6.2109060	0.9196210	4.1876260
C	-5.6064280	2.0581730	2.5291570
H	-5.4292940	1.7643480	1.4952580

C	-4.2718600	2.2356650	3.2695440
O	-4.2307470	2.1908260	4.5025420
C	-6.4215790	3.3603330	2.5605130
H	-6.6305020	3.6539340	3.5929860
H	-5.8670440	4.1678820	2.0734500
N	-3.1999670	2.4610790	2.4842500
H	-3.2714320	2.4257900	1.4727080
C	-1.8554170	2.6688580	3.0015420
H	-1.9034390	3.3969900	3.8182960
C	-1.0235310	3.2365190	1.8408190
O	-1.3253900	3.0010250	0.6639830
C	-1.2291120	1.3627440	3.5275050
H	-1.1760810	0.6199300	2.7267310
N	0.0524190	3.9602470	2.1995300
H	0.2955940	4.1166570	3.1728230
C	1.0195170	4.4788820	1.2456010
C	0.5007650	5.7393950	0.5282220
H	0.3093130	6.5383990	1.2500580
H	-0.4292130	5.4992360	0.0092270
H	1.2239660	6.1010200	-0.2083580
C	-6.2624680	-2.0993300	3.8614370
H	-7.3659460	3.2237280	2.0284860
H	-1.8475320	0.9693230	4.3362710
H	-0.2211970	1.5426440	3.9121950
H	1.2236180	3.7026660	0.4990800
H	-6.6649500	-2.9218080	4.4569510
H	-5.7233880	-2.5122030	3.0038700
H	-5.5558820	-1.5386670	4.4803170
C	2.3010780	4.7754500	2.0476290
N	3.4097240	4.9909910	1.3041560
H	3.3382820	4.9205510	0.2985140
O	2.2765670	4.8300910	3.2794400
N	8.2443670	3.8478290	1.6069720
N	16.8158750	-2.8957360	-1.7822950
O	8.6031240	5.2059580	-0.1941680
O	7.8192570	2.4328900	3.3491640
O	17.2155640	-1.4517670	-3.5162380
O	16.3631860	-4.2927740	-0.0152750
C	8.9261500	4.2023040	0.4346080
C	10.0351840	3.3196230	0.0114230
C	10.3580490	2.1548970	0.7495820
C	9.6100760	1.8284570	1.9069860
C	8.4982610	2.6928850	2.3607840
C	9.9209200	0.6856830	2.6252500
H	9.3395330	0.4472830	3.5086370
C	10.9684350	-0.1462200	2.2180660
H	11.1732830	-1.0274540	2.8126840
C	11.7346510	0.1362330	1.0851770
C	11.4313670	1.3116570	0.3266900
C	12.1751440	1.6645300	-0.8442070
C	11.8188740	2.8211330	-1.5410960
C	10.7638520	3.6376310	-1.1227640
H	10.5042630	4.5308690	-1.6795240
C	13.2855280	0.8023070	-1.2735910
C	14.0630230	1.0912570	-2.3970310
H	13.8639960	1.9759030	-2.9887180
C	15.1171860	0.2636020	-2.7974040
H	15.7086290	0.5083550	-3.6721310
C	15.4221110	-0.8824140	-2.0821830
C	14.6612660	-1.2146240	-0.9375050
C	13.5853020	-0.3743340	-0.5172670
C	12.8377170	-0.7320250	0.6486660
C	13.1854660	-1.8979520	1.3341540
C	14.2383030	-2.7162170	0.9116420
H	14.4890610	-3.6174390	1.4591070
C	14.9773740	-2.3869990	-0.2126460

C	16.0878910	-3.2714630	-0.6377710
C	16.5459810	-1.7412300	-2.5287930
C	7.1564360	4.7329950	2.0562870
H	7.4328530	5.7467890	1.7644350
C	5.8026980	4.3484220	1.4485230
H	5.5313500	3.3369630	1.7674000
H	5.8918400	4.3430850	0.3558280
C	17.9385980	-3.7939920	-2.2011110
H	17.9067390	-4.5910450	-1.4596220
C	19.2969540	-3.0936700	-2.0863130
H	19.4375640	-2.6827120	-1.0818390
H	19.3981270	-2.2883780	-2.8149040
C	17.6853730	-4.4180750	-3.5778030
H	17.7270650	-3.6732000	-4.3732860
H	16.7096140	-4.9127170	-3.6061740
H	12.3599910	3.1122440	-2.4324150
H	12.6387900	-2.1968060	2.2195820
C	4.7083050	5.3327240	1.8746330
H	20.0908980	-3.8261190	-2.2633220
H	18.4512770	-5.1763120	-3.7693550
H	7.1193410	4.6665400	3.1438910
H	4.9812310	6.3522800	1.5737130
H	4.5796710	5.3298190	2.9588280
H	-6.9931750	-0.6223440	-1.8657790

Extended Cor-(Ala)₄-PDI_{opt} in toluene

Energy total = -5475.32586830 a.u.

Symbol	X	Y	Z
O	-9.8842970	-3.1950720	0.9015760
C	-3.6547710	0.0982410	-0.5472150
C	-2.3017870	-0.2225830	-0.2463240
H	-1.4976690	0.4964570	-0.1804760
C	-2.2317550	-1.5976720	-0.0426520
H	-1.3428190	-2.1692310	0.1836940
C	-3.5420190	-2.1373710	-0.2244940
C	-4.0903990	-3.4420180	-0.2792260
C	-5.4344930	-3.6845060	-0.6540830
C	-6.1022930	-4.9735880	-0.6186380
H	-5.6474320	-5.9168940	-0.3501370
C	-7.4025070	-4.7513700	-0.9529990
H	-8.1970480	-5.4800300	-1.0283550
C	-7.5368450	-3.3237200	-1.2048300
C	-8.7689290	-2.6867760	-1.5244140
C	-8.9495540	-1.3242160	-1.8035320
C	-10.1769450	-0.6022000	-1.9945080
H	-11.1583470	-1.0522110	-1.9801420
C	-9.8797530	0.7271300	-2.1585190
H	-10.5842150	1.5360420	-2.2862430
C	-8.4565340	0.8952940	-2.0690790
C	-7.7074940	2.0885050	-2.0966080
C	-6.3318740	2.1298510	-1.7400590
C	-5.2777540	3.0258470	-2.0454930
H	-5.3774000	3.9300070	-2.6294300
C	-4.0825620	2.4825650	-1.5618810
H	-3.0877890	2.8849190	-1.6898120
C	-4.3864070	1.2471200	-0.9528600
N	-4.3529580	-1.0729750	-0.4868280
H	-5.3295460	-1.2731110	-0.7379050
N	-6.3323270	-2.7081300	-1.0375490
N	-7.9488250	-0.3801410	-1.8828640
N	-5.7596670	1.0800490	-1.0507090
H	-6.2816480	0.5804190	-0.3237140
C	-10.0162530	-3.5131860	-1.4197270
C	-10.5617260	-3.7656110	-0.1402910

C	-11.7174490	-4.5362180	0.0060740
H	-12.1334300	-4.7296730	0.9880220
C	-12.3451860	-5.0557660	-1.1304650
H	-13.2435690	-5.6541840	-1.0111840
C	-11.8305250	-4.8091530	-2.4005900
H	-12.3210540	-5.2125380	-3.2806280
C	-10.6706310	-4.0390800	-2.5351190
H	-10.2557070	-3.8447070	-3.5197900
C	-3.2113230	-4.5792960	0.0980420
C	-2.6793540	-4.6851680	1.3897470
C	-1.8409940	-5.7307010	1.7653020
C	-1.5139170	-6.7162040	0.8381040
C	-2.0272020	-6.6456690	-0.4539020
C	-2.8581100	-5.5862980	-0.8087230
F	-2.9880630	-3.7686110	2.3212610
F	-1.3577000	-5.8009380	3.0124620
F	-0.7113150	-7.7263470	1.1877240
F	-1.7065280	-7.5872630	-1.3508040
F	-3.3144100	-5.5480710	-2.0686370
C	-8.3633210	3.3507400	-2.5093660
C	-8.3467910	4.4852200	-1.6829650
C	-8.9343130	5.6893060	-2.0578220
C	-9.5737130	5.7897330	-3.2905190
C	-9.6151490	4.6848770	-4.1361220
C	-9.0110870	3.4932110	-3.7456410
F	-7.7672000	4.4307590	-0.4725300
F	-8.9027890	6.7453210	-1.2346150
F	-10.1453820	6.9399370	-3.6593060
F	-10.2180040	4.7803970	-5.3280250
F	-9.0528140	2.4669470	-4.6077170
C	-10.2882130	-3.4264070	2.2408850
H	-10.2660080	-4.4952640	2.4874130
H	-11.3040220	-3.0542860	2.4258560
C	-9.3409550	-2.7005720	3.1986850
O	-9.5205000	-2.7942080	4.4123720
N	-8.3527240	-1.9858900	2.6212410
H	-8.2809120	-1.9388340	1.6113950
C	-7.3895980	-1.2262540	3.3950900
H	-7.9054350	-0.8272900	4.2752900
C	-6.8923790	-0.0691170	2.5164480
O	-7.0096100	-0.1168810	1.2845580
N	-6.3092590	0.9511060	3.1759400
H	-6.1943080	0.9110690	4.1819430
C	-5.6235640	2.0609950	2.5216350
H	-5.4446960	1.7684160	1.4875810
C	-4.2900480	2.2561660	3.2594260
O	-4.2437810	2.2010730	4.4909250
C	-6.4562990	3.3519910	2.5529630
H	-6.6651070	3.6450570	3.5856510
H	-5.9151520	4.1661830	2.0618470
N	-3.2244750	2.5083520	2.4718250
H	-3.2965740	2.4701410	1.4603990
C	-1.8813380	2.7246920	2.9882210
H	-1.9324640	3.4571830	3.8012970
C	-1.0511880	3.2891250	1.8250520
O	-1.3513710	3.0504540	0.6491420
C	-1.2486600	1.4249350	3.5229180
H	-1.1949170	0.6763420	2.7275980
N	0.0249590	4.0158840	2.1809530
H	0.2740640	4.1714410	3.1529900
C	0.9933080	4.5239790	1.2234910
C	0.4781870	5.7798010	0.4954920
H	0.2888780	6.5853250	1.2105990
H	-0.4521240	5.5371390	-0.0216550
H	1.2022890	6.1343740	-0.2439830
C	-6.2072810	-2.0977800	3.8679940

H	-7.4004790	3.2012920	2.0244640
H	-1.8644430	1.0363430	4.3358310
H	-0.2404240	1.6113660	3.9040830
H	1.1942290	3.7411800	0.4824760
H	-6.5959980	-2.9238880	4.4675350
H	-5.6570020	-2.5051220	3.0149410
H	-5.5133680	-1.5198070	4.4857120
C	2.2754370	4.8215610	2.0244330
N	3.3856670	5.0342970	1.2795270
H	3.3145540	4.9605310	0.2743250
O	2.2523050	4.8783920	3.2547320
N	8.2144470	3.8677250	1.5913370
N	16.7766360	-2.9007750	-1.7762920
O	8.5607500	5.2068570	-0.2264390
O	7.7975510	2.4668080	3.3473760
O	17.1645010	-1.4723690	-3.5262960
O	16.3336870	-4.2799250	0.0076150
C	8.8885690	4.2111120	0.4109440
C	9.9967720	3.3248040	-0.0088160
C	10.3244800	2.1673680	0.7386860
C	9.5822630	1.8511350	1.9026170
C	8.4713890	2.7187790	2.3546830
C	9.8971680	0.7155770	2.6300900
H	9.3188360	0.4866360	3.5181150
C	10.9437240	-0.1189040	2.2255590
H	11.1527420	-0.9946000	2.8270890
C	11.7047920	0.1532030	1.0867180
C	11.3967310	1.3211880	0.3185670
C	12.1345620	1.6638270	-0.8592140
C	11.7732290	2.8135510	-1.5648210
C	10.7193040	3.6329950	-1.1493450
H	10.4544390	4.5211530	-1.7119180
C	13.2438540	0.7986270	-1.2856680
C	14.0160190	1.0769790	-2.4153640
H	13.8127940	1.9560080	-3.0142090
C	15.0692480	0.2466770	-2.8132240
H	15.6575340	0.4816870	-3.6928690
C	15.3784220	-0.8917260	-2.0883290
C	14.6234480	-1.2134020	-0.9368370
C	13.5484500	-0.3703540	-0.5194850
C	12.8069110	-0.7179300	0.6533330
C	13.1599350	-1.8769160	1.3477190
C	14.2119950	-2.6980110	0.9282680
H	14.4683100	-3.5941260	1.4816980
C	14.9448230	-2.3782890	-0.2024240
C	16.0551200	-3.2664130	-0.6240030
C	16.5018220	-1.7539510	-2.5330550
C	7.1302160	4.7579020	2.0383980
H	7.4104620	5.7699730	1.7434250
C	5.7749880	4.3777310	1.4311950
H	5.4982780	3.3691450	1.7546280
H	5.8664560	4.3679820	0.3385480
C	17.8980250	-3.8021280	-2.1920460
H	17.8706720	-4.5917670	-1.4422770
C	19.2558170	-3.0982940	-2.0923540
H	19.4022930	-2.6782300	-1.0924600
H	19.3507780	-2.2997140	-2.8291290
C	17.6378280	-4.4382990	-3.5619000
H	17.6725050	-3.6995430	-4.3633990
H	16.6634720	-4.9362460	-3.5799490
H	12.3101830	3.0964860	-2.4614640
H	12.6174590	-2.1678370	2.2385620
C	4.6851440	5.3693160	1.8519640
H	20.0501740	-3.8308390	-2.2674250
H	18.4044720	-5.1961400	-3.7523130
H	7.0923160	4.6926650	3.1261080

H	4.9652570	6.3868970	1.5501320
H	4.5522080	5.3691890	2.9357410
H	-6.9753390	-0.6408900	-1.8621770

Folded Cor-(Ala)₄-PDI_{opt} with hydrogen bond to PDI in chloroform
 Energy total = -5475.33455241 a.u.

Symbol	X	Y	Z
O	-3.4783740	2.5676580	4.0698280
C	-2.7233040	1.9138720	5.0774560
H	-3.3748740	1.4345230	5.8186530
H	-2.0646690	2.6146870	5.6053340
C	-1.8606650	0.8172140	4.4523070
O	-1.1210100	0.1491910	5.1760520
N	-1.9892800	0.6453530	3.1209280
H	-2.6267240	1.2299720	2.5935730
C	-1.3338590	-0.4394320	2.4129780
H	-0.3004450	-0.5198130	2.7648400
C	-1.3378070	-0.1076270	0.9138920
O	-2.0805990	0.7733390	0.4553790
N	-0.5248510	-0.8792600	0.1621780
H	0.0787950	-1.5572020	0.6251670
C	-0.5537570	-0.8860970	-1.2942580
H	-1.3143870	-0.1676680	-1.5970230
C	0.8021480	-0.4824530	-1.8940760
H	1.5878780	-1.1655160	-1.5594620
H	0.7632280	-0.5105420	-2.9869320
C	-2.0404840	-1.7878720	2.6664600
H	1.0568770	0.5342340	-1.5839690
H	-2.0437920	-1.9864330	3.7400050
H	-3.0739810	-1.7513410	2.3093370
H	-1.5178650	-2.6045220	2.1641760
C	-0.9489270	-2.2919140	-1.7753840
O	-0.4432930	-3.3008090	-1.2746980
N	-1.8588980	-2.3466560	-2.7776500
H	-2.2307090	-1.4796030	-3.1467630
C	-2.1634240	-3.5821860	-3.5151080
C	-2.6632120	-4.7198490	-2.5895450
O	-2.3565790	-5.8888550	-2.7997930
C	-0.9939700	-4.0476000	-4.3845140
H	-0.1264100	-4.2799700	-3.7640710
H	-0.7263990	-3.2653210	-5.0997050
H	-1.2746060	-4.9493840	-4.9303250
N	-3.4957240	-4.3266180	-1.5885930
H	-3.7224900	-3.3446610	-1.5250460
C	-4.1657380	-5.2364310	-0.6556180
C	-5.0735600	-6.2616220	-1.3454420
C	-3.2235480	-5.9041860	0.3741600
O	-3.6622530	-6.7845170	1.1184160
H	-3.0122260	-3.3265260	-4.1602880
H	-4.8049760	-4.5902140	-0.0448430
H	-5.5118170	-6.9123720	-0.5872600
H	-4.5052470	-6.8692680	-2.0506760
H	-5.8766220	-5.7438160	-1.8753730
N	-1.9698950	-5.4131090	0.4690200
H	-1.6608250	-4.6914050	-0.1722050
N	2.4795170	-4.4446830	2.1443520
N	12.2694880	0.7291530	-0.6520780
O	1.3665100	-2.4714860	1.8905530
O	3.5875870	-6.4384570	2.3231540
O	11.1237990	2.7027550	-0.8559940
O	13.3509460	-1.2863720	-0.4372810
C	2.4394610	-3.0828720	1.8558330
C	3.7131750	-2.4204700	1.5131830
C	4.9190820	-3.1613070	1.4572050

C	4.9027890	-4.5482090	1.7403420
C	3.6414110	-5.2367820	2.0899280
C	6.0817220	-5.2738990	1.6844040
H	6.0550060	-6.3351620	1.9038490
C	7.2856440	-4.6476870	1.3488680
H	8.1804730	-5.2560150	1.3187890
C	7.3493090	-3.2832130	1.0575350
C	6.1445010	-2.5125400	1.1119510
C	6.1348270	-1.1093520	0.8295000
C	4.9231110	-0.4185770	0.9045440
C	3.7285060	-1.0618990	1.2399580
H	2.8002840	-0.5043690	1.2890190
C	7.3947040	-0.4434370	0.4688380
C	7.4601890	0.9204880	0.1763330
H	6.5669680	1.5311680	0.2104750
C	8.6637030	1.5442620	-0.1691210
H	8.6909450	2.6045180	-0.3926700
C	9.8397800	0.8158220	-0.2316390
C	9.8208310	-0.5684760	0.0568140
C	8.5974460	-1.2153400	0.4109870
C	8.6088990	-2.6169720	0.6959760
C	9.8212270	-3.3055660	0.6173060
C	11.0138990	-2.6624310	0.2700560
H	11.9433220	-3.2172830	0.2153280
C	11.0254510	-1.3060790	-0.0099130
C	12.3031330	-0.6503870	-0.3764960
C	11.1022700	1.5019840	-0.6022580
C	1.1990830	-5.1043080	2.4714950
H	0.6546420	-4.4277520	3.1326310
C	0.3744390	-5.3869000	1.2103850
H	0.8717730	-6.1481420	0.6005210
H	0.3429360	-4.4704010	0.6175810
C	13.5664940	1.3817450	-1.0196590
H	14.2783510	0.5588380	-0.9722860
C	13.9875780	2.4316720	0.0142180
H	13.9982010	2.0022620	1.0207390
H	13.3231790	3.2964490	0.0063430
C	13.5488500	1.9094850	-2.4584180
H	12.8664300	2.7526740	-2.5720870
H	13.2560730	1.1199890	-3.1574100
H	4.8850920	0.6438560	0.7009760
H	9.8625020	-4.3671720	0.8252320
C	-1.0629690	-5.8150970	1.5398000
H	15.0028000	2.7695190	-0.2168540
H	14.5573970	2.2388200	-2.7278420
H	1.4429880	-6.0166240	3.0136450
H	-1.3887380	-5.3507520	2.4823520
H	-1.1460940	-6.8958910	1.6838740
C	-3.6611720	0.8269890	-3.1503550
C	-4.2963150	-0.1032600	-4.0183310
H	-3.9615760	-0.3667350	-5.0124150
C	-5.4373910	-0.5771070	-3.3689310
H	-6.1585750	-1.2756640	-3.7687810
C	-5.5184650	0.0686770	-2.1011810
C	-6.4861450	0.1171120	-1.0627500
C	-6.3937810	1.0325080	0.0112600
C	-7.2694590	1.0677790	1.1713260
H	-8.1188590	0.4221770	1.3458150
C	-6.7882630	2.0345920	1.9974270
H	-7.1810540	2.3345550	2.9581700
C	-5.6169190	2.6074590	1.3443360
C	-4.8009730	3.6178560	1.9244000
C	-3.6431940	4.1749910	1.3588670
C	-2.7105430	5.0912330	1.9562240
H	-2.8154390	5.5128440	2.9445200
C	-1.6782310	5.2973700	1.0779520

H	-0.8004920	5.9047890	1.2432140
C	-1.9235270	4.5262910	-0.1086100
C	-1.1213660	4.3967780	-1.2564550
C	-1.4067180	3.4488020	-2.2775600
C	-1.1231130	3.4229460	-3.6640210
H	-0.5339980	4.1585670	-4.1930810
C	-1.8394650	2.3683480	-4.2388810
H	-1.9115150	2.1412400	-5.2933750
C	-2.5622350	1.7282530	-3.2125540
N	-4.4138930	0.8633020	-2.0098450
H	-4.3614030	1.5036880	-1.2064810
N	-5.4093860	1.9935570	0.1446800
N	-3.1327960	3.8854560	0.1140930
N	-2.2501950	2.3838340	-2.0327030
H	-2.2580570	1.9029800	-1.1275770
C	-5.1250150	4.0643190	3.3201880
C	-4.4187170	3.5030250	4.4072630
C	-4.6882670	3.9030720	5.7186670
H	-4.1414550	3.4776350	6.5518600
C	-5.6768320	4.8631630	5.9551330
H	-5.8830010	5.1687830	6.9765490
C	-6.3889440	5.4239410	4.8976640
H	-7.1548310	6.1697900	5.0841680
C	-6.1050790	5.0223080	3.5887440
H	-6.6491350	5.4563800	2.7550480
C	-7.6094910	-0.8520000	-1.1283200
C	-7.3734790	-2.2329760	-1.1350490
C	-8.3980130	-3.1684740	-1.2217630
C	-9.7179470	-2.7332680	-1.3012380
C	-9.9940230	-1.3689050	-1.2944220
C	-8.9490660	-0.4521010	-1.2165550
F	-6.1126150	-2.6998000	-1.0366180
F	-8.1251670	-4.4803320	-1.2192470
F	-10.7131940	-3.6202070	-1.3820330
F	-11.2609680	-0.9457060	-1.3819230
F	-9.2627520	0.8511020	-1.2401200
C	0.0498630	5.2850170	-1.4405960
C	1.3303960	4.7563540	-1.6648980
C	2.4451710	5.5633270	-1.8649430
C	2.3064840	6.9483120	-1.8405100
C	1.0525450	7.5102930	-1.6192080
C	-0.0512740	6.6838640	-1.4305660
F	1.5208390	3.4262330	-1.6712090
F	3.6514040	5.0162580	-2.0648160
F	3.3715100	7.7329030	-2.0267560
F	0.9110370	8.8415240	-1.6080020
F	-1.2420340	7.2737750	-1.2498320
H	-3.6547220	3.3428090	-0.5557100

Folded Cor-(Ala)₄-PDI_{opt} with hydrogen bond to PDI in toluene
Energy total = -5475.32309308 a.u.

Symbol	X	Y	Z
O	-3.1954090	2.6730580	4.0805840
C	-2.4509120	1.9469620	5.0454110
H	-3.1068350	1.4990430	5.8023300
H	-1.7246110	2.5880540	5.5604000
C	-1.6930730	0.8048630	4.3665820
O	-0.9690270	0.0782010	5.0459080
N	-1.8975610	0.6625810	3.0401190
H	-2.5130100	1.3001230	2.5492890
C	-1.3530620	-0.4558640	2.2927960
H	-0.3190260	-0.6245120	2.6099280
C	-1.3765840	-0.0978930	0.8004210

O	-2.0438860	0.8575010	0.3774760
N	-0.6698170	-0.9334410	0.0096470
H	-0.0996800	-1.6598770	0.4388990
C	-0.7487900	-0.9083360	-1.4431770
H	-1.5393110	-0.2045420	-1.7032190
C	0.5734940	-0.4539090	-2.0843900
H	1.3881390	-1.1225440	-1.7922770
H	0.4970900	-0.4585210	-3.1758330
C	-2.1545530	-1.7500930	2.5489840
H	0.8126980	0.5623560	-1.7604560
H	-2.1452820	-1.9618930	3.6200560
H	-3.1910660	-1.6311510	2.2190790
H	-1.7095300	-2.5986900	2.0246140
C	-1.1167910	-2.3150010	-1.9410320
O	-0.5844820	-3.3184030	-1.4596420
N	-2.0253790	-2.3730470	-2.9458900
H	-2.4310220	-1.5078040	-3.2821630
C	-2.2715450	-3.5918340	-3.7334410
C	-2.7452460	-4.7860550	-2.8645410
O	-2.3837960	-5.9293130	-3.1165220
C	-1.0688200	-3.9805520	-4.5952580
H	-0.2086520	-4.2115890	-3.9642950
H	-0.8116710	-3.1599780	-5.2708850
H	-1.3058250	-4.8680800	-5.1834400
N	-3.6208560	-4.4670970	-1.8730460
H	-3.8709470	-3.4950430	-1.7612850
C	-4.2679320	-5.4348260	-0.9811780
C	-5.0613390	-6.5191550	-1.7204630
C	-3.3358030	-6.0495800	0.0897140
O	-3.7706390	-6.9273370	0.8367110
H	-3.1167760	-3.3428840	-4.3863320
H	-4.9835550	-4.8454780	-0.4000970
H	-5.5023470	-7.1922050	-0.9837200
H	-4.4112290	-7.0903160	-2.3835220
H	-5.8620350	-6.0593270	-2.3061830
N	-2.0975100	-5.5223380	0.2075100
H	-1.7892780	-4.8032680	-0.4361890
N	2.3262470	-4.5322210	1.9739350
N	12.2331670	0.6348160	-0.3990230
O	1.2327070	-2.5490840	1.7097420
O	3.4189730	-6.5348760	2.1537320
O	11.1072980	2.6223750	-0.5813080
O	13.2934810	-1.3936820	-0.1985260
C	2.3011760	-3.1675880	1.6997140
C	3.5893940	-2.5073850	1.4052650
C	4.7928150	-3.2537150	1.3753000
C	4.7596210	-4.6450510	1.6336340
C	3.4845670	-5.3316150	1.9384280
C	5.9347950	-5.3775120	1.6001020
H	5.8928510	-6.4422250	1.8000940
C	7.1520840	-4.7528400	1.3128660
H	8.0441890	-5.3660040	1.2986510
C	7.2337440	-3.3835390	1.0504180
C	6.0323500	-2.6061810	1.0818310
C	6.0397100	-1.1976120	0.8271840
C	4.8287790	-0.5028510	0.8703800
C	3.6200980	-1.1453140	1.1535270
H	2.6921870	-0.5856150	1.1802230
C	7.3155680	-0.5312230	0.5286020
C	7.4008490	0.8396950	0.2768320
H	6.5108780	1.4559390	0.2994320
C	8.6194820	1.4639070	-0.0102410
H	8.6636640	2.5297330	-0.2030090
C	9.7916170	0.7282860	-0.0538110
C	9.7535900	-0.6630870	0.1961940
C	8.5147900	-1.3100190	0.4921060

C	8.5081550	-2.7182860	0.7428090
C	9.7181750	-3.4129210	0.6852150
C	10.9258800	-2.7701780	0.3931560
H	11.8541400	-3.3284580	0.3533070
C	10.9550940	-1.4072980	0.1498010
C	12.2495410	-0.7517230	-0.1570630
C	11.0705990	1.4157570	-0.3637740
C	1.0357990	-5.1870220	2.2704690
H	0.4832310	-4.5114130	2.9261190
C	0.2309220	-5.4580250	0.9946680
H	0.7361990	-6.2147490	0.3856730
H	0.2058600	-4.5366840	0.4087710
C	13.5452270	1.2866200	-0.7098550
H	14.2489860	0.4563730	-0.6663060
C	13.9428460	2.3031640	0.3659310
H	13.9249990	1.8437730	1.3590650
H	13.2821260	3.1708380	0.3657470
C	13.5716440	1.8575960	-2.1319180
H	12.8987900	2.7093500	-2.2384670
H	13.2931200	1.0919010	-2.8625580
H	4.8032510	0.5629290	0.6821630
H	9.7451590	-4.4798280	0.8675600
C	-1.2090210	-5.8901490	1.3040810
H	14.9653720	2.6430130	0.1728150
H	14.5897350	2.1864600	-2.3635450
H	1.2652480	-6.1046120	2.8103830
H	-1.5562290	-5.4071200	2.2299060
H	-1.2875970	-6.9679210	1.4714940
C	-3.7471500	0.9520020	-3.1181590
C	-4.4160140	0.0028780	-3.9378400
H	-4.1489000	-0.2510900	-4.9547930
C	-5.4981790	-0.4975320	-3.2091210
H	-6.2288570	-1.2141890	-3.5563990
C	-5.5088570	0.1531120	-1.9425590
C	-6.4022230	0.1791740	-0.8375610
C	-6.2692240	1.1080140	0.2179660
C	-7.0764540	1.1371720	1.4273990
H	-7.9016980	0.4773250	1.6552920
C	-6.5707810	2.1242280	2.2126710
H	-6.9142000	2.4294960	3.1904540
C	-5.4502830	2.7127030	1.4864950
C	-4.6171830	3.7383620	2.0137860
C	-3.4982510	4.3025870	1.3827780
C	-2.5426140	5.2304400	1.9242880
H	-2.5973230	5.6545750	2.9155710
C	-1.5636110	5.4429250	0.9892950
H	-0.6843120	6.0597780	1.1026890
C	-1.8674320	4.6655110	-0.1799550
C	-1.1331580	4.5436900	-1.3720340
C	-1.4705880	3.5944980	-2.3772800
C	-1.2760430	3.5799250	-3.7784120
H	-0.7302830	4.3255460	-4.3390130
C	-2.0172660	2.5208660	-4.3135700
H	-2.1562400	2.3008200	-5.3629190
C	-2.6652490	1.8674490	-3.2480480
N	-4.4249100	0.9785570	-1.9319270
H	-4.3293260	1.6166750	-1.1305740
N	-5.3011860	2.0927960	0.2826790
N	-3.0547520	4.0120240	0.1131690
N	-2.2841140	2.5181170	-2.0862250
H	-2.2382690	2.0318370	-1.1853140
C	-4.8656990	4.1852700	3.4249250
C	-4.1117860	3.6101920	4.4719170
C	-4.3117610	4.0037220	5.7975280
H	-3.7269350	3.5679870	6.5991700
C	-5.2770110	4.9723300	6.0885770

H	-5.4293400	5.2733480	7.1207860
C	-6.0335390	5.5483930	5.0711310
H	-6.7809660	6.3010970	5.3001160
C	-5.8196420	5.1525960	3.7471850
H	-6.4002830	5.5972320	2.9442830
C	-7.4709800	-0.8515450	-0.8069270
C	-7.1455770	-2.2136820	-0.7918190
C	-8.1066330	-3.2175360	-0.7949000
C	-9.4553850	-2.8706310	-0.8044070
C	-9.8202040	-1.5266530	-0.8125670
C	-8.8362590	-0.5405890	-0.8200290
F	-5.8506560	-2.5903460	-0.7482490
F	-7.7431150	-4.5070600	-0.7758470
F	-10.3931470	-3.8205260	-0.8042470
F	-11.1151190	-1.1905480	-0.8314120
F	-9.2347650	0.7381920	-0.8503590
C	0.0156190	5.4440780	-1.6253060
C	1.2849420	4.9279440	-1.9296040
C	2.3778470	5.7461100	-2.1957270
C	2.2278360	7.1299320	-2.1592100
C	0.9844040	7.6795580	-1.8596050
C	-0.0982970	6.8421790	-1.6057400
F	1.4865300	3.6002290	-1.9508330
F	3.5743250	5.2110250	-2.4706800
F	3.2715870	7.9250100	-2.4082900
F	0.8317190	9.0089170	-1.8358750
F	-1.2807020	7.4201080	-1.3505560
H	-3.6079460	3.4605560	-0.5233520

Folded Cor-(Ala)₄-PDI_{opt} without hydrogen bond to PDI in chloroform
Energy total = -5475.33298688 a.u.

Symbol	X	Y	Z
C	-4.4809710	1.6218700	-2.5455380
C	-5.5603700	0.8446280	-3.0468230
H	-5.7853550	0.6795870	-4.0919300
C	-6.2891180	0.3758650	-1.9515000
H	-7.1897690	-0.2204100	-1.9884560
C	-5.6703670	0.8748740	-0.7691750
C	-5.9973270	0.8637340	0.6127910
C	-5.2964710	1.6435380	1.5611380
C	-5.4973170	1.6084260	3.0008140
H	-6.2269280	1.0072050	3.5250990
C	-4.5757000	2.4462330	3.5465510
H	-4.4248110	2.6667830	4.5933820
C	-3.8046290	3.0069130	2.4425610
C	-2.6984230	3.8853060	2.6125100
C	-1.8960720	4.4132610	1.5884840
C	-0.7000140	5.2012340	1.7079070
H	-0.2708970	5.5236850	2.6446510
C	-0.2039920	5.4341260	0.4512940
H	0.7024760	5.9661150	0.2023660
C	-1.0704100	4.8086860	-0.5078780
C	-0.9457880	4.7609330	-1.9077350
C	-1.7875330	3.9498800	-2.7176430
C	-2.2216070	4.0751940	-4.0593110
H	-1.8856120	4.8323190	-4.7534630
C	-3.2444240	3.1477850	-4.2788890
H	-3.8499310	3.0580490	-5.1699010
C	-3.4443350	2.4352490	-3.0804120
N	-4.5789110	1.5798830	-1.1825810
H	-4.0677240	2.1164380	-0.4698620
N	-4.2688100	2.5166190	1.2577690
N	-2.0795110	4.2186950	0.2384930
N	-2.5189530	2.9151970	-2.1681190

H	-2.1550130	2.3322820	-1.4106080
C	-2.2655430	4.2045390	4.0136240
C	-1.1928760	3.4888370	4.5885930
C	-0.7635760	3.7629480	5.8895720
H	0.0710620	3.2232140	6.3220550
C	-1.4148140	4.7505770	6.6344790
H	-1.0781410	4.9587400	7.6456250
C	-2.4787390	5.4645650	6.0877910
H	-2.9813940	6.2321220	6.6672930
C	-2.8925470	5.1892510	4.7811220
H	-3.7181370	5.7420540	4.3427710
C	-7.1012640	-0.0322890	1.0418450
C	-7.0256870	-1.4153810	0.8347320
C	-8.0507760	-2.2844630	1.1883880
C	-9.2037780	-1.7778130	1.7821430
C	-9.3144380	-0.4089660	2.0106130
C	-8.2770910	0.4415090	1.6367420
F	-5.9120160	-1.9514670	0.2917420
F	-7.9307220	-3.6025570	0.9735760
F	-10.1961310	-2.6001420	2.1310530
F	-10.4246680	0.0844090	2.5717090
F	-8.4393730	1.7540650	1.8538340
C	0.0614070	5.6126980	-2.5830790
C	1.0149980	5.0579070	-3.4503140
C	1.9590390	5.8344120	-4.1138840
C	1.9755420	7.2129240	-3.9209030
C	1.0452180	7.8000360	-3.0682850
C	0.1036260	7.0053680	-2.4213250
F	1.0525000	3.7312620	-3.6489380
F	2.8592720	5.2630190	-4.9240110
F	2.8799650	7.9680520	-4.5504430
F	1.0483760	9.1271670	-2.8904290
F	-0.7902890	7.6221520	-1.6342600
O	-0.6178690	2.5457460	3.7776550
C	0.2603850	1.5697390	4.3161060
H	-0.0920560	1.2086410	5.2897850
H	1.2740430	1.9674170	4.4449290
C	0.3247160	0.3565350	3.3864720
O	1.0876780	-0.5702070	3.6674980
N	-0.5056070	0.3847970	2.3255190
H	-1.0777400	1.2063860	2.1700190
C	-0.7088460	-0.7506390	1.4455760
H	0.2370840	-1.2945490	1.3630170
C	-1.1266060	-0.2255990	0.0628590
O	-1.4891660	0.9456280	-0.1031770
N	-1.1162280	-1.1493390	-0.9218970
H	-0.8057090	-2.0953700	-0.7370090
C	-1.6744420	-0.9186430	-2.2469620
H	-2.3996540	-0.1082240	-2.1575970
C	-0.5985300	-0.5332990	-3.2772910
H	0.1417590	-1.3322170	-3.3723100
H	-1.0492540	-0.3555250	-4.2580440
C	-1.7791140	-1.7085890	2.0111800
H	-0.0946590	0.3816460	-2.9568930
H	-1.4516980	-2.0715570	2.9873960
H	-2.7348790	-1.1882310	2.1241470
H	-1.9272210	-2.5745800	1.3613140
C	-2.3766240	-2.2135060	-2.6764970
O	-1.8714710	-3.3125690	-2.4230540
N	-3.5407380	-2.0611920	-3.3482450
H	-3.8902310	-1.1212140	-3.4885740
C	-4.2100340	-3.1515090	-4.0735370
C	-4.5690140	-4.3494110	-3.1613620
O	-4.5598790	-5.4961210	-3.5988630
C	-3.4154560	-3.6058700	-5.2998860
H	-2.4421610	-3.9994820	-4.9998560

H	-3.2676820	-2.7639610	-5.9812550
H	-3.9581700	-4.3963230	-5.8195710
N	-4.9354280	-4.0319760	-1.8923810
H	-4.9316180	-3.0587380	-1.6231360
C	-5.3708330	-5.0124920	-0.8951910
C	-6.6419150	-5.7670650	-1.3017540
C	-4.2582050	-5.9853430	-0.4379870
O	-4.5543910	-6.9771460	0.2321420
H	-5.1673380	-2.7309750	-4.4032280
H	-5.6047110	-4.4242620	-0.0025640
H	-6.8934310	-6.4860710	-0.5209970
H	-6.4883610	-6.3021960	-2.2396940
H	-7.4703520	-5.0634010	-1.4177750
N	-2.9810250	-5.6399520	-0.7137420
H	-2.7809100	-4.8687600	-1.3415230
N	1.8160720	-5.5511450	0.4773860
N	11.6518750	0.2554330	0.5573740
O	0.9160390	-4.0404290	1.9302600
O	2.6998860	-7.0150320	-1.0442600
O	10.7233040	1.7370520	2.0377930
O	12.5169450	-1.2648420	-0.9321060
C	1.8872200	-4.3960530	1.2665270
C	3.1619430	-3.6465800	1.2589890
C	4.2527780	-4.0868840	0.4700850
C	4.1167930	-5.2474440	-0.3300650
C	2.8506830	-6.0154870	-0.3492050
C	5.1821270	-5.6748070	-1.1056150
H	5.0638710	-6.5642400	-1.7139760
C	6.3907950	-4.9718290	-1.1014680
H	7.1952060	-5.3457310	-1.7220460
C	6.5713210	-3.8232930	-0.3275700
C	5.4833000	-3.3604110	0.4782520
C	5.5938160	-2.1883500	1.2926460
C	4.4882110	-1.7901490	2.0463400
C	3.2853120	-2.5050440	2.0352310
H	2.4439370	-2.1612700	2.6285660
C	6.8621000	-1.4450820	1.3070560
C	7.0452220	-0.2978130	2.0820280
H	6.2409430	0.0761430	2.7027510
C	8.2563380	0.4016890	2.0898510
H	8.3760380	1.2898850	2.6995770
C	9.3231840	-0.0301650	1.3192150
C	9.1835450	-1.1881160	0.5194520
C	7.9505860	-1.9097950	0.5034060
C	7.8388370	-3.0781960	-0.3145190
C	8.9437550	-3.4717730	-1.0725610
C	10.1464110	-2.7582310	-1.0494820
H	10.9911990	-3.0838430	-1.6454000
C	10.2771420	-1.6248740	-0.2637350
C	11.5634890	-0.8898780	-0.2558400
C	10.5963750	0.7296330	1.3474480
C	0.5539920	-6.3152460	0.5154910
H	0.2596330	-6.3997460	1.5638010
C	-0.5621060	-5.6411790	-0.2876910
H	-0.2454780	-5.5071370	-1.3276140
H	-0.7390780	-4.6489330	0.1352030
C	12.9581360	0.9876850	0.5622820
H	13.5693980	0.4054560	-0.1258070
C	13.6265890	0.9461240	1.9408590
H	13.7186030	-0.0847330	2.2964720
H	13.0691110	1.5256380	2.6776620
C	12.8203780	2.4031570	-0.0091920
H	12.2351820	3.0486110	0.6467600
H	12.3479940	2.3790040	-0.9961020
H	4.5368550	-0.9040420	2.6665230
H	8.8908010	-4.3514550	-1.7013240

C	-1.8641570	-6.4430690	-0.2295150
H	14.6350990	1.3639130	1.8592530
H	13.8185190	2.8370520	-0.1260900
H	0.7796210	-7.3067540	0.1248920
H	-2.0908160	-6.7416490	0.7996240
H	-1.7724380	-7.3697930	-0.8121060
H	-2.9196620	3.7941090	-0.1213920

Folded Cor-(Ala)₄-PDI_{opt} without hydrogen bond to PDI in toluene

Energy total = -5475.32158714 a.u.

Symbol	X	Y	Z
C	-4.5220600	1.5954300	-2.5137320
C	-5.6012250	0.8100380	-3.0015450
H	-5.8428590	0.6496140	-4.0437730
C	-6.3107930	0.3320380	-1.8965700
H	-7.2082110	-0.2697070	-1.9222280
C	-5.6793780	0.8326370	-0.7226790
C	-5.9866880	0.8160320	0.6644600
C	-5.2815420	1.6023040	1.6030960
C	-5.4632300	1.5646120	3.0455740
H	-6.1790760	0.9551400	3.5790820
C	-4.5452720	2.4129620	3.5794060
H	-4.3833100	2.6354020	4.6240860
C	-3.7956260	2.9837270	2.4651820
C	-2.7006240	3.8789400	2.6218300
C	-1.9191430	4.4181960	1.5878450
C	-0.7346720	5.2260070	1.6922920
H	-0.3013300	5.5579900	2.6236610
C	-0.2570800	5.4639770	0.4301870
H	0.6371910	6.0106840	0.1695780
C	-1.1243900	4.8226910	-0.5181610
C	-1.0143620	4.7744140	-1.9185410
C	-1.8567300	3.9536250	-2.7186820
C	-2.3097840	4.0760390	-4.0536520
H	-1.9913770	4.8378140	-4.7509640
C	-3.3257930	3.1379710	-4.2607410
H	-3.9428230	3.0445230	-5.1434460
C	-3.5015290	2.4215330	-3.0613030
N	-4.5999820	1.5477750	-1.1496940
H	-4.0842580	2.0871660	-0.4418820
N	-4.2675810	2.4869460	1.2868770
N	-2.1155740	4.2191860	0.2409390
N	-2.5690170	2.9102040	-2.1609840
H	-2.1889860	2.3317130	-1.4075270
C	-2.2560260	4.2062220	4.0173250
C	-1.1481320	3.5273130	4.5698540
C	-0.7068960	3.8097620	5.8649020
H	0.1549470	3.2988810	6.2789260
C	-1.3815090	4.7674800	6.6274830
H	-1.0355680	4.9822470	7.6341250
C	-2.4805350	5.4440820	6.1036140
H	-3.0014660	6.1887460	6.6966740
C	-2.9058990	5.1619040	4.8022710
H	-3.7586490	5.6864300	4.3815470
C	-7.0773990	-0.0897510	1.1063180
C	-6.9963830	-1.4714210	0.8905740
C	-8.0109420	-2.3491480	1.2540670
C	-9.1584500	-1.8527790	1.8676000
C	-9.2740230	-0.4856500	2.1055480
C	-8.2475770	0.3737420	1.7209770
F	-5.8875020	-1.9977410	0.3282880
F	-7.8860950	-3.6646000	1.0296620
F	-10.1403110	-2.6827040	2.2259490
F	-10.3785180	-0.0025550	2.6853350

F	-8.4149270	1.6834070	1.9471600
C	-0.0235740	5.6350200	-2.6068690
C	0.9264280	5.0867170	-3.4824420
C	1.8552110	5.8707180	-4.1591140
C	1.8592670	7.2503180	-3.9709830
C	0.9319100	7.8310080	-3.1102670
C	0.0054520	7.0287830	-2.4501750
F	0.9752130	3.7601520	-3.6765590
F	2.7521960	5.3060780	-4.9767340
F	2.7487320	8.0122630	-4.6125680
F	0.9232610	9.1582330	-2.9371100
F	-0.8859160	7.6383620	-1.6555410
O	-0.5524270	2.6113120	3.7432660
C	0.3581750	1.6539360	4.2598780
H	0.0373900	1.2859750	5.2420870
H	1.3666210	2.0716780	4.3636400
C	0.4244520	0.4407640	3.3294780
O	1.2276070	-0.4591010	3.5812740
N	-0.4529770	0.4384770	2.3063670
H	-1.0470450	1.2468850	2.1650630
C	-0.6576660	-0.7068880	1.4400670
H	0.2952500	-1.2345910	1.3378390
C	-1.1179400	-0.2007150	0.0644460
O	-1.4905080	0.9664890	-0.1063390
N	-1.1299960	-1.1349550	-0.9115070
H	-0.8105030	-2.0781530	-0.7273460
C	-1.7097460	-0.9069120	-2.2274700
H	-2.4441100	-0.1064900	-2.1230710
C	-0.6534320	-0.5003970	-3.2701750
H	0.0946760	-1.2898290	-3.3821420
H	-1.1194880	-0.3203740	-4.2434380
C	-1.6917480	-1.6818760	2.0417000
H	-0.1560360	0.4182790	-2.9503490
H	-1.3365420	-2.0149890	3.0188070
H	-2.6603510	-1.1869010	2.1604550
H	-1.8211060	-2.5669510	1.4143270
C	-2.4009340	-2.2071490	-2.6577910
O	-1.8778760	-3.3009170	-2.4244590
N	-3.5770320	-2.0604310	-3.3126080
H	-3.9438460	-1.1232510	-3.4264930
C	-4.2416010	-3.1470060	-4.0485250
C	-4.5910540	-4.3621080	-3.1538890
O	-4.5906910	-5.4976040	-3.6161830
C	-3.4487780	-3.5818340	-5.2831810
H	-2.4707270	-3.9691360	-4.9906110
H	-3.3120200	-2.7332010	-5.9588420
H	-3.9859400	-4.3747170	-5.8046570
N	-4.9393090	-4.0674580	-1.8737460
H	-4.9226950	-3.1001570	-1.5851460
C	-5.3537710	-5.0661350	-0.8846230
C	-6.6213120	-5.8291520	-1.2861480
C	-4.2282290	-6.0349910	-0.4495100
O	-4.5077060	-7.0211780	0.2329440
H	-5.2029520	-2.7281790	-4.3694270
H	-5.5835330	-4.4917690	0.0181260
H	-6.8499660	-6.5640610	-0.5131920
H	-6.4742580	-6.3464940	-2.2349380
H	-7.4607150	-5.1345930	-1.3781000
N	-2.9575660	-5.6893010	-0.7579420
H	-2.7714300	-4.9200790	-1.3912160
N	1.8384660	-5.5384910	0.4120370
N	11.6732710	0.2708250	0.5838650
O	0.8864610	-3.9569940	1.7521700
O	2.7685440	-7.0569220	-1.0270220
O	10.7085710	1.7872350	2.0056270
O	12.5730860	-1.2868560	-0.8457530

C	1.8831180	-4.3493150	1.1499940
C	3.1641560	-3.6101680	1.1697060
C	4.2753290	-4.0728340	0.4229850
C	4.1591600	-5.2555720	-0.3470100
C	2.8963290	-6.0307360	-0.3691800
C	5.2432950	-5.7041720	-1.0831800
H	5.1386970	-6.6116470	-1.6671240
C	6.4512450	-4.9999030	-1.0687270
H	7.2710840	-5.3896820	-1.6588760
C	6.6140410	-3.8316990	-0.3206980
C	5.5068600	-3.3483190	0.4459840
C	5.5994280	-2.1588040	1.2372690
C	4.4774820	-1.7455670	1.9576390
C	3.2722830	-2.4563350	1.9293450
H	2.4216160	-2.0998280	2.5018030
C	6.8677070	-1.4159670	1.2646420
C	7.0335580	-0.2506760	2.0161670
H	6.2143370	0.1369340	2.6085640
C	8.2441110	0.4496820	2.0354090
H	8.3519150	1.3526050	2.6256110
C	9.3279710	0.0002360	1.2997810
C	9.2068080	-1.1766920	0.5251950
C	7.9744670	-1.8992460	0.4976780
C	7.8815610	-3.0866300	-0.2949830
C	9.0042290	-3.4969480	-1.0172200
C	10.2063880	-2.7827720	-0.9828970
H	11.0661370	-3.1202370	-1.5503530
C	10.3184530	-1.6312220	-0.2215660
C	11.6050920	-0.8953340	-0.2020690
C	10.5997730	0.7632770	1.3382560
C	0.5817700	-6.3115670	0.4573740
H	0.2678290	-6.3506910	1.5029210
C	-0.5287550	-5.6882830	-0.3928320
H	-0.2059510	-5.6139270	-1.4368800
H	-0.7108830	-4.6736870	-0.0304300
C	12.9776510	1.0060380	0.5982970
H	13.6051790	0.4070890	-0.0604320
C	13.6140880	1.0039990	1.9925600
H	13.7030790	-0.0167850	2.3769030
H	13.0364940	1.5995650	2.7004950
C	12.8482530	2.4057890	-0.0126780
H	12.2446580	3.0648040	0.6123950
H	12.4003640	2.3541850	-1.0099340
H	4.5120650	-0.8498260	2.5649670
H	8.9652500	-4.3911880	-1.6264550
C	-1.8306650	-6.4879930	-0.2917850
H	14.6223550	1.4248180	1.9236030
H	13.8470720	2.8415090	-0.1168700
H	0.8248780	-7.3174240	0.1166720
H	-2.0335770	-6.7718240	0.7467320
H	-1.7563890	-7.4238260	-0.8619410
H	-2.9513170	3.7765570	-0.1069700

Turn1,4-Cor-(Ala)₄-PDI_{opt} in chloroform

Energy total = -5475.32413890 a.u.

Symbol	X	Y	Z
C	9.0564150	2.8879030	-0.9033970
C	9.7374940	4.0874770	-1.2328860
H	10.7957730	4.1733330	-1.4350550
C	8.8186460	5.1343180	-1.1647820
H	9.0309660	6.1848110	-1.3034250
C	7.5532530	4.5957520	-0.7902190
C	6.3089430	5.1739230	-0.4208970

C	5.3303470	4.4524410	0.2931250
C	3.9538980	4.7591720	0.5003480
H	3.4521590	5.6258840	0.0947500
C	3.3734350	3.7429470	1.2263710
H	2.3338730	3.6648160	1.5081780
C	4.3607400	2.7493200	1.5071210
C	4.1868210	1.5256970	2.1748210
C	5.1115700	0.4550400	2.2519290
C	4.9517640	-0.7766790	2.9696790
H	4.0950040	-1.0202270	3.5800940
C	6.0639930	-1.5611130	2.7539620
H	6.2448090	-2.5481490	3.1541340
C	6.9529010	-0.8420500	1.8976760
C	8.2229460	-1.1840940	1.3759560
C	8.9432620	-0.3197870	0.5180620
C	10.3215330	-0.4031860	0.0666300
H	11.0047330	-1.2228650	0.2438890
C	10.5969050	0.7754530	-0.5819200
H	11.5319860	1.0733240	-1.0373000
C	9.3832010	1.5534780	-0.5307810
N	7.7508130	3.2448670	-0.6988210
H	7.0300330	2.5537970	-0.5726600
N	5.5370110	3.2033100	0.9035020
H	6.4403520	2.9787970	1.3008690
N	6.3358840	0.3641940	1.6284070
N	8.4062040	0.8655370	0.1069200
C	2.8627710	1.3184950	2.8512710
C	1.8244270	0.6163920	2.2018690
C	0.5912020	0.4263950	2.8335280
H	-0.2048570	-0.1174220	2.3394870
C	0.3853950	0.9384230	4.1171290
H	-0.5748730	0.7836390	4.5998220
C	1.3959220	1.6385430	4.7719190
H	1.2343460	2.0371810	5.7680990
C	2.6243490	1.8233310	4.1328440
H	3.4213200	2.3672660	4.6311970
C	6.0383870	6.5812190	-0.7962940
C	6.1550280	7.0226970	-2.1235040
C	5.9248180	8.3444580	-2.4914920
C	5.5570820	9.2756410	-1.5245580
C	5.4281190	8.8752920	-0.1978820
C	5.6736390	7.5508380	0.1504030
F	6.4795750	6.1577610	-3.0958890
F	6.0380770	8.7209040	-3.7714410
F	5.3284300	10.5462930	-1.8676900
F	5.0878410	9.7699620	0.7384850
F	5.5648270	7.2228790	1.4468190
C	8.8345860	-2.4765320	1.7848180
C	9.1318480	-3.4718610	0.8465100
C	9.7177060	-4.6823820	1.2029350
C	10.0324360	-4.9256270	2.5369170
C	9.7504200	-3.9600260	3.4989630
C	9.1658420	-2.7560760	3.1165310
F	8.8159600	-3.2884950	-0.4472150
F	9.9731040	-5.6132670	0.2754100
F	10.5965160	-6.0832400	2.8929260
F	10.0581730	-4.1868170	4.7822490
F	8.9294430	-1.8469810	4.0745190
O	2.1087540	0.1599070	0.9428770
C	1.0688520	-0.4158090	0.1573960
H	0.2256140	0.2760200	0.0501710
H	0.7047580	-1.3585790	0.5831270
C	1.5910960	-0.7346550	-1.2372340
O	0.8102990	-1.0643870	-2.1250300
N	2.9427780	-0.6649990	-1.3958120
C	3.5686390	-0.8527440	-2.6971620

H	2.7968400	-0.6879180	-3.4534570
C	4.0715830	-2.2855460	-2.9444950
O	4.3410850	-2.6511970	-4.0960000
C	4.7203790	0.1397400	-2.9050940
H	5.4892550	0.0187580	-2.1342180
N	4.2329620	-3.0815020	-1.8657670
H	3.9094650	-2.7444580	-0.9683650
C	4.8592410	-4.4061670	-1.9371830
C	3.8249380	-5.5086450	-2.2806970
O	3.6548530	-6.4979450	-1.5721940
C	5.6016260	-4.7130950	-0.6424150
H	4.9227720	-4.6884040	0.2154390
H	6.4044610	-3.9889830	-0.4913470
H	6.0323770	-5.7145460	-0.6905210
N	3.1232880	-5.2665700	-3.4221280
H	3.4151070	-4.4693040	-3.9831380
C	2.1499370	-6.2026590	-3.9846830
C	2.7738770	-7.5311080	-4.4292690
C	0.9274540	-6.4423770	-3.0698560
O	0.1990020	-7.4204680	-3.2418290
N	0.6633880	-5.4819610	-2.1522410
H	1.3406190	-4.7514740	-1.9827870
C	-0.4361730	-5.6037350	-1.2003730
H	-1.3075340	-5.9711340	-1.7507590
C	-0.1097620	-6.5774840	-0.0572420
H	-0.9592800	-6.6670160	0.6275970
H	0.7574010	-6.2172830	0.5014310
H	5.1833620	-0.0324590	-3.8785680
H	4.3450340	1.1656720	-2.8694180
H	5.5645030	-4.3609920	-2.7750300
H	1.7418100	-5.6989570	-4.8690970
H	0.1129040	-7.5629910	-0.4703960
H	2.0025540	-8.1735990	-4.8561350
H	3.2250770	-8.0427530	-3.5773910
H	3.5440360	-7.3451420	-5.1826270
H	3.4694120	-0.2450280	-0.6395970
C	-0.6864280	-4.1975670	-0.6420690
N	-1.9335020	-3.7053080	-0.7969260
H	-2.5909740	-4.2225900	-1.3631790
O	0.2221190	-3.5853900	-0.0715120
N	-5.6647220	-0.5620030	0.0663860
N	-16.9709510	1.0372750	0.2778040
O	-5.7379820	-1.3528490	2.2077360
O	-5.6048780	0.1462010	-2.1046720
O	-17.0093610	0.2219460	2.4185110
O	-16.8591560	1.8333460	-1.8742580
C	-6.3479020	-0.9028400	1.2422650
C	-7.8118430	-0.6907200	1.2523990
C	-8.4794230	-0.1828300	0.1112350
C	-7.7388710	0.1225290	-1.0567490
C	-6.2745810	-0.0847300	-1.1027420
C	-8.3915950	0.6172390	-2.1737440
H	-7.8125130	0.8438130	-3.0617390
C	-9.7745530	0.8223150	-2.1552580
H	-10.2395540	1.2121590	-3.0517290
C	-10.5458540	0.5369050	-1.0265440
C	-9.8941380	0.0178310	0.1373930
C	-10.6220240	-0.3057460	1.3266250
C	-9.9208610	-0.8040440	2.4268450
C	-8.5362590	-0.9949860	2.3930740
H	-8.0123370	-1.3834070	3.2590020
C	-12.0781020	-0.1044010	1.3514510
C	-12.8545580	-0.4097110	2.4712780
H	-12.3934060	-0.8133910	3.3637050
C	-14.2390650	-0.2108460	2.4858000
H	-14.8221220	-0.4560140	3.3660380

C	-14.8870510	0.3036640	1.3753030
C	-14.1410100	0.6262580	0.2180710
C	-12.7272480	0.4228710	0.1908310
C	-11.9999630	0.7519610	-0.9961430
C	-12.7007290	1.2679770	-2.0883420
C	-14.0847270	1.4669660	-2.0499380
H	-14.6071080	1.8698680	-2.9099100
C	-14.8091420	1.1518150	-0.9121680
C	-16.2745270	1.3734820	-0.8979380
C	-16.3558470	0.5066770	1.4190950
C	-4.2053590	-0.7574740	0.0468790
H	-3.8468530	-0.5692350	1.0593240
C	-3.8138730	-2.1689190	-0.4041900
H	-4.1913780	-2.3356220	-1.4199680
H	-4.2874210	-2.9033070	0.2560520
C	-18.4508690	1.2664390	0.2821260
H	-18.6391300	1.6809690	-0.7072570
C	-18.8604330	2.3164360	1.3208120
H	-18.2859830	3.2383020	1.1872680
H	-18.7165820	1.9550880	2.3397110
C	-19.2285230	-0.0490290	0.3993870
H	-19.0957850	-0.5119870	1.3780310
H	-18.9115900	-0.7565990	-0.3729730
H	-10.4434780	-1.0555770	3.3408830
H	-12.1785040	1.5294180	-2.9999220
C	-2.2973300	-2.3553760	-0.3744120
H	-19.9190700	2.5579200	1.1823320
H	-20.2939880	0.1537110	0.2512440
H	-3.7925130	-0.0099960	-0.6308410
H	-1.9133600	-2.2050690	0.6401720
H	-1.7967880	-1.6228250	-1.0206990
H	6.8205540	0.9779780	0.9654260

Turn1,4-Cor-(Ala)₄-PDI_{opt} in toluene

Energy total = -5475.31209905 a.u.

Symbol	X	Y	Z
C	8.8389990	3.0964490	-1.0684730
C	9.4646140	4.3191290	-1.4209600
H	10.5110770	4.4424170	-1.6614560
C	8.5129850	5.3330800	-1.3177890
H	8.6838070	6.3902420	-1.4625760
C	7.2819260	4.7509330	-0.8977120
C	6.0338040	5.2844650	-0.4782160
C	5.1095250	4.5282940	0.2711210
C	3.7332880	4.7883530	0.5352940
H	3.1876380	5.6395450	0.1542110
C	3.2163280	3.7517860	1.2800510
H	2.1924680	3.6384730	1.6040860
C	4.2462730	2.7908120	1.5177330
C	4.1411140	1.5616180	2.1891920
C	5.1067700	0.5256130	2.2319120
C	5.0225270	-0.7058460	2.9624310
H	4.2002230	-0.9772590	3.6074830
C	6.1561130	-1.4476120	2.7099640
H	6.3919420	-2.4225640	3.1109390
C	6.9827620	-0.7015280	1.8159750
C	8.2457060	-0.9955770	1.2497790
C	8.8978940	-0.1085160	0.3618800
C	10.2606380	-0.1409080	-0.1401900
H	10.9805780	-0.9333260	0.0133020
C	10.4666090	1.0441370	-0.8012320
H	11.3721470	1.3752620	-1.2919020
C	9.2268450	1.7757270	-0.7071020
N	7.5298940	3.4075370	-0.8160610

H	6.8389020	2.6911890	-0.6675730
N	5.3811600	3.2850350	0.8679720
H	6.3080210	3.0838090	1.2206970
N	6.3084610	0.4766620	1.5610240
N	8.3005350	1.0538920	-0.0325780
C	2.8516400	1.3064820	2.9132860
C	1.8343090	0.5288340	2.3186200
C	0.6329980	0.2931200	2.9946110
H	-0.1454980	-0.3100340	2.5432650
C	0.4373750	0.8352460	4.2672710
H	-0.4979270	0.6442200	4.7847880
C	1.4264290	1.6105920	4.8674700
H	1.2726740	2.0324040	5.8553150
C	2.6235670	1.8396460	4.1852410
H	3.4042770	2.4411220	4.6413790
C	5.7005580	6.6831670	-0.8352320
C	5.7420380	7.1318620	-2.1646100
C	5.4521060	8.4467590	-2.5159140
C	5.0987600	9.3624490	-1.5285820
C	5.0435690	8.9540320	-0.1989040
C	5.3478380	7.6370560	0.1319490
F	6.0505660	6.2807710	-3.1534850
F	5.4945780	8.8306980	-3.7974140
F	4.8130730	10.6255420	-1.8548210
F	4.7167890	9.8339520	0.7554550
F	5.3083190	7.3010210	1.4298210
C	8.9254770	-2.2576580	1.6464920
C	9.2282340	-3.2500980	0.7067370
C	9.8793470	-4.4305970	1.0515160
C	10.2555670	-4.6449760	2.3747570
C	9.9692730	-3.6815140	3.3381100
C	9.3187590	-2.5077750	2.9674020
F	8.8543440	-3.0946290	-0.5746320
F	10.1384600	-5.3598010	0.1240830
F	10.8821180	-5.7729030	2.7196140
F	10.3353180	-3.8808510	4.6101020
F	9.0797060	-1.5995480	3.9247710
O	2.1052260	0.0483320	1.0659830
C	1.0704720	-0.5897320	0.3225600
H	0.1940510	0.0616340	0.2283910
H	0.7627130	-1.5402850	0.7747810
C	1.5656770	-0.9087320	-1.0823340
O	0.7746220	-1.2754510	-1.9449580
N	2.9109550	-0.7961550	-1.2766070
C	3.5061280	-0.9685610	-2.5950360
H	2.7098180	-0.8292860	-3.3307860
C	4.0462850	-2.3857200	-2.8535580
O	4.2939500	-2.7466300	-4.0101640
C	4.6227910	0.0564320	-2.8342130
H	5.4143970	-0.0402270	-2.0828090
N	4.2669130	-3.1712090	-1.7762980
H	3.9544120	-2.8437240	-0.8716180
C	4.9367770	-4.4733710	-1.8654700
C	3.9299850	-5.6123400	-2.1696420
O	3.8102060	-6.5952600	-1.4441290
C	5.7317250	-4.7507370	-0.5956670
H	5.0803760	-4.7509410	0.2837010
H	6.5122720	-3.9973610	-0.4722620
H	6.1950880	-5.7368110	-0.6567570
N	3.1910780	-5.4043680	-3.2952050
H	3.4414870	-4.6026910	-3.8697250
C	2.2259850	-6.3719670	-3.8180060
C	2.8676190	-7.6962670	-4.2498100
C	1.0281930	-6.6213950	-2.8728560
O	0.3065920	-7.6060470	-3.0234310
N	0.7767070	-5.6588750	-1.9511090

H	1.4553070	-4.9266960	-1.7971340
C	-0.2864500	-5.8026460	-0.9617920
H	-1.1588130	-6.2107440	-1.4813870
C	0.1097050	-6.7461510	0.1836550
H	-0.7136090	-6.8544400	0.8975850
H	0.9805670	-6.3466350	0.7082160
H	5.0660340	-0.1062470	-3.8184090
H	4.2192710	1.0716040	-2.7919830
H	5.6113650	-4.4044220	-2.7266680
H	1.7876070	-5.8945430	-4.7026420
H	0.3533530	-7.7294960	-0.2227470
H	2.0976410	-8.3663710	-4.6345740
H	3.3562660	-8.1744380	-3.3993460
H	3.6097640	-7.5124600	-5.0315170
H	3.4395790	-0.3434890	-0.5409450
C	-0.5705680	-4.3958650	-0.4212070
N	-1.8198990	-3.9204740	-0.6215860
H	-2.4437990	-4.4463150	-1.2168560
O	0.3103380	-3.7656460	0.1707060
N	-5.5738640	-0.7536190	0.0762710
N	-16.8475530	1.0736120	0.2135210
O	-5.6579300	-1.4273930	2.2573080
O	-5.5067680	-0.1733990	-2.1323680
O	-16.8911490	0.4042940	2.4048480
O	-16.7277780	1.7235290	-1.9870080
C	-6.2610800	-1.0240160	1.2683670
C	-7.7229030	-0.7924960	1.2652100
C	-8.3841990	-0.3387830	0.0978120
C	-7.6405620	-0.1121350	-1.0860080
C	-6.1782040	-0.3390550	-1.1199130
C	-8.2867370	0.3268730	-2.2294510
H	-7.7034760	0.4924760	-3.1282180
C	-9.6663130	0.5545000	-2.2216320
H	-10.1271350	0.8991390	-3.1386950
C	-10.4404660	0.3489960	-1.0776670
C	-9.7953360	-0.1128880	0.1138090
C	-10.5259910	-0.3536220	1.3209370
C	-9.8312260	-0.8042560	2.4454960
C	-8.4502330	-1.0217000	2.4211830
H	-7.9296470	-1.3707530	3.3058460
C	-11.9771230	-0.1179940	1.3379400
C	-12.7554620	-0.3339810	2.4770120
H	-12.2987170	-0.6913110	3.3913830
C	-14.1347370	-0.1003820	2.4847790
H	-14.7207030	-0.2738930	3.3801030
C	-14.7755440	0.3592070	1.3467220
C	-14.0279860	0.5897410	0.1686940
C	-12.6193670	0.3522810	0.1492780
C	-11.8902790	0.5924900	-1.0577330
C	-12.5853040	1.0540170	-2.1775900
C	-13.9646090	1.2850930	-2.1476750
H	-14.4840890	1.6448600	-3.0284300
C	-14.6897410	1.0585800	-0.9898230
C	-16.1503280	1.3152440	-0.9851100
C	-16.2391390	0.6039260	1.3850650
C	-4.1150650	-0.9523880	0.0720820
H	-3.7621580	-0.7172230	1.0768230
C	-3.7183150	-2.3825130	-0.3100780
H	-4.0837050	-2.5925580	-1.3224130
H	-4.1989250	-3.0874800	0.3766960
C	-18.3207720	1.3422580	0.2097580
H	-18.5056640	1.6898820	-0.8058160
C	-18.6922640	2.4740240	1.1742370
H	-18.0995540	3.3703090	0.9665510
H	-18.5417270	2.1839480	2.2147450
C	-19.1321810	0.0603420	0.4273890

H	-19.0031310	-0.3331310	1.4363160
H	-18.8413920	-0.7096930	-0.2938390
H	-10.3569450	-0.9956300	3.3724250
H	-12.0612330	1.2469100	-3.1052300
C	-2.2014650	-2.5601170	-0.2528660
H	-19.7470670	2.7299650	1.0322140
H	-20.1930520	0.2810040	0.2718460
H	-3.6985710	-0.2384660	-0.6391190
H	-1.8345880	-2.3761940	0.7624680
H	-1.6934860	-1.8468080	-0.9147500
H	6.7471370	1.1029500	0.8771160

(Ala)₄-PDI_{opt} in toluene

Energy total = -2517.08514256 a.u.

Symbol	X	Y	Z
C	-5.3149520	-0.7097470	-3.2894470
H	-4.3580210	-0.2002610	-3.4156820
C	-5.3294200	-1.6552230	-2.1066720
O	-6.3613560	-2.2367390	-1.7431500
N	-4.1419930	-1.8549070	-1.4804960
H	-3.3567030	-1.2470900	-1.6977610
C	-4.0545390	-2.7308160	-0.3176500
H	-4.4535950	-3.7108010	-0.6028910
C	-2.5972420	-2.8716680	0.1261160
H	-2.2039470	-1.9032570	0.4462450
H	-2.5210020	-3.5668260	0.9662720
H	-1.9844870	-3.2540860	-0.6948310
C	-4.9028410	-2.1478970	0.8312560
O	-4.6990310	-1.0055910	1.2516270
N	-5.8678790	-2.9525550	1.3343500
H	-6.0512020	-3.8249700	0.8605290
C	-6.8118600	-2.5058430	2.3662900
C	-7.5811260	-1.2175500	1.9552870
O	-7.9673290	-0.4311970	2.8147420
C	-6.1525830	-2.3465390	3.7375050
H	-5.3659620	-1.5915650	3.6963180
H	-5.7210520	-3.2989730	4.0572910
H	-6.8989680	-2.0261420	4.4653140
N	-7.8391900	-1.1017270	0.6253310
H	-7.3810710	-1.7441120	-0.0142240
C	-8.5599770	-0.0046380	-0.0221890
C	-9.8911420	0.3603050	0.6467580
C	-7.7176840	1.2618620	-0.3057850
O	-8.2304760	2.1983050	-0.9227490
H	-7.5700310	-3.2951710	2.4289350
H	-8.7864610	-0.3800270	-1.0268100
H	-10.3755520	1.1361630	0.0514530
H	-9.7323990	0.7256120	1.6608780
H	-10.5422580	-0.5176070	0.6883240
N	-6.4186690	1.2544650	0.0671310
H	-6.0327590	0.4742980	0.5875720
N	-1.7104880	2.2368460	-0.8830820
N	9.2340560	-0.7606490	0.4315380
O	-2.0890180	0.3155890	-2.0584420
O	-1.3511640	4.0932960	0.4046000
O	8.8455440	-2.5989010	-0.8807640
O	9.5436050	1.0987730	1.7453970
C	-1.2939380	1.0322440	-1.4424780
C	0.1275510	0.6620280	-1.2779240
C	1.0046010	1.4770050	-0.5208480
C	0.5153460	2.6629460	0.0765020
C	-0.8945900	3.0744000	-0.0972580
C	1.3675790	3.4559560	0.8272330
H	0.9775180	4.3615310	1.2779730

C	2.7070420	3.0939960	0.9975530
H	3.3344230	3.7452490	1.5928480
C	3.2362240	1.9363620	0.4225940
C	2.3743450	1.1032350	-0.3597830
C	2.8487560	-0.0928820	-0.9867730
C	1.9489160	-0.8619190	-1.7285430
C	0.6077510	-0.4945710	-1.8708830
H	-0.0721660	-1.1071910	-2.4519310
C	4.2610300	-0.4702980	-0.8313290
C	4.7988290	-1.6129720	-1.4272330
H	4.1762910	-2.2578920	-2.0346460
C	6.1431110	-1.9665190	-1.2681700
H	6.5403580	-2.8586100	-1.7387500
C	6.9895350	-1.1815580	-0.5039230
C	6.4893960	-0.0132330	0.1160600
C	5.1191830	0.3583210	-0.0420500
C	4.6437660	1.5482640	0.5934450
C	5.5389090	2.3021430	1.3552010
C	6.8783670	1.9278100	1.5063820
H	7.5564310	2.5278080	2.1023000
C	7.3606230	0.7829010	0.8949460
C	8.7858530	0.4110400	1.0699980
C	8.4106120	-1.5834520	-0.3475850
C	-3.1187010	2.6382620	-1.0761420
H	-3.3883570	2.3695870	-2.0990060
C	-4.0588380	1.9490140	-0.0834880
H	-3.7648350	2.2040190	0.9400230
H	-3.9479410	0.8676690	-0.1864670
C	10.6736160	-1.1293920	0.6193210
H	11.0542910	-0.3241410	1.2463010
C	11.4446320	-1.1057170	-0.7049310
H	11.3145730	-0.1451730	-1.2130160
H	11.1245670	-1.9057110	-1.3734120
C	10.8234700	-2.4447000	1.3916520
H	10.4670920	-3.2963790	0.8109740
H	10.2736310	-2.4044520	2.3370400
H	2.2780810	-1.7720460	-2.2137090
H	5.2083820	3.2055660	1.8519540
C	-5.5237300	2.3351920	-0.3335820
H	12.5117640	-1.2315470	-0.4958690
H	11.8812100	-2.6009080	1.6262880
H	-3.1505020	3.7221310	-0.9688990
H	-5.6975880	2.5358290	-1.3983290
H	-5.7804630	3.2616030	0.1947700
H	-5.5449470	-1.2773790	-4.1962230
H	-6.1087040	0.0297310	-3.1572330

7. References

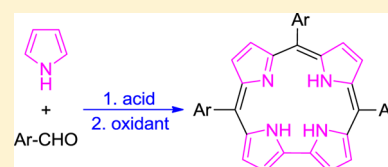
1. E. Schwartz *et al.*, "Helter-Skelter-Like" Perylene Polyisocyanopeptides. *Chemistry-a European Journal* **15**, 2536-2547 (2009).
2. R. Orłowski *et al.*, Covalently Linked Bis(Amido-Corroles): Inter- and Intramolecular Hydrogen-Bond-Driven Supramolecular Assembly. *Chemistry-a European Journal* **25**, 9658-9664 (2019).
3. D. D. Bao *et al.*, Electrochemical Oxidation of Ferrocene: A Strong Dependence on the Concentration of the Supporting Electrolyte for Nonpolar Solvents. *Journal of Physical Chemistry A* **113**, 1259-1267 (2009).
4. E. M. Espinoza *et al.*, Practical Aspects of Cyclic Voltammetry: How to Estimate Reduction Potentials When Irreversibility Prevails. *Journal of the Electrochemical Society* **166**, H3175-H3187 (2019).
5. E. M. Espinoza, J. M. Larsen, V. I. Vullev, What Makes Oxidized N-Acylanthranilamides Stable? *Journal of Physical Chemistry Letters* **7**, 758-764 (2016).
6. J. J. Markham, INTERACTION OF NORMAL MODES WITH ELECTRON TRAPS. *Reviews of Modern Physics* **31**, 956-989 (1959).
7. F. Ansbacher, A NOTE ON THE OVERLAP INTEGRAL OF 2 HARMONIC OSCILLATOR WAVE FUNCTIONS. *Zeitschrift Fur Naturforschung Part a-Astrophysik Physik Und Physikalische Chemie* **14**, 889-892 (1959).
8. G. Jones, X. Zhou, V. I. Vullev, Photoinduced electron transfer in alpha-helical polypeptides: dependence on conformation and electron donor-acceptor distance. *Photochemical & Photobiological Sciences* **2**, 1080-1087 (2003).
9. G. Jones *et al.*, Photoinduced electron transfer in arylacridinium conjugates in a solid glass matrix. *Journal of Physical Chemistry B* **111**, 6921-6929 (2007).
10. S. Upadhyayula *et al.*, Photoinduced dynamics of a cyanine dye: parallel pathways of non-radiative deactivation involving multiple excited-state twisted transients (vol 6, pg 2237, 2015). *Chemical Science* **6**, 3269-3269 (2015).
11. M. J. Frisch *et al.* (2009) Gaussian 09, Revision E.01. (Gaussian, Inc., Wallingford CT).

Synthesis of Corroles and Their Heteroanalogs

Rafał Orłowski, Dorota Gryko,* and Daniel T. Gryko*

Institute of Organic Chemistry, Polish Academy of Sciences, Kasprzaka 44-52, 01-224 Warsaw, Poland

ABSTRACT: Corroles have come a long way from being a curiosity to being a mainstream research topic. They are now regularly synthesized in numerous research laboratories worldwide with diverse specific aims in mind. In this review we present a comprehensive description of corroles' synthesis, developed both before and after 1999. To aid the investigator in developing synthetic strategies, some of the sections culminate in tables containing comparisons of various methodologies leading to *meso*-substituted corroles. The remaining challenges are delineated. In the second part of this review, we also describe the syntheses of isocorroles and heteroanalogs of corroles such as triazacorroles (corrolazines), 10-heterocorroles, 21-heterocorroles, 22-heterocorroles, *N*-confused corroles, as well as norcorroles. The review is complemented with a short outlook.



CONTENTS

1. Introduction	3102	10. Core-Modified Corroles	3126
2. β -Substituted Corroles	3103	10.1. <i>N</i> -Confused Corroles	3126
2.1. Classical Methods	3103	10.2. Heteroanalogues of Corroles	3127
2.1.1. Pyrrole Tetramerization	3103	10.2.1. 10-Heterocorroles	3127
2.1.2. Synthesis of β -Substituted Corroles from Tetrapyrrolic Intermediates	3104	10.2.2. Corrole Heteroanalogs Modified in Pyrrole Subunit	3130
2.2. Nonclassical Methods	3106	10.2.3. Triazacorroles (Corrolazines)	3130
2.2.1. Synthesis from Derivatives of 2,2'-Bipyrrole and Dipyrranes	3106	11. Norcorroles	3130
2.2.2. Contraction of Thiaphlorins	3107	12. Stability of Corroles	3131
3. <i>Meso</i> -Substituted A_3 -Corroles	3107	13. Summary and Outlook	3132
3.1. General Considerations	3107	Author Information	3133
3.2. Reaction under Neat Conditions	3110	Corresponding Authors	3133
3.3. Synthesis Using Al_2O_3 as a Solid Support	3111	Notes	3133
3.4. Synthesis in Acetic Acid	3111	Biographies	3133
3.5. Synthesis in Organic Solvents	3111	Acknowledgments	3133
3.6. Synthesis in Water–Methanol–HCl System	3111	References	3133
3.7. Synthesis via Porphyrin Ring Contraction	3112		
3.8. <i>N</i> -Alkyl Corroles	3112		
3.9. Guidelines for the Preparation of A_3 -Corroles	3112		
4. <i>Meso</i> -Substituted <i>trans</i> - A_2B -Corroles	3112		
4.1. General Considerations	3112		
4.2. Synthesis from Aldehydes and Dipyrranes	3113		
4.3. Synthesis from 2,2'-Bipyrrole and Dipyrrane–Diols	3117		
4.4. Synthesis from Alkyl Oxalyl Chlorides and Dipyrranes	3117		
4.5. Synthesis from Dipyrrane–Diols and Pyrrole	3118		
5. <i>cis</i> - A_2B -Corroles	3118		
6. ABC-Corroles	3118		
7. Conjugated Corrole Dimers	3119		
8. <i>Meso</i> - β -Substituted Corroles	3120		
8.1. Synthesis of Mono-Corroles Substituted at <i>Meso</i> and β -Positions	3120		
8.2. Face-to-Face Porphyrin–Corrole Systems	3123		
8.3. Cofacial Bis(Corrole) Dyes	3124		
9. Isocorroles	3124		

1. INTRODUCTION

Corroles (Figure 1) were discovered by serendipity by Kay and Johnson in 1964.¹ The formidable effort by the Johnson group² was oriented toward synthesis of the corrin skeleton and resulted

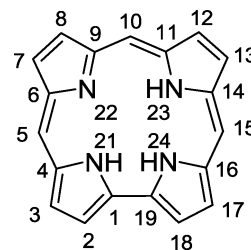


Figure 1. Structure and numbering of corrole.

Special Issue: Expanded, Contracted, and Isomeric Porphyrins

Received: July 6, 2016

Published: November 4, 2016

Mgr inż. Rafał Orłowski

Oświadczam, że mój wkład w powstanie poniższych publikacji polegał na:

1. Hydrogen Bond Involving Cavity NH Protons Drives Supramolecular Oligomerization of Amido-Corroles

Zsyntezowałem i zanalizowałem wszystkie związki podane w publikacji za wyjątkiem związków **11** i **12**. Wyhodowałem kryształ związku **9** nadający się do pomiarów rentgenografii strukturalnej. Przygotowałem szkic manuskrypt wraz z opisem części eksperymentalnej.

2. Covalently Linked Bis(Amido-Corroles): Inter- and Intramolecular Hydrogen Bond Driven Supramolecular Assembly

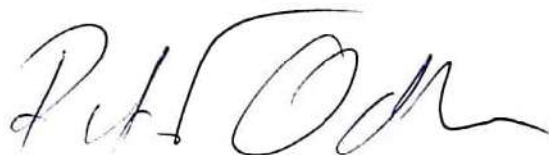
Zsyntezowałem i zanalizowałem wszystkie związki podane w publikacji. Dobrałem warunki umożliwiające przebieg reakcji oraz uzyskanie wysokich wydajności produktów. Wyhodowałem kryształy związków **5A**, **5B**, **6A**, **6B** nadające się do pomiarów rentgenografii strukturalnej. Wykonałem i zanalizowałem pomiary fotofizyczne. Przygotowałem szkic manuskrypt wraz z opisem części eksperymentalnej.

3. Role of intramolecular hydrogen bonds in promoting electron flow through amino acid and oligopeptide conjugates

Uczestniczyłem w tworzeniu koncepcji i metodyki badań. Zsyntezowałem i zanalizowałem wszystkie związki podane w publikacji. Asystowałem w trakcie prowadzenia wszystkich badań fotofizycznych, przygotowywania manuskryptu i części eksperymentalnej.

4. Synthesis of Corroles and Their Heteroanalogs

Dokonałem ogólnego przeglądu literatury i napisałem niektóre rozdziały oraz uczestniczyłem w scalaniu rozdziałów.



prof. dr hab. Daniel T. Gryko

Oświadczam, że mój wkład w powstanie poniższych publikacji polegał na:

1. Hydrogen Bond Involving Cavity NH Protons Drives Supramolecular Oligomerization of Amido-Corroles

Współpracowałem koncepcję badań, uczestniczyłem w planowaniu eksperymentów i w pisaniu manuskryptu.

2. Covalently Linked Bis(Amido-Corroles): Inter- and Intramolecular Hydrogen Bond Driven Supramolecular Assembly

Współpracowałem koncepcję badań, uczestniczyłem w pisaniu manuskryptu.

3. Role of intramolecular hydrogen bonds in promoting electron flow through amino-acid and oligopeptide conjugates

Współpracowałem koncepcję badań, uczestniczyłem w planowaniu eksperymentów, interpretacji wyników i w pisaniu manuskryptu.

4. Synthesis of Corroles and Their Heteroanalogs

Uczestniczyłem w pisaniu wstępnej wersji niektórych rozdziałów manuskryptu oraz w scalaniu rozdziałów i poprawianiu wersji finalnej przeglądu.





THE MARLAN AND ROSEMARY BOURNS
COLLEGE OF ENGINEERING

DEPARTMENT OF BIOENGINEERING
RIVERSIDE, CALIFORNIA 92521

phone: (951) 827-6239
fax: (951) 827-6416
e-mail: vullev@ucr.edu

February 27, 2021

To: Ph.D. Dissertation Committee of Mr. Rafał Orłowski
From: Valentine I. Vullev
Re: Contributions to the collaborative research published in the *Proc. Natl. Acad. Sci. USA*

Dear Committee Members:

Hereby, I declare that my contribution to the below mentioned publication is as follows:

1. Thermodynamic and kinetic analysis showing the role of intramolecular hydrogen bonds in promoting electron flow through amino-acid and oligopeptide conjugates

Rafał Orłowska, John A. Clark, James B. Derr, Eli M. Espinoza, Maximilian F. Mayther, Olga Staszewska-Krajewska, Jay R. Winkler, Hanna Jędrzejewska, Agnieszka Szumna, Harry B. Gray, Valentine I. Vullev, Daniel T. Gryko, "Role of intramolecular hydrogen bonds in promoting electron flow through amino-acid and oligopeptide conjugates," *Proc. Natl. Acad. Sci. USA*, 2020, in press.

Sincerely yours,

A handwritten signature in black ink, appearing to read "V. Vullev".

Valentine I. Vullev
Professor of Bioengineering, Chemistry,
Biochemistry, and Materials Science and Engineering
Fulbright U.S. Scholar Fellow (2018 – 2019)

Harry B. Gray, professor

I hereby declare that my contribution to the below mentioned publication is as follows:

1. Role of intramolecular hydrogen bonds in promoting electron flow through amino-acid and oligopeptide conjugates

I was host to Rafal Orłowski during his visit to Caltech. He performed photophysical experiments in the Caltech Beckman Institute laser spectroscopy laboratory. He analyzed data that were incorporated in the publication that has been accepted by the *Proceedings of the USA National Academy of Sciences*. I assisted in writing the paper.



Harry B. Gray

Arnold O Beckman Professor of Chemistry

California Institute of Technology

Pasadena, California, USA 91125



Instytut Chemii Organicznej
Polskiej Akademii Nauk

Prof. Dorota Gryko

Zespół XV

https://ww2.icho.edu.pl/gryko_group/

tel.: +48 22 343 20 51, fax: +48 22 343 66 81

dorota.gryko@icho.edu.pl

ul. M. Kasprzaka 44/52, 01-224 Warszawa

www.icho.edu.pl

Warszawa, 19.02.2020

OŚWIADCZENIE

Oświadczam, że mój wkład w powstanie poniższej publikacji polegał na napisaniu rozdziału 10 oraz redagowaniu i korekcie finalnej wersji manuskryptu.

„Synthesis of Corroles and Their Heteroanalogs”, R. Orłowski, D. Gryko, D. T. Gryko, *Chemical reviews*, **2017**, 117 (4), 3102-3137.

Z poważaniem,

**Dorota
Gryko**

Prof. Dorota Gryko

Digitally signed by
Dorota Gryko
Date: 2021.02.19
21:34:57 +01'00'

dr Olga Staszewska-Krajewska

Oświadczam, że mój wkład w powstanie poniższych publikacji polegał na:

1. Hydrogen Bond Involving Cavity NH Protons Drives Supramolecular Oligomerization of Amido-Corroles

Zaprojektowałam badania organizacji koroli za pomocą DOSY NMR, wykonałam pomiary i opracowałam wyniki. Uczestniczyłam w pisaniu publikacji w części dotyczącej NMR.

2. Covalently Linked Bis(Amido-Corroles): Inter- and Intramolecular Hydrogen Bond Driven Supramolecular Assembly

Badałam wpływ rozpuszczalników i temperatury na tworzenie się wiązań wodorowych; wykonałam pomiary NMR i opracowałam wyniki. Uczestniczyłam w pisaniu publikacji w części dotyczącej NMR.

3. Role of intramolecular hydrogen bonds in promoting electron flow through amino-acid and oligopeptide conjugates.

Zaprojektowałam i wykonałam eksperymenty NMR badanych związków i interpretowałam wyniki. Przygotowałam materiał do ESI w części dotyczącej NMR.


16.02.2021 *O. Krajewska*

Jay R. Winkler, PhD

I hereby declare that my contribution to the below mentioned publication is as follows:

1. Role of intramolecular hydrogen bonds in promoting electron flow through amino-acid and oligopeptide conjugates

I supervised the laser spectroscopic studies and co-wrote the manuscript.

 16 February 2021

Jay R. Winkler
California Institute of Technology

Prof. dr hab. Agnieszka Szumna
Kierownik zespołu IX



Instytut Chemii Organicznej
Polskiej Akademii Nauk

tel.: +48 22 343 23 20, fax: +48 22 632 66 81
Kasprzaka 44/42, 01-224 Warszawa
www.icho.edu.pl

Warszawa 16.02.2021

OŚWIADCZENIE

Oświadczam, że mój udział w publikacji:

“Role of intramolecular hydrogen bonds in promoting electron flow through amino-acid and oligopeptide conjugates.” Orłowski et al. *PNAS* **2021**

polegał na pracy strukturalnej nad modelem cząsteczek (przeszukania bazy danych krystalograficznej, stworzenie wstępnych założeń strukturalnych), planowaniu i konsultacji wyników obliczeń DFT i TD DFT oraz pracy nad tekstem publikacji dotyczącej tych wyników.

Z poważaniem,

Agnieszka Szumna

**Agnieszka
Szumna**

Elektronicznie podpisany przez
Agnieszka Szumna
Data: 2021.02.16 09:34:18
+01'00'

John A. Clark, PhD Candidate

I hereby declare that my contribution to the below mentioned publication is as follows:

1. Role of intramolecular hydrogen bonds in promoting electron flow through amino-acid and oligopeptide conjugates

I performed most photophysical and all electrochemical studies and analysis as well as assisted with writing the manuscript.

A handwritten signature in black ink that reads "John Clark". The signature is fluid and cursive, with the first name "John" and the last name "Clark" clearly distinguishable.

John A. Clark, PhD Candidate

University of California, Riverside

Department of Bioengineering

Maximilian F. Mayther

I hereby declare that my contribution to the below mentioned publication is as follows:

1. Role of intramolecular hydrogen bonds in promoting electron flow through amino-acid and oligopeptide conjugates

I aided with the synthetic schemes and conducted spectroscopic analysis on the corroles



Maximillian Mayther

Doctoral Candidate

University of California, Riverside

James B. Derr

I hereby declare that my contribution to the below mentioned publication is as follows:

1. Role of intramolecular hydrogen bonds in promoting electron flow through amino-acid and oligopeptide conjugates

I performed the deuterium exchanges and took the NMRs to confirm the exchange. I also performed transient absorption on the compounds



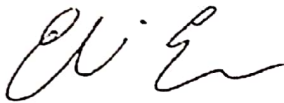
Sept. 28, 2020

Eli M. Espinoza, PhD

I hereby declare that my contribution to the below mentioned publication is as follows:

1. Role of intramolecular hydrogen bonds in promoting electron flow through amino-acid and oligopeptide conjugates

I helped perform the photophysical measurements: Transient absorption spectroscopy and quantum yields.



Eli Espinoza, PhD
Postdoctoral Scholar
University of California, Berkley
Department of Bioengineering

dr Mariusz Tasior

Oświadczam, że mój wkład w powstanie poniższej publikacji:

1. Hydrogen Bond Involving Cavity NH Protons Drives Supramolecular Oligomerization of Amido-Corroles

polegał na

*Przeprowadziłem syntezę opisanych wcześniej związków **11** i **12**, które R. Orłowski wykorzystał do syntezy koroń, byłem również zaangażowany w korektę manuskryptu.*

Mariusz Tasior



UNIwersytet
Warszawski



Oświadczam, że mój wkład w powstanie poniższych publikacji polegał na:

1. Hydrogen Bond Involving Cavity NH Protons Drives Supramolecular Oligomerization of Amido-Corroles, *Chem. Eur J.* **2017**, 23, 10195-10204

nadzorowaniu części związanej z charakterystyką strukturalną (rentgenowska analiza strukturalna na monokryształach) dwóch związków opisanych w pracy (**9** i **16**) i dyskusją wyników związanych z uporządkowaniem oraz oddziaływaniami w kryształach.

2. Covalently Linked Bis(Amido-Corroles): Inter- and Intramolecular Hydrogen Bond Driven Supramolecular Assembly, *Chem. Eur J.* **2019**, 25, 9658-9664.

nadzorowaniu części związanej z charakterystyką strukturalną (rentgenowska analiza strukturalna na monokryształach) dwóch układów opisanych w pracy (**5** i **6**), tworzących po 2 solwaty każdy i dyskusją uzyskanych wyników związanych z uporządkowaniem oraz występującymi oddziaływaniami w kryształach.

Prof. dr hab. Michał K. Cyrański
Pasteura 1
02-093 Warszawa
e-mail: mkc@chem.uw.edu.pl
Tel: 22 55 26 360

mgr. Grzegorz Cichowicz

Oświadczam, że mój wkład w powstanie poniższej publikacji polegał na:

1. Covalently Linked Bis(Amido-Corroles): Inter- and Intramolecular Hydrogen Bond Driven Supramolecular Assembly

Przeprowadziłem badania strukturalne metodą dyfrakcji rentgenowskiej czterech cząsteczek bisamidokoroli, opisałem je i zilustrowałem w manuskrypcie.

Grzegorz Cichowicz



UNIwersytet
Warszawski

Wydział Chemii



Warszawa, 25.02.2021

Oświadczam, że mój wkład w powstanie publikacji:

Orłowski, R.; Tasiór, M.; Staszewska-Krajewska, O.; Dobrzycki, Ł.; Schilf, W.;
Ventura, B.; Cyrański, M. K.; Gryko, D. T., „Hydrogen Bonds Involving Cavity NH
Protons Drive Supramolecular Oligomerization of Amido-Corroles”, *Chem. Eur. J.*,
2017, *23*, 10195-10204

polegał na wykonaniu pomiarów dyfrakcyjnych kryształów związków **9** i **16**, określeniu ich
struktury oraz przygotowaniu części manuskryptu dotyczącej badań rentgenostrukturalnych.

Łukasz Dobrzycki

dr inż. Hanna Jędrzejewska

Oświadczam, że mój wkład w powstanie poniższej publikacji polegał na:

1. Role of intramolecular hydrogen bonds in promoting electron flow through amino-acid and oligopeptide conjugates

Obliczenia DFT: optymalizacja geometrii oraz widma UV-Vis i ECD aminokwasowych i peptydowych pochodnych koroli.

Hanna Jędrzejewska

Barbara Ventura, PhD

I hereby declare that my contribution to the below mentioned publication is as follows:

1. „Hydrogen Bonds Involving Cavity NH Protons Drives Supramolecular Oligomerization of Amido-Corroles”, R. Orłowski, M. Tasiar, O. Staszewska-Krajewska, Ł. Dobrzycki, W. Schilf, B. Ventura, M. K. Cyrański, D. T. Gryko, *Chemistry–A European Journal*, **2017**, 23 (42), 10195-10204.

I have been in charge of the optical characterization of the monomer corroles in diluted solution at room temperature and at 77K and on the study of their self-assembly properties at optical concentrations. I participated in the writing of the manuscript.

Barbara Ventura

dr hab. Wojciech Schilf

Warszawa, 28.09.2020

IChO PAN

Zespół XVI

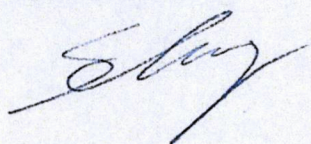
Oświadczenie

Oświadczam, że mój wkład w powstanie poniższych publikacji:

1. Hydrogen Bond Involving Cavity NH Protons Drives Supramolecular Oligomerization of Amido-Corroles
2. Covalently Linked Bis(Amido-Corroles): Inter- and Intramolecular Hydrogen Bond Driven Supramolecular Assembly

polegał na zaproponowaniu i przeprowadzeniu niektórych eksperymentów NMR. Konsultowałem również proces interpretacji widm NMR pod kątem badań strukturalnych.

Z poważaniem,
Wojciech Schilf



B. Org. 426/21

Biblioteka Instytutu Chemii Organicznej PAN

Org.-B.426/21



80000000342847